ANALYTICA CHIMICA ACTA

International monthly devoted to all branches of analytical chemistry
Revue mensuelle internationale consacrée à tous les domaines de la chimie analytique
Internationale Monatsschrift fur alle Gebiete der analytischen Chemie

ELSEVIER SCIENTIFIC PUBLISHING COMPANY
AMSTERDAM

Anal. Chim. Acta, Vol 72, No. 2, 225–460, October 1974
Published monthly
Completing Volume 72

Publication Schedule for 1974

Vol. **68**, No. **1**	January 1974	
Vol. **68**, No. **2**	February 1974	**(completing Vol. 68)**
Vol. **69**, No. **1**	March 1974	
Vol. **69**, No. **2**	April 1974	**(completing Vol. 69)**
Vol. **70**, No. **1**	May 1974	
Vol. **70**, No. **2**	June 1974	**(completing Vol. 70)**
Vol. **71**, No. **1**	July 1974	
Vol. **71**, No. **2**	August 1974	**(completing Vol. 71)**
Vol. **72**, No. **1**	September 1974	
Vol. **72**, No. **2**	October 1974	**(completing Vol. 72)**
Vol. **73**, No. **1**	November 1974	
Vol. **73**, No. **2**	December 1974	**(completing Vol. 73)**

Subscription price: Dfl. 492.00 plus Dfl. 36.00 postage. Subscribers in the U.S.A. and Canada receive their copies by airmail. Additional charges for airmail to other countries are available on request. For advertising rates apply to the publishers.

Subscriptions should be sent to:
Elsevier Scientific Publishing Company, P.O. Box 211, Amsterdam, The Netherlands.

GENERAL INFORMATION

Languages

Papers will be published in English, French or German.

Submission of papers

Papers should be sent to:

PROF. PHILIP W. WEST,
Coates Chemical Laboratories,
College of Chemistry and Physics,
Louisiana State University,
Baton Rouge 3,
La. 70803 (U.S.A.)

or to:

DR. A. M. G. MACDONALD,
Department of Chemistry,
The University,
P.O. Box 363
Birmingham B15 2TT (Great Britain)

Reprints

Fifty reprints will be supplied free of charge. Additional reprints (minimum 100) can be ordered at quoted prices. They must be ordered on order forms which are sent together with the proofs.

PRINTED IN THE NETHERLANDS

salon du laboratoire 1974

Paris, porte de Versailles

dec. 9th-14th 1974

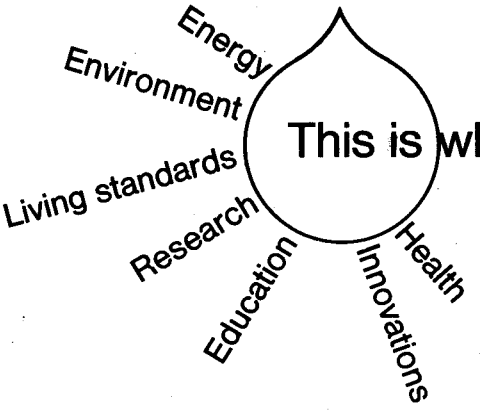

This is why Laboratories exist.

The 65th Physics Exhibition is being held along with the Salon du Laboratoire (Laboratory Exhibition); entrance formalities are communal.

The G.A.M.S. (Organisation for the propagation of spectroscopic and physico-chemical methods) will hold its 32nd Congress at the same time and place as the two Exhibitions.

The "Salon du Laboratoire" is organised by the "Association pour le Salon du Laboratoire"
10 avenue Hoche - 75382 PARIS CEDEX 08 - FRANCE - Tel. 622.38.00 ext. 528.

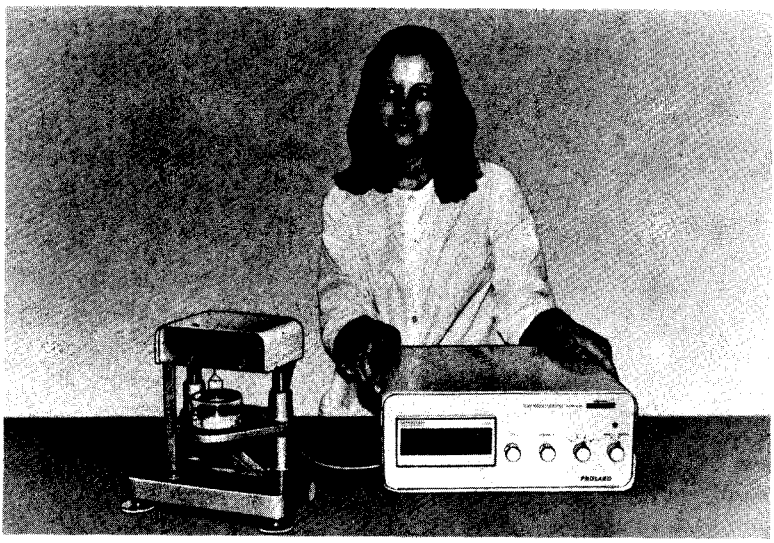

Tensiomètre PROLABO à équilibrage automatique et lecture numérique directe en dyne/cm

Ce nouveau tensiomètre automatique est destiné comme le tensiomètre Dognon-Abribat à la mesure précise des tensions superficielles et interfaciales. C'est un instrument élaboré aux possibilités très étendues:

- **Equilibrage automatique** par le jeu de servomécanismes.
- **Lecture numérique** sans facteur personnel.
- **Lecture directe de la tension en dynes par cm,** sans aucun calcul.
- **Enregistrement** de la tension superficielle sur un voltmètre enregistreur banal, donnant aussi une lecture directe en dyne/cm.

La méthode de mesure des tensions mise en oeuvre est celle de la lame mouillée ou de l'étrier NF T 73.060, immergé à l'interface liquide-air ou liquide-liquide.

Les mesures peuvent s'effectuer aussi bien en équilibre **statique** (méthode de Wilhelmy) que par arrachement **dynamique.**

Les résultats sont remarquablement **reproductibles;** la sensibilité de l'instrument est de **0,1 dyne/cm.**

Les mesures sont extrêmement **rapides:** à peine la lame ou l'étrier est-il immergé que l'appareil s'équilibre automatiquement, et la tension se trouve affichée sur le cadran en dyne/cm.

Les indications du tensiomètre étant **instantanées,** on peut suivre l'évolution de la tension au cours du temps, et **enregistrer** graphiquement ses variations.

Emplois • Les tensions superficielles des liquides, et les tensions interfaciales des liquides entre eux interviennent dans tous les phénomènes de surfaces, dans les problèmes de mouillage, de dispersion d'une poudre solide dans un liquide, de dispersion d'un liquide dans un autre liquide peu miscible, etc. . .

On comprend donc l'intérêt du tensiomètre pour l'étude des solutions détergentes, des liquides de traitement de minerais, des bains d'électrolyse, des colles, des peintures et vernis, des catalyseurs, des suspensions, des solutions colloïdales, etc. . . Sant compter l'étude des liquides biologiques.

La tension superficielle des liquides est une constante physique dont la mesure systématique se révèle fructueuse. Elle est à la fois un indice de pureté et de propreté superficielle.

Si le tensiomètre manuel de Dognon-Abribat est un excellent instrument lorsqu'il s'agit de faire épisodiquement quelques mesures ou d'organiser des travaux pratiques d'élèves, on préfèrera le nouveau tensiomètre automatique dans les laboratoires de recherches, les laboratoires de mesures physiques et les laboratoires de contrôle industriel devant exécuter de nombreuses mesures.

Le même tensiomètre convient pour faire rapidement et avec précision des mesures isolées ou en série, ou pour suivre et enregistrer en continu des tensions variables. Dans beaucoup de problèmes pratiques, l'étude des variations de la tension sous l'effet de divers paramètres est du plus haut intérêt. Ses qualités offrent des possibilités nouvelles pour l'étude scientifique des tensions superficielles et interfaciales et pour son exploitation pratique en milieu industriel.

PROLABO

12, Rue Pelée - 75-PARIS XIe
Téléphone 355.44.88
TELEX: PROLABO PARIS 68566
B.P. 200 75526 PARIS CEDEX 11

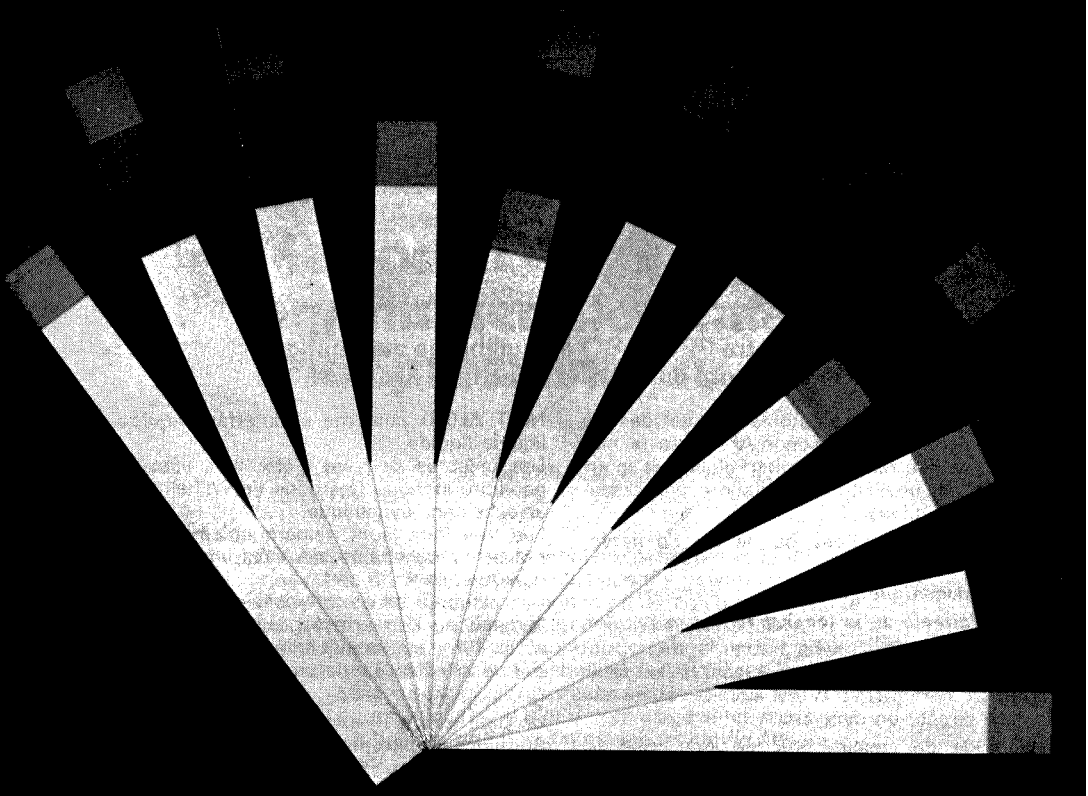

Analytical Chimica Acta, 72 (1974) 225–230

ANALYSIS FOR TRACE LEVELS OF BORON BY ION EXCHANGE–HOLLOW CATHODE EMISSION

E. H. DAUGHTREY, JR. and W. W. HARRISON

Department of Chemistry, University of Virginia, Charlottesville, Virginia 22901 (U.S.A.)

(Received 21st January 1974)

Trace analysis methods for the determination of boron have generally lacked the sensitivity necessary to determine normal boron levels in many samples, such as biological materials and natural waters, without preconcentration. For example, while atomic absorption spectrometry has been used to determine serum boron levels in two cases of lethal boron intoxication[1], the sensitivity obtained (5 p.p.m.) did not approach the normal (0.25 p.p.m.) boron level in blood. The boron concentration in plant and animal tissue ranges from tens of parts-per-million down to the parts-per-billion level[2]. Boron toxicity to various plants and the increasing boron concentration in surface waters has been a subject of study[3]. The average boron concentration in natural waters ranges from 13 p.p.b. in river water to 5 p.p.m. in sea water[2,4]. These lower concentration limits given here tax the sensitivity of most techniques for boron[5].

The use of the hollow-cathode emission (HCE) source for the determination of boron to the sub parts-per-billion level has been reported[6]. Conditions were optimized for the determination of boron, but interferences were observed in the attempted analysis of biological samples. In the present study, the elimination of organic and inorganic interferences by use of low-temperature RF ashing and ion-exchange separation is demonstrated. The analyses of several biological materials and natural water samples illustrate the utility of the hollow-cathode source for the trace determination of boron.

EXPERIMENTAL

Apparatus

The hollow-cathode source and associated vacuum system, spectrometer, and readout system have been previously described[6].

Reagents

All chemicals used were reagent-grade. Boron working solutions were made by dilution of 100 p.p.m. boric acid stock prepared by dissolution of boric acid in distilled, deionized water. Dowex 50W-X8 strongly acidic cation-exchange resin was made into a slurry with distilled, deionized water. Amberlite IR4B weakly basic anion-exchange resin was converted to the free base form by washing with 5% sodium hydroxide and rinsing with distilled, deionized water to remove excess of base. All solutions were stored in polyethylene bottles to minimize possible pick-up of boron from pyrex glassware.

Procedure

Ashing. All biological samples were dried at 110°C and weighed in quartz sample boats. Duplicate samples were placed in an RF low-temperature dry ashing furnace and ashed for 48 h with periodic stirring to achieve complete ashing of the samples. The samples were then removed and the ash weighed and dissolved in a few drops of 10% hydrochloric acid and diluted with distilled, deionized water to an appropriate volume, depending on the expected concentration of boron in the sample. Further dilution was sometimes necessary to adjust the concentration to the working range of the method.

Separation. The test solution (1 ml) was shaken in a polyethylene vial with a mixed ion-exchange resin slurry (5 ml of anion-exchange resin, 2 ml of cation-exchange resin, approximately 40% water by weight). The mixture was then centrifuged and 0.1-ml aliquots were taken for analysis from the solution over the resin.

Analysis. The 0.1-ml portion of test solution was placed in the cathode cavity and evaporated under an infrared lamp. The dried cathode was then placed in the cathode block, and the system was evacuated and flushed with argon. The fill gas pressure was adjusted to 0.7 torr and the discharge was initiated at low current and rapidly increased to the 200 mA operating value.

The spectrometer and associated readout produced a display of boron emission intensity at the 249.8-nm line as a function of time. The recorder trace showed a rapid rise in emission intensity followed by an exponential-like decay to a background level. This peak intensity was taken in each case; 10–20% r.s.d. was observed for 8–10 runs of each test solution. Blanks were run to determine the contribution to the emission intensity from the cathode material itself. The sputter-cleaning procedure of the cathodes has been previously described[6].

RESULTS AND DISCUSSION

Choice of separation technique

Attempts were made initially to analyze directly synthetic samples which contained p.p.b. of boric acid and 1000 p.p.m. sodium chloride, a first approximation of biological sample conditions. The response in boron emission intensity under these conditions was reduced and the peak broadened greatly with respect to the response from simple aqueous solutions. Also, the cathode surface was difficult to clean, requiring extensive sputtering at high currents, in addition to abrasive cleaning, to regenerate a suitable surface.

Because of these difficulties, a separation technique was sought. The most commonly used method for boron separation, distillation with methanol to form the volatile methyl borate, does not lend itself to the hollow-cathode emission technique, because a solution or solid sample is needed to deposit in the hollow-cathode cavity. The method is also time-consuming. Solvent extraction techniques involve the use of chelating agents or the formation of organo-boron compounds whose stability as solids and behavior in the discharge are potential causes of instability and interference. Ion-exchange techniques for the separation of boron have been used with success above the microgram level[5,7]. The separation is based on the non-absorption of boron as free boric acid by a mixed exchange resin

(strongly acidic cation, weakly basic anion) in acidic or neutral solution, whereas most ionic species will be absorbed by this resin mixture[5]. Any soluble, very weak, free acid should be similarly unaffected by the mixed resin, but there are few common inorganic acids that meet these solubility and K_a criteria. Organic acids which might be present in certain samples would be removed by the RF ashing. Although there should be no absorption of boric acid on weakly basic anion-exchange resins, some trace absorption (less than one microgram) varying with the manufacturer of the resin, has been reported[7]. Dilution of the sample solution by the resin mixture, plus any slight boron absorption on the resin, reduced the overall sensitivity for boron by about a factor of five. Considering the sensitivity of boron by hollow-cathode emission, this presents no serious problem.

Batch, rather than column, operation was chosen for the ion-exchange separation because column operation was more time-consuming and lacked the reproducibility from run to run obtained with the batch process. The exchange capacity of the batch process was not a limiting factor for the small sample quantities used in the study. No attempt was made to regenerate the resin after each run; the resin was discarded.

Studies with synthetic samples

Solutions containing 100 p.p.b. boron as boric acid and 0–5000 p.p.m. sodium as sodium chloride were analyzed after ion-exchange separation. The response in boron emission intensity was constant within experimental error as the sodium concentration was varied. The effects of 5000 p.p.m. potassium and 500 p.p.m. phosphoric acid addition were also investigated; no interference was found after separation of the boron by ion exchange. As a rigorous test of potential interference, an omnibus solution of 24 elements (normally used as a standard in spark-source mass spectrometry studies, each at a concentration of 100 p.p.m., all as the nitrate salts) was doped with 100 p.p.b. boron, treated by ion exchange, and analyzed. Again, no interference was observed from the other components of the solution.

A working curve was constructed, varying the boron concentration from 0–10 p.p.b. with a constant 1000 p.p.m. sodium chloride concentration (Fig. 1). The peak shape of the recording of emission intensity *versus* time was consistent with that observed for aqueous boron solutions[6].

Analysis of biological samples

Duplicate samples were taken of each of three biological samples: NBS Standard Orchard Leaves, NBS Standard Bovine Liver, and a human hair sample. Few literature values are available for the expected boron levels. The NBS Standard Orchard Leaves certificate of analysis[8] lists a non-certified value of 23 p.p.m., dry weight boron, as determined by the nuclear track technique. No NBS value is given for boron in the bovine liver sample. Average boron concentration in mammalian liver is reported as 0.48 p.p.m. by Bowen[2]. A range of 0.1 to tens of p.p.m. boron was found in 50 cat liver samples analyzed by mass spectrometry in this laboratory. No reported values for boron concentration in hair could be found.

Low-temperature dry ashing was chosen as the ashing technique because its

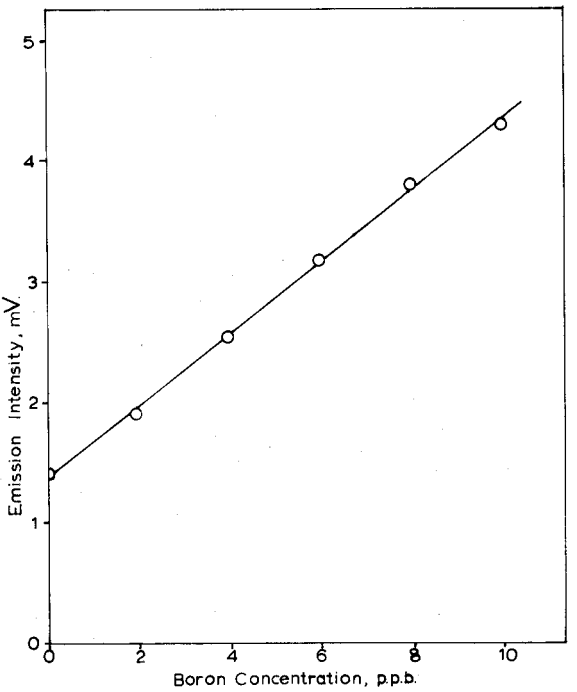

Fig. 1. Working curve for boron. Tube current, 200 mA; fill gas, argon at 0.7 torr. Points represent average of 8–10 runs with r.s.d. of $\pm$10–20%.

successful use has been reported in a colorimetric procedure[9]. Large boron losses have been reported by high-temperature ashing[1], which is thus eliminated from consideration. The nitric–perchloric acid wet digestion is not as trouble-free as the low-temperature dry ashing. Each of the samples ashed readily to completion and the resultant ash dissolved readily. The dissolved samples were diluted to the proper volume to fit on the working curve (Fig. 1), separated by ion exchange, and analyzed by hollow-cathode emission.

Analytical results were obtained both by direct comparison to the working curve and by standard addition methods. The latter involved addition of known amounts of boron to the sample before ion exchange. A comparison of the values obtained for the biological samples is given in Table I. The agreement of the duplicate samples with each other and the agreement between the standard addition and direct fit to the working curve are within the experimental uncertainty of the individual analyses. The higher deviation for the hair samples is probably due to the small sample size, yielding a small ash quantity and the low boron concentration.

Analysis of water samples

The determination of boron in solution samples was tested by running five water samples: freshly distilled, deionized water; "aged" distilled water (stored in a pyrex volumetric flask for 4 years); tap water (Charlottesville, Va. city water supply); river water (North Fork, Rivanna River, Charlottesville, Va.); and sea

TABLE I

COMPARISON OF BORON CONCENTRATIONS IN BIOLOGICAL SAMPLES BY DIRECT FIT TO WORKING CURVE AND BY STANDARD ADDITION

Sample	*Boron concentration (p.p.m., dry weight)*		
	Working curve		*Standard addition*
Hair 1	0.199		0.251
Hair 2	0.212		0.186
Average	0.205		0.218
		0.212 ± 0.020	
NBS Orchard Leaves 1	22.5		25.4
NBS Orchard Leaves 2	22.6		24.9
Average	22.55		25.15
		23.85 ± 1.3	
NBS Bovine Liver 1	2.19		1.92
NBS Bovine Liver 2	2.49		2.55
Average	2.34		2.24
		2.29 ± 0.23	

water (Atlantic Ocean, Virginia Beach, Va.). No attempt was made to obtain a range of representative samples from the various sources, as they were chosen only to illustrate the range of the present technique. Boron toxicity to plants has been reported as low as 500 p.p.b. (ref. 3) in water. A literature value for typical boron concenrations in river water is given as 13 p.p.b. (ref. 2). A range of 2–221 p.p.b. has been found in U. S. waters in this region[4]. Bowen lists a value of 4.6 p.p.m. boron in sea water.

The water samples were run without ashing. However, in the case of highly polluted water, ashing would be recommended. The analysis of the water samples is given in Table II. Standard addition methods were again used to verify working curve results. The tap water and river water boron values are within the range of expected concentrations. The Charlottesville city water is taken from the Rivanna River, so the agreement of the tap and river water samples suggests little change in boron levels from the treatment process[3]. The sea-water sample shows boron concentrations close to the nominal value.

TABLE II

BORON CONCENTRATIONS IN NATURAL WATER SAMPLES

Sample	*Boron concentration (p.p.b.)*	
	Working curve	*Standard addition*
Distilled, deionized water	Not detected	
"Aged" distilled water (see text)	7.7	7.5
Tap water	4.9	5.0
River water	6.0	6.1
Sea water	4,000	4,200

The ion exchange–hollow cathode emission technique can be used for a wide variety of sample types in the determination of boron. The presence of organics requires ashing, but this is also a requirement for many other trace element methods. The potential interference of high inorganic solids, such as the biological ashes or the sea water sample, can be eliminated by a rapid ion-exchange procedure. The advantageous sensitivity shown by hollow-cathode emission for an element (boron) which is difficult to determine at trace levels by other conventional techniques makes this a technique which could have valuable application.

SUMMARY

The demountable hollow-cathode source has been shown to be useful in the determination of boron to the sub-nanogram level. Its application to the analysis of biological materials and natural waters is illustrated. Low-temperature RF ashing and ion exchange are used to remove potential organic and inorganic interferences.

REFERENCES

1 H. Bader and H. Brandenberger, *At. Absorption Newslett.*, 7 (1968) 1.
2 H. J. M. Bowen, *Trace Elements in Biochemistry*, Academic Press, New York, 1966.
3 A. Waggolt, *Water Res.*, 3 (1969) 749.
4 J. F. Kipp and R. C. Kroner, *Trace Metals in Waters of the United States*, United States Department of the Interior, Washington, D.C., Survey 1962–1967.
5 A. A. Nemodrux and Z. K. Karolova, *Analtical Chemistry of Boron*, Ann Arbor-Humphrey Science Publishers, Ann Arbor, 1969.
6 E. H. Daughtrey and W. W. Harrison, *Anal. Chim. Acta*, 67 (1973) 253.
7 O. Samuelson, *Ion Exchange Separations in Analytical Chemistry*, Wiley, New York, 1963.
8 National Bureau of Standards Standard Reference Material 1571, Certificate of Analysis, United States Department of Commerce, Washington, D.C.
9 J. W. Mair and H. G. Day, *Anal. Chem.*, 44 (1972) 2015.

Analytica Chimica Acta, 72 (1974) 231–243

A CRITICAL STUDY OF THE APPLICATION OF GRAPHITE-FURNACE NON-FLAME ATOMIC ABSORPTION SPECTROMETRY TO THE DETERMINATION OF TRACE BASE METALS IN COMPLEX HEAVY-MATRIX SAMPLE SOLUTIONS

ROMANA B. CRUZ and JON C. VAN LOON

Departments of Geology, Chemistry and the Institute of Environmental Sciences and Engineering, University of Toronto, Toronto M5S 1A1 (Canada)

(Received 11th February 1974)

Since L'Vov[1] proposed in 1961 the use of a graphite crucible non-flame atomizer in conjunction with atomic absorption spectrometry, a proliferation of extravagant claims regarding the usefulness of non-flame atomizers have appeared in the literature. These include claims that limits of detection are generally several orders of magnitude lower than with flame atomizers and that selective volatilization of the matrix before the analyte or *vice versa* is a generally applicable method of reducing interference problems. If these contentions are true, then nonflame atomizers would be essential components of most atomic absorption installations.

Most of these claims for superiority have resulted from work done on simple matrix sample solutions, *e.g.* natural fresh waters and simple organic solutions. It is thus very important that a critical evaluation should be made under the more normal conditions of complex sample matrix types.

Critical evaluations of problems associated with the analysis of some specific sample types have been made. Barnard and Fishman[2] studied the determination of trace metals in water. They concluded that, "in general, determination of trace metals in water by direct comparison with aqueous standards is not practical because of interferences caused by ions, at low concentrations, common in natural waters". In this regard, the present authors have found that, with proper background correction, natural waters such as that from soft water lakes or rain, *etc.*, can be run directly against aqueous standards.

Segar and Gonzalez[3] critically evaluated the use of the graphite atomizer for the direct determination of trace metals in sea water. They concluded that direct analysis of sea water for Fe, Co, Ni, V and Mn can be achieved by means of a selected volatilization technique, with relatively poor precision, but high speed, compared to an extraction technique.

Other workers have reported non-flame procedures for determining trace elements in heavy matrix samples. In many of these cases, a prior extraction step is recommended to remove the analyte from the complex matrix. If an extraction is required, it is the present authors' opinion that in most instances, there would be little advantage to using a non-flame rather than a flame determinaton.

Direct analyses of specific organic sample types by the non-flame technique

have proved more successful. Papers on blood[4], urine[5] and polyester fibres[6] show the distinct advantage of this approach.

In the following critical evaluation of trace metal determination in heavy, complex, matrix solutions, a Perkin-Elmer Graphite Furnace was employed. Of the commercial offerings, this equipment seems to show distinct advantages of ease and reproducibility of sample introduction and reproducibility of experimental conditions. The tantalum ribbon (Instrumentation Laboratories) device has advantages when carbide formation might be a problem.

EXPERIMENTAL

Equipment and reagents

A Perkin-Elmer atomic absorption spectrophotometer Model 303 equipped with a PE HGA-70 heated graphite atomizer and a Sargent-Welch SRL recorder were employed. During the course of the research, the HGA-70 was replaced with tle new model HGA-2000. For flame comparison an Instrumentation Laboratories AA spectrophotometer Model 153 with a single-slot (high solids) burner was used.

Tables I and II give the operating conditions for the spectrophotometers and the heated graphite atomizer, determined to be optimal for heavy-matrix analysis.

TABLE I

INSTRUMENTAL PARAMETERS FOR PE ATOMIC ABSORPTION SPECTROPHOTOMETERS 303 AND HGA-2000

	Cd	*Co*	*Cu*	*Ni*	*Pb*	*Zn*
λ absorbing (nm)	228.9	240.9	324.8	232.0	217.0	213.9
λ background (nm)	226.8	239.3	296.1	231.6	220.4	210.4
Spectral slit width (nm)	0.65	0.20	0.20	0.065	0.65	0.65
HGA temperature (°C)						
Dry	125	125	125	125	1.25	125
Ash	500	1100	1100	1100	750	500
Atomize	1800	2500	2500	2500	2300	1800
Time (s)						
Dry	30	30	30	30	30	30
Ash	60	60	60	60	60	60
Atomize	20	15	15	15	15	20

TABLE II

INSTRUMENTAL PARAMETERS FOR IL 153

	Cd	*Co*	*Cu*	*Ni*	*Pb*	*Zn*
λ absorbing (nm)	228.8	240.7	324.8	232.0	217.0	213.9
λ background (nm)	226.4	239.3	324.3	231.6	220.4	217.6
Slit width (μm)	40	80	80	40	80	80
Scale expansion	1.0 ×	0.5 ×	0.5 ×	0.5 ×	0.25 ×	0.5 ×
Burner height (mm)	15	15	15	15	15	15
Flame type	stoich.	v. lean	lean	v. lean	stoich.	rich

With the HGA-2000, the drying, ashing, and atomization temperatures are continuously variable, whereas the drying and ashing temperatures are fixed with the HGA-70 and controlled by 7 program buttons; only the atomization temperature is variable for all programs. Programs 1 and 2 do not include an ashing stage and have only drying at 60°C and 100°C, respectively, and atomization in the cycle. Programs 3 to 7 include drying at 100°C, ashing at 230, 330, 490, 750, and 1100°C, respectively, and atomization at variable temperatures.

Gas flow within the graphite furnace was variable for the HGA-2000 and was fixed at the factory pre-set rate of 1.7 l min^{-1} for the HGA-70. With the HGA-2000, gas flow within the furnace can be momentarily stopped during the atomization stage, either manually or automatically. Such a condition causes the HGA-70 to shut off power supply to the furnace and hence is not applicable.

Argon and dry nitrogen were used as purge gases.

Standard solutions were prepared by dissolving the ncessary amount of high-purity metal in nitric acid and making appropriate dilutions with distilled water and nitric acid.

Solutions were introduced into the graphite furnace by a 10-μl Eppendorf micropipette with disposable polypropylene tips.

Peak height was used. Experimentation showed that integration did not improve results.

Spec-Pure reagents were difficult to procure for some salts used in preparing the heavy matrix solutions. Therefore blank solutions were read every time.

Trace elements studied

The six heavy metals, Cd, Co, Cu, Ni, Pb, and Zn were chosen for this study; these are the metals most commonly determined in geochemical and environmental samples. Multi-element standard solutions of these six metals were used to prepare calibration curves. No inter-element interference was observed when the absorption of a pure analyte solution was compared to that of the same analyte solution containing equal concentrations of each of the five remaining metals.

Matrices chosen

Three representative samples for analysis were chosen to cover the range of heavy-matrix types usually encountered in natural samples. Silicate rocks give an example of a mainly inorganic matrix. U.S.G.S. rock standards were utilized. Treated sewage sludge represents heavy matrix samples of intermediate composition with respect to both inorganic and organic matter. Standard sludges were obtained from the Canada Centre for Inland Waters (CCIW). Blood, although it may not be a stereotype of a geochemical sample, is an excellent medium for outlining the problems associated with trace-metal analysis in an organic heavy matrix. Blood also is an excellent sample type for observing sample stability problems with organic materials. In the case of blood, only lead, a relatively volatile element, was studied. As will be seen later in this work, the behaviour of the other trace components such as Cu, Co, Ni and Cd in this type of matter could be readily deduced. Blood samples were collected with heparinized capillary tubes from finger pricks.

Observations on calibration curves

The calibration curves were found to be linear only up to concentrations giving absorptions of about 50–60% regardless of the element and concentration, *e.g.* when calibration curves were made for three different copper analytical lines (324.7, 327.4, 222.6 nm with relative sensitivities of 1.0, 2.0 and 15.0 respectively), the linear cut-off was observed to be 50–60% absorption regardless of concentration. The curves bend towards the concentration axis at higher absorbances. Alkemade[7] gives an excellent discussion on the reasons for non-linearity of calibration curves.

Background correction

Because of the necessity to study the nature of matrix interference, background corrections were done manually by taking absorption readings of the heavy-matrix solutions at a nearby non-absorbing line of the element being determined (These lines are listed in Table I.) The non-linearity of absorbance curves necessitated the conversion of uncorrected absorbances first to concentration before the background absorbance was subtracted, instead of the more straightforward subtraction of the two absorbances.

The deuterium arc is a good continuum source for background correction over the analytical wavelengths range 200–300 nm. However, background compensation with this arc is limited to low background absorbance levels (of the order of about 40%) and to wavelengths where the arc emission is intense. Beyond these limits, the signal or the intensity of the background line or reference beam received by the photomultiplier becomes too weak and the signal is erratic.

Sample preparation

Rocks. Weigh 1 g of sample powder into a Teflon dish. Add 25 ml of 40% hydrofluoric acid and 2 ml of concentrated sulfuric acid. Evaporate over medium heat until fumes appear. Cool and slowly add 7 ml of concentrated nitric acid and 21 ml of concentrated hydrochloric acid. Evaporate over low heat. When dry, remove the excess of hydrochloric acid by adding nitric acid until brown fuming stops. Add about 15 ml of water. Filter into a 25-ml flask and dilute with washings to the mark. Analyze directly by flame a.a.s. Prepare further dilutions for HGA analysis (usually 1:250).

Treated sewage sludge. Weigh 0.5 g of sludge powder into a 100-ml beaker. Add 9 ml of concentrated hydrochloric acid and 3 ml of concentrated nitric acid. Cover the beaker with a watch glass and evaporate to dryness over medium heat. Add 1 ml of nitric acid, replace the cover and evaporate to dryness. Add 1 ml of nitric acid and filter into a 25-ml flask. Dilute to the mark. Make further dilutions as necessary.

Blood (see notes). Mark the level of blood inside the capillary. Blow out (as completely as possible) the sample into a dry 10-ml vial with a plastic cap. Dilute with 9 parts of distilled water (note (b)) blowing out the water 2 or 3 times after each separate addition. Swirl the solution gently to mix and replace the vial cap. Inject 10 μl into the graphite tube by the method described below. Add 10 μl of (1+1) ammonia liquor onto the sample inside the tube (note (c)).

Dry, ash, and atomize in the HGA-2000 (125, 750, 2300°C, respectively) for 40, 60 and 20 s, respectively.

Notes. (a) Blood should be frozen and analyzed within two days of collection. (b) Freezing and thawing, and dilution with distilled water all contribute to the haemolysis of blood cells. No need was found for recommended reagents such as Triton-X (ref. 4) or nitric acid. Some of these reagents only add to the matrix and perhaps contamination. (c) Addition of ammonia solution to the sample beforehand (*i.e.* during dilution) was found undesirable, owing to the precipitation of proteins on standing. The increased heterogeneity reduced precision. Ammonia minimizes frothing of the solution inside the tube[8].

Physical interferences

Physical problems were encountered in the introduction of blood solutions into the graphite furnace. The viscosity of the solution and the wetting of the hydrophobic polypropylene tip of the microlitre pipette caused errors in volume delivery. The drop of blood solution tended to form a bubble covering the injection hole of the graphite tube thus giving a reading that was different from that obtained when the drop was deposited on the bottom of the graphite tube (as occurs with the aqueous standard solutions). The sample position in the furnace affected the absorption because the height of the absorption peak depended not only on the number of absorbing atoms but also on their residence time in the path of the beam.

To solve the first problem, a "reversed" technique of pipetting was used[9]. The Eppendorf pipette has a plunger with two stops. In normal operation, depression to the first stop fills up the tip with the nominal volume of liquid. The second stop ensures the complete ejection of the contained liquid. In the "reverse" operation, the plunger is depressed all the way to the second stop to fill up the pipette tip with more than the nominal volume. Then the specified volume is delivered by depressing the plunger only to the first stop and touching the pipette tip to the lower lip of the injection hole of the graphite tube to wipe off ejected sample.

To prevent the drop of solution from covering the injection hole, the pipette tip was carefully wiped with tissue paper and care was taken not to touch the upper lip of the hole during introduction and withdrawal of the pipette. Thus by the above method the sample was deposited on the lower lip of the port so that during the drying, the sample drop rolled down reproducibly.

With the solutions of sewage sludges there was a slight problem owing to the wetting of the pipette tip. This was a consequence of the presence of organics and high concentrations of acid (nitric acid) used in preparing the solution. It was easily solved by frequently changing pipette tips.

Little problem was encountered with rock solutions.

RESULTS AND DISCUSSION

Chemical and Spectral interferences

Initial trace analysis of silicate rock solutions showed very large background absorbances caused by the heavy matrix, thus a detailed investigation of the nature of matrix interference was imperative. Simple heavy-matrix solutions were prepared

TABLE III

MATRIX INTERFERENCE IN NON-FLAME A.A.S.

Analyte conc.	*Matrix*	*Corrected absorbance*	*Background absorbance*	*Effect*[a]
Cd, 10 p.p.b.,	Pure	0.216		
	1% KNO_3	0.157	0.173	−
	1% $NaNO_3$	0.147	0.068	−
	0.5% $Fe(NO_3)_3$	0.223	0.009	+
	1% $Al(NO_3)_3$	0.143	0.000	−
	1% $CaCl_2$	0.000	0.393	−
	1% $Mg(NO_3)_2$	0.100	0.043	−
Co, 50 p.p.b.,	Pure	0.053		
	1% KNO_3	0.053	0.033	0
	1% $NaNO_3$	0.054	0.040	0
	0.5% $Fe(NO_3)_3$	0.070	0.043	+
	1% $Al(NO_3)_3$	0.051	0.304	0
	1% $CaCl_2$	0.000	0.330	−
	1% $Mg(NO_3)_2$	0.039	0.029	−
Cu, 25 p.p.b.,	Pure	0.046		
	1% KNO_3	0.037	0.012	−
	1% $NaNO_3$	0.038	0.010	−
	0.5% $Fe(NO_3)_3$	0.013	0.418	−
	1% $Al(NO_3)_3$	0.014	0.194	−
	1% $CaCl_2$	0.040	0.087	−
	1% $Mg(NO_3)_2$	0.037	0.014	−
Ni, 50 p.p.b.,	Pure	0.015		
	1% KnO_3	0.024	0.014	+
	1% $NaNO_3$	0.018	0.016	+
	0.5% $Fe(NO_3)_3$	0.029	0.053	+
	1% $Al(NO_3)_3$	0.020	0.257	+
	1% $CaCl_2$.	0.000	0.445	−
	1% $Mg(NO_3)_2$	0.020	0.031	+
Pb, 10 p.p.b.,	Pure	0.033		
	0.5% KCl	0.012	0.049	−
	0.5% NaCl	0.017	0.080	−
	1% $Fe(NO_3)_3$	0.000	0.049	−
	0.5% $Al(NO_3)_3$	0.029	0.179	−
	1% $MgCl_2$	0.033	0.000	0
	0.5% $CaCl_2$	0.016	0.027	−
Zn, 10 p.p.b.,	Pure	0.251		
	1% KNO_3	0.333	0.254	+
	1% $NaNO_3$	0.195	0.080	−
	0.5% $Fe(NO_3)_3$	0.066	0.592	−
	1% $Al(NO_3)_3$	0.334	0.214	+
	1% $CaCl_2$	0.062	0.376	−
	1% $Mg(NO_3)_2$	0.074	0.052	−

[a] Effect: + = enhancement; − = suppression; 0 = none.

from each salt and each analyte as follows: 1% and 0.5% KNO_3, $NaNO_3$, $Fe(NO_3)_3$, $Al(NO_3)_3$, $Mg(NO_3)_2$, KCl, NaCl, $MgCl_2$, and $CaCl_2$, as matrices for 10 p.p.b. solutions of Pb, Cd, Zn, 25 p.p.b. of Cu, and 50 p.p.b. of Ni and Co. These are the maximum levels of inorganic matrix that could be expected from

rock solutions, which are usually prepared by dissolving 1 g of rock powder with hydrofluoric acid into 25–50 ml of solution. Considering that 40–70% of silicate rocks or soils is silica, which is quantitatively removed by the hydrofluoric acid treatment, the rock solution is actually around 1–2% solids.

The instrumental conditions prescibed by the HGA-70 manual[10] were used, and 20 μl of each of the above solutions were run several times. With a few exceptions, smoke formation was observed and large non-specific absorption peaks were recorded at the atomization step.

Table III shows a compilation of the results.

Enhancement of atomic absorption was observed with Ni, Co, and Zn. But in most cases the corrected readings for the heavy-matrix solutions were lower than those for simple analyte solutions. This suppression seemed to be more severe with the relatively volatile elements such as Cd, Pb, and Zn. Calcium among the matrix salts causes the greatest suppression of analyte absorption.

The results obtained are in general agreement with recorded data[2,3,11,12]. There has however, been little correlation or analysis of these interference effects reported in the literature.

The frequent association of the more severe interferences observed, with systems containing relatively volatile analytes in a rather refractory matrix, suggested that it might be due to physical occlusion by the matrix. A simple experiment was performed to check this hypothesis. Solutions of 10 p.p.b. pure Cd, Cd with 1% $CaCl_2$, and 1% $CaCl_2$ blank were used. The results are presented in Table IV. Similarity in behaviour of systems 2 and 4, and the significant difference of system 3, supports the occlusion hypothesis of the solid phase before atomization. Further confirmation will be presented below under the discussion on atomization temperatures.

TABLE IV

EFFECT OF REFRACTORY MATRIX

System	*Absorbance*
1 5 p.p.b. Cd, 10 μl	0.046
2 5 p.p.b. Cd with 1% $CaCl_2$, 10 μl	0.019[a]
3 5 p.p.b. Cd, 10 μl, dried, plus 10 μl 1% $CaCl_2$	0.003[a]
4 1% $CaCl_2$, 10 μl, dried, plus 10 μl 5 p.p.b. Cd	0.015[a]
5 1% $CaCl_2$ blank	0.079

[a] Corrected readings.

Selective volatilization

In theory, the effect of the heavy matrix on analyte absorbance can be suppressed by the process of selective volatilization. Any two substances with different volatilities should be separable to some degree in the graphite furnace.

In practice, only the most volatile matrix was significantly removed by selective volatilization. Under this category fall organic matrices such as blood and,

to a certain extent, sludge. With organic matrices, relatively low ashing temperatures were sufficient for their removal. Therefore efficient selective volatilization was achieved even in the analysis of relatively volatile analytes such as lead. In the analysis for lead in blood, a large bulk of the organic matrix was easily vaporized during the first minute of ashing (dense smoke was emitted from the sides of the furnace). Thus at the atomization step only a very small background signal corresponding to around 5 p.p.b. lead was left, which could be due to the refractory calcium salts (9–11 mg% or 90–110 p.p.m. in blood) and other electrolytes such as potassium and sodium present in blood. It can be safely predicted that selective volatilization of organic matrices can be used in the determinations of the other metals like Cu, Co, Ni which have higher atomization temperatures than lead.

Attempts at selective volatilization of any of the inorganic matrix salts in trace analysis of Cd, Co, Cu, Ni, Pb, and Zn were not fruitful. Even at the highest ashing temperatures available with the HGA-70 (1100°C), the large bulk of the matrix invariably went off at the same time as the analyte during the subsequent atomization step.

Potential application of selective volatilization to inorganic matrices is limited to the cases where the differences in volatilities between matrix and analyte is quite large *e.g.* Na and K salts with Ni and Co. Even in this category selective volatilization was not complete. Background absorbance of a nickel solution containing 1% sodium nitrate cannot be eliminated even with ashing periods as long as 5 min at 1100°C. Under this condition, therefore, direct analysis will not yield good results.

However, Segar and Gonzalez[3] reported a qualified success for selective volatilization in the determination of Ni, Co, V, and Mn in sea water. They concluded, with reservations, that use of selective volatilization makes direct analysis of sea water for these metals possible. However, it is important to realize that sea water matrix is largely the easily volatilized sodium chloride. Samples of concern in the present study contain high levels of refractory Ca, Fe, and Al salts. Selective volatilization can do little to reduce chemical and spectral interference with this inorganic type of heavy matrix.

The reverse process of selective volatilization of analyte was equally unsatisfactory. In the determination of zinc and of cadmium in 1% aluminium nitrate or magnesium nitrate solutions at the manufacturer's recommended atomization voltage (1500°C), a broad background peak for the matrix appeared at around 1 s after the absorption peak. Resolution of the absorption peak from the background peak was achieved by successively lowering the atomization temperature, but at the expense of suppression of the analyte absorption by the refractory matrix.

The observed strong sample-composition dependence of non-flame a.a.s. puts into serious question earlier claims to the contrary, which in turn were responsible for much of the intense interest in this technique.

Method of standard additions

As an alternative to the selective volatilization method of interference suppression, several authors recommend the method of standard additions[2,3,12].

Since the standards are incorporated with the sample, viscosity and chemical environments are closely duplicated in both standard and sample. This method is potentially very useful if the heavy-matrix samples being analysed at any one time have unknown or widely differing matrix compositions.

The method of standard additions was tried on simple heavy-matrix solutions. Readings must be corrected for background absorption. Values obtained for 10 p.p.b. zinc samples ranged from 11 to 20 p.p.b. depending on the matrix constituents present.

Zinc values obtained were consistently high. The reason is the non-linearity of the calibration curve at higher absorbance levels. Because elements done by the non-flame technique often have very short linear regions in their calibration curve (*e.g.* Zn, Pb and Cd in this study), the routine use of the method of standard additions is hazardous.

The failure of the standard addition and selective volatilization methods to eliminate matrix problems in these complex solutions is a serious criticism of the non-flame technique for many applications.

Other variable parameters

Effect of the nature of purge gas. Argon is the most popular purge gas. Less expensive nitrogen has been used from time to time in place of argon. It has been shown[13] that the analytical sensitivity is sometimes less and sometimes the same in nitrogen compared to argon. This is attributed to the greater atomic weight of argon which seems to enhance its atom-stabilizing capacity. It was thought that the purge gas might affect the matrix differently from the analyte.

TABLE V

INFLUENCE OF THE NATURE OF PURGE GAS ON BACKGROUND ABSORBANCE

Background line (nm)		*Absorbance*	
		In argon	*In nitrogen*
239.3	(Co)	0.023	0.012
226.8	(Cd)	0.378	0.271
231.6	(Ni)	0.175	0.110
220.4	(Pb)	0.094	0.162
210.4	(Zn)	0.599	0.489

Table V shows a comparison of background absorbances of a standard rock solution at different non-absorbing wavelengths. As much as 50% decrease (with an average of about 25%) in matrix absorbance was obtained in switching from argon to nitrogen, while analytical absorbance was decreased by less than 10%.

Although with nitrogen there is the possibility of cyanogen formation at elevated temperatures (5000°C), no problem was encountered at the temperatures of the furnace (*ca.* 3000°C) that could be attributed to the strong cyanogen absorption in the u.v. region.

Nitrogen, in these applications, is then the purge gas of choice.

Influence of flow rate. Flow rate studies have been reported previously[13–15]. Optimal flow rates were chosen on the basis of sensitivity and precision in the absence of matrix[13]. However, it is conceivable that with the complicated interactions of parameters that affect atomic absorption, the flow rate of purge gas could have different influences on the analyte atoms and on the predominant matrix species. Thus optimization of flow rate in the presence of heavy matrix seems imperative to achieve a balance of sensitivity and reduced interference in heavy-matrix analysis.

Four different flow rates were studied (1.0, 2.5, 3.5 l min^{-1}) and the rate of 2.5 l min^{-1} was found to be optimal. Although this level of gas flow did not yield the maximal absorbance at the analyte wavelength, it did give the maximal difference between this and the background absorbance.

When flow-rate optimization experiments are done, attention must be given to the stabilization of flow rate after each adjustment. With the HGA-2000 it takes more than 1 min for the flow rate to adjust and remain constant after each setting.

Ashing time. Experimentation showed it was not worthwhile to use much more than 30 s at any ashing temperature to "ash" a sample. During this period of time, the furnace attained its equilibrium temperature and almost all of the salts that are volatile at that temperature were volatilized.

Atomization temperature. Except for Cd, Zn, and Pb, the atomization temperatures used in all the analyses done in this study were those commonly used by other workers.

In the past, workers studying interferences in non-flame a.a.s. used atomization temperatures determined to be optimal for simple aqueous solutions of the element[2,3,10,15]. What is considered optimal for ideal solutions was assumed to be so for non-ideal heavy-matrix solutions. This assumption may be seriously deficient in the case of the more volatile elements (*e.g.* Pb, Zn and Cd).

It is interesting to note that the more serious matrix interference effects reported in the literature[2,3] are usually associated with Cd, Zn, and Pb. It was suggested above that suppression of the analyte absorbance by heavy matrices was due to physical occlusion by salts. Experimentation was done to see if an increase in atomization temperature, above that recommended by most authors for simple solutions, might decrease the problem.

For cadmium, most workers use an atomization temperature of 1500°C. Others used an even lower temperature found to be optimal for simple aqueous solutions[3]. In this work, a temperature of 1800°C was chosen for cadmium as well as for zinc. This is a compromise between the problems arising at various temperatures from spectral and chemical interference. Though undesirable, the increased spectral interference (background absorbance) at higher atomization temperatures, becomes acceptable when weighed against the elimination of occlusion. The optimal atomization temperatures for Co, Cu, and Ni are near the maximal graphite furnace temperatures, at which solid-state occlusion is negligible.

Addition of reagents. The anion of a simple salt determines its volatility. Perchlorates, formates, and oxalates are rather unstable at relatively low temperatures. In particular, the formates and oxalates are thought to leave behind the metallic element on decompositon, permitting direct atomization and better

selective volatilization because of the lower volatility and the greater separation between the boiling points of the metals.

Dried 10-μl rock solutions (BCR-1, 1:5) being analyzed for nickel were treated with 10 μl each of 0.1 *M* solutions of perchloric acid, formic acid, and ammonium oxalate in the graphite furnace.

Formic acid and ammonium oxalate did not at all change the analytical or the background aborbance. The quantities used were intended to be in large excess compared to the sample, so that in spite of the instability, the formation of the formate or the oxalate of the metals and matrix would be favoured. Apparently no such reaction took place.

Perchloric acid gave very dense, white, pungent-smelling fumes during the ashing step even at very low temperatures (330°C). There was a slight decrease in background signal of treated samples at the nickel background line, compared to the untreated samples. When zinc was determined on similarly treated samples, most of the zinc was lost. Therefore the use of perchloric acid was discontinued.

Detection limit

Detection limits were estimated for the elements in heavy inorganic matrix solutions. The detection limit, in this case, is taken to be that concentration of an element which gives a signal 2 standard deviations above background, *or*, the concentration, in the present authors' judgment and experience, that can be reliably detected. A comparison of flame and flameless results is given in Table VI. The matrix chosen for this test contained high levels of the most troublesome constituents *e.g.* calcium and aluminium, but these types of matrices are commonly encountered in routine atomic absorption work. Data in this table indicate that there is little advantage to either the flame or the flameless technique.

TABLE VI

COMPARISON OF FLAME AND NON-FLAME DETECTION LIMITS IN HEAVY MATRIX SOLUTION (p.p.b.)

	Flame	*Flameless*
Cd	10	2
Co	10	30
Cu	30	12
Ni	40	80
Pb	30	10
Zn	10	3

Analysis of heavy matrix samples

A variety of rock and sludge samples were analysed by the procedures above, by both the flame and non-flame technique (Table VII). These values are the means on at least 3 determinations. No significant differences exist between the numercial values obtained by each technique for the methods tested.

Blood samples were analysed by the non-flame method and the results are compared with those obtained by anodic stripping voltammetry in Table VIII. Good agreement was obtained.

TABLE VII

ANALYSIS OF U.S.G.S. ROCK STANDARDS AND TREATED SEWAGE SLUDGE BY FLAME AND NON-FLAME A.A.S.

(All figures are in p.p.m.)

	AGV-1		*BCR-1*		*A (lime-treated)*[a]		*B($FeCl_3$-treated)*[a]	
	HGA	*Flame*	*HGA*	*Flame*	*HGA*	*Flame*	*HGA*	*Flame*
Cd	n.d.[b]	n.d.	n.d.	n.d.	1	1	19	14
Co	11.8	12.0	29.9	30.0	—	—	—	—
Cu	54.2	50.5	18.3	18.5	148	150	1314	1200
Ni	13.1	15.6	16.0	14.5	2	6	25	28
Pb	8.5	11.0	9.8	9.0	92	90	920	980
Zn	109.0	99.0	147.0	144.0	705	700	5600	5200

[a] Samples A and B are standard sludges from CCIW; A comes from Newmarket, B comes from North Toronto.
[b] Not detected.

TABLE VIII

LEAD ANALYSIS IN CAPILLARY BLOOD SAMPLES BY NON-FLAME A.A.S. AND ANODIC STRIPPING VOLTAMETRY (A.S.V.)

Sample no.	*Non-flame a.a.s.*	*A.s.v.*[a]
1	49	52
2	54	54
3	61	61
4	40	41
5	41	44
6	30	26

[a] From Dr. T. M. Roberts, unpublished data.

Conclusions

For the base metals studied in heavy inorganic matrices, non-flame atomic absorption spectrometry appears to offer little advantage over flame techniques. In organic matrices, the technique may have some advantage.

Work presently underway in this laboratory suggests that for some elements which are normally hard to do by flame a.a.s., *e.g.* Sn, As, Sb, *etc.*, the non-flame technique in a controlled atmosphere may be very useful. Results on these studies will appear soon.

The authors would like to express their appreciation to the National Research Council of Canada for a grant in support of this research, and to J. Lichwa, J. Kinrade, D. Dupak and T. M. Roberts for help with sampling and experimentation.

SUMMARY

Because of the extravagant claims made for the usefulness of non-flame

atomic absorption spectroscopy, a critical evaluation of its performance in heavy matrix solutions, for selected trace heavy metals, was made. Studies of physical and chemical interference problems are presented for a range of inorganic and organic matrices. Often quoted remedies (*e.g.* selective volatilization, standard addition *etc.*) for solution of the more serious problems were found to be of little help in most cases. The influence of variables such as nature and flow rate of purge gas, ashing temperature and atomization temperature are also evaluated. Analyses for Cd, Cu, Pb, Zn, Ni, Co were done on samples by flame and non-flame methods in high solids solutions. While there appears to be an advantage to the non-flame method in dealing with sample solutions of high organic content, no advantage is apparent for either technique with highly inorganic matrices.

REFERENCES

1 B. V. L'Vov, *Spectrochim. Acta*, 17 (1961) 761.
2 W. M. Barnard and M. J. Fishman, *At. Absorption Newslett.*, 12 (1973) 118.
3 D. A. Segar and J. G. Gonzalez, *Anal. Chim. Acta*, 58 (1972) 7.
4 N. P. Kubasik, M. T. Volosin and M. H. Murray, *Clin. Chem.*, 18 (1972) 410.
5 M. P. Amos, P. A. Bennett, K. G. Brodie and P. W. Lung, *Anal. Chem.*, 43 (1971) 211.
6 J. D. Kerber, *At. Absorption Newslett.*, 10 (1971) 104.
7 C. Th. J. Alkemade, *Appl. Opt.*, 7 (1968) 1261.
8 P. Hansen, *The Flameless AAS as a New Technique for Microanalytical Trace Determination*, Perkin Elmer Corp., Bodenseewerk, Uberlingen, (1971).
9 G. E. Peterson, private communication.
10 *Standard Conditions for the Heated Graphite Atomizer HGA 70*, Perkin Elmer Corp. Bodenseewerk, 1971.
11 D. Alger, R. G. Anderson, I. S. Maines and T. S. West, *Anal. Chim. Acta*, 87 (1971) 280.
12 D. C. Manning and G. Fernandez, *At. Absorption Newslett.*, 10 (1971) 65.
13 L. Ebdon, G. F. Kirkbright and T. S. West, *Anal. Chim. Acta*, 61 (1972) 15.
14 S. Dipierro and G. Tessari, *Talanta*, 18 (1971) 707.
15 T. S. West and K. Williams, *Anal. Chim. Acta*, 45 (1969) 27.

Analytica Chimica Acta, 72 (1974) 245–250

ATOMIC-ABSORPTION SPECTROMETRIC DETERMINATION OF CADMIUM, LEAD AND ZINC IN SALTS OR SALT SOLUTIONS BY HANGING MERCURY DROP ELECTRODEPOSITION AND ATOMIZATION IN A GRAPHITE FURNACE

F. O. JENSEN, JAN DOLEZAL* and F. J. LANGMYHR
Department of Chemistry, University of Oslo, Oslo 3 (Norway)
(Received 25th February 1974)

The determination of trace metals in salts or salt solutions is frequently complicated by serious interferences of the matrix. The trace metals have normally to be isolated, *e.g.* by extraction, ion exchange, *etc.*, before the determinations can be performed.

The present paper describes a method in which metals are deposited from a salt solution on to a hanging mercury drop, the mercury is transferred to a graphite furnace and removed by evaporation, and the metals are finally determined by atomic absorption spectrometry.

While this principle of separation is well known, and has been utilized by various authors[1–4] in connection with atomic absorption spectrometric analysis of salt matrixes, the proposed method of determination has—to the authors' best knowledge—only been employed by Fairless and Bard[5]. These authors used a "West" type of furnace to atomize copper which had been separated from sea water by deposition on a hanging mercury drop.

EXPERIMENTAL

Apparatus

The separations were made in the cell and with the electrodes shown in Fig. 1. The double-walled cylindrical glass cell (capacity about 100 ml) was equipped with a plastic cover and a bottom tap. Before and during electrolysis, water of temperature 25.0 ± 0.1°C was circulated through the jacket. The cover had three holes; one for a tube by which nitrogen was introduced, one for a stirrer, and one for the electrodes.

A micrometer hanging mercury drop electrode (Metrohm E-410) served as the cathode. A salt bridge connected the solution with a standard saturated calomel electrode; the end of the tube forming the bridge was separated from the solution by a plug of filter paper. The mercury capillary and the end of the bridge were held closely together by polytetrafluoroethylene fasteners.

Circulation in the cell was obtained with a variable speed stirrer (Multiflex Constant).

* On leave from Department of Analytical Chemistry, Charles University, Prague, Czechoslovakia.

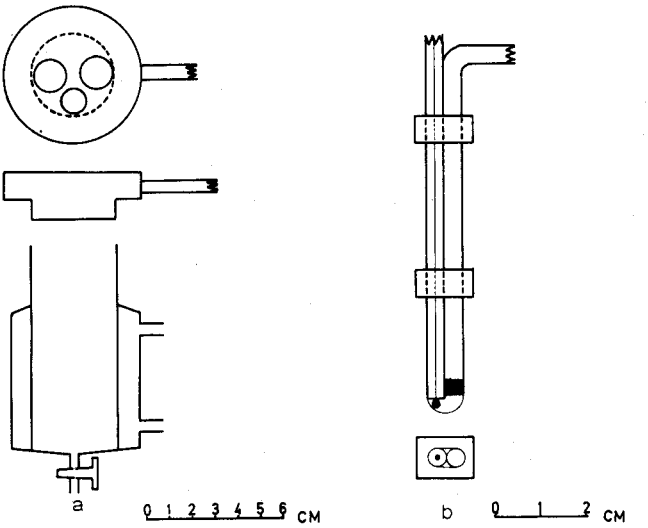

Fig. 1(a). The electrolytic cell with cover; (b) detail showing the connection of the mercury capillary with the end of the salt bridge.

It is important that the relative positions of the electrodes, the stirrer and the nitrogen tube are not changed, and that the rate of stirring is constant.

A washing cell of the same construction as the electrolysis cell (but without the heating jacket) was also made.

The electrolytic current was drawn from an Elliott Tinsley polarograph Mark 200.

The atomic absorption measurements were made with a Perkin-Elmer 303 spectrophotometer equipped with a deuterium arc source background corrector. The signals from the photometric detector were registered with a 2-channel recorder; one of the channels plotted the peak (in percent absorption) and the other recorded the integrated peak area, after transformation of the percent absorption signals into absorbance by means of a logarithmic amplifier, and integration with a home-made electronic integrator.

The construction of the graphite furnace has been described elsewhere[6].

Before evaporation and atomization, the mercury drops were transferred to small home-made graphite boats, the dimensions of which are given in Fig. 2. The graphite was of the quality used for making the furnace.

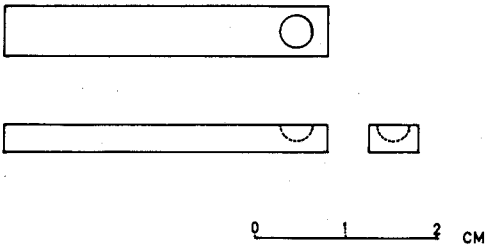

Fig. 2. The construction of the graphite boat.

The wash solution was stored in a 3-l bottle with a bottom outlet.

The electrolytic cell, the stirrer, the inlet tubes and the electrodes were siliconized with $(CH_3)_2SiCl_2$ (Fluka, puriss.).

Reagents and solutions

Standard solutions were prepared from reagent-grade (E. Merck) $3\,CdSO_4 \cdot 8\,H_2O$, lead nitrate and zinc sulphate heptahydrate. The potassium chloride was of "Suprapur" quality (E. Merck). The gases employed were nitrogen (purity 99.99% by volume) and argon (purity 99.9% by volume).

Water was purified by double distillation in a quartz still.

Solutions (10^{-2} *M*) of cadmium, lead and zinc were prepared from the salts listed above; other concentrations were prepared by dilution just before use.

A 10^{-5} *M* potassium chloride solution was prepared for washing purposes.

Samples

The method was tested by analyzing sea water and samples prepared from reagent-grade potassium chloride (Riedel-de Haën). The sample of sea water was collected and stored in a 5-l plastic bottle which had been cleaned with nitric acid and distilled water.

Procedure

Transfer 50 ml of the solution to be analyzed, and—when required—a volume of metal standard solution, to the electrolytic cell. Place the cover with the electrodes, the stirrer and the nitrogen tube in the cell, stir, and remove the oxygen from the solution by passing nitrogen for 12 min. During electrolysis, introduce nitrogen above the solution.

Form the mercury drop by turning the micrometer screw two divisions, which gives a drop having a surface of 1.80 mm^2. Electrolyze the solutions at the following potentials for the following times: cadmium, 1.0 V for 11 min; lead, 1.0 V for 11 min; and zinc, 1.3 V for 4 min. In all cases, stop the stirring 1 min before the electrolysis is finished.

At the proper time, lower the cell without interrupting the current (the small volume of sample solution hanging on the combined tips of the electrodes maintains the current), and replace the electrolysis cell by a washing cell which contains 50 ml of wash solution. Open the bottom tap and add 150 ml of wash solution at the same rate at which the cell is emptied. After the washing, and still without interrupting the current, remove the cell, and transfer the mercury to a preheated and cooled graphite boat by turning the micrometer until the mass of the drop makes it fall. Store the graphite boats in a covered Petri dish. The boats should not be touched by hand, but be handled with forceps. Precautions should be taken to avoid scraping the interior surface of the furnace and the boats, as this may release impurities, particularly zinc, from the graphite.

The various settings of the spectrophotometer were adjusted as specified in the instrument manual. The hollow-cathode lamps and the deuterium background corrector were heated for at least 1 h before the start of the measurements. The wavelengths employed were: for cadmium, 228.8 nm; for lead, 217.0 nm; and for zinc, 213.8 nm. After a preheated graphite boat with the mercury drop

had been transferred to the furnace, the mercury was removed by a 3-min evaporation at 440°C (earlier experiments demonstrated that the metals to be determined were not lost at this temperature), and the metals were then atomized by a 30-s heating at maximum voltage (260 V which gives about 1700°C after 30 s).

Blanks were run for the empty boat, and for the mercury; in the mercury, only traces of zinc were detected.

RESULTS AND DISCUSSION

To demonstrate the feasibility of the technique, analyses of sea water and of potassium chloride were carried out.

Analysis of sea water

Preliminary studies demonstrated a strong adsorption of metals from sea water onto the glass of the electrolytic cell; after standing for 1 h in the cell, the metal concentrations were reduced by up to 50%. This effect was pronounced for sea water; in 0.5 *M* potassium chloride the effect was negligible. In order to avoid this strong adsorption, the electrolytic cell, the stirrer, the nitrogen tube, and the electrodes were coated with silicone. This treatment reduced the adsorption but did not completely remove it. The problem of adsorption was solved by filling the cell with 50 ml of the solution to be analyzed, leaving it in the cell for at least 30 min, discarding it, and then doing the analysis on a new portion.

The determinations were made by the standard addition technique, 0.1–0.7 ml of 10^{-4} *M* metal solution being added to the sample solution in the cell; the resulting integrated peak areas were plotted as a function of the amounts of metal added. All measurements were made in duplicate, and the best fit of the standard addition curve was calculated by the method of least squares.

For comparison the same analyses were also performed by stripping voltammetry.

The results from the analysis of sea water are listed in Table I.

TABLE I

STRIPPING VOLTAMMETRIC AND ATOMIC ABSORPTION SPECTROMETRIC DETERMINATION OF CADMIUM, LEAD AND ZINC IN SEA WATER

Element	*Concentration ($\mu g\ l^{-1}$)*	
	Stripping volt	*A.a.s.*
Cadmium	11	14
Lead	42	39
Zinc	19	16

Analysis of reagent-grade potassium chloride

Cadmium, lead and zinc were also determined in commercial reagent-grade potassium chloride by the procedure given above. For the determination of cadmium and zinc, potassium chloride solutions containing 50 g l^{-1} were prepared; lead was determined in solutions having the concentration 100 g l^{-1}. The potentials and

the times of electrolysis were the same as those employed in the analyses of sea water.

The analytical results are listed in Table II. The precision of the present technique was established by a series of separate experiments; for each of the three elements the relative standard deviation was found to be in the range 10–15%.

TABLE II

ATOMIC ABSORPTION SPECTROMETRIC DETERMINATION OF CADMIUM, LEAD AND ZINC IN REAGENT-GRADE POTASSIUM CHLORIDE

Element	*Concentration* ($\cdot 10^{-5}$%)
Cadmium	1.6
Lead	2.5
Zinc	9.5

Conclusion

The main advantage of the proposed technique is that it makes it possible to determine trace metals in salt matrixes by atomic absorption spectrometry. The methods can be expected to be applicable also to the other alkaline chlorides, and to magnesium or the alkaline earth chlorides. The method can also be used for direct determination of impurities in mercury.

Compared to stripping voltammetry, the method opens the possibility of determining those metals, for which the stripping voltammetric peaks cannot be resolved. With the graphite furnace used, it would be possible to determine Cu, Mn, Ga, In and Tl as well as the metals tested here.

A disadvantage is that only a fraction of the metals present in solution is separated and atomized; this reduces the sensitivity of the method. This disadvantage could perhaps be removed, if all the metal were deposited on the mercury drop, *e.g.* according to the principle described by Huderová and Stulík[7], although modifications would be necessary to this procedure.

SUMMARY

Atomic absorption spectrometric methods are described for the determination of trace amounts of cadmium, lead and zinc in salts or salt solutions. The metals are separated from the salt matrix by electrolysis on a hanging mercury drop electrode, the mercury is transferred to a graphite boat and removed by evaporation, and the metals are determined by atomization. The feasibility of the technique was tested by analysis of sea water and of reagent-grade potassium chloride. For comparison the three metals were also determined in the sea water by stripping voltammetry, good agreement being found.

REFERENCES

1 H. Brandenberger and H. Bader, *Helv. Chim. Acta*, 50 (1967) 1409.
2 H. Brandenberger, *Chimia*, 22 (1968) 449.

3 T. F. Hartley and D. H. Ellis, *Proc. Soc. Anal. Chem.*, 9 (1972) 281.
4 C. Fairless and A. J. Bard, *Anal. Lett.*, 5 (1972) 433.
5 C. Fairless and A. J. Bard, *Anal. Chem.*, 45 (1973) 2289.
6 F. J. Langmyhr and Y. Thomassen, *Z. Anal. Chem.*, 264 (1973) 122.
7 L. Huderová and K. Štulík, *Talanta*, 19 (1972) 1285.

Analytica Chimica Acta, 72 (1974) 251–259

DOSAGE DU PLATINE PAR SPECTROMÉTRIE D'ABSORPTION ATOMIQUE

PARTIE I. MISE AU POINT D'UNE MÉTHODE D'ANALYSE DANS LES COMPLEXES ORGANOMÉTALLIQUES ET DE COORDINATION

J. P. MACQUET, J. HUBERT et T. THEOPHANIDES*

Département de Chimie, C.P. 6210, Université de Montréal H3C 3V1, P.Q. (Canada)

(Reçu le 21 janvier 1974)

Le but de cette étude est le dosage du platine en solution aqueuse dans divers complexes organométalliques simples et dans des polymères de type DNA-Pt[24], sans destruction préalable. On décrit la mise au point d'une méthode simple, ne nécessitant qu'un appareillage de routine. Les résultats obtenus pour une série de complexes du platine(II) et (IV), avec divers ligands, seront donnés dans un second article[25].

Le dosage du platine par absorption atomique et le problème des interférences ont déjà fait l'objet de multiples travaux[1–23]. Strasheim et Wessels[3] proposent sulfate et nitrate de cuivre comme tampon spectrochimique afin de pallier à l'effet dépressif des interférences; Schnepfe et Grimaldi[10] et Sen Gupta[11] utilisent les sulfates de cadmium et de cuivre; Van Loon[13] le lanthane; Jansen et Umland[14] le cuivre(II) et le sodium(I); Pitts *et al.*[15] le lanthane; Mallett *et al.*[19] le lanthane, l'uranium et le vanadium; Adriaenssens et Verbeek[20] le cyanure de potassium. L'emploi d'une flamme oxyde nitreux–acétylène[15] s'est avéré très efficace pour éviter des interférences; mais la sensibilité est alors inférieure à celle obtenue avec une flamme air–acétylène.

PARTIE EXPÉRIMENTALE

Appareillage

Cette étude est effectuée à l'aide d'un appareil Perkin–Elmer 403 avec brûleur (à prémélange et fente axiale de 10 cm), et bloc de contrôle des gaz (pression et débit), d'une lampe platine à cathode creuse Perkin–Elmer, et d'un enregistreur Perkin–Elmer 165 pour détermination des limites de détection et des sensibilités avec expansion d'échelle.

Réactifs

Sels de platine, $(NH_4)_2[PtCl_4]$, $K_2[PtCl_4]$, $K_2[PtCl_6]$, qualité "Specpure" (Johnson Matthey); trioxyde de lanthane, qualité "Reagent" (Matheson, Coleman & Bell); phosphates, qualité "Reagent" (J. T. Baker, BDH, Fisher, Merck); les phosphates de potassium déliquescents[26a] ont été séchés au préalable à 120°C, pendant 24 h.

Mise au point expérimentale

Les mesures ont été effectuées dans des conditions classiques[27]. Toutes les absorbances indiquées sont nettes (déduction de l'absorbance du tampon); elles représentent la moyenne de trois lectures (300 mesures), obtenues sans expansion d'échelle. Les concentrations en platine sont déterminées à l'aide d'une courbe d'étalonnage. Dans le cas du lanthane on n'observe aucun problème d'encrassement du brûleur et de stabilité de la flamme; les phosphates, après utilisation prolongée (2–3 h), rendent la flamme vacillante en raison d'un dépôt de particules solides sur le brûleur. Les conditions optimales d'utilisation sont résumées dans le Tableau I. Les meilleures sensibilités (voir Tableau II) ont été obtenues dans les conditions standard, sans expansion d'échelle (1,2 p.p.m. pour le lanthane et 1,3 p.p.m. pour les phosphates), ce qui améliore par un facteur de 2 les valeurs données par Perkin Elmer[27]. Avec une expansion d'échelle de 10, on arrive à 0,16 p.p.m. en présence de lanthane, et 0,17 p.p.m. en présence de phosphates, ce qui est, à notre con-

TABLEAU I

CONDITIONS EXPÉRIMENTALES DE LA MÉTHODE DE DOSAGE

Variables		*Lanthane ($LaCl_3$)*	*Phosphate (K_3PO_4)*
Position du brûleur[a]	Avant–arrière	Fente du brûleur coincidant avec le faisceau	
	Hauteur	5–7 mm	3,5–4,5 mm
Débit des gaz	Air[b]	15,6–20,0 l min^{-1}	18,3–21,2 l min^{-1}
	Acétylène[c]	3,2–3,8 l min^{-1}	3,1–3,3 l min^{-1}
Longueur d'onde		265,9 nm	
Fente		ouverture de fente = 1,0 mm largeur de la bande spectrale 0,7 nm	
Ampérage de la lampe		30 mA	

[a] Par rapport au centre du faisceau.
[b] Pression = 30 psig, acétylène: pression = 8 psig, débit = 3,2 l min^{-1}.
[c] Pression = 8 psig, air: pression = 30 psig, débit = 19,2 l min^{-1}.

TABLEAU II

INFLUENCE DES LONGUEURS D'ONDE CARACTÉRISTIQUES DU PLATINE SUP L'ABSORBANCE[a] ET COMPARAISON DES DIVERSES SENSIBILITÉS

λ (nm)	*Absorbance*		*Sensibilités (en p.p.m.)*[b]		
	Lanthane	*Phosphate*	*Lanthane*	*Phosphate*	*Perkin–Elmer*[27]
262,8	0,092	0,088	2,6	2,7	5,3
265,9	0,220	0,200	1,2	1,3	2,2
283,0	0,052	0,054	4,4	4,2	7,4
306,5	0,120	0,111	2,0	2,2	4,6

[a] $(NH_4)_2[PtCl_4]$: 50 p.p.m. Pt, $LaCl_3$: 20000 p.p.m. La^{3+} dans l'acide chlorhydrique 0,5 *M*. K_3PO_4: 30000 p.p.m. PO_4^{3-} dans l'eau.
[b] P.p.m. correspondant à 1% d'absorption.

naissance, la sensibilité la meilleure pour un dosage du platine par absorption atomique, avec flamme air–acétylène. Les limites de détection sont identiques à celles donnés par Perkin–Elmer, c'est-à-dire 0,05 p.p.m. Le domaine d'utilisation de la méthode s'étend de 1 à 100 p.p.m.

RÉSULTATS ET DISCUSSION

Le problème des interférences dans le dosage du platine a déjà été entrevu[3,10,11,13–15,17,19,20]. Lockyer et Hames[2] n'ont pas trouvé d'interférences dans une flamme air–gaz de ville.

Le lanthane est souvent utilisé comme tampon en spectrométrie d'absorption atomique, afin d'éviter des interférences, en particulier lors du dosage du platine[11,13,15,19]. Nous avons examiné l'influence de certains ions tels que K^+, NH_4^+ et Cl^- (voir Fig. 1). NH_4^+ a le moins d'influence; on recommande par conséquent l'utilisation du sel de platine correspondant[27]. Nos résultats concordent avec ceux de Pitts *et al.*[15].

À notre connaissance, aucune étude n'a été effectuée sur l'influence de divers paramètres tels que concentration et acidité, pouvant modifier le rôle des tampons spectrochimiques. En effet, dans le cas d'une solution de 50 p.p.m. de platine par exemple, si x p.p.m. d'un tampon A annulent l'effet des ions perturbateurs, il n'est pas certain que la même quantité de A jouera le même rôle pour une solution de 100 ou de 200 p.p.m. de platine (voir Fig. 2). Pour que la méthode

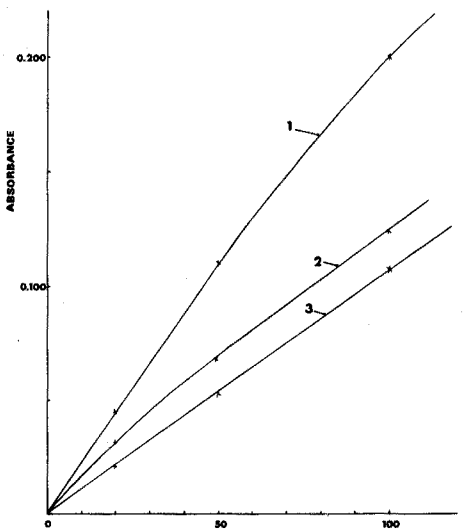

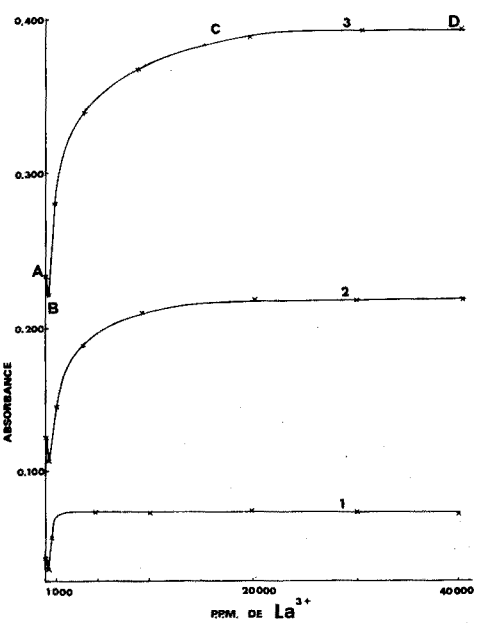

Fig. 1. Sels de platine dans H_2O. (1) $(NH_4)_2[PtCl_4]$, (2) $K_2[PtCl_4]$, (3) $K_2[PtCl_6]$.

Fig. 2. Influence du lanthane ($LaCl_3$, HCl 0,5 *M*) sur l'absorbance d'une solution de $(NH_4)_2[PtCl_4]$ contenant: (1) 20 p.p.m., (2) 50 p.p.m., (3) 100 p.p.m. de Pt.

soit valable dans le domaine d'utilisation proposé, il faut que l'effet du tampon soit le même, quelle que soit la concentration du métal.

Une première étude permet de choisir les tampons convenant le mieux pour le tétrachloroplatinate d'ammonium $(NH_4)_2[PtCl_4]$ (voir Tableau III). Ils doivent être effectifs dans n'importe quel milieu et ils ne doivent pas faire précipiter les complexes DNA-Pt. Le chlorure de lanthane donnant la meilleure absorbance, nous en avons déterminé la concentration optimum pour une absorbance constante: 500 à 100 p.p.m. de lanthane pour 20 p.p.m. de platine; 10000 à 20000 p.p.m. pour 50 p.p.m. de platine et 20000 pour 100 p.p.m. de platine (Fig. 2). L'atomisation est influencée par les réactions qui ont lieu en phase aqueuse (formation de composés stables, changement des propriétés physiques de la solution) et par celles qui s'effectuent en phase gazeuse (formation d'oxydes, etc.). L'atomisation d'un élément va dépendre des équilibres qui vont coexister en solution et dans la flamme. L'addition d'éléments étrangers (interférences, tampons) en déplaçant ces équilibres, déterminera l'absorbance de l'élément à doser.

TABLEAU III

INFLUENCE DE LA NATURE DU TAMPON SPECTROCHIMIQUE SUR L'ABSORBANCE DU PLATINE

Concentration en platine $((NH_4)_2[PtCl_4])$ *(p.p.m.)*	$NaCl^a$	$NaNO_3$	Na_2SO_4	$Na_2S_2O_3$	$Na_3PO_4{}^b$
50	0,124	0,173	0,172	0,172	0,190
100	0,187	0,290	0,319	0,285	0,302
	$CuCl_2{}^a$	$Cu(NO_3)_2$	$CuSO_4$	$LaCl_3{}^c$	$K_3PO_4{}^b$
50	0,106	0,165	0,173	0,220	0,200
100	0,176	0,300	0,323	0,390	0,341

[a] 30000 p.p.m. Na^+, 30000 p.p.m. Cu^{2+} dans l'acide chlorhydrique 0,1 *M*.
[b] 30000 p.p.m. PO_4^{3-} dans l'eau.
[c] 20000 p.p.m. La^{3+} dans l'acide chlorhydrique 0,5 *M*.

Le platine peut réagir avec l'oxygène aux températures élevées[29–30], et donner des oxydes, Pt_xO_2, à 1200°C[28]. Alcock et Hooper[29] établirent par la suite que $x=1$ et que la réaction avec l'oxygène était la suivante:

$$Pt(s)+O_2(g) \rightleftharpoons PtO_2(g) \qquad (1)$$

Kubaschewski[30] a montré que la quantité de $PtO_2(g)$ augmente rapidement avec la température de 900°C à 1700°C. Si l'on admet que l'équilibre (1) existe dans la flamme et que $PtO_2(g)$ est l'espèce qui masque l'absorbance du platine, on peut expliquer la forte diminution de sensibilité observée par Pitts *et al.*[15] dans une flamme oxyde nitreux–acétylène. En effet, la différence de température entre cette flamme (*ca.* 2700°C)[31] et la flamme air–acétylène est de l'ordre de 400°C.

Afin de mieux comprendre l'influence complexe des ions gênants sur le degré

d'atomisation du platine, examinons le cas très simple du mélange $(NH_4)_2[PtCl_4]$+ KCl (50 p.p.m. Pt). La courbe d'absorbance en fonction de l'addition de chlorure de potassium se divise en deux parties: la première, A–B, indique une forte décroissance de l'absorbance (45%) et la seconde, B–C, est un plateau (absorbance pratiquement constante dans le domaine étudié: $K^+/Pt^{2+} = 2 \rightarrow 8$). La cassure de la courbe en B cErrespond à un rapport molaire $K^+/Pt^{2+} \approx 2$. L'atomisation d'une même quantité de platine à partir d'une solution de $K_2[PtCl_4)$ donne la même valeur d'absorbance qu'en B. Ce résultat confirme celui obtenu par Pitts *et al.*[15]. La décroissance A→B correspondrait donc au déplacement des ions ammonium par le potassium. En B, le platine serait sous forme $K_2[PtCl_4]$ et le plateau B→C correspondrait à l'atomisation de $K_2[PtCl_4]$ et de KCl en excès. Dans ce cas, les ions étrangers (surtout K^+) agiraient comme des interférences chimiques en phase condensée.

La Fig. 2 représente la variation de l'absorbance en fonction du rapport La^{3+}/Pt^{2+}. Par analogie avec la courbe précédente (Absorbance *vs.* K^+/Pt^{2+}), la partie A→B de ces courbes peut s'interpréter par la formation de composés thermiquement stables entre le lanthane et le sel de platine. Le minimum de la courbe ci-dessus, correspondant à une décroissance de l'absorbance de 10%, est moins bien défini que dans le cas du potassium. L'imprécision de ce minimum ne permet pas de donner une stoechiométrie bien définie au(x) composé(s) qui se forme(nt)[15]. La partie B→C de la Fig. 2 indique une augmentation d'absorbance de 83% correspondant à une formation de Pt(g) plus importante. Si l'on suppose que $PtO_2(g)$ est l'espèce qui masque l'absorbance du platine, la croissance B→C pourrait s'expliquer par la réaction du lanthane La(g) en excès avec l'oxygène pour prévenir la formation de $PtO_2(g)$, et/ou par la réduction de l'oxyde $PtO_2(g)$ par La(g)[15]. La grande stabilité de La_2O_3[32] et la comparaison de sa chaleur de formation (-145 kcal mole^{-1} par atome d'oxygène)[26b,33] avec celle de PtO_2 (-20 kcal mole^{-1} par atome d'oxygène)[30] favorisent la formation de Pt(g). La partie C→D de la Fig. 2 correspondrait à un nouvel état d'équilibre entre les diverses espèces. Le lanthane peut donc agir comme interférence (partie AB), puis comme tampon spectrochimique idéal (partie CD).

La courbe 1 de la Fig. 3 nous montre l'influence de l'acidité (HCl) sur une solution de platine contenant 20000 p.p.m. de La^{3+}; les variations d'abosrbance sont minimes et non significatives. L'effet tampon du lanthane reste donc le même quelle que soit l'acidité. L'augmentation d'absorbance en présence de 20000 p.p.m. de La^{3+} est de 83%, ce qui double presque la sensibilité (voir Tableau II).

Le dosage du platine dans les complexes DNA-Pt indique de fortes interférences[24], provenant sans doute des phosphates contenus dans le DNA. Comme nous le verrons plus loin (Fig. 5), leur influence est très importante: diminution de 60% de l'absorbance en présence de orthophosphate tripotassique. Willis[34] et Smith et Winefordner[35] ont trouvé le même effet lors du dosage du calcium en présence de phosphates; de même Yofe *et al.*[36] dans le dosage du strontium et du baryum par émission. Malheureusement, l'utilisation du lanthane n'est pas possible, il se forme un précipité, empêchant le dosage. Le lanthane en effet réagit avec les polynucléotides[37]. Par contre le sulfate de sodium ou l'orthophosphate de potassium conviendrait mieux comme tampon spectrochimique. Nous avons choisi le phosphate, donnant une absorbance maximale. Beaucoup

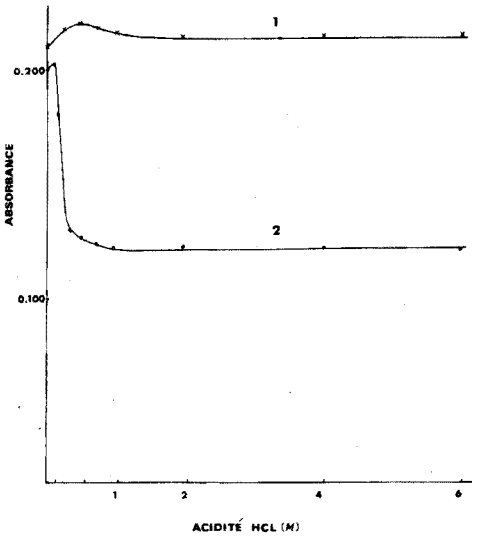

Fig. 3. Influence de l'acidité (HCl) sur l'absorbance d'une solution de $(NH_4)_2[PtCl_4]$ (50 p.p.m. de Pt) contenant (1) $LaCl_3$ (20000 p.p.m. La^{3+}), (2) K_3PO_4 (30000 p.p.m. PO_4^{3-}).

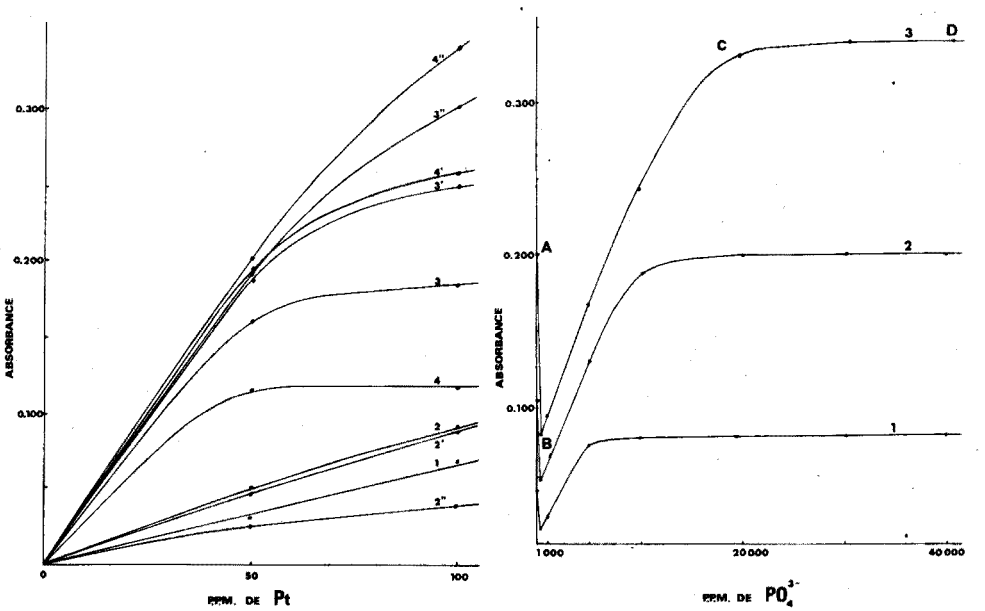

Fig. 4. Influence des différents phosphates (30000 p.p.m. PO_4^{3-} dans l'eau) sur l'absorbance d'une solution de $(NH_4)_2[PtCl_4]$ (50 p.p.m. de Pt) contenant: (1) H_3PO_4; (2) (2'), (2'') $(NH_4)H_2PO_4$, $(NH_4)_2HPO_4$, $(NH_4)_3PO_4$; (3), (3'), (3'') NaH_2PO_4, Na_2HPO_4, Na_3PO_4; (4), (4'), (4'') KH_2PO_4, K_2HPO_4, K_3PO_4.

Fig. 5. Influence des phosphates ($K_3PO_4 \cdot H_2O$) sur l'absorbance d'une solution de $(NH_4)_2[PtCl_4]$ contenant: (1) 20 p.p.m., (2) 50 p.p.m., (3) 100 p.p.m. de Pt.

de sels métalliques[38–41] sont exclus puisqu'ils se complexent avec le DNA en formant un précipité.

Les orthophosphates monoacide, diacide et neutre des sels d'NH_4^+, de Na^+, de K^+ ont été examinés. La Fig. 4 résume les résultats obtenus et permet de choisir l'orthophosphate tripotassique. On constate que les sels de Na^+ et de K^+ se comportent de la même façon. Cependant, les sels de sodium perturbent la stabilité de la flamme.

La Figure 5 donne la quantité de phosphates nécessaire à une atomisation maximale du platine: 5000 p.p.m. de phosphate pour 20 p.p.m. Pt, 10000 p.p.m. pour 50 p.p.m. Pt et 20 à 30000 p.p.m. pour 100 p.p.m. Pt. L'évolution générale de ces courbes correspond à celle obtenue pour le lanthane. Cependant la décroissance de l'absorbance dans la partie A→B (60%) est nettement plus significative dans le cas des phosphates et le minimum (B) est mieux défini; la valeur d'absorbance correspondante est sensiblement la même que celle d'une solution de $K_2[PtCl_4]$. La partie BCD de la courbe 3 (Fig. 5) étant analogue à celle de la courbe 3 (Fig. 2), on peut envisager un mécanisme similaire. L'excès de phosphate serait réduit par le potassium et la forme réduite du phosphore agirait de la même manière que le lanthane, pour donner des oxydes de phosphore. Il semble que la présence simultanée du potassium et des phosphates soit requise pour obtenir un effet tampon efficace. En effet, le potassium sous forme de chlorure interfère[15] (Fig. 1). De même, les phosphates sous forme d'acide orthophosphorique produisent une diminution sensible de l'absorbance (Fig. 4, courbe 1). Le remplacement du proton par l'ion NH_4^+ a peu d'influence (Fig. 4, courbes 2 à 2″), alors que la présence d'un métal alcalin (Na^+, K^+) augmente fortement l'absorbance (Fig. 4, courbes 3 à 3″ et 4 à 4″). L'acidité du milieu joue un rôle prépondérant; on observe une nette augmentation de l'absorbance lors du passage $MH_2PO_4 \rightarrow M_3PO_4$ (M=Na, K) (Fig. 3, courbes 2 et 4). Pitts *et al.*[15] attribuent cette influence à la formation de polyphosphates peu volatils. En général, la présence simultanée d'un métal et d'un oxanion semble nécessaire, les oxacides[15] et les chlorures de métaux individuellement (Tableau III) ne présentant aucun effet tampon. On peut noter que l'absorbance (50 p.p.m. Pt) est plus faible en présence de phosphate (0,200) qu'en présence de lanthane (0,220); ceci serait dû à une différence de stabilité entre La_2O_3 et oxydes de phosphore[26]. On peut prévoir des tampons spectrochimiques autres que lanthane et phosphate à partir des valeurs de chaleur de formation. L'uranium et le vanadium, utilisés par Mallett *et al.*[19], constituent d'excellents tampons. Ils forment des oxydes dont la chaleur de formation est inférieure à celle de PtO_2. L'augmentation d'absorbance en présence de 30000 p.p.m. de PO_4^{3-} dans l'eau est de 82%; ce qui double la sensibilité (Tableau II).

Si l'on admet que sur les plateaux CD des Figs. 2 et 5, la plus grande partie du platine est sous forme gaz, on voit qu'en l'absence des tampons spectrochimiques ($LaCl_3$, K_3PO_4), on ne peut détecter que 55% de Pt(g).

Cette méthode est simple, rapide et précise; elle présente les caractéristiques suivantes: domaine d'utilisation de 1 à 100 p.p.m., sensibilité de 1,2 p.p.m. dans les conditions normales et 0,16 p.p.m. avec expansion d'échelle; limites de détection de 0,05 p.p.m., indépendance de l'acidité du milieu pour le lanthane et inhibition des interférences. Tous les composés de platine (sels, complexes) donnent des courbes identiques à la Fig. 6, en présence des tampons spectrochimiques, et

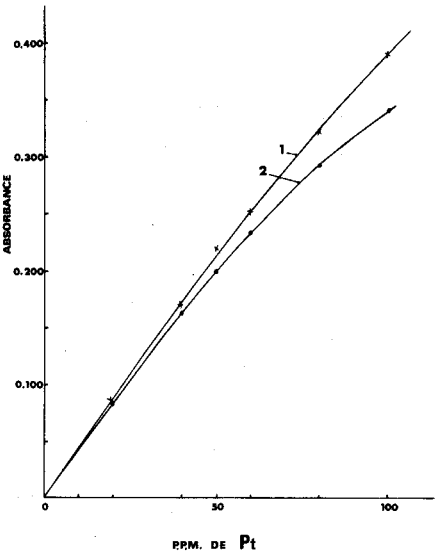

Fig. 6. Courbes standard: (1) $LaCl_3$ (20000 p.p.m. La^{3+}, HCl 0,5 *M*), (2) K_3PO_4 (30000 p.p.m. PO_4^{3-}, H_2O).

peuvent être utilisés comme étalons. L'utilisation de 20000 p.p.m. de lanthane(III) dans l'acide chlorhydrique 0,5 *M* ou de 30000 p.p.m. de phosphate dans l'eau va permettre le dosage du platine dans divers types de complexes.

Deux des auteurs (J. P. M. et J. H.), détenteurs d'une bourse post-grade du Conseil National de Recherches du Canada, tiennent à exprimer toute leur gratitude envers cet organisme. L'aide financière du Conseil National de Recherches du Canada a été grandement appréciée.

RÉSUMÉ

Une méthode simple et rapide, par absorption atomique, est proposée pour le dosage du platine, sous forme de complexe, en milieu aqueux sans destruction préalable. Les divers paramètres pouvant influencer l'absorbance sont étudiés. L'utilisation de divers tampons spectrochimiques est nécessaire, afin d'éviter des interférences perturbant l'absorbance. Parmi ceux-ci, citons le lanthane (20000 p.p.m. dans l'acide chlorhydrique 0,5 *M*) et les phosphates (30000 p.p.m. dans l'eau), jusqu'alors considérés comme ions perturbateurs. La méthode utilisée ne fait appel à aucune modification de l'appareillage standard, les lectures étant faites directement en absorbance, sans expansion d'échelle. Le domaine d'utilisation de la méthode s'étend de 1 à 100 p.p.m.

SUMMARY

A simple fast method for the determination of platinum in complexes in aqueous solution by atomic absorption spectrometry, without previous destruction

of complexes, is reported. Several parameters affecting absorbance measurements are discussed. The use of some spectrochemical buffers was necessary in order to prevent interference effects. Lanthanum (20,000 p.p.m. in 0.5 *M* hydrochloric acid) and phosphate (30,000 p.p.m. in water) were used as buffers. The method requires only standard equipment without scale expansion. The concentration range is 1–100 p.p.m. of platinum.

BIBLIOGRAPHIE

1 A. C. Menzies, *Anal. Chem.*, 32 (1960) 898.
2 R. Lockyer et G. E. Hames, *Analyst*, 84 (1959) 385.
3 A. Strasheim et G. J. Wessels, *Appl. Spectrosc.*, 17 (1963) 65.
4 V. L. Ginzburg, D. M. Livsic et G. I. Satarina, *Z. Anal. Chem.*, 214 (1965) 140.
5 I. Rubeska et J. Stupar, *Absorption Newslett.*, 5 (1966) 69.
6 C. E. Mulford, *At. Absorption Newslett.*, 5 (1966) 88.
7 H. C. Van Rensburg et P. B. Zeeman, *Anal. Chim. Acta*, 43 (1968) 173.
8 R. T. Swider, *At. Absorption Newslett.*, 7 (1968) 111.
9 P. B. Zeeman et J. A. Brink, *Analyst*, 93 (1968) 388.
10 M. M. Schnepfe et F. S. Grimaldi, *Talanta*, 16 (1969) 591.
11 J. G. Sen Gupta, *Anal. Chim. Acta*, 58 (1972) 23.
12 K. M. Aldous, R. M. Dagnall et T. S. West, *Analyst*, 94 (1969) 347.
13 J. C. Van Loon, *Z. Anal. Chem.*, 246 (1969) 122.
14 A. Janssen et F. Umland, *Z. Anal. Chem.*, 251 (1970) 101.
15 A. E. Pitts, J. C. Van Loon et F. E. Beamish, *Anal. Chim. Acta*, 50 (1970) 181, 195.
16 A. E. Pitts et F. E. Beamish, *Anal. Chim. Acta*, 52 (1970) 405.
17 A. Simonsen, *Anal. Chim. Acta*, 49 (1970) 368.
18 G. Pannetier et P. Toffoli, *Bull. Soc. Chim. France*, 7 (1972) 2977.
19 R. C. Mallett, D. C. G. Pearton, E. J. Ring et T. W. Steele, *J. S. Afr. Chem. Inst.*, 25 (1972) 219; *Talanta*, 19 (1972) 181.
20 E. Adriaenssens et F. Verbeek, *At. Absorption Newslett.*, 12 (1973) 57.
21 B. D. Guerin, *J.S. Afr. Chem. Inst.*, 25 (1972) 230.
22 J. G. Sen Gupta, *Anal. Chim. Acta*, 63 (1973) 19.
23 E. V. Elliott et K. R. Stever, *At. Absorption Newslett.*, 12 (1973) 60.
24 J. P. Macquet et T. Theophanides, en préparation.
25 J. P. Macquet et T. Theophanides, *Anal. Chim. Acta*, 72 (1974) 261.
26 *Handbook of Chemistry and Physics*, CRC, 50th edn., 1969–1970, (a) p. B-145, (b) p. D-45.
27 *Analytical Methods for Atomic Absorption Spectrophotometry*, Perkin–Elmer, Sept. 1968.
28 A. Schneider et U. Esch, *Z. Elektrochem.*, 49 (1943) 55.
29 C. B. Alcock et G. W. Hooper, *Proc. Roy. Soc. A*, 254 (1960) 551.
30 O. Kubaschewski, *Platinum Metals Rev.*, 15 (1971) 134.
31 J. B. Willis, *Appl. Optics*, 7 (1968) 1295.
32 M. Foex et J. P. Traverse, *Rev. Int. Hautes Temp. Réfract.*, 3 (1966) 429.
33 C. S. G. Phillips et R. J. P. Williams, *Inorganic Chemistry. I. Principles and Non-Metals*, Oxford University Press, 1965, p. 499.
34 J. B. Willis, *Anal. Chem.*, 33 (1961) 556.
35 R. Smith et J. D. Winefordner, *Spectrosc. Lett.*, 1 (1968) 157.
36 J. Yofe, R. Avni et M. Stiller, *Anal. Chim. Acta*, 28 (1963) 331.
37 G. L. Eichhorn et J. J. Butzow, *Biopolymers*, 3 (1965) 79.
38 S. Katz, *J. Amer. Chem. Soc.*, 74 (1952) 2238.
39 G. L. Eichhorn, *Nature*, 194 (1962) 474.
40 G. L. Eichhorn et P. Clark, *J. Amer. Chem. Soc.*, 85 (1963) 4020.
41 J. J. Butzow et G. L. Eichhorn, *Biopolymers*, 3 (1965) 95.

Analytica Chimica Acta, 72 (1974) 261–267

DOSAGE DU PLATINE PAR SPECTROMÉTRIE D'ABSORPTION ATOMIQUE

PARTIE II. RÉSULTATS ANALYTIQUES SUR LES COMPLEXES ORGANOMÉTALLIQUES D'INTÉRÊT BIOLOGIQUE: EFFET *CIS-TRANS*

J. P. MACQUET et T. THEOPHANIDES
Département de Chimie, C.P. 6210, Université de Montréal, Montréal H3C 3V1, P.Q. (Canada)
(Reçu le 21 janvier 1974)

A la suite de la mise au point d'une méthode de dosage des complexes de platine(II) et (IV), nous avons été amenés à effectuer une étude sur l'analyse du platine dans des sels simples ainsi que dans des complexes organométalliques, de coordination et d'intérêt biologique, afin de vérifier la validité de la méthode[1].

Tous les résultats présentés dans ce travail ont été obtenus par simple dosage (solutions à 50 p.p.m. de platine). Le pourcentage de platine dans les différents complexes varie de 14 à 65%. Deux types de composés de platine sont à considérer: tout d'abord, les composés solubles dans l'eau, analysés tels quels sans destruction préalable; ensuite, les insolubles, traités à l'eau régale, afin de transformer le platine(II) en H_2PtCl_6; l'acidité finale est ajustée à 0,5 *M*. L'utilisation de tampons spectrochimiques s'avère nécessaire pour masquer les interférences dans une flamme air–acétylène[1–9]. Cependant, les phosphates sont sans effet en milieu acide[1].

PARTIE EXPÉRIMENTALE

Les appareils, les produits chimiques et le processus expérimental sont les mêmes que ceux décrits précédemment[1]. Les complexes étudiés ont été préparés et identifiés dans ce laboratoire.

La calcination des phosphines et des arsines s'effectue dans un four, modèle Lindberg.

RÉSULTATS ET DISCUSSION

Afin de démontrer la nécessité des tampons spectrochimiques, nous avons entrepris une étude comparée dans l'eau, dans l'eau +30000 p.p.m. de phosphate, dans l'acide chlorhydrique 0,5 *M* et dans l'acide chlorhydrique 0,5 *M* +20000 p.p.m. de lanthane.

Sels de platine

Le Tableau I reflète deux tendances: tout d'abord, en utilisant comme étalon le sel d'ammonium $(NH_4)_2[PtCl_4]$, on se rend compte qu'il est impossible de doser $K_2[PtCl_4]$, sans tampon spectrochimique. En effet, l'ion potassium a un

TABLEAU I

L'ANALYSE DES SELS DE PLATINE

Platine introduit (50 p.p.m.)	*Platine trouvé (p.p.m.)*			
	Eau[a]	*Acide chlorhydrique*[b] *(0,5 M)*	*Phosphate*[c] *(30000 p.p.m. dans l'eau)*	*Lanthane*[d] *(20000 p.p.m. dans l'acide chlorhydrique 0,5 M)*
$K_2[PtCl_4]$	31,0	24,0	50,8	49,9
$K_2[PtCl_6]$	24,4	23,2	49,0	50,0
$[Pt(NH_3)_4][PtCl_4]$[e]	52,8	52,3	50,5	50,6

[a] Courbe standard[1]: $(NH_4)_2[PtCl_4]$ dans l'eau.
[b] Courbe standard: $(NH_4)_2[PtCl_4]$ dans l'acide chlorhydrique 0,5 *M*.
[c] Courbe standard[1]: $(NH_4)_2[PtCl_4]$ dans l'eau + 30000 p.p.m. PO_4^{3-} (K_3PO_4).
[d] Courbe standard[1]: $(NH_4)_2[PtCl_4]$ dans l'acide chlorhydrique 0,5 *M* + 20000 p.p.m. La^{3+} ($LaCl_3$).
[e] Dissous dans l'ammoniaque à chaud, puis repris à l'eau après évaporation de l'ammoniaque.

effet dépressif plus important que l'ion ammonium[1,5]. Les absorbances mesurées sont dans l'eau: 0,110, 0,068 et 0,53 et dans l'acide chlorhydrique 0,5 *M*: 0,135, 0,066 et 0,063 pour les trois sels $(NH_4)_2[PtCl_4]$, $K_2[PtCl_4]$ et $K_2[PtCl_6]$ (50 p.p.m. Pt). Par contre, dans le cas du sel de Magnus $[Pt(NH_3)_4][PtCl_4]$ dissous dans l'ammoniaque, le déplacement des chlorures conduit à $[Pt(NH_3)_4]Cl_2$, donnant une absorbance supérieure à celle de $(NH_4)_2[PtCl_4]$. Ceci montre que les ammines coordonnées au platine ont un effet exaltant. L'utilisation des tampons spectrochimiques ($LaCl_3$ et K_3PO_4) inhibe l'effet dépressif du potassium, ainsi que l'effet exaltant des NH_3; les valeurs obtenues sont en accord avec les valeurs attendues.

Complexes organométalliques

Le Tableau II montre que l'effet dépressif, causé par les interférences, dans l'eau et en milieu acide 0.5 *M*, est complètement supprimé par addition de tampon.

TABLEAU II

L'ANALYSE DES COMPLEXES ORGANOMÉTALLIQUES

Platine introduit (50 p.p.m.)	*Platine trouvé (p.p.m.)*			
	Eau	*Acide chlorhydrique (0,5 M)*	*Phosphate (30000 p.p.m. dans l'eau)*	*Lanthane (20000 p.p.m. dans l'acide chlorhydrique 0,5 M)*
$K[Pt(ac)Cl_3]$[a]	i[b]	31,0	i	50,1
$K[Pt(C_2H_4)Cl_3]$	36,2	40,4	49,8	50,6
$K[Pt(ac_1)Cl_3]$[c]	38,9	42,2	49,8	50,3
trans-$Pt(ac_1)$(lutidine)Cl_2	i	46.8	i	50,6

[a] ac = Tétraméthyl-2,2,5,5-hexyne-3.
[b] Insoluble.
[c] ac_1 = Diméthyl-2,5-hexyne-3-diol-2,5.

On peut noter que les absorbances obtenues en milieu acide chlorhydrique 0,5 *M* sont généralement supérieures à celles obtenues dans l'eau. Les deux complexes, $K[Pt(C_2H_4)Cl_3]$ et $K[Pt(ac_1)Cl_3]$, ont été analysés en milieu aqueux sans destruction préalable.

Complexes de coordination

Les résultats sont résumés dans le Tableau III. La majorité des complexes de coordination étudiés sont du type Pt-amine (ammoniac; pyridine (py), éthylènediamine(en), diéthylènetriamine(dien)). Dans le premier cas, l'absorbance d'une quantité constante de platine (50 p.p.m.) dans l'eau et en mileu légèrement acide (0,5 *M*) se trouve exaltée (allant jusqu'à doubler pour *trans*-$Pt(NH_3)_2Cl_2$). Dans le cas des ligands bidentates et tridentates, il y a dépression très marquée par rapport aux ammines monodentates. Cette différence est significative et peut être liée à l'effet de chélation.

TABLEAU III

L'ANALYSE DES COMPLEXES DE COORDINATION

Platine introduit (50 p.p.m.)	*Platine trouvé (p.p.m.)*			
	Eau	*Acide chlorhydrique (0,5 M)*	*Phosphate (30000 p.p.m. dans l'eau)*	*Lanthane (20000 p.p.m. dans l'acide chlorhydrique 0,5 M)*
cis-$Pt(NH_3)_2Cl_2$	56,2	62,0	50,6	50,3
trans-$Pt(NH_3)_2Cl_2$	87,3	103,9	50,0	49,6
$[Pt(NH_3)_4]Cl_2$	54,3	61,8	50,2	50,6
cis-$Pt(py)_2Cl_2$[a]	62,3	67,1	49,5	49,8
trans-$Pt(py)_2Cl_2$[a]	62,3	66,3	50,1	50,3
$[Pt(py)_4]Cl_2$	67,8	71,8	49,3	50,7
$Pt(en)Cl_2$	29,8	28,7	50,5	50,8
$Pt(en)Cl_4$	36,4	36,3	49,5	49,5
[Pt(dien)Cl]Cl	29,3	28,7	49,8	49,2
cis-$Pt(P\emptyset_3)_2Cl_2$[b]	—	43.5	—	48,4
cis-$Pt(As\emptyset_3)_2Cl_2$[c]	—	36,3	—	48,0

[a] Dissous dans l'ammoniaque à chaud, puis repris à l'eau après évaporation de l'ammoniaque.
[b] $P\emptyset_3$ = triphénylphosphine.
[c] $As\emptyset_3$ = triphénylarsine.

Effet cis et trans

Nous avons noté une particularité dans le cas des complexes *cis* et *trans* (tableau IV). En comparant les absorbances des composés *cis*- et *trans*-$Pt(NH_3)_2Cl_2$, on observe une absorbance supérieure pour le complexe trans par rapport au complexe *cis* de 55% dans l'eau et de 68% dans l'acide chlorhydrique 0,5 *M*). Dans la série des complexes platine–nucléoside, il est possible de distinguer l'isomère *cis* de l'isomère *trans* par simple mesure de l'absorbance. Dans le cas des complexes *cis*- et *trans*-$Pt(py)_2Cl_2$, on ne retrouve pas cet effet, car ils sont dissous dans l'ammoniaque à chaud, pour donner un mélange de *cis*- et de *trans*-

TABLEAU IV

EFFET *CIS* ET *TRANS* EN MILIEU AQUEUX

Complexes platine (50 p.p.m. Pt)	*Absorbance*	
	Eau	*Acide chlorhydrique (0,5 M)*
cis-$Pt(NH_3)_2Cl_2$	0,123	0,138
trans-$Pt(NH_3)_2Cl_2$	0,178	0,204
$Pt(en)Cl_2$	0,066	0,069
cis-$[Pt(NH_3)_2(guanosine)_2]$-$Cl_2 \cdot 2H_2O$	0,046	0,051
trans-$[Pt(NH_3)_2(guanosine)_2]Cl_2$	0,117	0,138
cis-$Pt(guanosine)_2Cl_2 \cdot 2HCl$	0,045	0,043
$[Pt(en)(guanosine)_2]Cl_2 \cdot 2H_2O$	0,053	0,060
cis-$[Pt(NH_3)_2X_2]Cl_2$	0,045	0,046
cis-$Pt(inosine)_2Cl_2$	0,046	0,045

TABLE V

EFFET *CIS* ET *TRANS* EN MILIEU ORGANIQUE

Complexes platine (100 p.p.m. Pt)	*Absorbance*	
	Chloroforme	*Acétone*
cis-$Pt(py)_2Cl_2$	0,510	—
trans-$Pt(py)_2Cl_2$	0,650	—
cis-$Pt(NH_2{-}CH_3)_2I_2$	—	0,348
trans-$Pt(NH_2{-}CH_3)_2I_2$	—	0,685

$[Pt(py)_2(NH_3)_2]Cl_2$ ou un mélange de $[Pt(py)_4]Cl_2$ et de $[Pt(NH_3)_4]Cl_2$ (Tableau III). Par contre, ces complexes étant solubles dans le chloroforme, on retrouve le même effet *cis–trans* (Tableau V).

Le phénomène observé dans les complexes *cis* et *trans* semble indépendant du solvant; il se retrouve même dans le cas où les atomes de chlore sont remplacés par de grosses molécules, telles l'adénosine, la guanosine, etc... (Tableau VI). En présence des tampons spectrochimiques (K_3PO_4 et $LaCl_3$) tous les effets dépressifs et exaltants dus aux divers ligands sont supprimés et les résultats obtenus sont très satisfaisants.

Dans le cas de *cis*-$Pt(triphénylphosphine)_2Cl_2$ le % de platine (24,67% Pt calculé) trouvé par absorption atomique est plus meilleur que le % trouvé par calcination (23,88% Pt par s.a.a. et 32 à 36% par calcination). Les arsines ont donné des résultats identiques par calcination et par absorption atomique. Il semble que dans le cas des phosphines, il se forme des phosphures très stables (p.f. $\approx$ 1500°C) qui faussent les résultats obtenus par calcination (900°C).

Complexes d'intérêt biologique (Tableau VI)

Les complexes platine–hématoporphyrine[10] comprenant la platino-hémato-

:LEAU VI

ULTATS ANALYTIQUES, PRÉCISION

posés[a]	% *Pt calculé*	% *Pt trouvé*			
		Eau	*Acide chlorhydrique 0,5 M*	*Phosphate (30000 p.p.m. dans l'eau)*	*Lanthane (20000 p.p.m. dans l'acide chlorhydrique 0,5 M)*
$^{2}PtCl_4]$	47,00	18,61	21,62	47,75 (+0,75)[b]	46,91 (−0,09)[b]
$^{2}PtCl_6]$	40,14	13,33	19,11	39,34 (−0,80)	40,14 (0,00)
$NH_3)_4][PtCl_4]$	65,03	68,67	68,02	65,68 (+0,65)	65,81 (+0,78)
$t(ac)Cl_3]$	40,76	—	25,27	—	40,84 (+0,08)
$t(C_2H_4)Cl_3]$	52,91	38,31	42,48	52,70 (−0,21)	53,54 (+0,63)
$t(ac_1)Cl_3]$	40,41	31,44	34,11	40,25 (−0.16)	40,65 (+0,24)
$-Pt(ac_1)(lut)Cl_2$	37,87	—	35,45	—	38,32 (+0,45)
$'t(NH_3)_2Cl_2$	65,03	73,09	80,64	65,81 (+0.78)	65,42 (+0,39)
$-Pt(NH_3)_2Cl_2$	65,03	113,54	135,13	65,03 (0,00)	64,51 (−0,52)
$NH_3)_4]Cl_2$	58,40	63,42	72,18	58,63 (+0,23)	59,10 (+0,70)
$'t(py)_2Cl_2$	46,01	57,33	61,75	45,55 (−0,46)	45,83 (−0,18)
$-Pt(py)_2Cl_2$	46,01	57,33	61,00	46,10 (+0,09)	46,29 (+0,28)
$py)_4]Cl_2$	33,52	45,45	48,13	33,05 (−0,47)	33,99 (+0,47)
$n)Cl_2$	59,84	35,66	34,35	60,44 (+0,60)	60,79 (+0,95)
$n)Cl_4$	49,13	35,77	35,67	48,64 (−0,49)	48,64 (−0,49)
lien)Cl]Cl	52,87	30,98	30,35	52,66 (−0,21)	52,02 (−0,85)
$'t(P\emptyset_3)_2Cl_2$	24,67	—	21,46	—	23,88 (−0,79)
$'t(As\emptyset_3)_2Cl_2$	22,20	—	16,18	—	21,31 (−0,89)
$H_4^{2+}PtCl_4^{2-}$	20,80	—	15,81	—	21,50 (+0,70)
$I_2 \cdot PtCl_2$	22,56	—	18,86	—	22,02 (−0,54)
Pt	24,64	—	21,48	—	24,74 (+0,10)
$)_2Cl_2$	24,37	—	10,92	—	24,71 (+0,34)
$)_2Br_2$	21,94	—	8,78	—	21,98 (+0,04)
$A)_2Cl_2$	17,20	—	8,26	—	18,06 (+0,86)
$MA)]Cl_3$	43,20	—	19,87	—	43,72 (+0,52)
$OA)_2Cl_2$	37,97	—	39,87	—	38,73 (+0,76)
$Pt(NH_3)_2G_2]Cl_2 \cdot 2H_2O$	21,61	9,29	9.81	21,61 (0,00)	21,82 (+0,21)
$-[Pt(NH_3)_2G_2]Cl_2$	22,51	25,12	27,60	23,32 (+0,81)	23,41 (+0,90)
$n)G_2]Cl_2 \cdot 2H_2O$	21,00	10,63	11,17	20,24 (−0,76)	20,50 (−0,50)
$,Cl_2 \cdot 2HCl$	21,54	9,70	9,23	21,24 (−0,30)	21,32 (−0,22)
$_4]Cl_2$	13,94	5,94	6,32	13,24 (−0,70)	13,60 (−0,34)
$Pt(NH_3)_2X_2]Cl_2$	22,46	9,21	9,16	22,81 (+0,35)	22,28 (−0,18)
$'t(In)_2Cl_2$	24,31	10,45	10,21	24,94 (+0,63)	24,31 (0,00)
$fP)_2$	25,61	—	17,00	—	24,94 (−0,67)
$n)MP]Cl$	33,99	15,57	8,84	33,31 (−0,68)	33,58 (−0,41)
$fP)Cl_2$	35,44	—	25,73	—	36.15 (+0.71)
$fP_1)_2$	24,64	—	17,45	—	23,75 (−0,89)
$MP_1)In_2]Cl$	18,57	8,21	2,15	18,38 (−0,19)	17,68 (−0,89)

ıssaire: ac: Tétraméthyl-2,2,5,5-hexyne-3, ac_1: diméthyl-2,5-hexyne-3-diol-2,5, lut: lutidine, dien: diéthylènetriamine, : triphénylphosphine, $As\emptyset_3$: triphénylarsine, HPH_2: hématoporphyrine, HPH_4^{2+}: hématoporphyrine diacide, dénosine, TA: tétraacétyladénosine, MA: 9-méthyladénosine, OA: 1-oxyadénosine, G: guanosine, X: xanthosine, osine, MP: 6-mercaptopurine, MP_1: 2-amino-6-mercaptopurine.

s valeurs entre parenthèses correspondent à l'écart des pourcentages trouvés par rapport aux pourcentages ılés.

porphyrine HP.Pt, et les produits secondaires $HPH_4^{2+}PtCl_4^{2-}$ et $HPH_2 \cdot PtCl_2$ ont été analysés avec succès, après destruction dans l'eau régale. De plus, toute une série de complexes Pt–nucléoside[11,12], nouvellement isolés dans ce laboratoire, a pu être analysée par absorption atomique. Ces complexes font partie d'une étude qui englobe l'interaction des bases puriques, pyrimidiques, des nucléosides, des nucléotides et des acides nucléiques avec différents sels de platine: $K_2[PtCl_4]$, *cis*- et *trans*-$Pt(NH_3)_2Cl_2$, *cis*- et *trans*-$Pt(py)_2Cl_2$, $Pt(en)Cl_2$. Comme dans le cas du *cis*- et *trans*-$Pt(NH_3)_2Cl_2$, en l'absence de tampon spectrochimique, on retrouve une augmentation de l'absorbance (160% dans le cas de mesures) dans l'eau et 170% dans l'acide chlorhydrique 0,5 *M* pour les complexes guanosine. Dans le cas du complexe $[Pt(en)G_2]Cl_2 \cdot 2H_2O$, on retrouve les caractéristiques du complexe *cis*-$[Pt(NH_3)_2G_2]Cl_2 \cdot 2H_2O$.

Une étude est en cours sur les variations d'absorbance entre complexes *cis* et complexes *trans*. Elle présente un grand intérêt pour l'identification d'isomérie géométrique des complexes. Les premiers résultats obtenus avec l'inosine et la guanosine montrent une isomérie *cis* de ces complexes. Comme dans les cas précédents, les tampons spectrochimiques annulent l'effet dépressif (complexes *cis*) ou exaltant (complexes *trans*) dû aux interférences (nucléoside, NH_3, en, Cl). Cependant, dans le cas du composé *trans*-$Pt(NH_3)_2Cl_2$ (non ionique), son absorbance dans l'eau et dans l'acide chlorhydrique 0,5 *M* est identique à celle obtenue sur les plateaux CD des Figs. 2 et 5 de l'article précédent[1]. De plus, en présence des tampons orthophosphate de potassium et chlorure de lanthane, aucune variation significative de l'absorbance n'est détectée. Par contre, la diminution de l'absorbance par addition de potassium ne correspond à aucune formation de complexe stable comme dans le cas des composés ioniques[1,5]. L'interférence causée par le chlorure de potassium, dans ce processus, semble être physique.

Les résultats (Tableau VI) correspondent à une seule détermination du platine. Le pourcentage de platine dans les complexes étudiés varie de 14 à 65%. La moyenne des écarts entre les pourcentages de platine trouvés et calculés est de +0.008% (23 composés) dans le cas des phosphates et de +0.05% (38 composés) dans le cas du lanthane. La précision du dosage dépend du pourcentage de platine dans le complexe. Cette précision varie de 0 à 5% pour l'ensemble des 61 dosages effectués en présence de chlorure de lanthane et d'orthophosphate de potassium. La moyenne des erreurs relatives sur l'ensemble des résultats (61 mesures) est de 1,5%. La précision, la reproductibilité et la sensibilité de cette méthode la rendent très fiable et bien adaptée au dosage du platine dans les complexes.

Un des auteurs (J. P. M.) détenteur d'une bourse post-grade du Conseil National de Recherches du Canada, tient à exprimer sa reconnaissance envers cet organisme. Tous nos remerciements au Conseil National de Recherches du Canada pour le support financier qu'il nous a accordé.

RÉSUMÉ

Un dosage du platine par absorption atomique est appliquée à différentes séries de complexes, dans divers milieux, avec et sans tampon spectrochimique. L'utilisation d'orthophosphate de potassium et de chlorure de lanthane comme

tampons élimine toute interférence. La reproductibilité et la précision des résultats sont très satisfaisantes. Dans le cas des phosphines, cette méthode s'avère supérieure à la calcination, couramment utilisée. De plus, en l'absence de tampons spectrochimiques, les complexes de platine de formule générale *cis*- et *trans*-$PtL_2L'_2$ (où L,L' sont des ligands) solubles dans l'eau présentent une différence d'absorbance très nette, permettant de distinguer un composé *cis* d'un composé *trans*, dans une série donnée. Le même effet est observé dans les solvants organiques.

SUMMARY

An atomic-absorption spectrometric method is reported for the determination of platinum in a series of platinum complexes, with and without the use of spectrochemical buffers. The use of potassium phosphate and lanthanum chloride as buffer eliminated interference effects. The results were reproducible and accurate Platinum phosphine complexes were easily analysed. The *cis*- and *trans*-$PtL_2L'_2$ (L,L' are ligands) complexes soluble in water gave significant differences in absorbance in the absence of spectrochemical buffers, so that absorbance measurements differentiated *cis*- and *trans*-compounds in a given series. The *cis–trans* effect was also detected in organic solvents.

BIBLIOGRAPHIE

1 J. P. Macquet et T. Theophanides, *Anal. Chim. Acta*, 72 (1974) 251.
2 M. M. Schnepfe et F. S. Grimaldi, *Talanta*, 16 (1969) 591.
3 J. G. Sen Gupta, *Anal. Chim. Acta*, 58 (1972) 23.
4 A. Janssen et F. Umland, *Z. Anal. Chem.*, 251 (1970) 101.
5 A. E. Pitts, J. C. Van Loon et F. E. Beamish, *Anal. Chim. Acta*, 50 (1970) 181.
6 A. Simonsen, *Anal. Chim. Acta*, 49 (1970) 368.
7 R. C. Mallett, D. C. G. Pearton, E. J. Ring et T. W. Steele, *J.S. Afr. Chem. Inst.*, 25 (1972) 219.
8 R. C. Mallett, D. C. G. Pearton, E. J. Ring et T. W. Steele, *Talanta*, 19 (1972) 181.
9 E. Adriaenssens et F. Verbeek, *At. Absorpt. Newslett.*, 12 (1973) 57.
10 J. P. Macquet et T. Theophanides, *Can. J. Chem.*, 51 (1973) 219.
11 N. Hadjiliadis et T. Theophanides, à être publié.
12 P. C. Kong et T. Theophanides, *Inorg. Chem.*, 13 (1974) 1167.

Analytica Chimica Acta, 72 (1974) 269–274

THE SIMULTANEOUS DETERMINATION OF CARBON AND OXYGEN IN SEMICONDUCTOR SILICON BY HELIUM-3 ACTIVATION ANALYSIS

C. VANDECASTEELE*, F. ADAMS and J. HOSTE

Institute for Nuclear Sciences, Rijksuniversiteit Gent, Proeftuinstraat 86, B-9000 Gent (Belgium)

(Received 20th March 1974)

In recent years, considerable interest has been taken in the influence of trace elements on the physical properties of semiconductor silicon. The influence of carbon and oxygen on these properties has been the subject of several investigations. Methods have been developed for the determination of carbon in silicon by charged-particle activation analysis. Deuteron activation[1,2] through the $^{12}C(d,n)^{13}N$ reaction was shown to provide a convenient determination. Activation with low-energy (2.3 MeV) deuterons[2] allowed an interference-free carbon determination with a detection limit of 0.2 p.p.m. Helium-3 activation based on $^{12}C(^3He,\alpha)^{11}C$ has also been applied[1,3,4]. Nozaki *et al.*[3] and Engelmann *et al.*[1] used a chemical separation for ^{11}C and ^{18}F (formed from carbon and oxygen, respectively). This, however, makes the determination of both elements after one irradiation difficult.

In a recent paper[5], the authors have reported results for oxygen in silicon by alpha and helium-3 activation. Because of the large cost of charged-particle activation analysis, it appeared worthwile to determine carbon and oxygen simultaneously after one helium-3 irradiation. By irradiating a few thin muscovite foils placed in front of the sample, the use of two different standard substances[3,4], *e.g.* silicon dioxide and carbon, and measurement of the beam intensity as a means of standardization can be avoided. These muscovite foils serve both as a standard for the oxygen determination and as a flux monitor for the carbon determination.

Nuclear data—interferences

Table I lists the nuclear reactions on which the determinations of carbon and oxygen are based. The radionuclides ^{11}C and ^{18}F are both β^+-emitters with half-lives of 20.3 and 109.8 min, respectively. The main interfering reactions are also indicated.

The error on the carbon determination caused by oxygen can be corrected for, but usually the correction is negligible. The nitrogen concentration in high-purity silicon samples is normally between 1 and 5 p.p.b. (ref. 7). Boron concentrations are also at this level or lower in undoped samples[8].

For the oxygen determination, the interference of fluorine and sodium is negligible at the concentration levels considered[5]. This is proved by the fact that

* Aspirant of the N.F.W.O.

TABLE I

REACTIONS OF CARBON AND OXYGEN WITH HELIUM-3 PARTICLES AND MAIN INTERFERING REACTIONS[6]

Reaction	*Concentration (p.p.m.) for equal activity to 1 p.p.m. C*	*Reaction*	*Concentration (p.p.m.) for equal activity to 1 p.p.m. O*[a]
$^{12}C(^{3}He, \alpha)^{11}C$		$^{16}O(^{3}He, p)^{18}F$ $^{16}O(^{3}He, n)^{18}Ne \xrightarrow{\beta^+} {}^{18}F$	
Interfering reactions		*Interfering reactions*	
$^{9}Be(^{3}He, n)^{11}C$	3.3	$^{19}F(^{3}He, \alpha)^{18}F$	20
$^{10}B(^{3}He, d)^{11}C$	2.0	$^{23}Na(^{3}He, 2\alpha)^{18}F$	25
$^{11}B(^{3}He, t)^{11}C$			
$^{14}N(^{3}He, \alpha d)^{11}C$	70		
$^{16}O(^{3}He, 2\alpha)^{11}C$	100		

[a] For 15-MeV incident energy[6].

activation with two different particles of largely different energies (helium-3 and alpha) yields similar results for oxygen.

It has been shown[3] that the formation of ^{11}C or ^{18}F by spallation reactions of the silicon matrix does not occur appreciably below about 20 MeV; 14 MeV was chosen, since a further increase in energy would not lead to a substantial increase in sensitivity.

Standardization method

The oxygen results were calculated from the activity in the sample and in the muscovite foils placed in front of the sample, by applying the usual equivalent thickness method[5]. Since it was not possible to find a standard material with a precisely known oxygen and carbon content and with a good heat resistance, so that it could stand high charged particle beam intensities, another solution was adopted for the carbon determination. Thus, the carbon concentration was deduced from the ratio of the ^{11}C activity in the sample to the ^{18}F activity, by means of the simultaneously determined oxygen concentration. The ratio V_E of the "integral cross-sections" for the $^{12}C(^{3}He, \alpha)^{11}C$ and the $O(^{3}He, x)^{18}F$ reactions was determined for various energies from the irradiation of a stack of mylar foils, exceeding the range. Because the average cross-section for a given reaction and particle energy is independent of the matrix[9,10], this will also be the case for the V_E values. Once determined for mylar, the V_E value can thus be used for other matrices as well.

$$V_E = \frac{\int_0^{R_{mylar}} \sigma_C(dx)_{mylar}}{\int_0^{R_{mylar}} \sigma_O(dx)_{mylar}} = \frac{\int_0^{R_{Si}} \sigma_C(dx)_{Si}}{\int_0^{R_{Si}} \sigma_O(dx)_{Si}} \quad (1)$$

where

σ_C = cross-section (cm^2) for $C(^3He, \alpha)^{11}C$ at a depth x in the matrix,
σ_O = cross-section for $O(^3He, x)^{18}F$ at a depth x in the matrix,
R = total range (mg cm^{-2}) of the charged particles of energy E in mylar or silicon.

The carbon concentration can then be calculated from:

$$\text{p.p.m.}_C = \text{p.p.m.}_O \cdot \frac{A_C}{A_F} \cdot \frac{S_F}{S_C} \cdot \frac{1}{V_E} \cdot \frac{e^{-\lambda_F t}}{e^{-\lambda_C t}} \cdot \frac{M_C}{M_O} \quad (2)$$

where p.p.m._C, p.p.m._O = carbon or oxygen concentration (p.p.m.), A_C, A_F = ^{11}C or ^{18}F activity t min after irradiation, S_C, S_F = saturation factor for ^{11}C or ^{18}F, λ_C, λ_F = decay constant for ^{11}C or ^{18}F, M_C, M_O = carbon and oxygen atomic mass.

EXPERIMENTAL

The main features of the experimental procedure have been described in detail elsewhere[5]. It essentially consists of the following steps.

(1) Irradiation with 20-MeV ^3He particles at an intensity up to 2 μA for times of 10–40 min, depending on the expected carbon and oxygen concentration. The sample is placed in a water-cooled holder with 3 muscovite foils (about 20 μm thick) in front.

(2) Chemical etching to remove a surface layer of at least 40 μm. The muscovite foils and the etching reduce the energy on the silicon layer corresponding to the depth of etching to about 14 MeV.

(3) Coincidence counting of the induced 511-keV annihilation radiation with two 7.5×7.5-cm NaI (Tl) detectors. Counting is started about 1 h after irradiation to insure the decay of ^{30}P ($T_{\frac{1}{2}}$ = 2.5 min). During 40 min, the sample is periodically counted for 200 s with a 100-s waiting time. Afterwards, the decay is further followed for about 4 h with a waiting and counting cycle depending on the ^{18}F activity (typically a 200-s count every 20 min for a sample containing 10 μg O g^{-1} and a 1000-s count every 40 min for a sample containing 60 ng O g^{-1}).

(4) Counting of the muscovite standard foils in a *ca.* 20 times lower geometry than that of the sample, about 6 h after irradiation. The geometry reduction is obtained by placing the two detectors about 40 cm apart. The second and the third foil are used as standards. The counting data are corrected for dead-time counting losses.

(5) Analysis of the decay data with the CLSQ[11] computer program, with weighted least squares.

(6) Calculation of the oxygen content from the activity in standards and sample[5] and of the carbon content by means of eqn. (2). The appropriate V_E value is obtained by linear interpolation.

For the determination of the V_E values, a stack of 20 mylar foils with a thickness gradually decreasing from 3.7 to 1.2 mg cm^{-2} was irradiated for 20 min with a 20-nA beam of 20 MeV helium-3 particles. Exactly 36 min after the irradiation, the foils were counted consecutively for 20 s with a waiting time of

40 s between each. Four measurements were carried out for each foil. Afterwards, the two NaI(Tl) detectors were placed closer to each other, thus improving the detection efficiency by a factor of 5. Three further counts were then made for each foil with a 1-h time lapse between each. The count data were analysed with the CLSQ-program, the iterations being started with half-lives of 10.0 min, 20.3 min and 109.8 min. After iteration, mean half-lives of respectively 19.5 and 107 min were obtained for the decay curve components attributed to ^{11}C and ^{18}F.

The ^{18}F and ^{11}C activities obtained in each foil were corrected for decay to the end of irradiation. The ratio V_E could then be calculated at different helium-3 energies from

$$V_E = \frac{f_O}{f_C} \cdot \frac{\sum_i A_C^i}{\sum_i A_F^i} \cdot \frac{S_F}{S_C} \cdot \frac{M_C}{M_O} \tag{3}$$

where f_O, f_C = weight fractions of oxygen and carbon in mylar (0.333 and 0.625); $\Sigma_i A_C^i \Sigma_i A_F^i$ = sum of the decay-corrected ^{11}C and ^{18}F activities in the foils starting with the foil which the particles reach with energy E.

RESULTS AND DISCUSSION

In the present paper only the results for carbon will be discussed, as a thorough discussion of the oxygen results has been given previously[5].

The assumption that V_E is independent of the matrix was investigated. The V_E values could, indeed, also be calculated from:

$$V_E = \frac{f_O}{f_C} \cdot \frac{\sum_i \frac{A_C^i \Delta_{Si}^i}{\Delta_{mylar}^i}}{\sum_i \frac{A_F^i \Delta_{Si}^i}{\Delta_{mylar}^i}} \cdot \frac{S_F}{S_C} \cdot \frac{M_C}{M_O} \tag{4}$$

where Δ_{Si}^i = the thickness (mg cm^{-2}) in silicon corresponding to the same energy loss as that in the ith mylar foil with thickness Δ_{mylar}^i. Δ_{Si}^i values were obtained after application of the modified range energy transformation program[5,12].

Table II compares the V_E values obtained by both calculation methods from the same experimental data.

TABLE II

COMPARISON OF THE V_E VALUES OBTAINED BY TWO CALCULATION METHODS

Incident energy (E, MeV)	*Ratio of integral cross-sections (V_E)*	
	Eqn. (3)	*Eqn. (4)*
14.36	0.988	0.984
13.50	0.956	0.953
12.60	0.917	0.914
11.65	0.892	0.889
10.63	0.837	0.836
9.99	0.773	0.774

TABLE III

DETERMINATION OF CARBON AND OXYGEN IN SILICON

Sample	*Carbon ($\mu g\ g^{-1}$)*		*Oxygen ($\mu g\ g^{-1}$)*	
	Values	*Average*	*Values*	*Average*
Czochralski				
1	2.4 ± 0.1^a	2.6 ± 0.3^b	9.9 ± 0.1^a	10.1 ± 0.1^b
	2.8 ± 0.1		10.2 ± 0.1	
2	0.9 ± 0.1	1.15 ± 0.35	6.2 ± 0.05	5.1 ± 1.5
	1.4 ± 0.1		4.1 ± 0.04	
3	1.8 ± 0.2		10.9 ± 0.1	
4	2.9 ± 0.1		5.6 ± 0.05	
Floating zone				
5	0.116 ± 0.017	0.122 ± 0.007	0.067 ± 0.006	0.062 ± 0.014
6	0.117 ± 0.020		0.072 ± 0.007	
	0.127 ± 0.013		0.052 ± 0.002	
7	0.053 ± 0.022		0.079 ± 0.002	

[a] Standard deviation from the least-squares fitting of the decay curve.
[b] Standard deviation on one determination.

Results for carbon and oxygen are given in Table III. It is clear that, in the present non-destructive determination, both the sensitivity and the precision of the carbon determination depend strongly on the oxygen concentration. Indeed, the ^{11}C activity is superimposed on a varying ^{18}F background. For a 40-min irradiation, which can be considered as optimal for the carbon determination, at 2 μA with 14 MeV helium-3 particles (on the layer corresponding to the depth of etching). 1 p.p.b. of oxygen gives an induced ^{18}F activity of 1.6 c.p.m., and 1 p.p.b. of carbon gives 1.4 c.p.m., 1 h after irradiation. Under these conditions, with a 5-min counting time to check the ^{11}C half-life, one calculates a determination limit[13] of 38 p.p.b. of carbon in the presence of 50 p.p.b. of oxygen, and of 290 p.p.b. of carbon in the presence of 5 p.p.m. of oxygen.

The dependence of the carbon result on the carbon/oxygen concentration ratio also explains the relatively large error estimates for carbon obtained from the least squares analysis of the decay curve for samples 1–4 (on average about 7% compared to about 1% for oxygen). These samples contain on average about 4 times more oxygen than carbon. The determined carbon concentrations for crystals from commercial sources are in general agreement with those recently reported by other workers who applied activation analysis. This is so both for the czochralski (a few p.p.m.)[2,4,7,8] and the floating zone samples (about 100 p.p.b.)[7]. Infrared spectrometry[4,7] and mass spectrometry[14] gave similar results. As part of a program sponsored by EURISOTOP, the results for sample 1 (2.6 ± 0.3 p.p.m.) could be compared with results obtained by other methods in other laboratories for samples taken from the same ingot. Photon activation[15] and infrared spectrometry[16] yielded concentrations of 2.1 ± 0.8 and 2.3 ± 0.7 p.p.m., respectively.

Grateful acknowledgement is made to R. Kieffer for technical assistance,

to the "Comité de gestion du cyclotron" of Louvain-La-Neuve (U.C.L.) for the use of the cyclotron, to the operating staff of the cyclotron and to the scientists of the "Laboratoire de chimie nucléaire" for kind cooperation. The authors express their gratitude to Dr. L. De Laet (Metallurgy Hoboken) for providing part of the samples and to the N.F.W.O. and the I.I.K.W. for financial support.

SUMMARY

A non-destructive method for the simultaneous determination of carbon and oxygen in silicon by helium-3 activation analysis is described. The determination is based on a simplified standardization method. The method was applied to samples containing 0.05–3 p.p.m. of carbon and 0.05–10 p.p.m. of oxygen. The determination limit of carbon varies from 30 to 300 p.p.b. depending on the oxygen concentration.

REFERENCES

1 C. Engelmann and A. Marschal, *Radiochem. Radioanal. Lett.*, 6 (1971) 189.
2 J. Martin and E. Haas, *Z. Anal. Chem.*, 259 (1972) 97.
3 T. Nozaki, Y. Yatsurugi and N. Akiyama, *J. Radioanal. Chem.*, 4 (1970) 87.
4 C. Gross, G. Gaetano, T. Tucker and J. Baker, *J. Electrochem. Soc.*, 119 (1972) 926.
5 C. Vandecasteele, F. Adams and J. Hoste, *Anal. Chim. Acta*, in press.
6 C. Engelmann, *J. Radioanal. Chem.*, 7 (1971) 281.
7 T. Nozaki, Y. Yatsurugi, N. Akiyama, Y. Endo and Y. Makide, *Intern. Meeting on Activation Analysis, Paris, Oct. 1972, Paper C 44; J. Radioanal. Chem.*, 19 (1974) 109.
8 C. Engelmann, J. Gosset and J. Rigaud, *Radiochem. Radioanal. Lett.*, 5 (1970) 319.
9 E. Ricci and R. Hahn, *Anal. Chem.*, 39 (1967) 794.
10 P. Kuin and J. Reynders, *Int. Conf. Mod. Trends in Activation Analysis, Paris, Oct. 1972, Paper M 73; J. Radioanal. Chem.*, 16 (1973) 403.
11 J. Cumming, *BNL Report 6470.*
12 H. Rook, *Dissertation*, Texas A and M University, 1969.
13 L. Currie, *Anal. Chem.*, 40 (1968) 586.
14 J. Baker, T. Tucker, T. Moyer and N. Buschert, *J. Appl. Phys.*, 39 (1968) 4365.
15 C. Engelmann, personal communication.
16 M. Millett, personal communication.

Analytica Chimica Acta, 72 (1974) 275–283

NUCLEAR MAGNETIC RESONANCE STUDIES OF THE MICROSCOPIC PROTONATION OF L-CYSTEINE

DOUGLAS B. WALTERS* and DONALD E. LEYDEN

Chemistry Department, University of Georgia, Athens, Georgia 30602 (U.S.A.)

(Received 4th February 1974)

Relative concentrations of the microspecies present when L-cysteine dissociates were determined by n.m.r. spectroscopy. The microscopic dissociation scheme for L-cysteine[1] is shown below. The carboxyl group is not included in the scheme because this site dissociates in the region of pH 2 and is completely dissociated before dissociation of the amino and sulfhydryl sites.

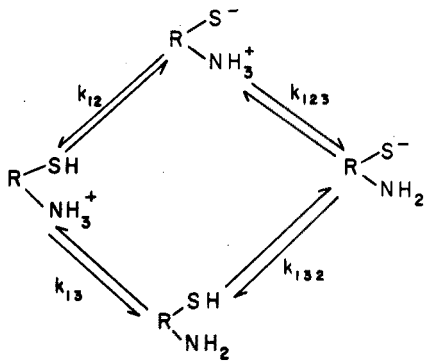

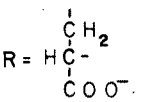

By supplementing potentiometric data with n.m.r. data in a manner previously described[2], the relative concentrations of the microspecies were determined. Table I

TABLE I

pK_a VALUES OF COMPOUNDS USED

Compound	*Observed values at 0.5 M*			*Literature values at 0.5 M*			*Ref.*
	pK_1	pK_2	pK_3	pK_1	pK_2	pK_3	
L-Cysteine	2.02	8.48	10.48	1.96	8.18	10.28	3
L-Cysteine methyl ester	—	6.54	9.06	—	6.56	8.99	4
S-Methyl-L-Cysteine	2.02	—	8.92	—	—	8.97	5

* Present address: Tobacco and Health Laboratory, Russell Research Center, ARS, USDA, Athens, Georgia 30604, U.S.A.

shows the microscopic pK_a values of the compounds studied.

The microscopic protonation scheme for L-cysteine is of interest for several reasons: variation of reported values for the microspecies indicates that the question of the dissociation of L-cysteine has not been resolved[3,5–10]; n.m.r. has been used in similar studies of EDTA[11] and tetracycline antibiotics[2]; although n.m.r. studies of L-cysteine have been done[12–14], the results were not applied to the protonation scheme; and L-cysteine has two acidic sites with K_a values in close proximity, resulting in a simultaneous dissociation of the amino and sulfhydryl groups.

EXPERIMENTAL

Spectra were recorded with a Varian A-60 n.m.r. spectrometer at ambient probe temperature of 40°C. Calibrations were made with a Hewlett Packard 241A audio oscillator and 5233L electronic counter. Sodium 3-(trimethylsilyl)propane sulfonate was the internal reference compound. Line positions are estimated to be better than ± 0.01 p.p.m.

When necessary, spectra were analyzed by computer synthesis by means of LAOCOON-III[15], a FORTRAN program processed by an IBM 7094 computer. The simultaneous equations used to obtain values of f_i were solved by a program from the University of Georgia Computer Center and processed by an IBM 1620 computer.

pH measurements were made at room temperature with a Leeds and Northup Model 7403-Al pH meter equipped with miniature electrodes and standardized with National Bureau of Standard buffers. Corrections were not made for glass electrode errors at either pH extreme.

pK_a values were determined by potentiometric titration in aqueous solutions with standard 6 *M*, CO_2-free potassium hydroxide (Baker AR grade), using a semiautomatic recording device previously described[3]. pK_a values in D_2O were determined in the same manner. The KOD solution used as the titrant was prepared by reacting reagent grade potassium metal with CO_2-free D_2O (Columbia Organic, 99.8%) in a nitrogen atmosphere. A layer of ether covered the D_2O to slow the reaction rate. The ether was then removed by warming the KOD solution with hot water while passing a stream of nitrogen over the surface. pK_a values were calculated by standard methods[16].

L-cysteine hydrochloride hydrate, S-methyl-L-cysteine, and L-cysteine methyl ester were California Biochem. Corp., A grade eagents. Except for L-cysteine, the compounds were used without further purification. Analysis of L-cysteine showed 0.05% iron. Iron has a catalytic effect on L-cysteine and was removed by a procedure described elsewhere[17].

ANALYSIS OF NMR RESULTS

The n.m.r. spectrum of L-cysteine is strongly pH-dependent. Protons of primary interest are those on the carbon atoms α- and β- to the amino group. The β- carbon protons are adjacent to an asymmetric site, and are expected to display magnetic nonequivalence[18]; they are therefore designated A and B. The α-carbon proton is designated C or X. Methyl protons of the L-cysteine

derivatives will not be discussed, since they are not relevant to this study. Acid protons undergo rapid exchange with the solvent; hence, their spectra appear as a weighted average of all environments.

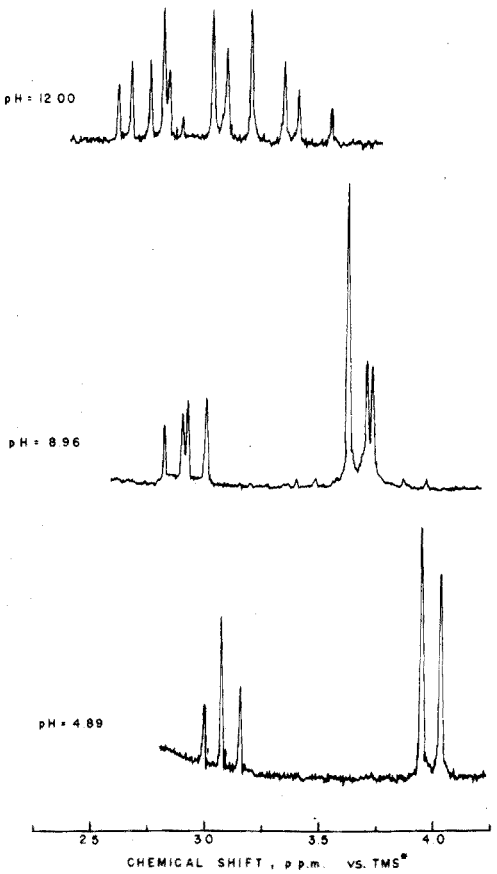

Fig. 1. N.m.r. spectra of L-cysteine.

Figure 1 shows typical spectra of L-cysteine in the pH range investigated. Types of spectra observed can be described in terms of two pH regions. In acidic solutions, five line A_2X spectra were observed that were analyzed by standard procedures[19]. The A_2X spectrum prevails until the region of the second pK_a (*ca.* pH 8.5) of L-cysteine. The spectrum then undergoes a rapid transition with pH variation, first to an A_2B then to an ABC spectrum. The ABC spectra were analyzed by means of LAOCOON III. Table II shows the obtained spectral parameters that are in good agreement with literature values[13].

Figure 2 shows the chemical shift values of the –CH and $-CH_2$ protons of L-cysteine *versus* pH. Solid lines were drawn by requiring symmetry about the microscopic pK_a values (horizontal dashed lines). Dashed lines in the titration

TABLE II

SPECTRAL PARAMETERS IN Hz

Compound	*n*	*δA*	*δB*	*δC or X*	J_{AC}	J_{BC}	J_{AB}
L-Cysteine	0	149.4	172.0	187.0	3.40	9.13	−12.44
0.5 *M* H_2O	1	167.0	173.1	215.4	3.87	7.13	−14.0
	2	184.5		239.9	4.98		—
	3	190.5		264.9	5.02		—
L-Cysteine	0	168.3		216.0	5.25		—
Methyl ester	1	175.2		231.7	5.02		—
0.5 *M* H_2O	2	191.1		267.0	4.98		—
S-Methyl-L-Cysteine	0	164.8		202.3	7.0		—
0.5 *M* H_2O	1	180.5		233.5	7.0		—
	2	190.8		261.2	7.1		—

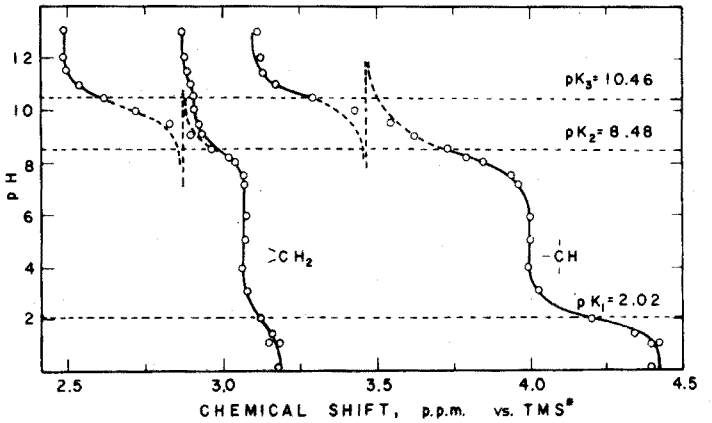

Fig. 2. Chemical shift data for L-cysteine at various pH values.

curves represent the expected curve, assuming no overlap of dissociation, and were based on symmetry about pK_a. Figures 3 and 4 are similar plots for S-methyl-L-cysteine and L-cysteine methyl ester, respectively.

Table III lists the total chemical shift change of the –CH and $-CH_2$ protons in the compounds studied. These values represent differences in chemical shift observed when all acidic sites are completely deprotonated and when they are completely protonated. The $-CH_2$ protons in L-cysteine have two values because

TABLE III

TOTAL OBSERVED CHEMICAL SHIFT CHANGES (P.P.M.)

Compound	*–CH*		*–CH_2*
L-Cysteine	1.30	0.69	0.31 (mean 0.50)
L-Cysteine methyl ester	0.85		0.38
S-Methyl-L-cysteine	0.98		0.43

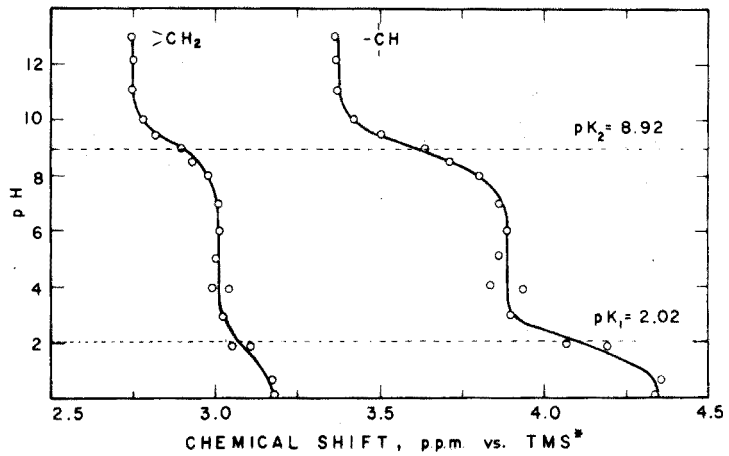

Fig. 3. Chemical shift data for S-methyl-L-cysteine at various pH values.

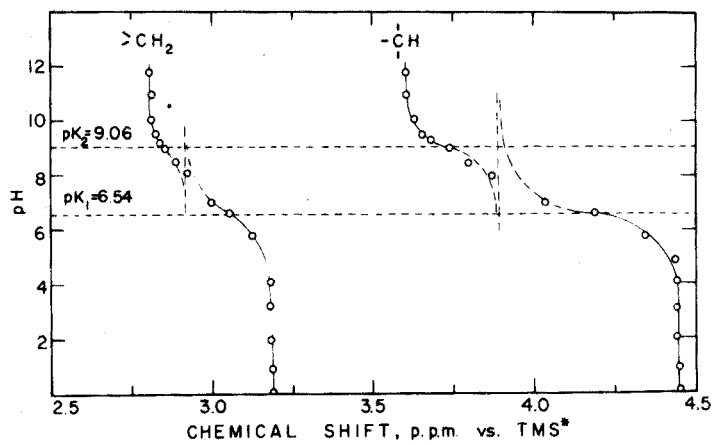

Fig. 4. Chemical shift data for L-cysteine methyl ester at various pH values.

the magnetic nonequivalence of these protons, resulting from asymmetry, is enhanced enough at high pH to become measurable. Protonation of the functional sites causes a larger shift of the proton which is initially at higher field in the completely deprotonated molecule. The largest total chemical shift change for both the –CH and $-CH_2$ protons is with L-cysteine, where all three acidic sites undergo dissociation. The next largest total chemical shift change is with L-cysteine methyl ester, because the carboxyl group is no longer participating in the acid–base reactions.

The difference between the total chemical shift change of the compounds studied shows the effect of protonation of a particular site on either the –CH or $-CH_2$ proton chemical shift. These values are called protonation shift constants. For example, the difference between the total –CH chemical shift in L-cysteine and that in S-methyl-L-cysteine gives the chemical shift change in the –CH proton which would result from complete protonation of the sulfhydryl group. Similarly, the

TABLE IV

PROTONATION SHIFT CONSTANTS (P.P.M.)[a]

Group	*–CH*	*–CH_2*
–COOH	0.45	0.12
–NH_3	0.53	0.31
–SH	0.32	0.07
Total	1.30	0.50

[a] Obtained with 0.5 *M* solutions.

protonation shift constant for the carboxyl group can be obtained from data for L-cysteine and L-cysteine methyl ester. Attempts to obtain chemical shift data on L-cysteine betaine, synthesized in this laboratory by existing methods[22], were of limited success because of the rapid decomposition of the compound in basic solution. Therefore, amino site protonation shifts were obtained as the difference between the total chemical shift change for L-cysteine and the sum of the sulfhydryl and carboxyl protonation shift constants. In the case of L-cysteine, the two –CH_2 protons undergo different chemical shift changes over the pH range used. These protons undergo equal chemical shift changes in the derivatives studied. To relate the observed change in L-cysteine to those in their derivatives, the mean for value for the total chemical shift change for the –CH_2 protons in L-cysteine was used. Table IV gives values of the protonation shift constants.

The fraction of time each of the functional sites is protonated may be represented by f_i, the average fraction of time during the ith site is protonated. A set of simultaneous equations may be written as follows:

$$\delta_0^{CH} = \Sigma_i^n f_i \delta_i^{CH} \tag{1}$$

$$\delta_0^{CH^2} = \Sigma_i^n f_i \delta_i^{CH^2} \tag{2}$$

$$\Sigma_i^n f_i = n \tag{3}$$

In eqn. (1), δ_0^{CH} is the total observed chemical shift change of the –CH proton upon addition of n equivalents of acid, and δ_i^{CH} is the protonation shift constant for the –CH proton for complete protonation of ith site, where n is the total number of sites. Similarly, in eqn. (2), $\delta_0^{CH^2}$ is the total observed chemical shift change of the –CH_2 protons upon the addition of n equivalents of acid and $\delta_i^{CH^2}$ is the protonation shift constant for the ith site. Equation (3) is a normalizing equation that sets the total fraction protonated equal to the equivalents of acid present. Because the carboxyl group is not involved in the microscopic scheme, only the amino and sulfhydryl sites need consideration. Unknowns are the fraction of time the amino site (f_A) and the sulfhydryl site (f_s) are protonated. Since there are two unknowns and three equations, the system is overdetermined and is best solved by the technique of obtaining the minimum residual[2,11] (R^2) of the equations in the form

$$(\delta_0 - \Sigma_i^n f_i \delta_i)^2 = R^2 \tag{4}$$

Table V shows the per cent protonation of the amino, carboxyl and sulfhydryl sites in L-cysteine at various values of n.

TABLE V

PERCENT PROTONATION OF THE BASIC SITES AT VARIOUS VALUES OF n

Compound	n	*–SH*	$-NH_3^+$	*–COOH*
L-Cysteine	1	60.0±0.6	39.4±0.6	0.6±1.3
(0.5 *M* H_2O)	2	100.0±0.7	100.0±0.6	0.0±1.3
	3	99.4±0.7	101.3±0.6	99.3±1.3
L-Cysteine	1	50.4±1.6	49.4±1.2	0.2±0.2
(0.75 *M* H_2O)	2	100.0±0.8	100.0±1.2	0.0±0.4
	3	100.0±0.8	100.0±1.2	100.0±0.4
L-Cysteine	1	48.8±0.5	50.7±0.5	0.5±1.2
(1.0 *M* H_2O)	2	100.0±0.7	100.0±0.5	0.0±1.2
	3	99.3±0.7	99.5±0.5	101.2±1.2
L-Cysteine	1	60.3±0.2	39.4±0.9	0.2±1.2
(0.5 *M* D_2O)	2	102.8±0.3	99.2±0.9	2.0±1.2
	3	102.8±0.3	99.2±0.9	99.8±1.2

DISCUSSION

As explained above, the portion of the total microscopic protonation scheme of L-cysteine of interest is the pH region in which the amino and sulfhydryl sites are being protonated. Results may be expressed as the ratio, R, of the concentrations of species I to species II.

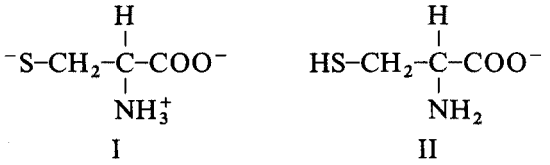

I II

This ratio represents the point on the titration curve after the addition of n equivalents of acid to the completely deprotonated amino acid. Table V gives the per cent average protonation of the various sites for three values of n. With these values, when $n=1$, R is calculated to be 0.66, 0.98, 1.04 for the 0.5 M, 0.75 M, and 1.00 M solutions, respectively. The value for R for the 0.5 M solution of L-cysteine is in good agreement with the value obtained from extrapolation of calorimetric results to the ionic strength corresponding to the 0.5 M solution. To the extent that comparisons between the present data and calorimetric data[5] are valid, the results show that the value of R is about 1.2 at low ionic strength, decreases to 0.6 at an ionic strength of 2.2 M and subsequently increases again at higher ionic strength values. The calorimetric method gave values of R ranging from 1.2 at zero ionic strength to 0.7 at an ionic strength of 1.0 M. These results were obtained in different ionic strength regions by different methods and neither gave the divergence of results reported earlier.

The trend toward lower values of R with increasing ionic strength is probably a result of the different effect of ionic strength on the dissociation of the positively charged protonated amino group and the neutral protonated sulfhydryl group. Dissociation of the amino group does not involve charge separation and therefore,

is not expected to vary with ionic strength as much as the dissociation of the sulfhydryl site which does involve charge separation. This has been reported previously[5]. Hence, an initial decrease in the value of R with increasing ionic strength is observed. This is largely a result of the decrease in the value of the microconstant pk_{13} in Fig. 1. At very high ionic strengths the activity coefficients commonly begin to increase and become greater than unity. Consequently, the value of R is expected to increase as the value of pk_{13} again becomes larger with increasing ionic strength. The results of the 0.75 M and 1.00 M solutions show this to be the case.

Protonation data in D_2O (Table V) was obtained to determine if any solvent isotope effects could be observed. Such effects generally depend upon the nature of the acidic site in question and the pK_a of this site. Groups having similar pK_a values often exhibit similar isotope effects. Because the microscopic distribution of the protons depends on the relative values of the microconstants pk_{12} and pk_{13}, and since these may have similar effects, it is not too surprising that the protonation data are the same, within experimental error, for the two solvents.

Conclusions

The order and relative magnitudes of the protonation shift constants for the compounds investigated are in agreement with those expected from inductive effect considerations. For example, the –COOH and $-NH_3^+$ protonation shift constants for $-CH_2$ protons can be compared with 0.05 p.p.m. and 0.25 p.p.m., respectively, tabulated previously[2] for carboxylic acids and primary amines. There is no basis for a valid comparison of –CH shifts with the earlier data. One interesting exception is noticed. Protonation of the sulfhydryl group gives rise to a chemical shift change in the –CH proton which is three times that observed for the $-CH_2$ protons. From simple inductive effect and bond distance considerations, this is not the expected result. One explanation is a hydrogen bond between sulfur and the amino group. However, studies of the relative reactivity of hydrogen atoms in sulfur compounds, indicate that hydrogen atoms bonded to the carbon β to sulfur are significantly more reactive than those bonded to the carbon to sulfur[22,23]. This effect could be, partly, the result of non-bonded interactions between sulfur and hydrogen atoms resulting in an increased electron density about the hydrogen nucleus. Such interactions may cause significant changes in the chemical shift of the proton involved and are reasonable from steric considerations. Martin and Mathur[13] showed that the preferred rotamer of L-cysteine, with respect to the carbon–carbon bond, is the one in which the sulfhydryl group is *anti* to the carboxylate group:

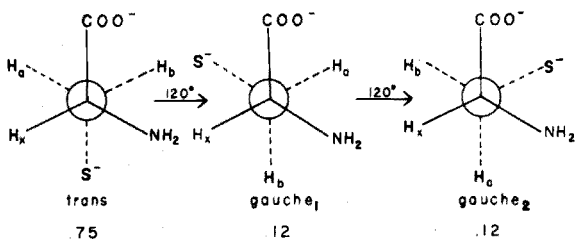

Models indicate that in this configuration the distance between the sulfur

atom and the –CH proton is small enough to permit some type of interaction. Similar compounds under current investigation show this interaction to be somewhat general with the extent being dependent upon relative rotamer populations[23].

The authors wish to express their sincere appreciation for support of this research by the National Institute of Health, Public Health Service Research Grant GM-13935.

SUMMARY

The protonation scheme of L-cysteine has been investigated by nuclear magnetic resonance. Chemical shift data as a function of pH are given for L-cysteine, L-cysteine methyl ester and S-methyl-L-cysteine. Use of derivatives of L-cysteine permits determination of the effect of protonation of the amino, sulfhydryl and carboxylic sites on the chemical shift of the –CH and $-CH_2$ protons. On the basis of these results, a set of simultaneous equations was written whose solution yielded the fraction of protonation of each site upon the addition of n equivalents of acid to the initially completely deprotonated molecule.

REFERENCES

1 J. T. Edsall and J. Wyman, *Biophysical Chemistry*, Vol. 1, Academic Press, New York, 1958, p. 497.
2 J. L. Sudmeier and C. N. Reilley, *Anal. Chem.*, 36 (1964) 1698.
3 E. J. Cohn and J. T. Edsall, *Proteins, Amino Acids and Peptides*, Reinhold, New York, 1943, p. 85.
4 J. P. Greenstein and M. Winitz, *Chemistry and Amino Acids*, Vol. 1, Wiley, New York, 1961, p. 642.
5 D. P. Wrathall, R. M. Izatt and J. J. Christensen, *J. Amer. Chem. Soc.*, 86 (1964) 4779.
6 E. Elson and J. R. Edsall, *Biochemistry*, 1 (1962) 1.
7 L. R. Ryklan and C. L. A. Schmidt, *Arch. Biochem. Biophys.*, 5 (1944) 89.
8 R. E. Benesch and R. Benesch, *J. Amer. Chem. Soc.*, 77 (1955) 5877.
9 S. J. Rogers, *J. Chem. Soc.*, 46 (1969) 239.
10 G. E. Clement and T. P. Hartz, *J. Chem. Educ.*, 48 (1971) 395.
11 J. L. Sudmeier and C. N. Reilley, *Anal. Chem.*, 36 (1964) 1707.
12 K. G. R. Packler, *Spectrochim. Acta*, 20 (1964) 581.
13 R. B. Martin and R. Mathur, *J. Amer. Chem. Soc.*, 87 (1965) 1965.
14 F. Taddei and L. Pratt, *J. Chem. Soc., London*, (1964) 1553.
15 A. A. Bothner-By and S. Costellano, *Laocoon III*, Carneige Mellon Institute, Pittsburgh, Pa.
16 A. Albert and E. P. Serjeant, *Ionization Constants of Acids and Bases*, Methuen, London, 1962.
17 D. E. Leyden and W. R. Morgan, *Can. J. Biochem.*, 45 (1967) 611.
18 H. S. Gutowsky, *J. Chem. Phys.*, 37 (1962) 2196.
19 J. A. Pople, W. G. Schneider and J. J. Bernstein, *High Resolution Nuclear Magnetic Resonance*, McGraw-Hill, New York, 1959.
20 A. Loewenstein and J. D. Roberts, *J. Amer. Chem. Soc.*, 82 (1960) 2705.
21 M. P. Schubert, *J. Biol. Chem.*, 111 (1935) 671.
22 T. A. Kampmeir, R. P. Greer, A. J. Meskin and R. M. D'Silva, *J. Amer. Chem. Soc.*, 88 (1966) 1257.
23 D. E. Leyden and D. B. Walters, *Spectrochim Acta, Part A* 25 (1969) 1869.

Analytica Chimica Acta, 72 (1974) 285–293

STUDIES IN ATOMIC FLUORESCENCE SPECTROMETRY

PART II. INTERFERENCE EFFECTS IN THE DETERMINATION OF TIN WITH VARIOUS PREMIXED FLAMES

D. P. HUBBARD* and R. G. MICHEL

Department of Chemistry and Biology, Sheffield Polytechnic, Sheffield S1 1WB (England)

(Received 11th March 1974)

West *et al.*[1] have described the determination of tin by atomic fluorescence spectrometry, quoting a detection limit of 0.1 p.p.m. with a nitrogen-separated argon–oxygen–hydrogen flame. Several severe interferences were found when flame conditions that gave optimal sensitivity were used, but the use of a leaner flame minimized these interferences.

In the atomic absorption determination of tin, detection limits of 0.03 p.p.m. have been obtained[2] with cool flames. However, the less sensitive nitrous oxide–acetylene flame has been preferred in practice[3,4], because interferences are less than in the cooler hydrogen flames. Where sensitivity is not adequate, the traditional method of concentration by solvent extraction techniques has been used[5,6].

Nakahara *et al.*[7] have investigated the large number of interferences with the atomic absorption of tin in the nitrogen–hydrogen, argon–hydrogen, and air–hydrogen flames. Iron(III) chloride was found to be very effective in eliminating interferences from most other elements. Six acids were also found to interfere seriously with the atomic absorption determination but the effect of iron(III) chloride on the acid interferences was not reported. The use of iron(III) chloride was satisfactorily applied to a direct method for the determination of tin in copper-base alloys and steel. The sensitivity for 1% absorption, 0.12 p.p.m. in the argon–hydrogen flame, was similar to that obtained by solvent extraction methods[5,6] and up to an order of ten better than the various other direct methods that employ the nitrous oxide–acetylene flame[3,4].

The argon–hydrogen flame is often used for atomic fluorescence spectrometry because the fluorescence quenching abilities of argon and hydrogen are poor. In view of the potential usefulness of atomic fluorescence, discussed in reviews by Winefordner and Elser[2], and Kirkbright and West[8], it was decided to make a detailed investigation of the interference effects encountered in the atomic fluorescence determination of tin with argon–oxygen–hydrogen, argon–hydrogen, and argon-separated air–acetylene flames. The interference effects in the argon-separated nitrous oxide–acetylene flame were not studied because of the poor detection limit obtained in this work with this flame; the poor signal was probably due to the large quenching effect of the flame gases on the emitted fluorescence.

* Present address: Department of Chemistry, University of Otago, Box 56, Dunedin, New Zealand.

A comparison between the results obtained by Nakahara *et al.*[7] and those obtained during this study indicated that the interferences in both the atomic absorption and atomic fluorescence of tin show the same basic trends. In the atomic fluorescence determination of tin, iron(III) chloride eliminated most interferences from the elements tested for any of the three flames. However, it was not as effective in removing the interference of the acids tested.

EXPERIMENTAL

Apparatus

The atomic fluorescence instrument used has already been fully described[9].

Fixed instrumental conditions. The lock-in-amplifier gain was kept at maximum. The time constant at the lock-in-amplifier was 4.7 s for solutions containing more than 0.1 p.p.m. tin, and 18.2 s for concentrations below 0.1 p.p.m. The electrodeless discharge lamp was thermostated at 385°K and operated at 40-W incident microwave power in a $\frac{1}{4}$-wave cavity. The lamp was modulated at a frequency of 10 KHz and the percentage modulation was the maximum that the equipment could deliver. The monochromator entrance and exit slits were fixed at 100 and 150 μm, respectively.

Reagents

Spectrographically standardized tin (1 g) was dissolved in the minimum of concentrated (analytical reagent-grade) hydrochloric acid, and the solution was diluted to 1 l with 0.4 *M* hydrochloric acid. Except where otherwise stated all solutions were made up in 0.4 *M* hydrochloric acid to keep the pH less than 1.5. Above pH 1.5, dilute solutions of tin are unstable[10]. Solutions made up with 0.4 *M* hydrochloric acid were stable for at least two weeks, whereas pure aqueous solutions were stable for less than 1 h. Other reagents were of analytical grade or spectrographically standardized metals.

RESULTS AND DISCUSSION

Choice of gas flow rates, flame separation and most sensitive wavelengths for each flame

The gas flow rates in the premixed air–acetylene, argon–hydrogen, argon–oxygen–hydrogen and nitrous oxide–acetylene flames were optimized by observing the atomic fluorescence signal from 10 p.p.m. tin solutions, except for the nitrous oxide-supported flame when a 1000 p.p.m. tin solution was used (Table I).

Argon separation of the argon–oxygen–hydrogen flame increased the signal by 30% but there was no attendant decrease in flame noise levels; this modification was therefore considered unjustified, especially in view of the large amount of argon required. This contrasts with the very useful increase in signal-to-noise ratio—by a factor of 3.8—obtained by separation of the air–acetylene flame[9], and with the ten-fold improvement in detection limit obtained by argon separation of the nitrous oxide–acetylene flame in the present work.

The oxygen flow in the argon–oxygen–hydrogen flame is critical as reported by West *et al.*[1]. However, the variations in signal with hydrogen flow reported by West *et al.* could not be reproduced on the present instrument. The optimal flows

TABLE I

GAS FLOW RATES AND SPECTRAL LINES GIVING OPTIMAL SENSITIVITY FOR TIN IN VARIOUS FLAMES

Flame	*Gas flow rates (l min^{-1})*		*Optimal wavelength (nm)*
	Unseparated flame	*Argon-separated flame (argon flow 6.0 l min^{-1})*	
Air	3.7	3.7	303.4
Acetylene[9]	1.25	0.9	
Argon	3.7	—	317.5
Hydrogen	1.0	—	
Argon	3.7	3.7	303.4
Hydrogen	1.0	1.0	
Oxygen	0.5	0.5	
Nitrous oxide	3.7	3.7	284.0
Acetylene	3.2	3.2	

in both the argon–hydrogen and argon–oxygen–hydrogen flames were found to be the same (Table I); in the argon–hydrogen flame and in the argon-separated argon–oxygen–hydrogen flame, the signal decreased rapidly with increasing hydrogen flow rate, whereas in the unseparated argon–oxygen–hydrogen flame, the signal decreased only slowly up to 2 l H_2 min^{-1}.

Variation in flame height with respect to the monochromator entrance slit gave very little variation in fluorescence. Benetti *et al.*[11] have indicated that their optical system did not allow a specific flame zone to be observed or excluded, and the present optical arrangement was very similar.

The atomic fluorescence spectra of tin in each of the four flames listed in Table I were obtained and showed similar characteristics to the fluorescence spectrum in the argon–oxygen–hydrogen flame[1]. The most sensitive lines in each flame are listed in Table I; these are the same wavelengths as found by West *et al.*[1] except for the nitrous oxide–acetylene flame which they did not study. The most sensitive line in each flame was selected for the detailed work on interferences because preliminary observations indicated that interferences were not significantly different at other wavelengths.

The effect of acids

In the argon flames and the air–acetylene flame, the effect of five acids on the atomic fluorescence of tin was determined by measuring aqueous 10 p.p.m. tin solutions. The effects in the three flames (Fig. 1) are similar to those found by Nakahara *et al.*[7] and Juliano and Harrison[12] for the atomic absorption of tin.

An aqueous 10 p.p.m. tin solution containing 1% hydrofluoric acid gave enhancements of the fluorescence signal between 26 and 92% in the three flames.

The effect of elements

The interferences of twenty-seven elements, including iron, on the atomic

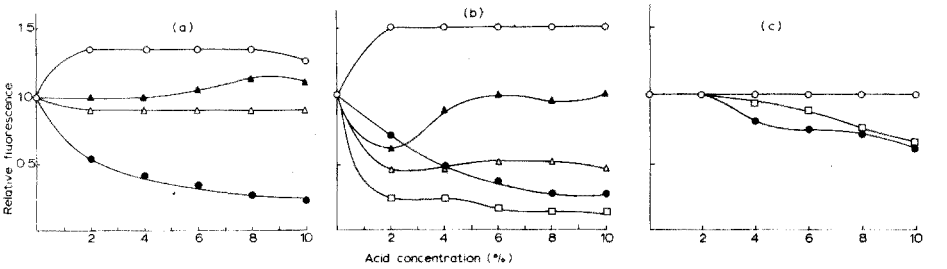

Fig. 1. The effect of acids on tin fluorescence (10 p.p.m. Sn). (a) In the argon–oxygen–hydrogen flame; (○) hydrochloric acid, (●) sulphuric and phosphoric acids, (△) nitric acid, (▲) perchloric acid. (b) In the argon–hydrogen flame; (○) hydrochloric acid, (●) sulphuric acid, (□) phosphoric acid, (△) nitric acid, (▲) perchloric acid. (c) In the air–acetylene flame; (○) hydrochloric, perchloric and nitric acids, (□) phosphoric acid, (●) sulphuric acid.

fluorescence of 10 p.p.m. tin were studied. The concentration of tin in 0.4 *M* hydrochloric acid was kept constant at 10 p.p.m. and the concentration of each element varied between 25 and 1000 p.p.m. All the interference effects increased with increase in concentration of the element. The magnitudes of the interferences at a 100 p.p.m. concentration of each interfering element are given in Table II.

TABLE II

INTERFERENCES ON THE ATOMIC FLUORESCENCE OF TIN

(10 p.p.m. tin, 100 p.p.m. interfering ion. Results expressed as the ratio of the fluorescence of tin in the presence of the interfering ion to the fluorescence of tin alone. All solutions were made up with 0.4 *M* hydrochloric acid unless the particular salt used was insoluble in acid. In such cases alternative dissolution conditions were used. Measurements were made at the most sensitive wavelength of each flame)

Element	*Relative fluorescence*			*Element*	*Relative fluorescence*		
	Air–C_2H_2	*Ar–H_2*	*Ar–O_2–H_2*		*Air–C_2H_2*	*Ar–H_2*	*Ar–O_2–H_2*
Al[a]	1.19	0.87	1.00	Mn[b]	1.06	1.00	1.00
Al[b]	1.30	0.76	0.95	Mo[e]	1.27	1.02	0.97
As[c]	1.20	0.91	0.96	Nb[f]	1.14	1.00	1.00
Bi[a]	1.15	0.97	1.01	Ni[b]	1.03	0.84	1.00
Ba[d]	1.05	0.98	1.00	Pb[d]	1.00	1.07	1.00
Ca[a]	1.11	0.95	1.00	Rb[a]	1.00	0.74	0.97
Cd[a]	1.00	1.00	1.00	Sb[a]	1.00	1.02	1.05
Ce[d]	1.14	0.88	1.07	Sr[d]	1.04	0.83	1.00
Co[a]	1.00	1.00	1.00	Ti[g]	1.28	1.07	1.13
Cr[d]	1.05	0.85	1.00	Tl[h]	1.00	0.80	0.96
Cu[d]	1.11	1.12	1.00	V[b]	1.06	0.94	0.95
Fe[d]	1.00	1.10	1.00	W[i]	1.00	1.04	1.00
Fe[a]	1.00	1.10	1.00	Zn[d]	1.00	1.02	0.99
La[a]	1.14	0.90	1.03	Zn[b]	1.00	1.05	0.98
Mg[d]	1.04	0.99	1.00	Zr[a]	1.16	0.79	0.93

[a] As chloride. [b] As sulphate. [c] As sodium arsenite. [d] As nitrate. [e] As ammonium salt. [f] As pentoxide. [g] As metal. [h] As carbonate. [i] As sodium tungstate.

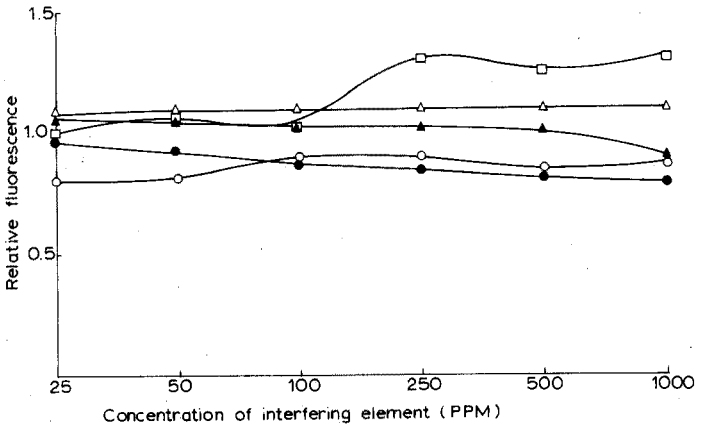

Fig. 2. Examples of the variation of interference effect with concentration of interfering ion, 10 p.p.m. tin. Results expressed as the ratio of the fluorescence of tin in the presence of interfering ion to the fluorescence of tin alone; flame, argon–hydrogen. (○) Aluminium, (●) arsenic, (△) iron, (▲) molybdenum, (□) antimony.

The interferences were not linear with concentration; some examples given in Fig. 2 illustrate the trends observed.

Interferences in atomic fluorescence are usually expected to be similar to those in atomic absorption. The main types of interference are common to both techniques, and Winefordner *et al.*[13] have indicated that fluorescence quenching from matrix elements is unlikely at levels below 1000 μg ml^{-1}.

In this work neither the magnitudes nor the nature, *i.e.* enhancement or depression, of the interferences in the argon–hydrogen flame correlated with those reported by Nakahara *et al.*[7] for the atomic absorption of tin. However, this observation was not unexpected because the stoichiometry of the argon–hydrogen flame used here was different from the stoichiometry of the flame used by Nakahara *et al.*[7], whose gas flows were 7.2 l H_2 min^{-1} and 4.5 l A min^{-1}. Browner *et al.*[1] have shown that flame conditions have a marked affect on interferences with tin fluorescence in the argon–oxygen–hydrogen flame.

The effects of a few elements on the fluorescence of tin in neutral aqueous solution were studied for comparison with the interferences in 0.4 *M* hydrochloric acid solution. The measurements were taken soon after preparation of the aqueous solutions; the results are given in Table III. It can be seen that 0.4 *M* hydrochloric acid tends to reduce interferences in general, but for some elements, *e.g.* chromium, the interference changes from an enhancement in aqueous solution to a depression in the acid solution.

The effect of iron(III) on interferences

The effect of both iron(III) chloride and iron(III) nitrate on the atomic fluorescence of tin were the same (Fig. 2 and Table II). In view of the findings of Nakahara *et al.*[7] that iron(III) chloride eliminated the interference of most elements in the atomic absorption determination of tin, it was reasonable to suppose that iron would have a similar effect on the atomic fluorescence of tin. Figure 3

TABLE III

INTERFERENCES WITH TIN ATOMIC FLUORESCENCE FROM AQUEOUS SOLUTION

(10 p.p.m. tin, 100 p.p.m. interfering ion; all solutions made up with deionized water. Argon–hydrogen flame at 317.5 nm; the same metal salts were used as in Table II, superscripts [a] to [i]

Element	*Relative fluorescence*	*Element*	*Relative fluorescence*	*Element*	*Relative fluorescence*
Al[a]	1.46	Fe[a]	2.07	Pb[d]	2.17
As[c]	1.04	Mn[b]	1.52	Ti[g]	1.84
Co[a]	2.28	Mo[e]	1.76	V[b]	1.24
Cr[d]	1.11	Nb[f]	1.26	W[i]	1.44
Cu[d]	2.04	Ni[b]	1.12		

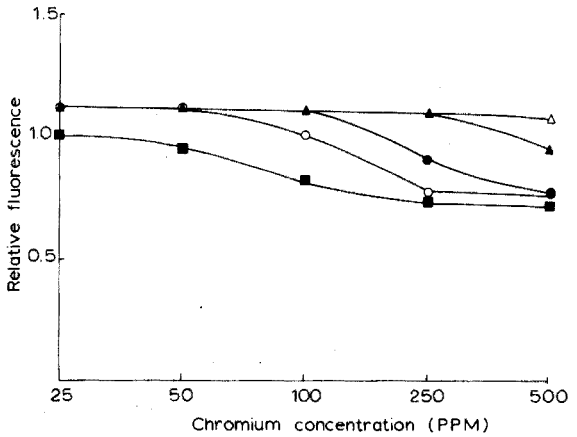

Fig. 3. Effect of iron on the interference from chromium. Solutions 0.4 *M* in hydrochloric acid, 10 p.p.m. tin. Flame, argon–hydrogen. Concentrations of iron added (■) 0 p.p.m., (○) 25 p.p.m., (●) 100 p.p.m., (▲) 500 p.p.m., (△) 1000 p.p.m.

shows how the addition of iron(III) chloride affects the interference of chromium on tin fluorescence in the argon–hydrogen flame; the interference of chromium is eliminated in the presence of 1000 p.p.m. iron. Thus the effect of iron in both atomic absorption[7] and atomic fluorescence is the same. Iron (1000 p.p.m.) similarly removed the interference from chromium in the argon–oxygen–hydrogen and air–acetylene flames, as well as eliminating the interference from most of the other elements studied (Table IV). Iron was as effective in removing interferences in the argon–oxygen–hydrogen flame as it was in the argon–hydrogen flame but was most effective in the air–acetylene flame. In deciding which flame to use for a particular matrix, both the better sensitivity of the argon flames and the interference effects in all three flames must be taken into account.

The effect of iron on the interference from acids

In the argon flames, 1000 p.p.m. iron failed to remove the interference from the acids studied except for hydrochloric acid. In the acetylene flame, only phosphoric,

sulphuric and hydrofluoric acids interfered (Table V). The enhancement, in the argon flames, from iron in the presence of hydrochloric acid is the same as the enhancement from iron in neutral aqueous 10 p.p.m. tin solutions.

TABLE IV

THE EFFECT OF IRON ON THE INTERFERENCE FROM OTHER ELEMENTS

(10 p.p.m. tin, 1000 p.p.m. iron(III) chloride. Results expressed as the ratio of the fluorescence of tin in the presence of 100 p.p.m. interfering ion and 1000 p.p.m. iron to the fluorescence of tin in the presence of 1000 p.p.m. iron alone. All solutions made up with 0.4 *M* hydrochloric acid. Elements were added in the forms indicated in Table II)

Element	*Relative fluorescence*			*Element*	*Relative fluorescence*		
	Air–C_2H_2	*Ar–H_2*	*Ar–O_2–H_2*		*Air–C_2H_2*	*Ar–H_2*	*Ar–O_2–H_2*
Al	1.00	1.00	1.00	Mn	1.00	1.00	1.00
Al	1.58	0.96	1.00	Mo	1.00	0.90	1.00
As	1.00	1.00	1.07	Nb	1.31	1.02	1.05
Bi	1.00	1.00	1.00	Ni	1.00	0.81	1.00
Ba	1.00	1.02	1.02	Pb	1.00	1.00	1.00
Ca	1.00	1.00	1.00	Rb	1.00	1.00	1.00
Cd	1.00	1.00	1.00	Sb	1.00	0.84	0.89
Ce	1.08	1.00	1.02	Sr	1.00	1.00	1.02
Co	1.00	1.00	1.00	Ti	1.35	1.04	1.02
Cr	1.00	1.00	1.00	V	1.00	0.98	0.94
Cu	1.00	1.00	1.00	W	1.00	1.00	1.00
Fe	1.00	1.00	1.00	Zn	1.00	0.98	1.00
La	1.19	1.00	1.00	Zn	1.00	1.00	1.00
Mg	1.00	0.96	0.96	Zr	1.46	1.00	1.00

TABLE V

THE EFFECT OF IRON ON INTERFERENCES FROM ACIDS

(10 p.p.m. tin; all solutions made up with deionized water. Results expressed as the ratio of the fluorescence of tin in the presence of acid and 1000 p.p.m. iron to the fluorescence of the aqueous tin solution containing neither acid nor iron)

Acid	*Concentration of acid (% (v/v))*	*Relative fluorescence*		
		Air–C_2H_2	*Ar–H_2*	*Ar–O_2–H_2*
Hydrochloric	10	1.00	2.08	2.52
Phosphoric	10	0.69	0.19	0.22
Nitric	10	1.00	1.27	1.31
Sulphuric	10	0.47	0.23	0.29
Perchloric	10	1.00	1.23	1.27
Hydrofluoric	1	1.20	1.96	1.68
0.4 *M* Hydrochloric acid, no iron(III) chloride		1.00	1.52	1.36
Aqueous tin, no acid, 1000 p.p.m. iron(III)-chloride		1.00	2.08	2.52

The effect of organic solvents

Aqueous tin solutions (10 p.p.m.) containing 10% concentrations of a range of organic liquids were nebulized, and the fluorescence was measured. In the argon flames, acetone, acetic acid, ethanol and methyl ethyl ketone all depressed the fluorescence of tin. Acetic acid gave the smallest depression (36.5%), and methyl ethyl ketone the largest (92.7%). Iron (1000 p.p.m.) had a releasing effect in all cases but not enough to restore the signal completely. In the air–acetylene flame all the organic liquids enhanced the signal by 5%, and the addition of 1000 p.p.m. iron had no effect.

Analytical curves and detection limits

Analytical curves in all three flames were linear between the detection limit and 250 p.p.m. The calibration solutions used to obtain the analytical curves were 0.4 *M* in hydrochloric acid and each contained 1000 p.p.m. iron(III) chloride.

The work described here was carried out with the instrumentation described in Part I of this series[9]. After the work had been completed, two of the original mirrors were replaced by larger diameter, better quality mirrors. Also the electrodeless discharge lamp was thermostated to allow control of its radiant output[14]. Detection limits obtained when the new mirrors, thermostated lamp and a 18.2-s time constant were used, were: 0.05 p.p.m. in the argon-separated air–acetylene flame; 0.006 p.p.m. in the argon–oxygen–hydrogen and argon–hydrogen flames, and 3 p.p.m. in the argon-separated nitrous oxide–acetylene flame. These detection limits are the concentrations of standard solutions containing 1000 p.p.m. iron(III) chloride which gave a signal-to-noise ratio of two.

A more detailed account of the effect of the thermostated lamp and the new mirrors will be given in Part III.

CONCLUSIONS

Interelement effects in both the atomic absorption and the atomic fluorescence spectrometry of tin follow the same basic trends. The use of iron(III) chloride to eliminate the interferences has a similar effect in both techniques. The detection limit for the determination of tin by atomic fluorescence with the argon–hydrogen or the argon–oxygen–hydrogen flame is nearly an order of magnitude lower than the published figures for the atomic absorption method. The detection limit in the argon-separated air–acetylene flame is similar to the atomic absorption detection limits for the argon–hydrogen flame. The best reported detection limits for atomic fluorescence determinations of metals have usually been obtained with cool flames where the power yield of fluorescence is high. However, Browner and Manning[15] have pointed out that practical analyses often require the use of higher temperature flames (*e.g.* air–acetylene and nitrous oxide–acetylene) which often give few interferences. The present work shows that tin atomic fluorescence with the air–acetylene flame can give low detection limits, whereas in atomic absorption it is necessary to use the interference-prone cool flames to achieve the same sensitivity.

Although the potential of atomic fluorescence has been appreciated for some time, applications of the technique have been limited, mainly because of the difficulties encountered during operation of microwave-excited electrodeless discharge lamps.

In this work, it was found that the reproducibility of the spectral radiance and stability of the tin lamp were considerably improved by introduction of temperature control.

The authors acknowledge with thanks the Science Research Council for the provision of an S.R.C. (CAPS) studentship for one of us (R.G.M.). Our thanks are also due to BISRA, the Corporate Laboratories of the British Steel Corporation, for the loan of equipment.

SUMMARY

The interference effects are reported for 27 elements, 6 acids and 4 organic liquids on the atomic fluorescence determination of tin with argon–hydrogen, argon–oxygen–hydrogen and argon-separated air–acetylene flames. The addition of 1000 p.p.m. iron(III) eliminates most interferences from the elements but not from the acids. The basic trends in the interference effects in the argon–hydrogen flame for the atomic absorption and atomic fluorescence determinations of tin are similar. The detection limit, for an 18.2-s time constant, in the argon–oxygen–hydrogen and argon–hydrogen flames is 0.006 p.p.m. and in the air–acetylene flame it is 0.05 p.p.m. These detection limits are significantly better than previously reported limits. Analytical curves in all three flames studied are linear between the detection limits and 250 p.p.m.

REFERENCES

1 R. F. Browner, R. M. Dagnall and T. S. West, *Anal. Chim. Acta*, 46 (1969) 207.
2 J. D. Winefordner and R. C. Elser, *Anal. Chem.*, 43(4) (1971) 24A.
3 J. A. Bowman, *Anal. Chim. Acta*, 42 (1968) 285.
4 T. M. Quarrell, R. J. W. Powell and H. J. Cluley, *Analyst (London)*, 98 (1973) 443.
5 K. E. Burke, *Analyst (London)*, 97 (1972) 19.
6 J. B. Headridge and A. Sowerbutts, *Analyst (London)*, 97 (1972) 442.
7 T. Nakahara, M. Munemori and S. Musha, *Anal. Chim. Acta*, 62 (1972) 267.
8 G. F. Kirkbright and T. S. West, *Chem. Br.*, 8 (1972) 428.
9 D. P. Hubbard and R. G. Michel, *Anal. Chim. Acta*, 67 (1973) 55.
10 A. E. Smith, *Analyst (London)*, 98 (1973) 209.
11 P. Benetti, N. Omenetto and G. Rossi, *Appl. Spectrosc.*, 25 (1971) 57.
12 P. O. Juliano and W. W. Harrison, *Anal. Chem.*, 42 (1970) 84.
13 J. D. Winefordner, S. G. Schulman and T. C. O'Haver, *Luminescence Spectrometry in Analytical Chemistry*, Vol. 38 in *Chemical Analysis*, Wiley-Interscience, New York, 1972.
14 R. F. Browner and J. D. Winefordner, *Spectrochim. Acta, Part B*, 25 (1973) 263.
15 R. F. Browner and D. C. Manning, *Anal. Chem.*, 44 (1972) 843.

Analytica Chimica Acta, 72 (1974) 295–305

METAL COMPLEXES OF AROMATIC SCHIFF BASE COMPOUNDS

PART 1. THE FLUORESCENCE PROPERTIES OF ALUMINIUM AND GALLIUM COMPLEXES OF AROMATIC SCHIFF BASES AND THEIR USE IN FLUORIMETRY

KIYOTOSHI MORISIGE

Department of Fundamental Education, Faculty of Science and Technology, Kinki University, Kowakae, Higashi-Osaka (Japan)

(Received 18th February 1974)

Aromatic Schiff base compounds, of the salicylidene-*o*-aminophenol type, have been studied as useful fluorimetric reagents for aluminium, magnesium, and other metal ions[1–7]. Argauer and White synthesized 31 aromatic Schiff bases, and investigated the fluorescence properties of aluminium complexes in 95% ethanol solution and magnesium complexes in dimethylformamide (DMF), to elucidate the effect of substituent groups[7]. However, as they obtained the fluorescence intensities of all the complexes under the same conditions, *i.e.* excitation at 420 nm and emission at 510 nm, the effect of the substitution on the fluorescence spectrum was not considered.

o,o'-Dihydroxy Schiff base compounds, in analogy with *o,o'*-dihydroxyazo compounds[8–10], form fluoresent gallium complexes. Nevertheless, most of the research so far has dealt with aluminium, magnesium[7], and scandium[11] complexes, but not gallium complexes.

The author has synthesized 87 Schiff bases, most of which are derived from salicylidene-*o*-aminophenol (2-hydroxyaniline-*N*-salicylidene), and compared the fluorescences of aluminium, gallium and other metal complexes in 8% DMF solution. The present paper describes the fluorescence properties of the aluminium and gallium complexes with 9 Schiff bases, *i.e.* 2-hydroxyaniline-*N*-salicylidene and eight derivatives, of which the fluorescence sensitivities were more than twice that of 2-hydroxyaniline-*N*-salicylidene. The optimal conditions for the fluorimetric determination of aluminium and gallium were also established.

EXPERIMENTAL

Apparatus and materials

Fluorescence measurements were made with a Hitachi fluorescence spectrophotometer, Model 204 (the source is a 150-W Xenon lamp). A Hitachi–Horiba glass electrode pH Meter, Model M-5, was used for the pH measurements.

Schiff base compounds. The nine Schiff bases used in this investigation are listed in Table I. Compounds II–VII are derivatives of compound I (2-hydroxyaniline-*N*-salicylidene). A sulfo-, methoxy-, chloro-, ethoxy-, or carboxy group was

TABLE I ELEMENTAL ANALYSIS OF SCHIFF BASE COMPOUNDS

Compd. no.	*Schiff base compound*		*Elemental analysis (%)*			*Amino component*	*Aldehyde component*
			C	*H*	*N*		
I	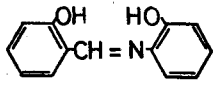	2-Hydroxyaniline-*N*-salicylidene	*Found* 72.90 *Calcd.* 73.16	5.10 5.16	6.65 6.75	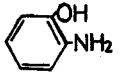	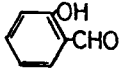
II	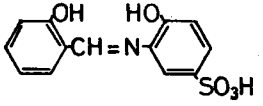	2-Hydroxy-5-sulfoaniline-*N*-salicylidene	*Found* 53.15 *Calcd.* 53.20	3.70 3.75	4.90 4.77	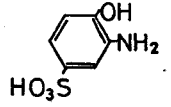	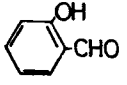
III	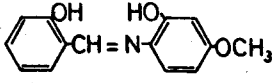	2-Hydroxy-4-methoxyaniline-*N*-salicylidene	*Found* 69.00 *Calcd.* 69.07	5.30 5.34	5.71 5.76	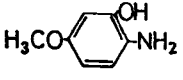	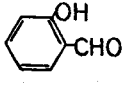
IV	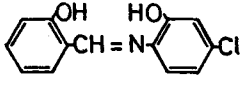	2-Hydroxy-4-chloroaniline-*N*-salicylidene	*Found* 62.81 *Calcd.* 62.98	4.00 4.04	5.55 5.65	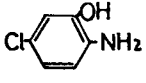	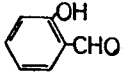
V	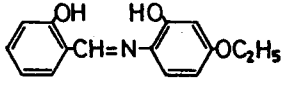	2-Hydroxy-4-ethoxyaniline-*N*-salicylidene	*Found* 69.81 *Calcd.* 69.97	5.70 5.83	5.37 5.44	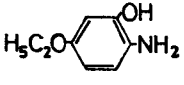	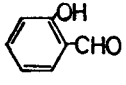
VI	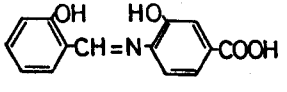	2-Hydroxy-4-carboxyaniline-*N*-salicylidene	*Found* 65.20 *Calcd.* 65.31	4.20 4.28	5.38 5.44	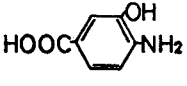	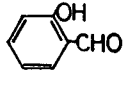
VII	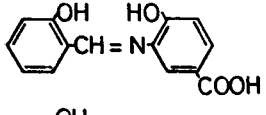	2-Hydroxy-5-carboxyaniline-*N*-salicylidene	*Found* 65.18 *Calcd.* 65.31	4.19 4.28	5.32 5.44	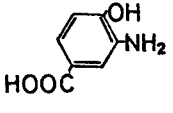	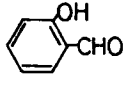
VIII	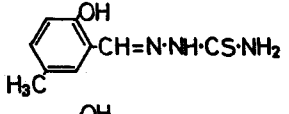	2-Hydroxy-5-methylbenzaldehyde thiosemicarbazone					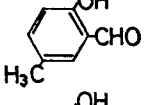
IX	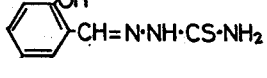	2-Hydroxy-5-chlorobenzaldehyde thiosemicarbazone					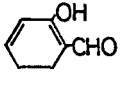

substituted for the hydrogen atom at the *m*- or *p*-position on the *N*-ring of compound I. Compounds VIII and IX are benzaldehyde thiosemicarbazones. These compounds were synthesized by condensation of salicylaldehyde with the appropriate amino compounds at 100°C for 30 min[12]. The products obtained were purified by repeated recrystallization from ethanol, and were dried at room temperature over silica gel in a desiccator.

Schiff base solution. Schiff base (0.1 g) was dissolved in *N*,*N*-dimethylformamide (Dotite Spectrosol solvent) and diluted to 100 ml.

Standard solutions of aluminium and gallium. A stock solution of aluminium was prepared by dissolving 1.6803 g of aluminium in water containing 5 ml of concentrated hydrochloric acid, and diluting the solution to 100 ml. The stock solution was diluted with water to make a standard solution containing 1.00 μg Al ml^{-1}. A stock solution of gallium was prepared by dissolving 0.1344 g of Ga_2O_3 (99.99%) with 10 ml of 6 *M* hydrochloric acid, and diluting to 100 ml with water (1 mg Ga ml^{-1}). The stock solution was diluted with 0.1 *M* hydrochloric acid to give a standard solution of 1.00 μg Ga ml^{-1}.

Uranine and quinine sulfate standard solutions. Uranine (0.1 g; Nakarai Chemicals Ltd.) was dissolved in 100 ml of water, and the solution was diluted with water to give solutions containing 0.125–1.00 μg ml^{-1}. Quinine (0.1 g; Nakarai Chemicals Ltd.) was dissolved in 100 ml of 0.1 *M* sulfuric acid, and the solution was diluted with 0.1 *M* sulfuric acid to give solutions containing 0.1–1.00 μg ml^{-1}. These solutions were employed as reference standards of fluorescence in adjusting the sensitivity of the instrument.

General procedure

To 10–15 ml of a sample solution containing an appropriate amount of aluminium ion or gallium ion, add the quantity of 0.1% Schiff base solution and 0.5–2 ml of 20% ammonium acetate solution. Adjust the pH value to the required value with a dilute hydrochloric acid solution or an ammonia solution, and then dilute the solution to 25 ml with water. If the reaction is slow, warm the solution at 50°C for 10 min after the final dilution. Measure the fluorescence intensity at the optimal excitation and maximal fluorescence wavelengths, using an uranine solution or a quinine solution as the reference standard*.

FLUORESCENCE PROPERTIES OF METAL–SCHIFF BASE COMPLEXES

Most of O,O′- or O′,S-coordinating Schiff base compounds synthesized react with aluminium and gallium ions to form fluorescent complexes. Table II shows the fluorescence properties of the complexes with compounds I–IX; in all cases, the complexes have a 1:1 metal–ligand ratio.

Aluminium and gallium complexes with compounds I–VII emit greenish yellow fluorescence, whereas the gallium complexes with compounds VIII and IX show blue fluorescence. The latter two compounds do not react with aluminium.

The fluorescence intensities of the aluminium complexes obtained under the

* The fluorescence spectra were not corrected, since the present research was done principally for analytical purposes.

TABLE II

OPTIMAL FLUORESCENCE CONDITIONS FOR ALUMINIUM AND GALLIUM COMPLEXES WITH SCHIFF BASE COMPOUNDS

Compd. no.	*Ion*	$\lambda_{excitation}$ *(nm)*	$\lambda_{emission}$ *(nm)*	*pH*	*Standing time*	*Relative fluorescence intensity*[a]	
						Net intensity per 1 μg metal	*Reagent blank*
I	Al	405	505	5.8	50°C, 10 min.	51.9	17.5
	Ga	410	515	4.0	5 min., room temp.	6.6	4.0
II	Al	405	480	5.5	50°C, 10 min.	125.0	4.6
	Ga	410	490	3.7	5 min., room temp.	22.2	2.0
III	Al	420	505	5.0	50°C, 10 min.	120.7	12.4
	Ga	420	510	3.3	5 min., room temp.	17.6	3.6
IV	Al	405	490	5.3	50°C, 10 min.	122.7	4.2
	Ga	410	500	3.8	5 min., room temp.	20.7	1.5
V	Al	415	495	5.5	50°C, 10 min.	113.0	3.8
	Ga	415	510	3.7	5 min., room temp.	15.2	1.5
VI	Al	415	505	5.6	50°C, 10 min.	101.6	7.4
	Ga	420	510	3.5	5 min., room temp.	28.1	5.5
VII	Al	400	490	5.0	50°C, 10 min.	102.6	2.5
	Ga	400	495	3.5	5 min., room temp.	20.3	1.2
VIII	Al	—	—	—	—	—	—
	Ga	385	465	4.5	5 min., room temp.	10.8	6.7
IX	Al	—	—	—	—	—	—
	Ga	385	450	4.5	5 min., room temp.	17.5	11.0

[a] Fluorescence intensities were measured at maximal fluorescence wavelength. The sensitivity of the fluorimeter was regulated by setting the fluorescence of the standard uranine solution (0.125 μg ml^{-1}) at 100 div., 488 nm/510 nm.

optimal conditions increase in the following order: compound I $<$VI$\leqslant$VII$<$V-$<$III$\leqslant$IV$<$II; or with respect to the substituent group: (hydrogen)$<$carboxy-$<$ethoxy-$<$methoxy-$\leqslant$chloro-$<$sulfo- group.

For the gallium complexes, the order is I$<$VIII$<$V$<$IX$\leqslant$III$<$VII$\leqslant$IV-$\leqslant$II$<$VI. An interesting fact concerning the effect of the substitution is that

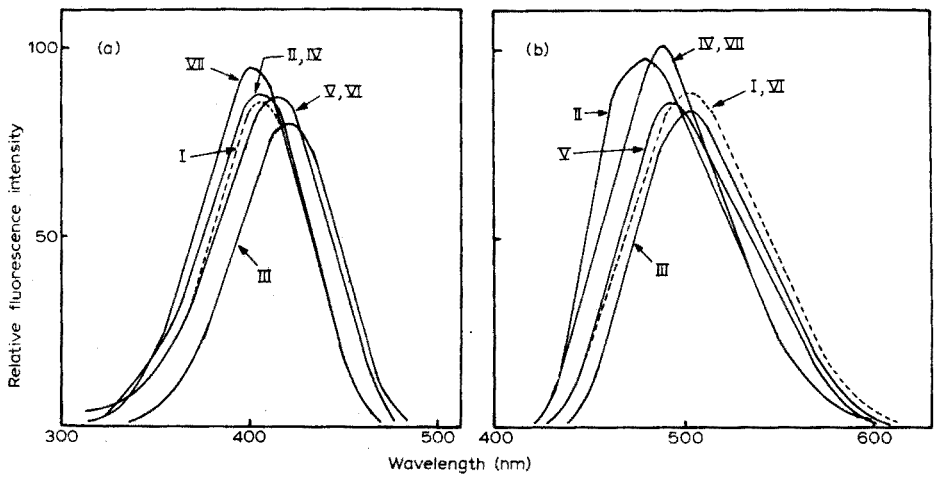

Fig. 1. Excitation (a) and emission (b) spectra of aluminium complexes with Schiff base compounds. Emission and excitation wavelengths for (a) and (b), respectively, were as follows: Compound I, λ_{em} 505 nm, λ_{ex} 405 nm. Compound II, λ_{em} 480 nm, λ_{ex} 405 nm. Compound III, λ_{em} 505 nm, λ_{ex} 420 nm. Compound IV, λ_{em} 490 nm, λ_{ex} 405 nm. Compound V, λ_{em} 495 nm, λ_{ex} 415 nm. Compound VI, λ_{em} 505 nm, λ_{ex} 415 nm. Compound VII, λ_{em} 490 nm, λ_{ex} 400 nm.

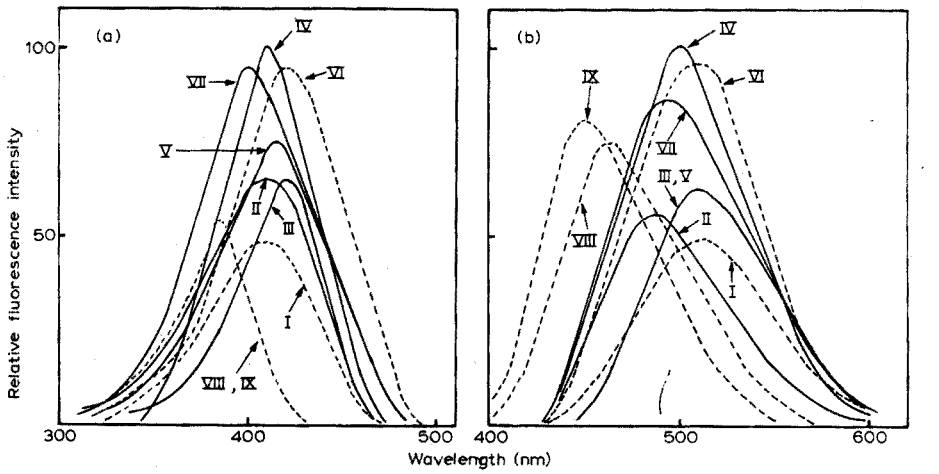

Fig. 2. Excitation (a) and emission (b) spectra of gallium complexes with Schiff base compounds. Emission and excitation wavelengths for (a) and (b), respectively, were as follows: Compound I, λ_{em} 515 nm, λ_{ex} 410 nm; Compound II, λ_{em} 490 nm, λ_{ex} 410 nm. Compound III, λ_{em} 510 nm, λ_{ex} 420 nm. Compound IV, λ_{em} 500 nm, λ_{ex} 410 nm. Compound V, λ_{em} 510 nm, λ_{ex} 415 nm. Compound VI, λ_{em} 510 nm, λ_{ex} 420 nm. Compound VII, λ_{em} 495 nm, λ_{ex} 400 nm. Compound VIII, λ_{em} 465 nm, λ_{ex} 385 nm. Compound IX, λ_{em} 450 nm, λ_{ex} 385 nm.

substitution on the *N*-ring of the azomethine compounds intensifies, while substitution on the α-ring reduces, the fluorescence of the complexes, although the evidence for the latter effect is not presented here. The effect of substitution on the α-ring will be reported later.

Excitation and emission spectra of the aluminium and gallium complexes are shown in Figs. 1 and 2. Effective excitation wavelengths are 400–420 nm for the aluminium complexes, and 385–420 nm for the gallium complexes. The fluorescence bands of these complexes lie in the region from 400 to 600 nm; the fluorescence maxima of the aluminium complexes occur at wavelengths of 480–505 nm, and those of the gallium complexes at wavelengths of 450–515 nm. As shown in Figs. 1(b) and 2(b), substitution on the *N*-ring shifts the maximum to shorter wavelengths; the blue shift is significant in the case of benzaldehydethiosemicarbazones.

From these results, compounds II, IV and VII appear to be favorable reagents for the determination of aluminum, while compounds II, VI, VII, VIII and IX are suitable for gallium, because of low blank fluorescence and their excellent stability. Moreover, compounds VIII and IX are selective reagents for gallium, because they do not react with aluminium.

FLUORIMETRIC DETERMINATION OF ALUMINIUM AND GALLIUM

As described above, Schiff bases are useful fluorimetric reagents, and the analytical conditions were therefore investigated.

Effect of standing time

Because the reactions of all the Schiff bases with aluminium are very slow, the solutions must be warmed at 50°C for 10 min after the pH adjustment. Gallium complexes show full fluorescence immediately after the pH adjustment. The fluorescence is stable for 3 h at least. Figures 3 and 4 show the stability of some of the fluorescent complexes of aluminium and gallium.

Effect of pH

The effect of pH on the fluorescence intensity of the metal complexes is indicated in Fig. 5. Aluminium complexes show maximal fluorescence in the pH region 5–5.8, and gallium complexes in the pH region 3.5–4.5.

Effect of reagent concentration

Various amounts of 0.1% Schiff base solution were added to the solution containing 1–2 μg of aluminium or 3–5 μg of gallium, and the fluorescence intensity was measured at the optimal pH. Figure 6 shows the results obtained from the aluminium–compound II, IV, and VII systems and the gallium–compound II, VI, VII, VIII and IX systems. The Figure indicates that the addition of 2 ml of 0.1% reagent solution is adequate in all cases.

Calibration curves

Figures 7 and 8 present the calibration curves for the aluminium–compound II, IV and VII systems and the gallium–compound II, VI, VII, VIII and IX

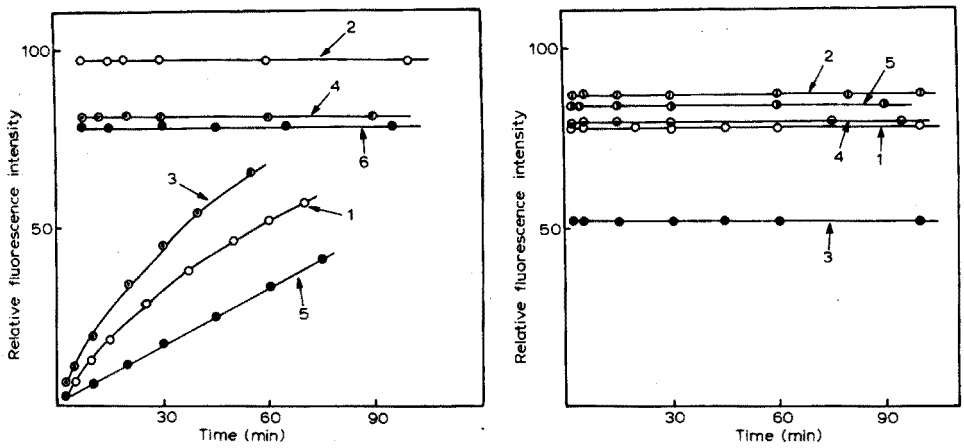

Fig. 3. Stability of fluorescence intensity of aluminium–Schiff base complexes. In all cases, 1 μg Al was used. (1) Compound II, room temp., 405 nm/480 nm, fluorimeter readings set at 10 div. with 1.0 μg uranine/ml reference solution. (2) Compound II, digested at 50°C for 10 min., 405 nm/480 nm, 10 div. (3) Compound IV, room temp., 405 nm/490 nm, 20 div. (1.0 μg/ml uranine). (4) Compound IV, digested at 50°C for 10 min., 405 nm/490 nm, 20 div. (5) Compound VII, room temp., 400 nm/490 nm, 15 div. (0.5 μg/ml uranine). (6) Compound VII, digested at 50°C for 10 min., 400 nm/490 nm, 15 div.

Fig. 4. Stability of fluorescence intensity of gallium–Schiff base complexes. 5 μg of gallium was used (except for line 4) and reactions proceeded at room temperature. (1) Compound II, 410 nm/490 nm, 30 div. (1.0 μg/ml uranine). (2) Compound VI, 420 nm/510 nm, 20 div. (0.25 μg/ml uranine). (3) Compound VII, 400 nm/495 nm, 10 div. (0.5 μg/ml uranine). (4) Compound VIII, 3 μg Ga, 385 nm/465 nm, 10 div. (0.25 μg/ml quinine). (5) Compound IX, 385 nm/450 nm, 10 div. (0.5 μg/ml quinine).

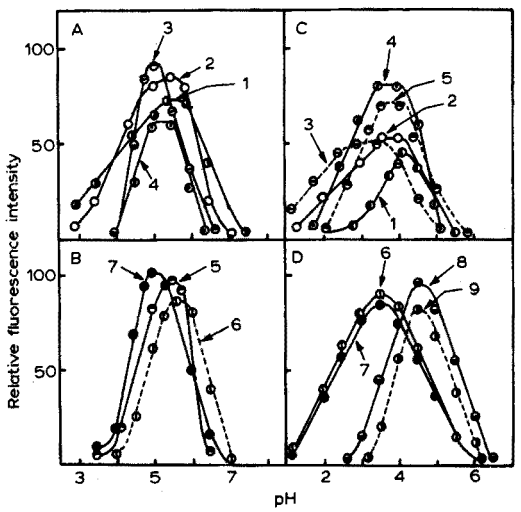

Fig. 5. Effect of pH of solution on fluorescence intensity. A-(1) Al–compound I; A-(2) Al–compound II; A-(3) Al–compound III; A-(4) Al–compound IV; B-(5) Al–compound V; B-(6) Al–compound VI; B-(7) Al–compound VII; C-(1) Ga–compound I; C-(2) Ga–compound II; C-(3) Ga–compound III; C-(4) Ga–compound IV; C-(5) Ga–compound V; D-(6) Ga–compound IV; D-(7) Ga–compound VII; D-(8) Ga–compound VIII; D-(9) Ga–compound IX.

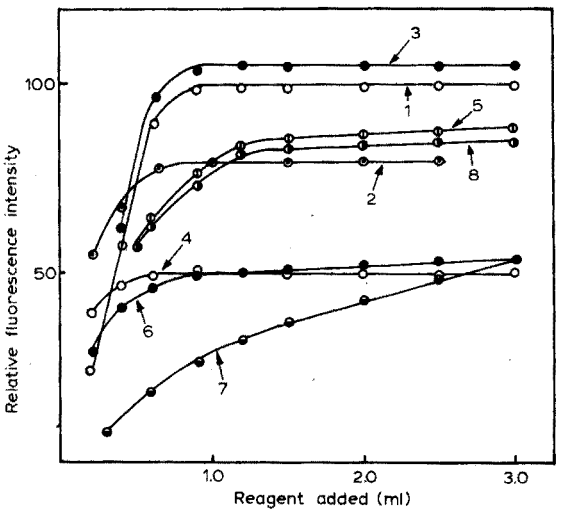

Fig. 6. Effect of reagent concentration. (1) Al–compound II, 1 μg Al, 405 nm/480 nm 10 div. *vs.* 1.0 μg uranine/ml. (2) Al–compound IV, 1 μg Al, 405 nm/490 nm 20 div. *vs.* 1.0 μg uranine/ml. (3) Al–compound VII, 2 μg Al, 400 nm/490 nm 10 div. *vs.* 0.5 μg uranine/ml. (4) Ga–compound II, 5 μg Ga, 410 nm/490 nm 20 div. *vs.* 1.0 μg uranine/ml. (5) Ga–compound VI, 5 μg Ga, 420 nm/510 nm 20 div. *vs.* 0.25 μg uranine/ml. (6) Ga–compound VII, 5 μg Ga, 400 nm/495 nm 10 div. *vs.* 0.5 μg uranine/ml. (7) Ga–compound VIII, 3 μg Ga, 385 nm/465 nm 10 div. *vs.* 0.5 μg quinine/ml. (8) Ga–complex IX, 3 μg Ga, 385 nm/450 nm 10 div. *vs.* 0.5 μg quinine/ml.

systems, respectively. The sensitivity of the fluorimeter was set with 0.125–1 μg ml^{-1} uranine solution as the reference standard, except for the gallium–compound VIII and IX systems, where 0.1 –0.5 μg ml^{-1} quinine solution (0.1 *M* sulfuric acid) was used.

Aluminium and gallium can be determined within a relative error of 3% in the following concentration ranges: for aluminium, 0.002–2 μg/25 ml with compound II and 0.005–3 μg/25 ml with compound IV or VII; for gallium, 0.05–5 μg/25 ml with compound II, 0.1–6 μg/25 ml with compound VI, 0.1–7 μg/25 ml with compound VII or IX, and 0.2–7 μg/25 ml with compound VIII.

Effect of diverse ions

The interferences of foreign cations in 100-fold amounts on the determination of aluminium or gallium ions were studied. For the determination of aluminium, no interference is caused by antimony(III), arsenic(III), barium(II), beryllium(II), boron(III), bismuth(III), cadmium(II), calcium(II), cerium(IV), europium(III), germanium(IV), lanthanum(III), magnesium(II), manganese(II), mercury(II), selenium(IV), strontium(II), thallium(I), tungsten(VI), yttrium(III) or zinc(II). Chromium(VI), cobalt(II), copper(II), gallium(III) and iron(III) cause negative errors. Indium(III), molybdenum(VI), nickel(II) and scandium cause negative errors with compound VII, but do not interfere with compounds II and IV. Tin(IV) gives a positive error with compound II, but a negative error with compound IV.

For the determination of gallium, negative errors are caused by chromium-(VI), copper(II), molybdenum(VI) and iron(III); cerium(IV), nickel(II), and tungsten(VI) cause negative errors with compounds VIII and IX, but do not

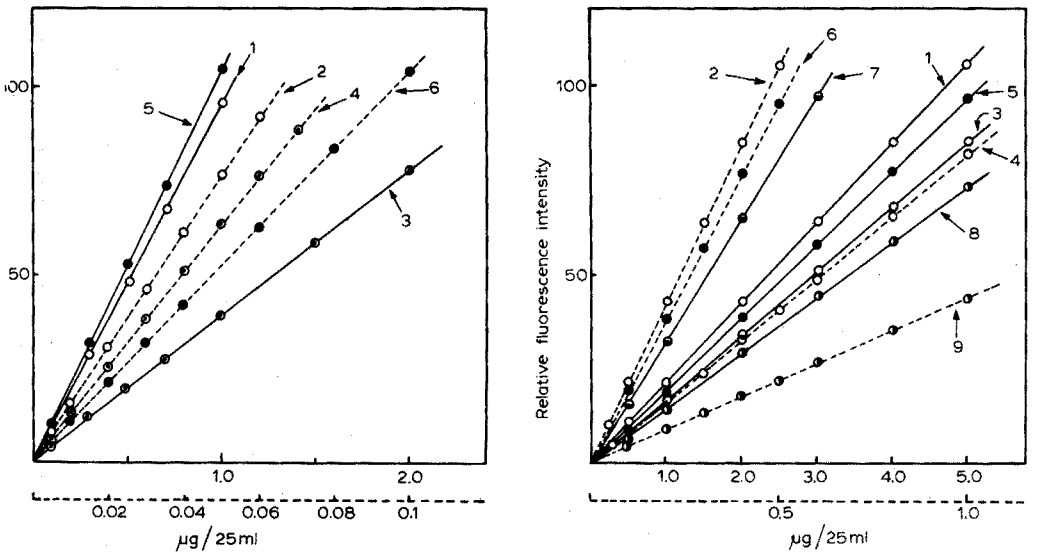

Fig. 7. Calibration curves for aluminium. (1) Al-compound II, 405 nm/480 nm, 10 div. *vs.* 1.0 μg uranine/ml. (2) Al-compound II, 40 div. *vs.* 0.25 μg uranine/ml. (3) Al-compound IV, 405 nm/490 nm 10 div. *vs.* 1.0 μg uranine/ml. (4) Al-compound IV, 80 div. *vs.* 0.25 μg uranine/ml. (5) Al-compound VII, 400 nm/490 nm. 20 div. *vs.* 0.5 μg uranine/ml. (6) Al-compound VII, 100 div. *vs.* 0.25 μg uranine/ml.

Fig. 8. Calibration curves for gallium. (1) Ga-compound II, 410 nm/490 nm, 40 div. *vs.* 1.0 μg uranine/ml. (2) Ga-compound II, 100 div. *vs.* 0.25 μg uranine/ml. (3) Ga-compound VI, 420 nm/510 nm, 20 div. *vs.* 0.25 μg uranine/ml. (4) Ga-compound VI, 100 div. *vs.* 0.25 μg uranine/ml. (5) Ga-compound VII, 400 nm/495 nm, 20 div. *vs.* 0.5 μg uranine/ml. (6) Ga-compound VII, 100 div. *vs.* 0.25 μg uranine/ml. (7) Ga-compound VIII, 385 nm/465 nm, 15 div. *vs.* 0.25 μg quinine/ml. (8) Ga-compound IX, 385 nm/450 nm, 10 div. *vs.* 0.5 μg quinine/ml. (9) Ga-compound IX, 15 div. *vs.* 0.25 μg quinine/ml.

interfere in other systems. Cobalt(II) causes negative errors, except in the compound VI and VII systems. Tin(IV) gives positive errors in the compound II, VI and VII systems, but negative errors in other systems. Indium(III) gives positive errors in the compound VIII and IX systems. Aluminium(III) causes positive errors, except in the gallium–compounds VIII or IX system.

Determination of metal–ligand ratio

The metal–ligand ratios in the aluminium and gallium complexes with Schiff bases could not be estimated fluorimetrically by the mole-ratio method or by the continuous variations method. Accordingly, the kinetic method, which had been successfully used for the complexes with azo compounds[8–10], was applied. The results for the aluminium–compound II, IV and VII complexes are indicated in Fig. 9, which indicates a metal–ligand ratio of 1:1. Table III summarizes the results of the elemental analyses of the aluminium complexes with compounds I, II, III, IV and VII, and the gallium complexes with compound I. The results again indicate that the metal–ligand ratios are 1:1 in these crystalline complexes.

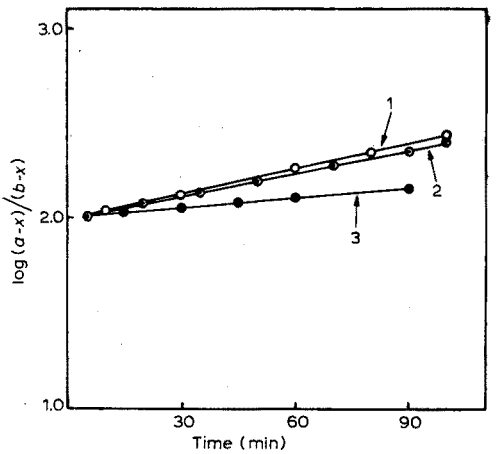

Fig. 9. Kinetics of complex formation as indicated by fluorescence; a is initial concentration of compound II, IV and VII, b is initial concentration of aluminium, and x is concentration of complex as indicated by fluorescence. (1) Al–compound II system, $a=300$ μmol, $b=3$ μmol; (2) Al–compound IV system, $a=300$ μmol, $b=3$ μmol; (3) Al–compound VII system, $a=300$ μmol, $b=3$ μmol.

TABLE III

ANALYSIS OF METAL–SCHIFF BASE COMPLEXES

Compd. no.	*Chemical formula*	*N (%)*		*Metal (%)*	
		Found	*Calcd.*	*Found*	*Calcd.*
I	$C_{13}H_9NO_2 \cdot Al \cdot 3H_2O$	4.72	4.79	9.25	9.24
I	$C_{13}H_9NO_2 \cdot Ga \cdot 3H_2O$	4.10	4.18	20.65	20.81
II	$C_{13}H_9NO_5S \cdot Al \cdot 3H_2O$	3.85	3.76	7.40	7.25
III	$C_{14}H_{11}NO_3 \cdot Al \cdot 3H_2O$	4.25	4.34	8.27	8.38
IV	$C_{13}H_8NO_2Cl \cdot Al \cdot 3H_2O$	4.12	4.28	8.18	8.26
VII	$C_{14}H_9NO_4 \cdot Al \cdot 3H_2O$	4.09	4.16	7.80	8.03

The author is investigating the fluorescence characteristics and chemical composition of metal complexes with various Schiff bases, and their application to fluorimetric analysis. The results will be reported later.

The author expresses his appreciation to Professor Tsunenobu Shigematsu (Institute for Chemical Research, Kyoto University), Professor Yasuharu Nishikawa and Assistant Professor Keizō Hiraki (Faculty of Science and Technology, Kinki University), and Professor Masayuki Tabushi (Tohoku Women's College) for their kind advice and suggestions.

SUMMARY

As fluorimetric reagents for aluminium and gallium, 87 Schiff base compounds were synthesized. Nine of these proved to be sensitive reagents, and the fluorescence properties of the aluminium and gallium complexes were studied. 2-Hydroxy-5-

sulfoaniline-*N*-salicylidene and 2-hydroxy-5-carboxyaniline-*N*-salicylidene were excellent in regard to sensitivity and stability. 2-Hydroxy-5-methylbenzaldehyde-thiosemicarbazone and 2-hydroxy-5-chlorobenzaldehyde-thiosemicarbazone formed fluorescent complexes with gallium but not aluminium, and are recommended as selective reagents for gallium. In all cases, 1:1 metal–ligand complexes are formed. Optimal reaction conditions and interference studies are described.

REFERENCES

1 R. M. Dagnall, R. Smith and T. S. West, *Talanta*, 13 (1966) 609.
2 N. B. Lebed and R. P. Pantaler, *Zavod. Lab.*, 31 (1965) 163.
3 R. M. Dagnall, R. Smith and T. S. West, *Chem. Ind.*, (1965) 1499.
4 V. V. Klimov, O. S. Didkovskaya, A. N. Kazachenko, *Zavod. Lab.*, 28 (1962) 652.
5 A. K. Babko and S. L. Lisichenok, *Ukr. Khim. Zh.*, 35 (1969) 98.
6 Z. Holzbecker, *Chem. Listy*, 52 (1958) 430.
7 R. J. Argauer and C. E. White, *Anal. Chem.*, 36 (1964) 2141.
8 K. Hiraki, *Bull. Chem. Soc. Jap.*, 45 (1972) 789.
9 K. Hiraki, *Bull. Chem. Soc. Jap.*, 45 (1972) 1395.
10 K. Hiraki, *Bull. Chem. Soc. Jap.*, 46 (1973) 2438.
11 G. F. Kirkbright, T. S. West and G. Woodward, *Analyst (London)*, 91 (1966) 23.
12 C. Donald, J. Freeman, and C. E. White, *J. Amer. Chem. Soc.*, 78 (1956) 2678.

Analytica Chimica Acta, 72 (1974) 307–314

ÉTUDE QUANTITATIVE D'ÉQUILIBRES CHIMIQUES EN SOLUTION DANS LES SELS FONDUS PAR SPECTROPHOTOMÉTRIE D'ABSORPTION

APPLICATION AU NEPTUNIUM

R. LYSY*, G. LANDRESSE** et G. DUYCKAERTS
Institut de Radiochimie, Université de Liège au Sart Tilman, B-4000 Liège (Belgique)
(Reçu le 30 avril 1974)

Dans un article précédent[1], nous avons décrit quelques propriétés chimiques du neptunium dans l'eutectique LiCl–KCl fondu en suivant les différentes réactions d'oxydo-réduction par spectrophotométrie d'absorption visible et proche i.r. Ce travail a comme but l'étude quantitative de réactions chimiques du neptunium dans le même eutectique et principalement de la réaction d'oxydo-réduction:

$$NpO_2^+ + 4\,HCl \rightleftharpoons Np^{4+} + 2\,H_2O + \tfrac{1}{2}\,Cl_2 + 3\,Cl^- \qquad (1)$$

L'évolution de l'équilibre (1) en fonction des pressions partielles en H_2O, HCl et Cl_2 est suivie par spectrophotométrie d'absorption.

APPAREILLAGES ET MANIPULATIONS

L'installation spectrophotométrique ainsi que le dispositif permettant le contrôle des pressions partielles en H_2O et HCl ont déjà été décrits[2,3]. La mesure du débit de chlore gazeux a été effectuée au moyen d'un débitmètre à flotteur sphérique en rubis, préalablement étalonné. La préparation des réactifs ainsi que les différentes manipulations des solutions de neptunium sont mentionnées dans une publication antérieure[1].

RÉSULTATS EXPÉRIMENTAUX ET DISCUSSION

Pour pouvoir effectuer l'étude quantitative de la réaction (1) par exemple, nous avons vérifié la loi de Beer–Lambert et déterminé les coefficients d'extinction des principales bandes des états d'oxydation III, IV et V du neptunium dans l'eutectique LiCl–KCl à 450°C (Fig. 1 et Tableau I). La concentration totale en neptunium est calculée d'après la relation:

$$c = \frac{1000\rho w}{M(W + xw)} \qquad (2)$$

* Chercheur agréé à l'Institut Interuniversitaire des Sciences Nucléaires.
** Chargé de Recherches au Fonds National de la Recherche Scientifique.

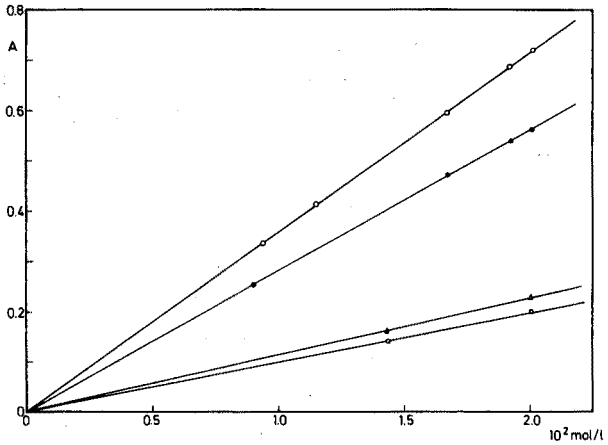

Fig. 1. Vérification de la loi de Beer–Lambert dans l'eutectique LiCl–KCl à 450°C. (○) Np(IV) à 935 nm; $\varepsilon^4_{935\,nm}=35{,}85$. (●) Np(V) à 990 nm; $\varepsilon^5_{990\,nm}=28{,}25$. (△) Np(III) à 1375 nm; $\varepsilon^3_{1375\,nm}=11{,}50$. (□) Np(III) à 1450 nm; $\varepsilon^3_{1450\,nm}=10{,}05$.

TABLEAU I

VARIATION DES COEFFICIENTS D'EXTINCTION MOLAIRE AVEC LA TEMPÉRATURE

T (°C)	ε^3_{1450} ($l\ mol^{-1}\ cm^{-1}$)	ε^3_{1375} ($l\ mol^{-1}\ cm^{-1}$)	ε^4_{935} ($l\ mol^{-1}\ cm^{-1}$)	ε^5_{990} ($l\ mol^{-1}\ cm^{-1}$)
400	11,2	12,6	37,8	32,35
450	10,0	11,5	35,85	28,3
500			34,8	26,3
550	9,0	10,35	34,4	23,95
600			33,9	22,7

dans laquelle c=concentration (mol. l^{-1}), ρ=poids spécifique du solvant à la température d'expérience, w=poids de Cs_2NpCl_6 ou $Cs_3NpO_2Cl_4$ (g), M=poids moléculaire de Cs_2NpCl_6 ou $Cs_3NpO_2Cl_4$, W=poids de solvant (g), xw=correction pour la participation de CsCl au solvant après fusion; $x=0{,}47$ pour Cs_2NpCl_6, $x=0{,}62$ pour $Cs_3NpO_2Cl_4$.

Le Tableau I représente la variation des coefficients d'extinction molaire en fonction de la température.

Détermination des concentrations dans une solution contenant Np^{4+} et NpO_2^+

Pour déterminer les concentrations en Np^{4+} et NpO_2^+ en solution (Fig. 2), la position de la ligne de base doit être fixée au préalable. L'absorption à 1237 nm est uniquement due à Np^{4+}; il en est de même en ce qui concerne NpO_2^+ à 1125 nm. On peut mesurer ainsi, sur des bains contenant uniquement soit Np^{4+}, soit NpO_2^+ les valeurs de x et y définies comme suit:

$$A^4_{1173}/A^4_{1237}=x \tag{3}$$

$$A^5_{1173}/A^5_{1125}=y \tag{4}$$

Par combinaison de (3) et (4) on obtient, pour le spectre du mélange

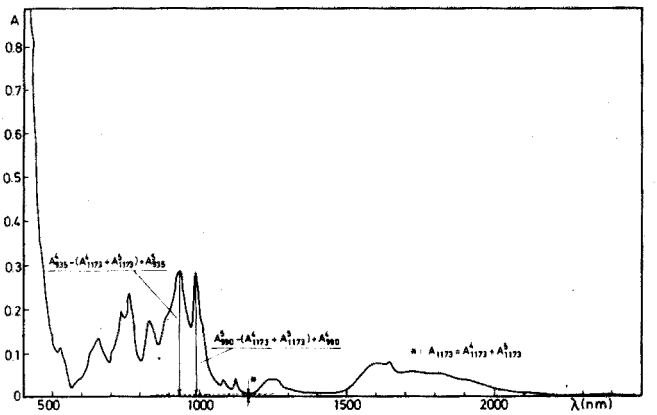

Fig. 2. Spectre d'une solution de Np^{4+} et NpO_2^+ dans l'eutectique LiCl–KCl à 450°C.

$$A_{1173} = A^4_{1173} + A^5_{1173} = xA_{1237} + yA_{1125} \tag{5}$$

En mesurant A_{1237} et A_{1125} on détermine aisément la position de la ligne de base.

Les concentrations sont déterminées à partir des deux bandes d'absorption principales, pour Np^{4+} à 935 nm et NpO_2^+ à 990 nm. Les deux bandes d'absorption étant relativement proches, il faut tenir compte de l'absorption des deux espèces aux deux longueurs d'onde considérées. En résolvant le système d'équation suivant:

$$A_{935} = (\varepsilon^4_{935} c_4 + \varepsilon^5_{935} c_5) l \tag{6}$$

$$A_{990} = (\varepsilon^5_{990} c_5 + \varepsilon^4_{990} c_4) l \tag{7}$$

on calcule (avec $l = 1{,}00$ cm) c_4 et c_5 qui désignent respectivement les concentrations en Np^{4+} et NpO_2^+.

Étude de la réaction d'oxydo-réduction NpO_2^+–Np^{4+}

La loi de Guldberg et Waage appliquée à la réaction (1) s'écrit:

$$[Np^{4+}] P^2_{H_2O} P^{\frac{1}{2}}_{Cl_2} / [NpO_2^+] P^4_{HCl} = K \tag{8}$$

L'expression (8) peut encore s'écrire:

$$\ln \frac{[Np^{4+}]}{[NpO_2^+]} = \ln \frac{c_4}{c_5} = \ln K - \ln \frac{P^2_{H_2O} P^{\frac{1}{2}}_{Cl_2}}{P^4_{HCl}} \tag{9}$$

Si on porte $\ln c_4/c_5$ en fonction de $\ln(P^2_{HO} P^{\frac{1}{2}}_{Cl_2}/P^4_{HCl})$, on doit obtenir une droite de pente unitaire dont l'ordonnée à l'origine donne la valeur du $\ln K$. Les expériences ont été réalisées aux températures de 450, 500, 550 et 600°C et les résultats sont repris dans le Tableau II. Figure 3 montre l'évolution du $\ln c_4/c_5$ en fonction de $\ln (P^2_{H_2O} P^{\frac{1}{2}}_{Cl_2}/P^4_{HCl})$. Les valeurs des pentes correspondent, aux erreurs expérimentales près, à la valeur théorique, ce qui confirme la stoechiométrie de la réaction (1). Le calcul des valeurs de K aux différentes températures est immédiat (Tableau III) et l'évolution du $\ln K$ en fonction de $1/T$ est représentée à la Fig. 4.

Dans le domaine de température prospecté, nous obtenons une droite dont la pente et l'ordonnée à l'origine fournissent les valeurs moyennes des variations

TABLEAU II

ÉTUDE DE LA RÉACTION D'OXYDO-RÉDUCTION NpO_2^+—Np^{4+}

T (°C)	$c_{tot} \cdot 10^2$ (mol l^{-1})	P_{tot} (mm Hg)	P_{HCl} (atm)	P_{Cl_2} (atm)	$P_{H_2O} \cdot 10^2$ (atm)	$\ln \frac{P_{H_2O}^2 P_{Cl_2}^{\frac{1}{2}}}{P_{HCl}^4} \cdot 10^7$	$c_4 \cdot 10^2$ (mol l^{-1})	$c_5 \cdot 10^2$ (mol l^{-1})	$\ln \frac{c_4}{c_5} \cdot 10^2$
450	2,69	750	0,463	0,163	0,376	7,13	1,12	1,58	4,27
	2.32	750	0,590	0,093	0,317	5,53	0,18	2,20	2,08
	2,32	750	0.603	0,073	0,324	5,37	0,62	1,69	3,60
	2,32	750	0,692	0,104	0,199	4,02	0,62	1,69	3,61
	2,32	750	0,709	0,079	0,207	3,86	1,36	0.96	4,96
	2,32	749	0,629	0,050	0.320	4,99	1,53	0,80	5,25
	2,00	748	0,771	0,101	0,117	2,51	1,83	0.26	6,55
	2,00	744	0,575	0,183	0,230	5,33	0,80	1,27	4,15
	1,61	751	0,649	0,121	0,227	4,62	0,77	0,82	4,55
	1,61	751	0,656	0,123	0,218	4,50	0,76	0,82	4,52
	1,61	750	0,529	0,047	0,324	4,98	0,61	0,99	4,11
	1,61	749	0,538	0,059	0,405	6,17	0,26	1,38	2,94
	1,61	750	0,768	0,029	0,198	2,96	1,33	0,29	6,13
500	1,98	750	0,440	0,166	0,397	7,45	0,061	1,94	1,15
	1,98	750	0,700	0,099	0,196	3,92	0,95	1,03	4,52
	1,98	753	0,766	0,099	0,131	2,75	1,50	0,48	5,74
	1,98	752	0,539	0,160	0,302	6,07	0,25	1,73	2,65
	1,98	751	0,693	0,126	0,176	3,86	0,97	0,99	4,59
	1,98	753	0,786	0,090	0,120	2,43	1,60	0,36	6,10
550	2,25	748	0,808	0,062	0,119	2,11	1,83	0,39	6,14
	2,25	748	0,707	0,113	0,171	3,67	1,17	1,01	4,75
	2,25	748	0,713	0,129	0,148	3,42	1,29	0.92	4,95
	1,94	751	0,797	0,069	0,127	2,35	1,55	0,38	6,02
	1,94	750	0,656	0,147	0,192	4,34	0,75	1,20	4,13
	1,94	750	0,436	0,168	0,399	7,50	0,041	1,96	0,74
600	1,91	750	0,760	0,108	0,124	2,72	1,25	0,66	5,25
	1,91	749	0,737	0,132	0,122	2,91	1,08	0,85	4,85
	1,91	748	0,674	0,164	0,152	3,81	0,77	1,15	4,20
	1,91	748	0,496	0,258	0,241	6,19	0,11	1,81	1,80
	1,91	754,5	0,806	0,059	0,133	2,31	1,41	0,53	5,60

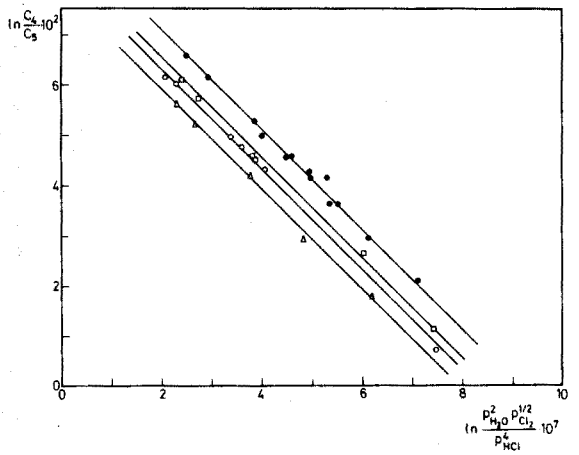

Fig. 3. Évolution du degré d'avancement de la réaction d'oxydo-réduction NpO_2^+–Np^{4+} en fonction de $\ln P^2_{H_2O} P^{\frac{1}{2}}_{Cl_2} / P^4_{HCl}$ dans l'eutectique LiCl–KCl (●) 450°C, (□) 500°C, (○) 550°C, (△) 600°C.

TABLEAU III

ÉTUDE DE LA RÉACTION $NpO_2^+ + 4\ HCl \rightleftharpoons Np^{4+} + 2\ H_2O + \frac{1}{2}\ Cl_2 + 3\ Cl^-$

$K = ([Np^{4+}] P^2_{H_2O} P^{\frac{1}{2}}_{Cl_2}) / ([NpO_2^+] P^4_{HCl})$

T (°C)	n^a	*Pente*	$K \cdot 10^6$ $atm^{(-\frac{1}{2})}$	*ln K*	ΔG (*kJ mol*$^{-1}$)^b
450	13	(0,97 ± 0,05)	(9,3 ± 0,4)	−11,60	(70 ± 1)
500	6	(0,96 ± 0,04)	(5,1 + 0,2)	−12,19	(78 ± 2)
550	6	(1,01 ± 0,04)	(4,2 ± 0,1)	−12,38	(85 + 2)
600	5	(0,97 ± 0,06)	(2,7 ± 0,5)	−12,80	(93 ± 3)

[a] n = Nombre de mesures.
[b] $\Delta H = (-40 \pm 6)$ kJ mol^{-1}; $\Delta S = (-152 \pm 15)$ J mol^{-1} °K^{-1}.

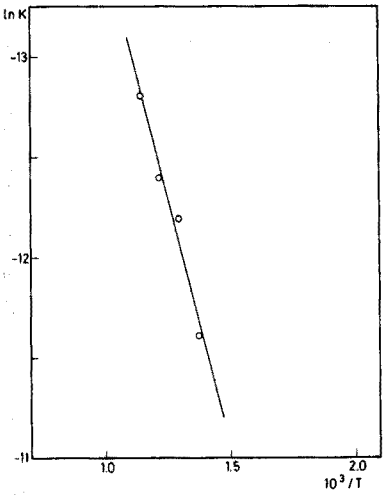

Fig. 4. Évolution de ln K en fonction de l'inverse de la température (°K).

enthalpique et entropique de la réaction (1) (Tableau III). La variation d'enthalpie libre de la réaction a également été calculée aux différentes températures (Tableau III). Une augmentation de température déplace l'équilibre dans le sens de la formation du neptunyle pentavalent, ce qui confirme les résultats de l'étude qualitative antérieure.

Étude de la réaction d'oxydo-réduction NpO_2^{2+}–NpO_2^+

Une solution contenant les espèces neptunyles(VI) et (V) dans l'eutectique LiCl–KCl à 400°C peut être obtenue sous une pression de chlore de 1 atmosphère. Dans ces conditions, le calcul des concentrations (Tableau IV) en NpO_2^+ et NpO_2^{2+} permet le calcul de la constante d'équilibre de la réaction:

$$NpO_2^+ + \tfrac{1}{2}\,Cl_2 \rightleftharpoons NpO_2^{2+} + Cl^- \qquad (10)$$

à savoir

$$[NpO_2^{2+}]/[NpO_2^+]P_{Cl_2}^{\frac{1}{2}} = K_1 \qquad (11)$$

De l'application de l'équation de Nernst à l'équilibre (10), il vient

$$E_{eq} = E^0_{NpO_2^{2+}/NpO_2^+} + 0{,}134 \log [NpO_{2+}^2]/[NpO_2^+] = E^0_{Cl_2/Cl} + 0{,}134 \log P_{Cl_2}^{\frac{1}{2}} \qquad (12)$$

ou encore

$$E^0_{NpO_2^{2+}/NpO_2^+} = 0{,}134 \log 1/K_1 = 0{,}220 \text{ V} \qquad (13)$$

en prenant comme référence le couple Cl_2/Cl^- ($E^0_{Cl_2/Cl} = 0$ V). Cette valeur du potentiel normal nous permet de compléter (en traits interrompus) le diagramme potentiel—pO^{2-} relatif au neptunium (Fig. 5) établi par Martinot et Duyckaerts[4] à partir de mesures de potentiels statiques et de la détermination du produit de solubilité de NpO_2.

TABLEAU IV

ÉTUDE DE LA RÉACTION $NpO_2^+ + \frac{1}{2}\,Cl_2 \rightleftharpoons NpO_2^{2+} + Cl^-$ [a]

$K_1 = ([NpO_2^{2+}]/[NpO_2^+]P_{Cl_2}^{\frac{1}{2}})$

Exp. n°.	A_{990}	A_{1440}	$c_5 \cdot 10^2$ *(mol l^{-1})*	$c_6 \cdot 10^2$ *(mol l^{-1})*
1	0,645	0,018	1.994	0,046
2	0,646	0,017	1,997	0,043
3	0,644	0,019	1,991	0,049

[a] $c_{tot} = 2{,}040 \cdot 10^{-2}$ mol l^{-1}, $K_1 = (2{,}3 \pm 0{,}1) \cdot 10^{-2}$ atm$^{(-\frac{1}{2})}$, $E^0_{NpO_2^{2+}/NpO_2^+} = 0{,}220$ V.

Étude de l'équilibre $2\,HCl + O^{2-} \rightleftharpoons H_2O + Cl^-$

La constante d'équilibre de la réaction

$$2\,HCl + O^{2-} \rightleftharpoons H_2O + Cl^- \qquad (14)$$

peut s'écrire

$$P_{H_2O}/P^2_{HCl}[O^{2-}] = k \qquad (15)$$

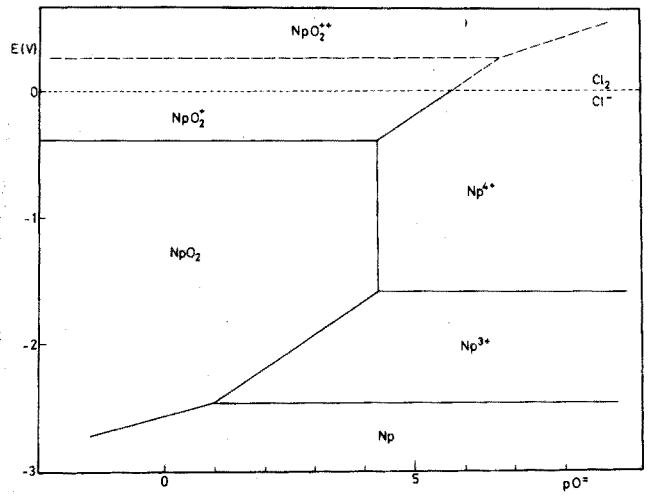

Fig. 5. Diagramme potentiel–pO^{2-} du neptunium dans l'eutectique LiCl–KCl à 400°C. $[Np^{3+}]=[Np^{4+}]=[NpO_2^+]=[NpO_2^{2+}]=10^{-2}$ mol l^{-1}.

Martinot et Duyckaerts[4] ont déterminé à 400°C dans l'eutectique LiCl–KCl la valeur du produit de solubilité du dioxyde de neptunium ainsi que la constante d'équilibre de la réaction:

$$NpO_2\downarrow + \tfrac{1}{2}\,Cl_2 \rightleftharpoons NpO_2^+ + Cl^- \qquad (16)$$

avec

$$[NpO_2^+]/P_{Cl_2}^{\frac{1}{2}} = K_2 \qquad (17)$$

La valeur de la constante d'équilibre de la réaction (1) est déterminée par extrapolation à 400°C de nos mesures. Nous avons ainsi, à 400°C, $K=10^{-4.8}$ $atm^{(-\frac{1}{2})}$, $K_2=10^{+0.89}$ mol l^{-1} $atm^{(-\frac{1}{2})}$ et $L_{NpO_2}=10^{-10.5}$. De ces valeurs, on tire $k=10^{3.8}$ 1 mol^{-1} atm^{-1}.

Nous devons faire remarquer que l'erreur sur la valeur de k dépend de celles sur les valeurs de K_2 et de L, cette dernière pouvant être entâchée d'une erreur importante; nous avions calculé cette même constante à partir de nos expériences sur l'uranium et nous avions obtenu une valeur de $k=10^{5.2}$ 1 mol^{-1} atm^{-1}; cette discordance entre les deux résultats montre bien qu'il faut attacher une signification très réservée à cette grandeur. Il y aurait sans doute lieu de faire des mesures plus exactes des produits de solubilité de UO_2 et NpO_2.

Nous remercions vivement l'Institut Interuniversitaire des Sciences Nucléaires et le Fonds National de la Recherche Scientifique pour l'intérêt constant apporté à nos travaux et le soutien financier accordé à notre laboratoire.

RÉSUMÉ

Les auteurs ont examiné de façon quantitative les réactions suivantes:

$$NpO_2^+ + 4\,HCl \rightleftharpoons Np^{4+} + 2\,H_2O + \tfrac{1}{2}\,Cl_2 + 3\,Cl^-$$

$$NpO_2^+ + \tfrac{1}{2}\,Cl_2 \rightleftharpoons NpO_2^{2+} + Cl^-$$
$$2\,HCl + O^{2-} \rightleftharpoons H_2O + Cl^-$$

dans un eutectique fondu de LiCl–KCl en déplaçant les équilibres par barbotages de gaz de compositions connues et en mesurant les concentrations des différentes espèces de neptunium à l'équilibre par spectrophotométrie d'absorption. Les constantes d'équilibre relatives aux trois réactions valent:

$K = (9{,}3 \pm 0{,}4) \cdot 10^{-6}$ atm$^{(-\frac{1}{2})}$; $K_1 = (2{,}3 \pm 0{,}1) \cdot 10^{-2}$ atm$^{(-\frac{1}{2})}$;
$k = 10^{3{\cdot}8}$ l mol^{-1} atm^{-1}.

On en a déduit la valeur du potentiel standard du couple NpO_2^{2+}/NpO_2^+ ($E^0 =$ 0,220 V par rapport à l'électrode normale de chlore).

SUMMARY

The following reactions:

$$NpO_2^+ + 4\,HCl \rightleftharpoons Np^{4+} + 2\,H_2O + \tfrac{1}{2}\,Cl_2 + 3\,Cl^-$$
$$NpO_2^+ + \tfrac{1}{2}\,Cl_2 \rightleftharpoons NpO_2^{2+} + Cl^-$$
$$2\,HCl + O^{2-} \rightleftharpoons H_2O + Cl^-$$

have been examined quantitatively. The reactions were studied in fused LiCl–KCl sparged with gas mixtures of definite compositions. The concentrations of the different neptunium species were measured by absorption spectrophotometry. The values of respective equilibrium constants are:

$K = (9.3 \pm 0.4) \cdot 10^{-6}$ atm$^{(-\frac{1}{2})}$; $K_1 = (2.3 \pm 0.1) \cdot 10^{-2}$ atm$^{(-\frac{1}{2})}$;
$k = 10^{3{\cdot}8}$ l mol^{-1} atm^{-1}.

The standard potential of the system NpO_2^{2+}/NpO_2^+ was determined to be $E^0 = 0.220$ V (*vs.* standard chlorine electrode).

BIBLIOGRAPHIE

1 R. Lysy, G. Landresse et G. Duyckaerts, *Bull. Soc. Chim. Belg.*, sous presse.
2 G. Landresse, *Anal. Chim. Acta*, 56 (1971) 29.
3 R. Lysy, G. Landresse et G. Duyckaerts, *Inorg. Nucl. Chem. Lett.*, sous presse.
4 L. Martinot et G. Duyckaerts, *Anal. Chim. Acta*, 66 (1973) 474.

Analytica Chimica Acta, 72 (1974) 315–321

A QUOTIENT METHOD OF EVALUATION FOR THE CATALYTIC–KINETIC DIFFERENCE METHOD

HEINER LUDWIG and HERBERT WEISZ

Lehrstuhl für Analytische Chemie, Chemisches Laboratorium der Universität Freiburg, Freiburg i. Br. (German Federal Republic)

(Received 19th April 1974)

In many analytical methods, the difference between two signals is used as the measuring quantity; one of these signals is caused by the sample and the other one by a known standard. In this way, interfering effects can often be largely compensated. A catalytic–kinetic difference method recently published[1] is based on this principle. A catalyzed reaction proceeds simultaneously in two separate mixtures. one containing a known standard amount of the catalyst (comparison system) and the other one an unknown amount of the catalyst (sample system). The courses of the reaction are followed simultaneously in both systems by a suitable measuring technique (photometry[1], potentiometry[1], thermometry[2] and conductometry[2]). Since both systems are initially equal except for the catalyst concentrations, the difference of the measured property must be zero initially. Then, because of the different catalyst concentrations, the difference of the two signals increases and reaches a maximum value. After the catalyzed reaction in both mixtures has been completed (equilibrium establishment), the difference is again zero.

For evaluation of the curve which shows the change of the difference of the two measured effects with time, the following quantities can be applied: the initial inclination of the curve[1,2], the size of the maximum[1], or the area under the entire curve[3]. Hitherto, one of these quantities was measured, and then a calibration graph was prepared by plotting the quantity directly against the catalyst concentration in the sample system.

In this paper a new procedure for evaluation is described. Here, the measured quantity (maximum of the difference in transmittance) is plotted not against the catalyst concentration in the sample system, but against the quotient of the two catalyst concentrations in the sample and in the comparison system. It is experimentally proved that a single calibration graph can be applied for the determination of several catalysts activating the same reaction. Furthermore, it is shown that the maximum of the difference in transmittance is independent of temperature, provided only that the temperature in both systems is equal.

The reaction between cerium(IV) and arsenic(III) catalyzed by iodide[4] as well as by osmium[5] serves to illustrate the procedure. The course of the reaction is followed photometrically by recording the difference in transmittance of the yellow cerium(IV) solutions with time.

EXPERIMENTAL

Equipment

For the measurements, a double-beam photometer (Kolorimeter Modell J, Lange, Berlin) connected with a recorder (Servogor, Metrawatt, Nürnberg) was used. For measurement, the vessel containing the catalyst standard concentration C_c (comparison) is always placed in the right compartment of the photometer, and the other vessel containing the unknown catalyst concentration C_s (sample) in the left compartment. Thus if $C_s > C_c$ (corresponding to a lower reaction rate in the right-hand vessel), the deflection on the photometer scale is to the right, and if $C_s < C_c$, to the left. The two interference filters used must show identical transmissibility, and the two photocells must have the same spectrophotoelectric sensitivity, so that two equal cerium(IV) concentrations in the cuvettes show equal signals (zero difference).

For zero adjustment of the measuring device, the two cuvettes (20 mm) contain twice-distilled water, corresponding to 100% transmittance for both cuvettes. The zero point (position 0 of the two resistance knobs of the photometer) is adjusted exactly to the middle of the recorder paper. Then, after both resistance knobs have been turned to position 5, the two photocells are, if necessary, balanced by one of the two iris diaphragms. The value of 0% transmittance for the right-hand cuvette is positioned to the right edge of the recorder paper, and that for the left-hand cuvette to the left edge.

In order to investigate the effect of temperature on the maximum of the difference in transmittance, the photometer was equipped with two thermostated cuvette holders. Mixing the solutions was performed by magnetic stirrers.

Solutions

Analytical reagent-grade chemicals and twice-distilled water were used for all solutions. Very dilute solutions were prepared daily from the stock solutions. In order to avoid losses by adsorption on the glass, all vessels were treated before use for two days with the respective solutions, which were then discarded.

Cerium(IV) sulphate solution. $7.5 \cdot 10^{-3}$ *M* in 0.3 *M* sulphuric acid.

Arsenic(III) solution. $8 \cdot 10^{-2}$ *M*. Dissolve 0.7914 g of arsenic trioxide in 10 ml of 1 *M* sodium hydroxide, add 12.5 ml of 4 *M* sulphuric acid and dilute to 100 ml with water.

Potassium iodide comparison solution. $2.5 \cdot 10^{-6}$ *M* (317 ng I ml^{-1}).

Osmium(VIII) stock solution. $7.84 \cdot 10^{-3}$ *M*. Dissolve osmium tetroxide in water, and standardize iodometrically.

Osmium(VIII) comparison solution. $9.8 \cdot 10^{-8}$ *M* (18.6 ng Os ml^{-1}).

Procedure

Into each of two cuvettes (20 mm), place 2 ml of cerium(IV) solution, 2 ml of arsenic(III) solution, and 1.25 ml of 4 *M* sulphuric acid and dilute to 9 ml with water. Start the catalyzed reaction with 1 ml of catalyst solution by use of a starting device[1], the right-hand pipette of the device containing 1 ml of the catalyst comparison solution, and the left-hand pipette 1 ml of the catalyst sample solution. Stir the solutions well. After the simultaneous start, the change of the difference in transmittance (420 nm) with time is registered by the recorder.

In order to avoid interferences, which may be caused by catalyst traces absorbed on the walls of the cuvettes, the vessels are cleaned after each determination with a (1+1) mixture of concentrated nitric and sulphuric acids.

RESULTS AND DISCUSSION

Relationship between the maximum of the difference in transmittance and the quotient of the catalyst concentrations

For different catalyst concentrations in the comparison system and in the sample system, the maximum of the difference in transmittance ΔT_{max} was measured as described. A first series of measurements was performed with iodide as catalyst, and a second series with osmium.

The results (Table I) show that the same value of ΔT_{max} is obtained for different catalyst concentrations in the comparison and in the sample system, if the quotient of concentrations is the same. The following two cases can occur.

BLE I

XIMUM OF THE DIFFERENCE IN TRANSMITTANCE FOR DIFFERENT CATALYST CONCEN ATIONS IN THE SAMPLE SYSTEM AND IN THE COMPARISON SYSTEM

= maximal needle deflection to the right; l = maximal needle deflection to the left.)

$[I]_s$ (/10 ml)	$[I]_c$	$Q = \frac{[I]_s}{[I]_c}$	$Q^* = \frac{[I]_c}{[I]_s}$	ΔT_{max} (%)	$[Os]_s$ (ng/10 ml)	$[Os]_c$	$Q = \frac{[Os]_s}{[Os]_c}$	$Q^* = \frac{[Os]_c}{[Os]_s}$	ΔT_{max} (%)
6	317	5.0		63.0(r)					
3.5	317		5.0	63.5(l)					
9	317	4.0		57.6(r)	74.4	18.6	4.0		56.4(r)
7	317		2.5	40.0(l)	7.44	18.6		2.5	40.0(l)
5	317	2.0		34.0(r)	37.2	18.6	2.0		31.6(r)
4	317		1.25	10.0(l)	14.9	18.6		1.25	11.8(l)
7	317	1.0	1.0	0					

(1) If the catalyst concentration in the sample system is higher than that in the comparison system ($C_s > C_c$), corresponding to a maximal deflection on the photometer to the right-hand side, the quotient is defined as follows:

$$Q = C_s/C_c, \quad \text{or} \quad C_s = C_c Q \tag{1}$$

(2) If the catalyst concentration in the sample system is lower than that in the comparison system ($C_s < C_c$), corresponding to a maximal deflection to the left-hand side, the quotient is defined as follows:

$$Q^* = C_c/C_s, \quad \text{or} \quad C_s = C_c/Q^* \tag{2}$$

Hence, the direction of the maximal deflection—to the right or left—indicates whether C_s is higher or lower than C_c.

The data in Table I illustrate that the maximum of the difference in transmittance is only a function of the quotient of the catalyst concentrations in the two

systems. It should be noted that the osmium-catalyzed reaction between cerium(IV) and arsenic(III) is faster, under the same conditions, than the iodide-catalyzed reaction; the rate constants differ by a factor of about 16 (ref. 6). However, by use of the above kinetic difference method, the same value of ΔT_{max} is obtained for both iodide and osmium, if the value of the quotient of the catalyst concentrations in the sample and in the comparison system is the same in both cases. Thus ΔT_{max} must be independent of the rate constant. This is also illustrated in Fig. 1, in which ΔT_{max} is plotted against the quotients Q or Q^*, as appropriate.

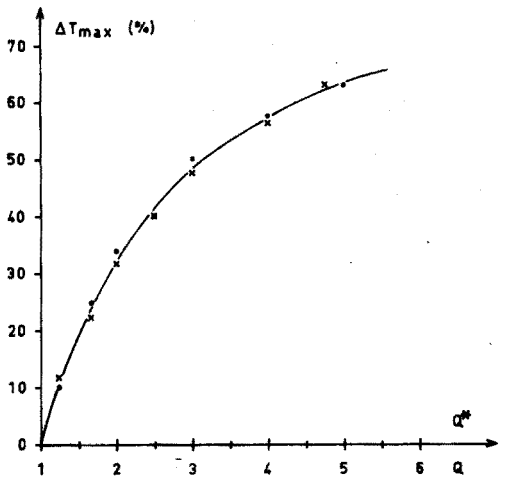

Fig. 1. Relationship between the maximum of the difference in transmittance and the quotient of the catalyst concentrations. (●) Iodide, (×) osmium.

Effect of temperature on the maximum of the difference in transmittance

The studies of the influence of temperature on ΔT_{max} were performed under the following conditions: $[I]_s = 2.5 \cdot 10^{-7}$ M, $[I]_c = 1.5 \cdot 10^{-7}$ M, $[Ce(IV)]_0 = 2.25 \cdot 10^{-3}$ M, $[As(III)]_0 = 8 \cdot 10^{-3}$ M, and $[H_2SO_4] = 0.6$ M. The temperature, equal in both vessels, was varied between 12 and 43°C. The results of these measurements (Table II) show that ΔT_{max} is independent of temperature. The effect of temperature on the transmittance of pure cerium(IV) solutions is practically negligible. This was proved by several experiments.

Theoretical treatment

The mathematical relationship between the maximum of the difference of the cerium(IV) concentrations in the two systems and the quotient of the catalyst concentrations is derived below. First, the iodide-catalyzed reaction is discussed.

TABLE II

EFFECT OF TEMPERATURE ON THE MAXIMUM OF THE DIFFERENCE IN TRANSMITTANCE

Temp. (°C)	12.4	18.3	23.0	30.3	35.0	43.3
ΔT_{max} *(%)*	30.4	30.5	30.0	31.2	31.0	30.3

If arsenic(III) is added in great excess, the change of the arsenic(III) concentration during the reaction can be neglected. The catalyzed reaction is then first order with respect to cerium(IV) and obeys the following rate law[6]:

$$-\frac{d[Ce(IV)]}{dt} = k^*[I][Ce(IV)] \tag{3}$$

where k^* is the rate constant. The cerium(IV) concentration given at time t after the start is obtained by integrating eqn. (3). This yields for the comparison system:

$$[Ce(IV)]_c = [Ce(IV)]_0 e^{-k^*[I]_c t} \tag{4}$$

and for the sample system:

$$[Ce(IV)]_s = [Ce(IV)]_0 e^{-k^*[I]_s t} \tag{5}$$

The indices c and s denote the concentrations in the comparison system and in the sample system, respectively. $[Ce(IV)]_0$ represents the initial concentration of cerium(IV), which is equal in both systems under the given conditions.

For different iodide concentrations in the two systems, the following difference of the cerium(IV) concentrations exists at time t:

$$\Delta[Ce(IV)] = [Ce(IV)]_c - [Ce(IV)]_s = [Ce(IV)]_0(e^{-k^*[I]_c t} - e^{-k^*[I]_s t}) . \tag{6}$$

This difference passes through a maximum value, $\Delta[Ce(IV)]_{max}$. In order to obtain the time t_{max}, at which this maximal difference occurs, eqn. (6) is first differentiated with respect to t, and then the resulting expression is set equal to zero and solved for time t_{max}:

$$t_{max} = \frac{\ln[I]_s - \ln[I]_c}{k^*([I]_s - [I]_c)} . \tag{7}$$

This value for t_{max} is substituted in eqn. (6), and rearrangement yields:

$$\Delta[Ce(IV)]_{max} = [Ce(IV)]_0 \, Q^{1/(1-Q)} - Q^{Q/(1-Q)} \tag{8}$$

where $Q = [I]_s/[I]_c$. If the quotient $Q^* = 1/Q$ is used, the expression obtained differs from eqn. (8) only by the negative sign of $\Delta[Ce(IV)]_{max}$. Equation 8 does not contain the rate constant k^*. Thus, the maximum of the difference of the cerium(IV) concentrations is independent of the rate constant, and, for a given initial concentration of cerium(IV), is only a function of the quotient of the two catalyst concentrations.

The osmium-catalyzed reaction between cerium(IV) and arsenic(III) is likewise first-order with respect to cerium(IV). Under the conditions mentioned above, this reaction obeys a rate law analogous to eqn. (3), although the rate constant is much greater than that of the iodide-catalyzed reaction[6]. The mathematical treatment applied to calculate the relationship between the maximum $\Delta[Ce(IV)]_{max}$ and the quotient Q for osmium as catalyst, yields the same expression as for iodide. This means that, under equal conditions, the calibration graphs representing $\Delta[Ce(IV)]_{max}$ as a function of Q are identical for both osmium- and iodide-catalysed reactions; thus, a calibration graph prepared with one catalyst can be used for the determination of the other.

Since eqn. (8) does not contain the rate constant k^*, $\Delta[Ce(IV)]_{max}$ is independent of temperature, provided that the temperatures in both vessels are equal. Temperature can therefore vary from determination to determination.

The determination of iodide and osmium

The results were obtained by use of a calibration graph, prepared with the iodide concentrations in the sample system ranging from $0.5 \cdot 10^{-7}$ M to $15.0 \cdot 10^{-7}$ M. The iodide concentration in the comparison system was always $2.5 \cdot 10^{-7}$ M (317 ng I/10 ml). Then, ΔT_{max} was plotted against Q and Q^*, respectively (compare Fig. 1). For evaluation of a measurement the following two cases can occur.

(1) When a deflection on the photometer scale to the right-hand side was obtained, the quotient Q was taken from the calibration graph, and the sample concentration was calculated by using eqn. (1) with respect to $[I]_c = 317$ ng/10 ml.

(2) If a deflection to the left-hand side was obtained, the quotient Q^* was taken, and the sample concentration was calculated by using eqn. (2).

The same calibration graph was also applied for the determination of osmium. The mode of evaluation was the same, except that the osmium concentration in the comparison system, $[Os]_c = 18.6$ ng/10 ml, was used.

Some results for the determinations are listed in Table III. Although the inclination of the calibration graph decreases with increasing value of Q, good reproducibility is obtained even for higher values of Q. For instance, an osmium determination of 88.4 ng Os/10 ml (corresponding to $Q = 4.75$) showed a standard deviation of ± 3.33 ng Os/10 ml (5 measurements).

TABLE III

DETERMINATION OF IODIDE AND OSMIUM

Iodide (ng/10 ml)		*Relative error (%)*	*Osmium (ng/10 ml)*		*Relative error (%)*
Given	*Found*		*Given*	*Found*	
57.1	56.8	−0.5	3.92	4.33	+10.5
63.5	58.5	−7.9	3.92	3.80	−3.1
127	133	+4.7	5.21	6.00	+15.2
279	276	−1.1	9.30	9.16	−1.5
317	317	±0	20.6	20.3	−1.5
381	405	+6.3	37.2	37.0	−0.5
381	390	+2.4	37.2	40.4	+8.6
431	434	+0.7	59.5	58.0	−2.5
711	713	+0.3	88.4	87.0	−1.6
1586	1556	−1.9	88.4	92.1	+4.2

The time required to reach the maximal difference ΔT_{max} depends on the catalyst concentrations and on the temperature. Under the given conditions (room temperature) it varies for the determination of iodide from about 2.5 to 14 min, and for that of osmium from about 3.5 to 20 min.

The quotient method described here is not limited to catalyzed reactions, in which the change of the concentration of a reactant is followed. Obviously, it can also be applied to reactions in which the change of the concentration of a product

is followed. This was proved by the determination of copper based on the reaction between hydrogen peroxide and 2,4-diaminophenol, where a red-brown product results. This catalyzed reaction proceeds by pseudo-first order kinetics. Furthermore, catalyzed reactions obeying a complicated rate law can likewise be used for the determination of the catalyst with this quotient method. The copper-catalyzed reaction between iron(III) and thiosulphate may serve as an example. Copper determinations with the catalytic–kinetic difference method based on this reaction have already been described[1]. It was experimentally proved that the quotient method of evaluation can also be employed in this case.

SUMMARY

A new variant of the catalytic–kinetic difference method is presented. The course of a catalyzed reaction, which proceeds simultaneously in two mixtures containing different catalyst concentrations, is followed by photometry. The maximum of the difference in transmittance being measured is a function of the quotient of the catalyst concentrations in the two mixtures and is independent of the rate constant. With this method of evaluation, a single calibration graph suffices for the determination of two different catalysts activating the same reaction. The maximum of the difference in transmittance is independent of temperature. The reaction between cerium(IV) and arsenic(III) catalyzed by iodide or osmium serves as an example. Two further examples are mentioned.

REFERENCES

1 H. Weisz and H. Ludwig, *Anal. Chim. Acta*, 55 (1971) 303.
2 S. Pantel and H. Weisz, *Anal. Chim. Acta*, 68 (1974) 311.
3 H. Ludwig, Dissertation, Freiburg University, 1973.
4 E. B. Sandell and I. M. Kolthoff, *J. Amer. Chem. Soc.*, 56 (1934) 1426.
5 R. D. Sauerbrunn and E. B. Sandell, *Mikrochim. Acta*, (1953) 22.
6 P. A. Rodriguez and H. L. Pardue, *Anal. Chem.*, 41 (1969) 1376.
7 H. Weisz and R. Rieger, Unpublished studies, Freiburg, 1974.

Analytica Chimica Acta, 72 (1974) 323–330

SUCCESSIVE PHOTOMETRIC TITRATION OF MANGANESE(VII), CHROMIUM(VI) AND VANADIUM(V) IN MIXTURES

S. SYAMSUNDER* and T. K. S. MURTHY

Chemical Engineering Division, Bhabha Atomic Research Centre, Trombay, Bombay 400085 (India)

(Received 2nd January 1974)

Manganese, chromium and vanadium are present together in a number of steels and their determination is of considerable interest. In general, the available methods involve oxidation of these constituents by persulphate to their highest oxidation states (VII, VI and V, respectively) and then titration with different combinations of reducing and oxidizing agents[1–5]. Recently[6], a photometric method has been proposed for the successive titration with iron(II) of chromium(VI) and vanadium(V) in mixtures. In the present study, a photometric titration of manganese(VII) in the presence of chromium(VI) with sodium nitrite, is described; in combination with the earlier method, this has made the simultaneous determination of all the three constituents possible.

EXPERIMENTAL

Reagents

Analytical reagent-grade chemicals were used. A *ca.* 0.1 *N* potassium permanganate solution was prepared and standardized against sodium oxalate. Potassium dichromate was dried at 150 °C for 2 h and stored; weighed aliquots were taken. A *ca.* 0.1 *N* solution of sodium vanadate was made by dissolving ammonium vanadate in 5 % (w/v) sodium carbonate solution and boiling to expel ammonia; the solution was standardized against iron(II) ammonium sulphate.

Iron(II) ammonium sulphate. Prepare a *ca.* 0.2 *M* solution in 0.25 *M* sulphuric acid. A constant titre can be maintained by adding cadmium powder[7].

Sodium nitrite. Prepare a *ca.* 0.1 *M* solution and standardize against permanganate[8]. Fresh solution should be made every week.

Silver(II) oxide. Prepare and test by the method of Hammer and Kleinberg[9].

Phosphoric acid. Oxidize reducing impurities by nitric acid treatment[10].

Apparatus

Absorption spectra were obtained on a Beckman Model B spectrophotometer. The cell compartment of this instrument was modified to carry out titrations[11]. The titration vessel was a 100-ml or 150-ml beaker, 5 cm in diameter. A 10-ml burette with 0.02-ml graduations was used.

---

* Present address: Nuclear Fuel Complex, Control Laboratory, Moula Ali, Cheralapalli Hyderabad 40 (India).

Preliminary studies

Initially, an attempt was made to find a titrant which could give separate end-points in the titration of mixtures of manganese(VII), chromium(VI) and vanadium(V). Iron(II), arsenic(III), nitrite and oxalate were tested but were unsatisfactory. The possibility of using a combination of two titrants was then considered. Since the earlier method[6] could be used to titrate a mixture of chromium(VI) and vanadium(V) with iron(II), only a method for titrating manganese(VII) in their presence was sought, so that the two procedures could be combined. Iron(II) failed to give a separate end-point for manganese both by potentiometric and photometric titration. Oxalate gave a premature end-point, and the absorbance towards the end of the titration did not vary linearly with the volume of titrant added, so that graphical extrapolation of the end-point was erroneous. Sodium nitrite was found to reduce permanganate smoothly to manganese(II) and detailed work was carried out only with this.

Procedure for titration of manganese(VII) in the presence of chromium(VI)

To an aliquot of permanganate in the titration vessel, add enough 2 *M* sulphuric acid and water to make the final acidity about 0.5 *M* and the volume 70 ml. Transfer the beaker to the titration assembly and adjust the speed of the magnetic stirrer to avoid vortex formation. Close the cover and introduce the burette through the hole in the cover so that its tip touches the solution. Set the wavelength scale at 620 nm and, keeping the shutter open, adjust the absorbance arbitrarily to about 1.5 by means of the slit-width control. If the solution is too deeply coloured to enable this adjustment to be made even after opening the slit to about 1 mm, keep it at this point and add nitrite slowly till the meter reading comes to about 1.5. Continue the titration, adding 0.2-ml portions and waiting for 30–40 s before noting the absorbance. Add the titrant until the absorbance remains nearly constant over a 0.5-ml range. Calculate the end-point by linear extrapolation of the plot of absorbance (corrected for volume change) against volume of titrant.

Procedure for simultaneous titration of manganese and chromium

Titrate an aliquot containing manganese(VII) and chromium(VI) for manganese as described above. Add phosphoric and sulphuric acids to make their final concentrations in the mixture 4 *M* and 1 *M*, respectively, and cool to ambient temperature. Change the titrant to iron(II) ammonium sulphate (0.2 *M*) and the wavelength to 470 nm. Titrate until the absorbance remains nearly constant over an addition of about 1 ml. Establish the end-point graphically. When calculating the chromium content, take into account the excess of nitrite added after the manganese end-point (see RESULTS).

Procedure for the simultaneous titration of manganese, chromium and vanadium

Follow the same procedure as for the Mn–Cr titration except that the wavelength, after the manganese titration, should be adjusted to 760 nm instead of 470 nm. Adjust the absorbance as close to zero as possible before starting the titration with iron(II).

RESULTS

Absorption spectra and choice of wavelength for titration

Though permanganate shows two strong absorption peaks in the range

520–550 nm, in order to cover a wider range of concentration, the less sensitive region at 620 nm was chosen for following the titration with nitrite. At this wavelength chromium(VI) has practically no absorption while chromium(III) and vanadium(V) absorb slightly. However, these ions should not be formed during this part of the titration.

Chromium(VI) in sulphuric acid has a strong absorption peak at about 350 nm, the intensity of which depends on acidity, but in the range 300–400 nm, vanadium(V) and iron(III) also show considerable absorption. However, at 470 nm, these ions show practically no absorption, whereas dichromate has a molar absorptivity of about 400, which is almost independent of acidity. Hence, the 470 nm wavelength was preferred for following the titration of chromium(VI). In the titration of Mn–Cr mixtures, therefore, after titration of the former with nitrite at 620 nm, the wavelength was changed to 470 nm and the titrant to iron(II).

Vanadium(IV) has an absorption peak at 760 nm where all other ions involved in the titration have practically no absorption. In the titration of Mn–Cr–V mixtures, after titration of manganese(VII) with nitrite, the wavelength was changed to 760 nm. The absorbance remains low until vanadium(IV) starts forming, when it increases rapidly and shows a break after all the vanadium(V) has been reduced.

Effect of acid concentration on the titration of manganese(VII) with nitrite

Aliquots of permanganate and dichromate were separately titrated photometrically with sodium nitrite solution at 620 and 470 nm, respectively, the sulphuric acid concentration of the solution being varied. In both cases the reaction became faster with increasing acidity. In the case of permanganate, the reaction rate was moderately fast in 0.5 *M* acid so that the titration could be followed; but it took 30–60 s for the reading to become steady after each addition of titrant. With dichromate, no detectable reduction took place up to 0.5 *M* acid, but at higher acidities (2 *M* and above) a slow reaction was noticed. Therefore, the acidity was limited to about 0.5 *M* for titrating manganese(VII) in the presence of chromium(VI). On addition of phosphoric acid–sulphuric acid mixture, after the manganese titration, the excess of nitrite present (above the stoichiometric quantity needed for reducing manganese(VII)) reacts with dichromate at a moderate rate. Therefore, when the chromium content is calculated, this excess must be taken into account, along with the iron(II) added to complete the titration. Attempts were made to avoid the need for this correction by adding urea or azide to decompose the excess of nitrite; unfortunately, an error of 2–4% in the chromium(VI) value arises from the chromium(VI)–nitrite reaction even in the few minutes necessary to establish the first end-point. Therefore, application of a stoichiometric correction for the excess of nitrite seems more appropriate.

The effect of acid concentration on the chromium–vanadium titration has already been discussed[6].

As an indication of the precision attainable under the recommended conditions, five titrations of permanganate (4 ml of 0.1071 *N*) showed a mean result of 2.15 ± 0.01 ml of 0.1995 *N* sodium nitrite (calculated value 2.15 ml), and addition of 100 mg of potassium dichromate had no effect on this result.

TABLE I

TITRATION OF MANGANESE–CHROMIUM MIXTURES

(Manganese(VII): sodium nitrite (0.2022 *M*) titrant in 0.5 *M* H_2SO_4 medium at 620 nm; initial volume 35 ml. Chromium(VI): iron(II) (0.1896 ***N***) titrant in 4 *M* H_3PO_4–1 *M* H_2SO_4 medium at 470 nm; initial volume, 70 ml.)

Expt.	*Manganese*				*Chromium*				
no.	*Mn taken (mg)*	*$NaNO_2$ added (ml)*	*Mn found (mg)*	*Rel. error (%)*	*Cr taken (a) (mg)*	*Excess $NaNO_2$ present (b) (ml)*	*Iron(II) added (ml)*	*Cr found (a+b) (ml)*	*Rel. error (%)*
1	11.72	5.29	11.76	+0.3	5.31	0.51	1.09	5.37	+1.2
2	9.38	4.24	9.42	+0.4	10.61	0.56	2.65	10.66	+0.5
3	7.03	3.17	7.03	0	21.85	0.44	6.21	21.95	+0.4
4	4.69	2.11	4.69	0	32.68	0.49	9.36	32.49	−0.6
5	2.35	1.07	2.38	+1.2	42.53	0.53	12.40	42.63	+0.2

TABLE II

TITRATION OF MANGANESE–CHROMIUM–VANADIUM MIXTURES

(Conditions as for Table I, except that the wavelength was 760 nm in the titrations with iron(II))

Mixture	*Manganese*			*Chromium*			*Vanadium*		
no.	*Present (mg)*	*Found (mg)*	*Rel. error (%)*	*Present (mg)*	*Found (mg)*	*Rel. error (%)*	*Present (mg)*	*Found (mg)*	*Rel. error (%)*
1	11.72	11.71	−0.1	5.37	5.40	+0.6	47.95	47.62	−0.7
2	9.38	9.35	−0.3	12.30	12.22	−0.7	33.21	33.37	+0.5
3	7.03	7.02	−0.1	21.39	21.37	−0.1	19.26	19.42	+0.8
4	9.26	9.21	−0.6	32.39	32.35	−0.1	9.63	9.56	−0.7
5	7.62	7.56	−0.8	5.16	5.24	+1.5	48.15	48.01	−0.3
6	14.07	14.12	+0.4	5.27	5.22	−0.9	5.29	5.17	−2.2
7	9.14	9.18	+0.4	10.36	10.27	−0.9	4.81	4.73	−1.6
8	4.57	4.62	+1.0	13.47	13.47	0	4.33	4.35	+0.5
9	7.03	7.02	−0.2	11.67	11.76	+0.8	2.41	2.37	−1.6
10	3.28	3.27	−0.3	50.75	50.78	+0.1	19.73	19.81	+0.4

Titration of synthetic mixtures of manganese(VII) and chromium(VI)

Synthetic mixtures of permanganate and dichromate were prepared and titrated by the procedure given above. A typical titration graph is shown in Fig. 1 and the results are summarized in Table I.

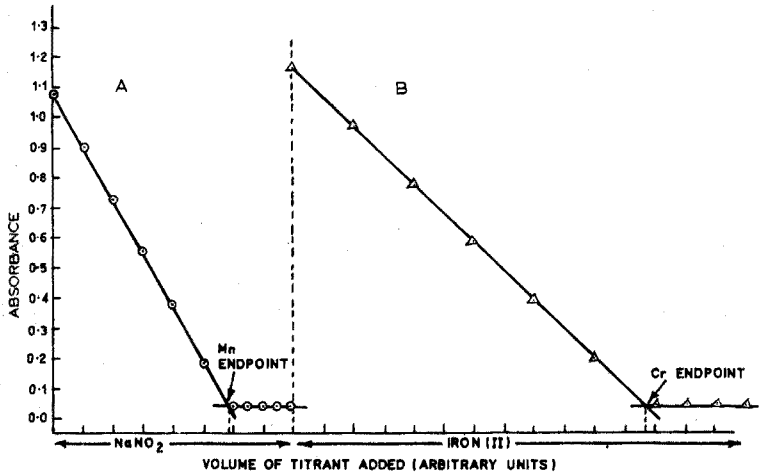

Fig. 1. Photometric titration of Mn(VII) and Cr(VI) mixture. A. Titration with $NaNO_2$ at 620 nm in 0.5 *M* H_2SO_4. B. Titration with Fe(II) at 470 nm in 4 *M* H_3PO_4–1 *M* H_2SO_4.

Titration of synthetic mixtures of manganese(VII), chromium(VI) and vanadium(V)

Synthetic mixtures of permanganate, dichromate and vanadate were titrated with nitrite (for Mn) and then with iron(II) (for Cr and V) as recommended above. The results are summarized in Table II and a typical titration graph is shown in Fig. 2. Mixtures 6–10 were prepared to correspond to the composition of some B.C.S. steel samples, nos. 251/1, 253/1, 258/1, 224/1, and 220/1, respectively.

Application of the method for the determination of manganese, chromium and vanadium in steel samples

The usefulness of the method was further tested by applying it to British Chemical Standard Steel no. 220/1, which has the following certified composition (%): W 6.89, Mo 5.20, Mn 0.28, Cr 5.13, V 2.09, Co 0.13, C 0.93, Si 0.24, S 0.047, P 0.029, Mn 0.28, Ni 0.16, Cu 0.15, Sn 0.021 and As 0.03. After some preliminary tests, the following procedure, consisting of chemical attack for dissolving the sample, oxidation of Mn, Cr and V to their highest oxidation states, and photometric titration, was adopted.

To 1.0 g of the sample, 5 ml of 10 *M* hydrochloric acid, 5 ml of 15 *M* nitric acid and 5 drops of 40 % hydrofluoric acid were added and the mixture was set aside until the reaction ceased. Then 5 ml of 60 % perchloric acid was added and the contents were evaporated to dryness. The residue was heated with 2.5 ml of sulphuric acid (*d.* 1.84) to dense fumes of sulphur trioxide. After cooling, 50–60 ml of distilled water was added and the mixture boiled for some time; the precipitated tungstic acid was then filtered off. The precipitate was washed

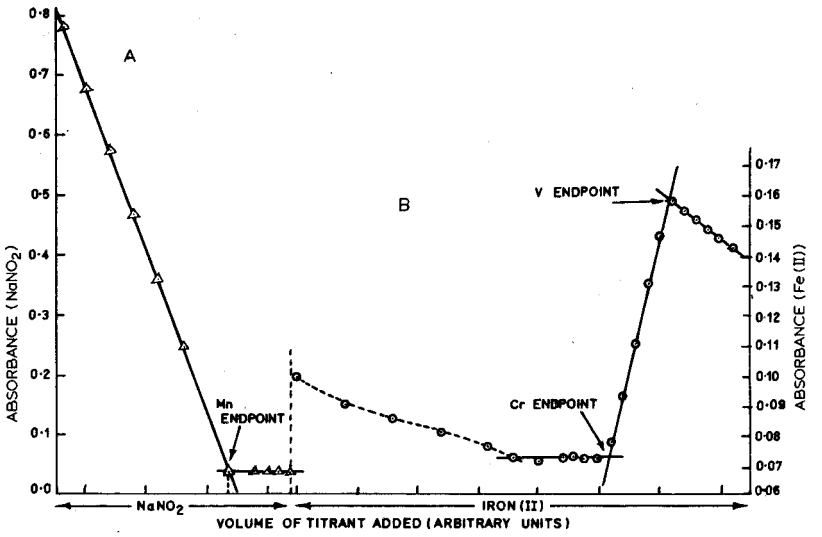

Fig. 2. Titration of Mn(VII), Cr(VI) and V(V) mixture. A. Titration with $NaNO_2$ at 620 nm in 0.5 *M* H_2SO_4. B. Titration with Fe(II) at 760 nm in 4 *M* H_3PO_4–1 *M* H_2SO_4.

with 1 % sulphuric acid and the combined filtrate and washings were evaporated to about 60 ml. This was transferred to the titration beaker and the total volume of the solution made up to 75 ml. About 0.6 g of silver(II) oxide was stirred into the solution which was then heated to 80 °C and set aside for about 30 min. The beaker was transferred to the titration compartment and photometric titration was carried out as in the case of synthetic mixtures of Mn–Cr–V. Five analyses of the sample gave mean results (with average errors) of 0.284 (0.005) % Mn, 5.13 (±0.02) % Cr, and 2.064 (±0.009) % V.

DISCUSSION

The small difference in the standard redox potentials of the systems:

$$MnO_4^- + 8\,H^+ + 5\,e \rightleftharpoons Mn^{2+} + 4\,H_2O, \qquad E^0 = 1.52\ V$$

$$Cr_2O_7^{2-} + 14\,H^+ + 6\,e \rightleftharpoons 2\,Cr^{3+} + 7\,H_2O, \qquad E^0 = 1.35\ V$$

accounts only partly for the difficulty in the titration of manganese(VII) in the presence of chromium(VI). Reactions involving multi-electron changes, as with permanganate and dichromate, are usually complex, and the rates of intermediate reactions decide the course of the titration of a mixture. Thus, iron(II) gives no separate end-point for manganese(VII) while oxalate[12] and thallium(I)[13] have been reported to be of some use. Kolthoff *et al.*[14] recommended a mixture of nitrite and arsenite; nitrite alone reacted slowly, especially near the end-point, and arsenite alone reduced manganese(VII) to an indefinite valency of about +3.3. Similar observations were made here. However, for sluggish reactions a photometric technique is more suitable than a potentiometric titration, primarily because the

end-point in a photometric titration is located by linear extrapolation of measurements at stages which are not affected by incomplete and simultaneous reactions. It was for this reason that the photometric titration of permanganate could be successfully carried out.

The use of oxalate for titration of manganese(VII) in the presence of chromium(VI)[12] was also examined in some detail. Difficulty was found in locating the end-point, and, under the conditions used, manganese was reduced to a state between +2 and +3. This titrant is also unsuitable because, though oxalate does not reduce chromium(VI) in moderately acidic solution, it interfered, causing negative error in the titration with iron(II), possibly by an induced reaction.

Nitrite was chosen as a suitable titrant for manganese(VII). Advantage was taken of the effect of acidity on the rate of reduction of manganese(VII) and chromium(VI). The titration of manganese was precise, as discussed earlier. Even though the titrant has to be changed to iron(II) to analyse mixtures, the procedure is much simpler than the normal procedures, where a sequential titration of the three constituents is impossible without intermediate reoxidation.

In the titration of Mn–Cr–V mixtures, the variation in absorbance was somewhat erratic during initial titration with iron(II). No valid explanation could be found for this, but a slow reaction between chromium(VI) and manganese(II) in the phosphate medium is suspected to be responsible. However, before the complete reduction of chromium(VI), the readings became constant enough to permit extrapolation for the end-point.

Only one standard sample of steel (no. 220/1) was chosen to show the validity of the method, but no difficulty should occur in extending this method to other types of steel. In the sample analysed, the tungsten content was high. Some authors have reported that the tungstic acid precipitate may carry down some vanadium, and it has been suggested that for every 10 mg of tungsten precipitated, about 0.01 mg of vanadium is lost[15]. If this correction is applied, the % vanadium in the steel reported above becomes higher by 0.01, bringing its value closer to the expected one.

SUMMARY

A method for the successive photometric titration of manganese(VII), chromium(VI) and vanadium(V) in mixtures, and its application for their determination in special steels, is described. Manganese is first titrated with sodium nitrite in 0.5 *M* sulphuric acid medium at 620 nm. The wavelength is then changed to 760 nm and the acidity to 4 *M* phosphoric acid–1 *M* sulphuric acid, and chromium and vanadium are successively titrated with iron(II) ammonium sulphate. The three end-points are determined graphically by the usual extrapolation technique. For calculating the chromium content, a correction is needed for the excess of nitrite added after the manganese end-point. The method was tested by analysing synthetic mixtures of manganese(VII)–chromium(VI), and manganese(VII)–chromium(VI)–vanadium(V). A sample of special steel (B.C.S. no. 220/1) was also analysed after oxidation of the metals to their highest oxidation states with silver(II) oxide.

REFERENCES

1 W. Hiltner and C. Marwin, *Z. Anal. Chem.*, 91 (1933) 401.
2 J. Brickel, *Ann. Chim. Anal.*, 25 (1943) 173.
3 J. Nummedal, *Chem. Abstr.*, 36 (1942) 3453.
4 I. M. Kolthoff and R. Belcher, *Volumetric Analysis*, Vol. III, Interscience, New York, 1957, p. 605.
5 N. H. Furman in W. W. Scott (Ed.), *Standard Methods of Chemical Analysis*, Vol. II, Van Nostrand, New York, 1959, p. 1479.
6 S. V. Parab, S. Syamsunder and T. K. S. Murthy, *Anal. Chim. Acta*, in press.
7 S. Syamsunder and T. K. S. Murthy, *Curr. Sci.*, 41 (1972) 503.
8 A. Berka, J. Vulterin and J. Zyka, *New Redox Titrants*, Pergamon, Oxford, 1965, p. 186.
9 W. Hammer and J. Kleinberg in John C. Ballar, Jr. (Ed.), *Inorganic Synthesis*, Vol. IV, McGraw-Hill, 1953, p. 12.
10 G. Gopala Rao and P. Kanta Rao, *Talanta*, 10 (1963) 1251.
11 S. V. Parab and T. K. S. Murthy, *Report B.A.R.C.-611*, Atomic Energy Commission (India), 1972.
12 G. Gopala Rao and U. Muralikrishna, *Anal. Chim. Acta*, 13 (1955) 8.
13 U. V. Rao, U. Muralikrishna and G. Gopala Rao, *J. Anal. Chem.*, 145 (1955) 12.
14 E. B. Sandell, I. M. Kolthoff and J. J. Lingane, *Ind. Eng. Chem., Anal. Ed.*, 7 (1935) 256.
15 N. H. Furman in W. W. Scott (Ed.), *Standard Methods of Chemical Analysis*, Vol. II, Van Nostrand, New York, 1959, p. 1458.

Analytica Chimica Acta, 72 (1974) 331–338

CHELATING ION-EXCHANGERS CONTAINING SALICYLIC ACID

F. VERNON and H. ECCLES

The Ramage Laboratories, Department of Chemistry and Applied Chemistry, University of Salford, Salford, M5 4WT, Lancs. (England)

(Received 6th January 1974)

The Kressman and Kitchener[1] technique for the preparation of ion-exchangers by copolymerization of phenol, formaldehyde and a phenolic compound containing an ionizable group, has been used with varying degrees of success for the production of chelating ion exchangers based on the salicyclic acid unit. Japanese workers[2–4] have described the preparation and properties of phenol–formaldehyde–salicylic acid condensates which were acid-catalysed and cured at 100°C. The resulting resins had low capacities and there was some evidence for decarboxylation at the curing temperature used. Davies *et al.*[5] prepared an alkali-catalysed, resorcinol–formaldehyde–salicylic acid resin of reasonably high capacity (Na^+ 2.4 and Cu^{2+} 1.6 mmole g^{-1}, respectively), and also a polystyrene-azo-salicylic exchanger (Na^+ 2.8 and Cu^{2+} 1.05 mmole g^{-1} capacities).

Degeiso *et al.*[6] examined the possibility of polymerizing salicylic acid with formaldehyde, leaving out the phenol cross-linking agent, and using a mild acid catalyst. The resulting polymer was of low molecular weight and insoluble in water, but soluble in alkali and ethanol. An almost theoretical sodium capacity was found, and metal complexes were obtained by precipitation from ethanolic alkaline solution. In later publications[7], the authors concluded that the resin had higher selectivity for uranyl ions than for other metal ions investigated, and used the resin in the extraction of uranium from ores. Rabek *et al.*[8] have stated that the formation of a linear high-molecular-weight polymer by condensation of salicylic acid with formaldehyde is impossible without the phenol cross-linking agent. Furthermore, their study of selectivity coefficients on salicylic and *p*-hydroxybenzoic acid resins proved that the salicylic-based exchanger showed no selectivity. From stability constant data[9] on metal salicylate complexes, stability constants decrease in the order $Fe^{3+} > Al^{3+} > Cu^{2+} > Ni^{2+} = Co^{2+} = Zn^{2+}$, and this is the order of selectivity expected from a salicylic acid exchanger. Two salicycylic acid-based condensation resins, a *p*-hydroxybenzoic acid resin and a polystyrene-azo-salicylic acid resin have been synthesized and their exchange properties are discussed and compared below.

EXPERIMENTAL

Salicylic acid resin preparation

Condensation resin 1. Sodium salicylate (0.5 mole), sodium hydroxide (0.12 mole) and 40% formaldehyde solution (0.25 mole CH_2O) were mixed and main-

tained at 40°C for 1 week. The product, a white solid, was easily crushed and was water-soluble. This product was mixed with resorcinol (0.5 mole) and formaldehyde solution (0.12 mole CH_2O) and heated at 100°C for 1 week. The red resin obtained was crushed and the 30–60 mesh fraction collected. This was washed with water, Soxhlet-extracted with ethanol for 16 h, and washed with 0.1 *M* hydrochloric acid and then with water until chloride-free. The resin was allowed to air-dry at room temperature.

Condensation resin 2. Salicylic acid (0.12 mole), phenol (0.03 mole), 40% formaldehyde solution (0.33 mole CH_2O) and sodium hydroxide (0.27 mole) were mixed with warming, then heated in a sealed container at 100°C for 2 days to give a purple gel. The gel was cured in air at 100°C for 4 days. The resultant resin was crushed, sieved, washed and Soxhlet-extracted in the same way as resin 1. The washing procedure after extraction was varied, the resin being washed with 0.1 *M* hydrochloric acid, water, 0.1 *M* sodium hydrogen carbonate solution and water, and then stored as the fully swollen sodium form.

Condensation resin 3. The preparation and washing procedures were as given for resin 2, but *p*-hydroxybenzoic acid replaced salicylic acid in the synthesis.

Polystyrene-azo-salicylic acid resin 4. Macroporous polystyrene beads (Amberlite XAD-2, Rohm and Haas Co.) were converted to poly(aminostyrene) by the method described previously[10] for polystyrene-azo-oxine. Poly(aminostyrene) (40 g) was diazotized and coupled with salicylic acid (0.3 mole) in alkaline solution at 0–5°C. The washing and extraction procedures were identical with those used for condensation resin 1.

Resin characterization

Water regain. Samples of the resins were allowed to stand in deionized water for 48 h. The resins were then filtered by suction and lightly pressed between filter papers to remove surface moisture. The moisture contents were determined by drying at 100°C for 48 h.

For elemental analyses, oven-dried resin samples were crushed to a fine powder and stored *in vacuo* over phosphorus pentoxide. The amine content of the poly(aminostyrene) was determined by titration with perchloric acid in acetic acid as described earlier[10].

Resin capacity determinations. The seven elements used in capacity determinations were aluminium, cobalt, copper, iron(III), nickel, uranium (as uranyl ion) and zinc. Capacity measurements were obtained for sodium acetate–acetic acid buffers which were 0.1 *M* in the metal ion concerned. The resin and buffered solution were equilibrated by shaking for 48 h, after which time the resin was filtered and washed with the appropriate buffer until the solution was metal-free. The metal was eluted from the resin with 4 *M* hydrochloric acid and determined spectrophotometrically.

The spectrophotometric methods used were as follows: diethyldithiocarbamate for copper[11], thiocyanate–acetone for cobalt[12], dimethylglyoxime for nickel[12], zincon for zinc[13], 8-hydroxyquinoline for aluminium[14] and uranium[11] and thioglycollic acid for iron[11].

Sodium capacities on the hydrogen form of each resin were determined to obtain the total carboxylic acid content. Weighed amounts of the fully swollen

resin were equilibrated by shaking for 18 h with a standard sodium carbonate solution. The resin was filtered and washed, and the combined filtrate and washings were boiled with an excess of standard hydrochloric acid solution to remove carbon dioxide. After cooling, the excess of acid was titrated with standard alkali, and the sodium capacity of the resin, corrected to a dry weight basis, was calculated.

Equilibration rates. From the capacity studies, the total capacity of each resin for copper at the optimal pH was known. Twice this theoretical quantity of copper ions was diluted with buffer to give an 0.05 *M* metal ion solution which was equilibrated with 1g of resin. With 8 equilibrations, the resin was removed from the solutions at various times over a period of 48 h and its copper content determined.

Column separation with resin 2.

An ion-exchange column (1 cm i.d.) was packed to a height of 10 cm with 4.5 g of fully swollen condensation resin 2 in the sodium form. The column was washed with 2 *M* hydrochloric acid, deionized water and a pH 7 acetate buffer. Aliquots (5 ml) of 100-p.p.m. iron(III), copper and manganese solutions were placed on the column which was then washed with ten bed volumes of deionized water at a rate of 2.5 ml min^{-1}. Ions retained were eluted with 2 *M* hydrochloric acid and determined by atomic absorption spectrometry.

As quantitative recoveries of the three elements were obtained, their determination in a brine sample was attempted. After equilibration of the resin with a pH 7 acetate buffer, a 1-l sample of brine was passed through the column at a rate of 2.5 ml min^{-1}, the eluate being retained. The column was washed with ten bed-volumes of deionized water, and the metal ions were eluted with 2 *M* hydrochloric acid. The eluate was evaporated to a small volume and made up to 25 ml with deionized water. The brine eluted from the column was spiked with iron, copper and manganese at concentrations of 0.5, 0.1 and 0.1 p.p.m. respectively. This solution was passed through the pH 7 buffered column a second time, the column was washed, and the ions were eluted with 2 *M* hydrochloric acid which was subsequently dilute to 100 ml. The ion concentrations of the two eluates were determined by atomic absorption spectrometry.

RESULTS AND DISCUSSION

The capacity *versus* pH contours for the polystyrene-azo-salicylic acid resin, which are given in Fig. 1, show good agreement between the formation of the metal resinates and the stability constants given for metal salicylate complexes. Hanelkova and Bartusek[9] have reported the logarithmic stability constants for the salicylate complexes as Al 14, Cu 10.64, Ni 6.95, Zn 6.85 and Co 6.72, and it is this order which is seen in Fig. 1, the resin exhibiting selectivity for aluminium and copper ions. From the nitrogen contents of the product from each stage of the synthesis and from the titres obtained for the residual amino groups, it was calculated that this resin contained 2.65 mmoles g^{-1} of nitro groups, 0.93 mmoles g^{-1} of amino groups and 0.63 mmoles g^{-1} of chelating units. As the functional groups of the chelating unit are acidic and phenolic, an independent check of the

number of chelating units was possible by measurement of the sodium capacity. The sodium capacity from sodium hydroxide was found to be 1.34 mmoles g^{-1} whilst that from sodium carbonate was 0.70 mmoles g^{-1} when only the carboxylic acid content was determined. The maximal capacity would, therefore, appear to be in the range 0.63–0.70 mmoles g^{-1}; this value is reached by pH 4.5 for aluminium ions and is exceeded above pH 4.8 for copper ions. The phenomenon of polystyrene-azo resins exceeding their maximal capacity for copper ions was observed in earlier work[15]; lone pair donation by nitrogen of the azo linkage bonding the copper to the resin was suggested as a possible explanation. The water regain of this resin was found to be 0.91 g g^{-1}, and equilibration rate studies gave a time to 50% resin capacity, $t_{\frac{1}{2}}$, of 24 min.

Figure 2 shows similar contours for metal ions with condensation resin 1; it can be seen that there is an overall similarity of the contours for this resin and the polystyrene-azo-salicylic acid resin with the notable exception of cobalt and nickel, the behaviour of which is reversed. There is no obvious explanation for the

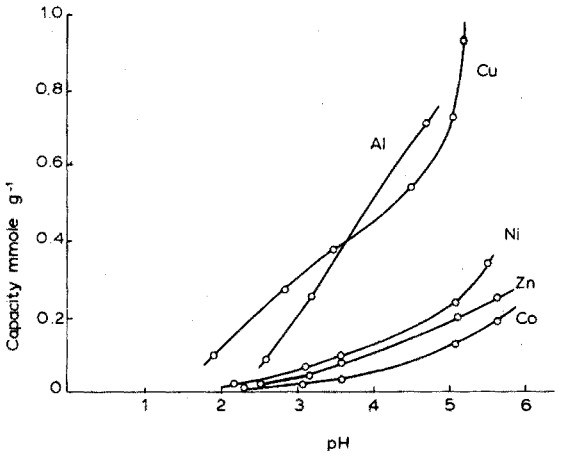

Fig. 1. Capacity *versus* pH curves for cations on polystyrene-azo-salicylic acid resin.

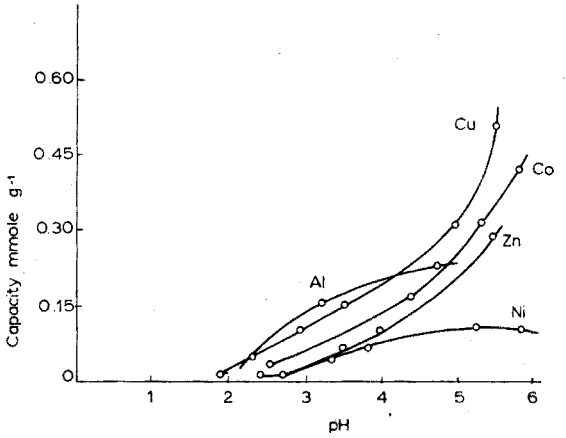

Fig. 2. Capacity *versus* pH curves for cations on salicylic acid condensation resin 1.

higher selctivity for cobalt over nickel on condensation resin 1. Stability constant data suggests that the higher selectivity will be for nickel as was found for the polystyrene resin, but, in this case, other effects must play a much larger role. As the resin is highly cross-linked (50%), differences in hydrated ionic radius could be a major contributory factor. However, Nightingale's values[16] for the hydrated ionic radii of cobalt, nickel and copper are 4.23, 4.04 and 4.19 Å, respectively, which would give a resin capacity order of nickel > copper > cobalt. Consideration of hydration energies of the ions also fails to produce a viable explanation.

The major difference in Figs. 1 and 2 lies in the selectivities of the two resins. The selectivity of the polystyrene resin is far higher than that of the condensation resin, where there is no large difference between aluminium and copper ions on one hand, and nickel, zinc and cobalt ions on the other. This loss of selectivity by the condensation resin can be explained by its high degree of cross-linking and tends to support the findings of Rabek *et al.*[8]. The resin selectivity is so low that, although selectivity can be seen in the contours, it is unlikely to become apparent by measurement of selectivity coefficients.

TABLE I

PROPERTIES OF THE ION EXCHANGERS STUDIED

Exchanger	*Chelating units from Na capacity (mmole g^{-1})*	*Water regain ($g\ g^{-1}$)*	*% Cross-linking*	*Time to 50% equilibration (min)*
Resin 1. Salicylic acid condensate	1.7	0.97	50	35
Resin 2. Salicylic acid condensate	2.9	2.6	20	5.5
Resin 3. *p*-Hydroxybenzoic acid condensate	2.4	1.6	20	Not determined
Resin 4. Polystyrene-azo-salicylic acid	0.7	0.91	"lightly cross-linked" (10% max)	24

The properties of the resins studied are summarized in Table I. The water regain of the condensation resin 1 was only slightly higher than that of the polystyrene resin 4. The time to 50% equilibration was slower for resin 1 than for resin 4, because of the greater degree of cross-linking. The sodium capacity (1.71 mmoles g^{-1}) was the maximum capacity expected for 1:1 complex formation. Unlike the polystyrene resin, the maximum observed capacity, which was 0.50 for copper at pH 5.5, is far less than the theoretical; this suggests that the majority of the sites are inaccessible owing to the dense, highly cross-linked nature of the resin.

Figure 3 shows the capacity for iron(III) ions as a function of pH for condensation resins 2 and 3. These salicylic and *p*-hydroxybenzoic acid condensates were prepared under identical conditions, in order to assess the selectivity of the salicylate resin over an equivalent hydroxybenzoic acid resin incapable of chelate

formation. From the contours, fairly high selectivity for iron(III) is seen with the salicylic acid exchanger, exhibiting a maximum of 1.0 mmoles g^{-1} at pH 5; the capacity of the *p*-hydroxybenzoic acid resin is at a minimum of 0.12 mmoles g^{-1} at this pH, being due only to the carboxylic acid group.

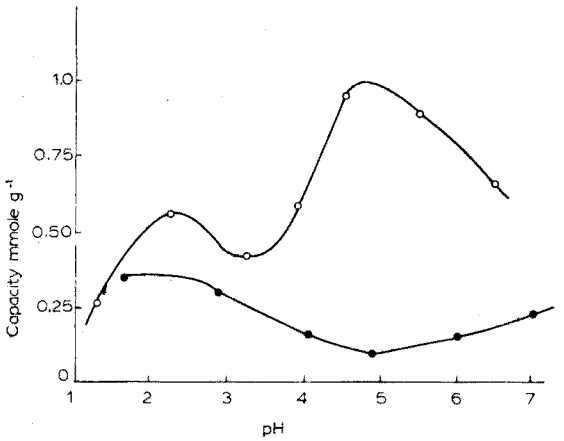

Fig. 3. Capacity *versus* pH curves for iron(III) on salicylic (○) and *p*-hydroxybenzoic (●) acid condensation resins in the presence of citrate.

Figure 3 gives reasonable although indirect proof of the existence of iron(III) on the salicylate resin at pH 5 as a chelate complex, as there was a competing ligand in solution. In order to keep the iron in solution to pH 7, it was necessary to determine resin uptakes from iron solutions containing an equimolar quantity of citrate. Thus, the contour suggests that for the salicylic acid resin, the stability of the metal resinate is higher than that of iron(III) citrate. In order to assess this however, it is necessary to have comparative capacities for iron(III) in the absence of citrate and to know the theoretical total capacity of the resin. The sodium capacities of these resins (Table 1) can be regarded as the maximal theoretical values. Iron(III) capacities in the absence of citrate were determined at pH 4, values of 1.7 and 1.0 mmoles g^{-1} respectively being obtained. Citric acid at pH 4 thus reduces the iron(III) capacity to 35% of its former value on the salicylic acid resin and to 16% of its former value on the *p*-hydroxybenzoic acid resin.

The high capacities of these two resins arise from their method of synthesis. The resins are about 20% cross-linked, and the first two days of curing in a sealed container gave swollen gels with no water loss. This technique resulted in resins having larger water regains than condensation resin 1 (Table I). The effects of the large water regain and reduced cross-linking of the salicylic acid condensation resin 2 can be seen in the rapid equilibration rate of this resin. In view of this equilibration rate, it was decided to use this resin for subsequent column work.

Uranium capacities

Unlike the resin described by Degeiso *et al.*[7], condensation resin 1 had a very low uranyl capacity (less than 0.01 mmoles g^{-1}) in the pH range 3–4; this was probably due to the presence of citrate as the stability constant for uranyl citrate is

known to be twice that of uranyl salicylate. A maximum in the capacity *versus* pH curve was found at pH 7.7 but even at this pH, the capacity for uranyl ions was only 0.02 mmoles g^{-1}. The polystyrene-azo-salicylic acid resin gave slightly higher capacities for uranyl ions in the presence of citrate. The optimal pH range was 3–4, in agreement with the findings of Degeiso *et al.*, the capacity being 0.14 mmoles g^{-1}. Measurement at the same pH in the absence of citrate gave a uranyl capacity of 0.25 mmoles g^{-1}. The capacity of this resin for uranium was found to depend on the nature of the co-ion in the absence of a backing electrolyte. With 0.05 *M* solutions, uranyl capacities of 0.18, 0.23 and 0.54 mmoles g^{-1} were obtained for nitrate, chloride and acetate co-ions, respectively. When a backing electrolyte of the sodium salt of the co-ion was used, the uranyl capacities increased for the chloride and nitrate systems as the backing electrolyte concentration increased, whilst for the acetate system the reverse was found.

In view of the poor performance of resin 1 and the disparity with the results of Degeiso *et al.*, condensation resin 2 was examined. The capacity for uranyl ions in the absence of citrate at pH 3.5 (acetate buffer) was found to be 1.7 mmoles g^{-1}. This high capacity demonstrates the high affinity of the resin for uranyl ions, in accordance with the results of previous workers, and also demonstrates the importance of the method of condensation polymerization selected. Although the iron and uranyl capacities on resin 2 are high, this is probably not the best salicylic acid resin which can be prepared. Further investigation of the various parameters of the synthesis may prove rewarding.

Column operation with condensation resin 2

The properties of condensation resin 2 suggested its suitability for column work. The determination of iron, copper and manganese in brine was chosen as a test of resin efficiency. When aliquots of 100-p.p.m. standard metal solutions were used, quantitative recoveries of the three ionic species from the column were obtained. However, when brine was spiked with iron, copper and manganese contents of 0.5, 0.1 and 0.1 p.p.m., respectively, the values found were 0.5, 0.1 and 0.015 p.p.m., after the ions had been collected by the resin, eluted and subsequently determined by atomic absorption spectrometry. At these levels, the iron and copper retentions by the column were quantitative, but manganese recovery was only 15%. Subsequent analyses of the unspiked brine showed iron and copper concentrations of 0.06 and 0.02 p.p.m. and, not surprisingly, no manganese was detected.

Conclusions

Salicylate-containing ion-exchange resins exhibit the selectivity which would be expected from examination of metal salicylate stability constants. This is the controlling factor in metal take-up by the resin, the effect of hydrated ionic radius playing at most a minor role. However, a lightly cross-linked, polystyrene-based exchanger demonstrated higher selectivities than a highly cross-linked dense condensation resin. A salicylate resin showed better selectivity for iron(III) than did an equivalent *p*-hydroxybenzoate resin and it is possible to produce salicylic acid condensation resins suitable for column operation. The resin used for column work showed selectivity for iron(III) and copper(II) ions over manganese and sodium ions. The results with the polystyrene-azo-salicylate resin confirmed the findings of Degeiso

et al. that the functional group shows selectivity for uranyl ions in the pH range 3–4.

SUMMARY

Condensation resins containing salicylic acid and *p*-hydroxybenzoic acid were synthesised; their ion-exchange properties were examined and compared with a polystyrene-azo-salicylic acid ion exchanger. The salicylic acid exchangers exhibited selectivity for copper, aluminium and uranyl ions in a manner predictable from the stability constants of the metal salicylates. The salicylate exchanger showed a higher selectivity for iron(III) than an equivalent *p*-hydroxybenzoic acid exchanger. One of the salicylic acid condensation resins was used successfully in column operation to determine the iron and copper contents of a brine.

REFERENCES

1 T. R. E. Kressman and J. A. Kitchener, *J. Chem. Soc., London*, (1949) 1190.
2 H. Kawake and M. Yanagita, *Rep. Sci. Res. Inst. (Japan)*, 28 (1952) 264.
3 S. Umezawa and U. Ohtsuka, *Japanese Patent 1598*, 1953; *Chem. Abstr.*, 48 (1954) 2290.
4 S. Matsumura and T. Kamiya, *Japanese Patent 1693*, 1953; *Chem. Abstr.*, 48 (1954) 3596.
5 R. V. Davies, J. Kennedy, E. S. Lane and J. L. Willans, *J. Appl. Chem.*, 9 (1959) 368.
6 R. C. Degeiso, L. G. Donaruma and E. A. Tomic, *J. Org. Chem.*, 27 (1962) 1424.
7 R. C. Degeiso, L. G. Donaruma and E. A. Tomic, *Anal. Chem.*, 34 (1962) 845; *Ind. Eng. Chem.*, 2 (1963) 43.
8 T. I. Rabek, J. Lindeman and B. Brekiesz, *Bull. Acad. Pol. Sci.*, 9 (1961) 555.
9 L. Hanelkova and M. Bartusek, *Collect. Czech. Chem. Comm.*, 34 (1969) 3722.
10 F. Vernon and H. Eccles, *Anal. Chim. Acta*, 63 (1973) 403.
11 A. I. Vogel, *Quantitative Inorganic Analysis*, 3rd edn., Longmans, London, 1962.
12 M. Pinta, *Detection and Determination of Trace Elements*, I.P.S.T., Jerusalem, 1966.
13 W. C. Johnson (Ed.), *Organic Reagents for Metals*, Vol. 2, Hopkin and Williams, Chadwell Heath, Essex, 1966.
14 C. H. R. Gentry and L. G. Sherrington, *Analyst (London)*, 71 (1946) 432.
15 H. Eccles and F. Vernon, *Anal. Chim. Acta*, 66 (1973) 231.
16 E. R. Nightingale, Jr., *J. Phys. Chem.*, 63 (1959) 1381.

Analytica Chimica Acta, 72 (1974) 339–343

EFFECTS OF QUATERNARY AMMONIUM BASES ON VALENCE-SATURATED BUT COORDINATION-UNSATURATED CHELATES

PART II. EXTRACTION OF MAGNESIUM 8-HYDROXYQUINOLINATE

SHINICHIRO NORIKI and MASAKICHI NISHIMURA

Analytical Chemistry Division, Department of Chemistry, Faculty of Fisheries, Hokkaido University, Hakodate 040 (Japan)

(Received 25th February 1974)

8-Hydroxyquinoline (oxine) forms chelates with many divalent metals. Among these, magnesium oxinate chelate is poorly extractable into inactive solvents such as benzene, 1,2-dichloroethane and nitrobenzene, because of formation of the magnesium oxinate dihydrate, which involves strongly coordinated water molecules[1,2]. If the coordinated water molecules in the chelate are replaced by other neutral organic molecules, *i.e.* if the coordination is saturated, the chelate can be extracted into inactive solvents. For this purpose, synergic extractions in the presence of n-butylamine[3], butylcellosolve[4,5] and pyridine[6] have been suggested.

In this paper, it is shown that the magnesium–oxine chelate can be quantitatively extracted into inactive solvents in the presence of a quaternary ammonium base, tetradecyldimethylbenzylammonium chloride (zephiramine), as the ternary complex $Mg(Q)_3(zeph)$. In the previous paper[7], the authors reported the peculiar effect of zephiramine on valence-saturated but coordination-unsaturated chelates, which changed to coordination-saturated chelates on higher coordination of the reagent in the presence of zephiramine. A similar effect was observed for the magnesium–oxine chelate.

EXPERIMENTAL

Reagents

Standard magnesium solution. A $1 \cdot 10^{-2}$ *M* magnesium sulfate solution was standardized with EDTA.

Oxine solution. A $1 \cdot 10^{-2}$ *M* solution was prepared by dissolving 0.726 g of 8-hydroxyquinoline in 500 ml of each organic solvent.

Zephiramine solution. A $5 \cdot 10^{-3}$ *M* solution was made by dissolving 0.920 g of tetradecyldimethylbenzylammonium chloride in 500 ml of water.

Organic solvents. Nitrobenzene, carbon tetrachloride, chloroform and 1,2-dichloroethane were used.

All the chemicals used were of analytical-reagent grade.

Procedure

The magnesium solution, borate buffer solution and the zephiramine solution

were placed into a separatory funnel, and diluted to 20 ml with water. The oxine–organic solvent solution (20 ml) was added and the funnel was shaken for 5 min. After the organic phase had been dried with anhydrous sodium sulfate, the absorbance was measured at 390 nm.

Distribution ratios were obtained by determining the magnesium concentration in the aqueous phase by atomic absorption spectrometry. All extractions were done in a thermostated room ($25 \pm 1\,^{\circ}C$).

RESULTS AND DISCUSSION

Composition of extracted chelate in the presence of zephiramine

The composition of the extracted magnesium chelate with oxine (HQ) in the presence of zephiramine (zeph) was examined by the equilibrium shift and continuous variations methods.

Dependences of log D, D being the distribution ratio, on pH and log[HQ] are shown in Figs. 1 and 2. All these plots gave straight lines with slopes of 3, which indicates that the extracted magnesium chelate has the composition $[Mg(Q)_3]^-$. The relationship between log D and log[zeph] is illustrated in Fig. 3. The results in Figs. 1–3 show that the extracted chelate has the composition $Mg(Q)_3(zeph)$. As indicated in Fig. 4, the continuous variations method confirmed this composition for the extracted chelate.

In the previous paper[7], the authors stated that zephiramine has the effect of changing a coordination-unsaturated chelate to an extractable coordination-saturated chelate by replacing water molecules with the same reagent used as a ligand, showing the examples of chelates with glyoxal bis-(2-hydroxyanil) and *o*-(salicylideneamino)phenol.

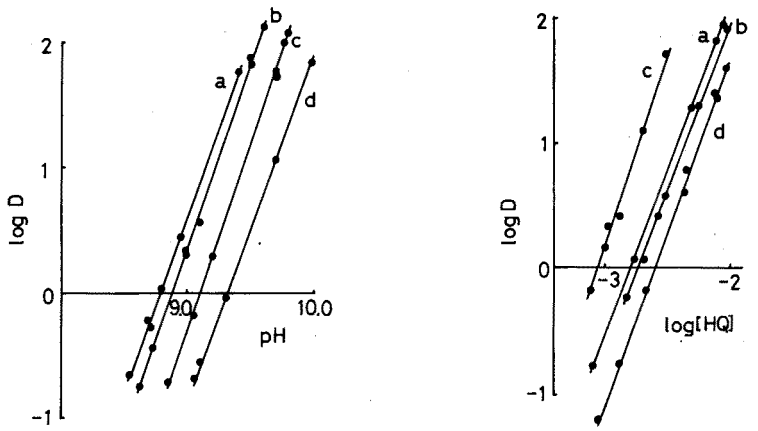

Fig. 1. Dependence of log D on pH in the extraction of magnesium oxinate with various solvents in the presence of zephiramine. $[Mg] = 1 \cdot 10^{-4}$ M, $[HQ] = 1 \cdot 10^{-2}$ M, and $[zeph] = 1 \cdot 10^{-3}$ M. (a) Nitrobenzene, (b) 1,2-dichloroethane, (c) chloroform, and (d) carbon tetrachloride.

Fig. 2. Dependence of log D on log[HQ] in the presence of zephiramine. $[Mg] = 1 \cdot 10^{-4}$ M, and $[zeph] = 1 \cdot 10^{-3}$ M. (a) Nitrobenzene at pH 9.50, (b) 1,2-dichloroethane at pH 9.50, (c) chloroform at pH 10.05, and (d) carbon tetrachloride at pH 9.80.

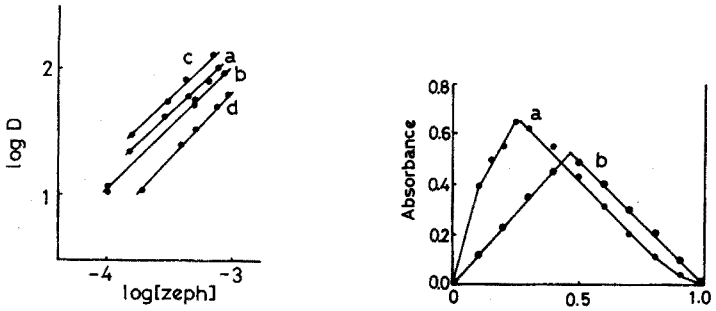

Fig. 3. Dependence of log D on log[zeph]. [Mg] = $1 \cdot 10^{-4}$ M. (a) Nitrobenzene at [HQ] = $1 \cdot 10^{-2}$ M and pH 9.50, (b) 1,2-dichloroethane at [HQ] = $1 \cdot 10^{-2}$ M and pH 9.50, (c) chloroform at [HQ] = $5 \cdot 10^{-3}$ M and pH 10.05, and (d) carbon tetrachloride at [HQ] = $1 \cdot 10^{-2}$ M and pH 9.80.

Fig. 4. Continuous variations method for magnesium–oxine and magnesium–zephiramine relationships. (a) [Mg]/[Mg] + [HQ]), [Mg] + [HQ] = $5 \cdot 10^{-4}$ M and [zeph] = $5 \cdot 10^{-4}$ M; (b) [Mg]/[Mg] + [zeph]), [Mg] + [zeph] = $1 \cdot 10^{-4}$ M and [HQ] = $5 \cdot 10^{-3}$ M.

In the case of the magnesium–oxine chelate, the same effect of zephiramine was observed. In the absence of zephiramine, magnesium forms the coordination-unsaturated chelate with two molecules of water. In the presence of zephiramine, however, the coordinated water molecules are expelled and one more ligand (HQ^-) coordinates to the central metal of the chelate, forming a coordination-saturated chelate, $[Mg(Q)_3]^-$. As a result, the coordination-saturated anionic chelate is extracted into organic solvents by coupling with the added zephiramine, as Mg-$(Q)_3$(zeph).

For the extraction, the following system can be considered:

$$Mg(H_2O)_6^{2+} + 2(HQ) \rightleftharpoons Mg(Q)_2 \cdot 2\,H_2O + 2\,H^+ + 4\,H_2O$$

$$Mg(Q)_2 \cdot 2\,H_2O + HQ + zeph^+ \rightleftharpoons [Mg(Q)_3]^-[zeph]^+ + H^+ + 2\,H_2O$$

Thus:

$$K_{ex} = \frac{[Mg(Q)_3(zeph)][H^+]^3}{[Mg^{2+}][HQ]^3[zeph^+]}$$

When nitrobenzene, 1,2-dichloroethane, chloroform or carbon tetrachloride is used, the extracted chelate has the same composition, but the nature of the organic solvent influences the extractability of the chelate. In the extraction of ion-association chelates, it has been generally said that the higher the dielectric constant of the organic solvent, the higher is the extractability. For the extractable magnesium–oxine chelate, the extraction constants (K_{ex}) and the dielectric constants of the organic solvents are listed in Table I and their relationship is shown in Fig. 5. The relationship shows a good agreement with the general rule for extractions by ion-association.

Effect of zephiramine on the pyridine adduct

Although zephiramine seems to have the ability to expel coordinated water molecules, it is also of interest to know the effect of zephiramine on coordinated neutral organic adducts. Nakaya and Nishimura[6] have pointed out that the ordinary

TABLE I

EXTRACTION CONSTANTS AND DIELECTRIC CONSTANTS OF THE ORGANIC SOLVENTS USED

	CCl_4	$CHCl_3$	$C_2H_4Cl_2$	$C_6H_5NO_2$
Dielectric constant (α)	2.2	4.8	10.4	34.8
$-\log K_{ex}$	18.5	18.0	17.7	17.3

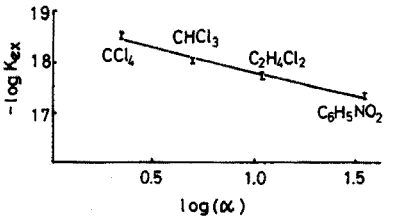

Fig. 5. Relationship between K_{ex} and dielectric constant.

magnesium–oxine chelate can be extracted into 1,2-dichloroethane by the synergic effect of pyridine, the composition of the extracted chelate being $Mg(Q)_2$(pyridine). The effect of zephiramine on the pyridine adduct of the magnesium–oxine chelate was investigated. In the presence of pyridine and absence of zephiramine, the distribution ratio (D) was measured; then zephiramine was added to the

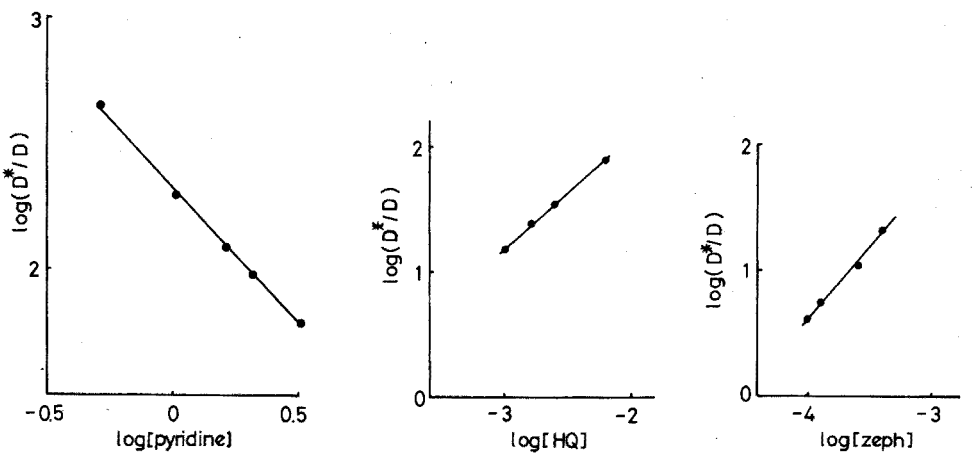

Fig. 6. Pyridine dependence for the formation of the Mg–oxine–zephiramine chelate from the Mg–oxine–pyridine chelate. $[Mg] = 1 \cdot 10^{-4}$ M, $[HQ] = 1 \cdot 10^{-2}$ M, $[zeph] = 1 \cdot 10^{-3}$ M, and pH = 9.50.

Fig. 7. Oxine dependence for the formation of the Mg–oxine–zephiramine chelate from the Mg–oxine–pyridine chelate. $[Mg] = 1 \cdot 10^{-4}$ M, $[zeph] = 1 \cdot 10^{-3}$ M, $[pyridine] = 0.5$ M, and pH = 9.50.

Fig. 8. Zephiramine dependence for the formation of the Mg–oxine–zephiramine chelate from the Mg–oxine–pyridine chelate. $[Mg] = 1 \cdot 10^{-4}$ M, $[HQ] = 1 \cdot 10^{-2}$ M, $[pyridine] = 0.5$ M, and pH = 9.50.

aqueous phase and the distribution ratio (D^*) was measured again. The influence of zephiramine is indicated by the value of D^*/D as a function of concentrations of pyridine, oxine and zephiramine which are added to the extraction system. Figs. 6–8 show that one molecule of pyridine is removed from the $Mg(Q)_2$(pyridine) chelate, and one more molecule of oxine and one molecule of zephiramine are involved in the chelate in the presence of zephiramine to form the $Mg(Q)_3$(zeph) chelate.

From the results presented here, it may be again concluded that zephiramine has an effect of changing a coordination-unsaturated chelate to a coordination-saturated chelate by expelling water or pyridine molecules with the same reagent; and if the resulting chelate has a negative charge, it can be extracted by ion-association with zephiramine present already in the solution.

SUMMARY

It is known that 8-hydroxyquinoline (HQ) forms a non-extractable chelate with magnesium, $Mg(Q)_2 \cdot 2\,H_2O$, and in the presence of pyridine an extractable chelate, $Mg(Q)_2$(pyridine). In these systems, the presence of a quaternary ammonium base, zephiramine, changes both the oxine chelates to the $Mg(Q)_3$(zeph) chelate which is extractable into inactive solvents. Zephiramine has the effect of expelling coordinated water or the pyridine molecule from a chelate to form a highly coordinated chelate with respect to the ligand.

REFERENCES

1 J. Starý, *The Solvent Extraction of Metal Chelates*, Pergamon, Oxford, 1964, p. 80.
2 J. Starý, *Anal. Chim. Acta*, 28 (1963) 132.
3 F. Umland and W. Hoffman, *Anal. Chim. Acta*, 17 (1957) 234.
4 C. L. Luke and M. E. Campbell, *Anal. Chem.*, 26 (1954) 1778.
5 S. J. Jankowski and H. Freiser, *Anal. Chem.*, 33 (1961) 776.
6 S. Nakaya and M. Nishimura, *Bunseki Kagaku*, 22 (1973) 733.
7 M. Nishimura, S. Noriki and S. Muramoto, *Anal. Chim. Acta*, 70 (1974) 121.

Analytica Chimica Acta, 72 (1974) 345–351

THE COULOMETRIC TITRATION OF ACIDS AND BASES IN *m*-CRESOL MEDIUM

M. BOS and E. A. M. F. DAHMEN

Department of Chemical Technology, Twente University of Technology, Enschede (The Netherlands)

(Received 2nd April 1974)

Coulometric titrations in non-aqueous solvents offer some distinct advantages over conventional titrations. First of all, it is possible to generate and use titrants which are unstable on storage. Moreover, the method is somewhat more sensitive: coulometric titrations can be carried out in the microequivalent range. There is no need for standardization of titrants, and the titration curves show better resolution because of the absence of dilution effects. Finally, coulometric titrations can easily be automated, as the parameters which control the titration are electrical.

However, several difficulties are involved in coulometric titrations in non-aqueous solvents. High cell resistances necessitate the use of high voltage sources and even with these the currents that can be obtained are generally low. The separation of the anode and cathode compartment of the cell when non-aqueous solvents are used can also be a problem. For liquids with a high viscosity, sintered glass discs are adequate but with other solvents loss of current efficiency can occur. Ion-exchange membranes which are very satisfactory for this purpose when water is the solvent[1], usually have too high resistances in organic media. When the course of a titration is followed by potentiometry with the glass electrode, as is mostly the case for the titration of acids and bases, sometimes the slow response of the glass electrode[2] makes rapid titrations impossible. Moreover, when the glass electrode is used, the generating current affects the pH reading. By proper cell design this effect can be minimized, but it is very difficult to overcome completely.

Many non-aqueous solvents have already been used for coulometric acid–base titrations, *e.g.* acetic acid/acetic anhydride[3,4], isopropanol[5], acetonitrile[3,6], tert-butanol[7] and tetrahydrofuran[8]. For tert-butanol and tetrahydrofuran—solvents of relatively low dielectric constant—it was necessary to add 0.2% water to generate base with 100% current efficiency[7,8]. When homoconjugation of the compound to be titrated can be expected, the use of solvents with relatively low dielectric constants can be advantageous, as this phenomenon has only a small influence on the accuracy of the titrations in these solvents[9]. However, the necessity of adding water nullifies this advantage, owing to decreased sharpness of the end-points.

In the present study, *m*-cresol (dielectric constant 12.3) was chosen as the solvent as it was expected that the electrogeneration of base would be possible from the solvent itself. Moreover, *m*-cresol is a good solvent for various types of compounds, *i.e.* polymers like "Terlenka". A study of the anodic oxidation of

bases in *m*-cresol[10] has shown that the determination of bases in *m*-cresol is possible by constant-potential coulometry. In coulometric titrations, the working electrode potential cannot be kept constant, as this would give rise to prohibitively long electrolysis times. Normally, coulometric titrations are run at constant current. Without precautions, the potential of the working electrode varies during the titration under these circumstances, which means that side reactions and loss of current efficiency can occur. To prevent this an excess of a very weak base can be added. For this purpose 0.2 *M* urea was added to the supporting electrolyte.

EXPERIMENTAL

Chemicals

m-Cresol (Baker, polymer characterization solvent) was purified by distillation (b.p. 201–201°C), drying for 24 h on molecular sieves (3 Å, Union Carbide) and a second distillation (b.p. 201–202°C). The product was used within a day of preparation. The water content was below 0.002% (Karl Fisher titration).

Tetraethylammonium perchlorate (TEAP, Eastman Kodak) and tetramethylammonium chloride (Eastman Kodak, reagent grade) were recrystallized from ethanol and dried *in vacuo* at 40°C before use.

2,4-Dinitrobenzenesulfonic acid (Eastman Kodak, reagent grade), benzenesulfonic acid (Riedel de Haen), trishydroxymethylaminomethane (Merck, Zur Analyse), picric acid (Merck, Zur Analyse), bromochlorophenol blue (Merck, Indikator), strychnine (Merck, Purum), iodoacetic acid (Merck, Zur Analyse), tribenzylamine (Eastman Kodak), 1,3-diphenylguanidine (Eastman Kodak), n-butylamine (Fluka, puriss.), triethylamine (Koch Light, puriss.) and tetramethylguanidine (Eastman Kodak, pract.) were used as received. Solutions of the acids in *m*-cresol were standardized against trishydroxymethylaminomethane (Merck, Urtitersubstanz). Solutions of the bases in *m*-cresol were standardized by titration with hydrochloric acid.

Apparatus

The coulometric titrations were carried out at room temperature in an H-type cell of which the titration compartment had a content of about 30 ml. The working electrode consisted of platinum gauze (area 4 cm^2). A platinum wire was used as auxiliary electrode. The course of the titration was followed by potentiometry with a glass electrode (Ingold, type HA 405) and an Ag/AgCl reference electrode filled with 0.1 *M* tetramethylammonium chloride in *m*-cresol. A salt bridge with 0.1 *M* TEAP in *m*-cresol was inserted between the reference electrode and the test solution. These electrodes were connected to a pH meter (Radiometer, type PHM 28). A Philips recorder (PM 8100) was used to record the titration curves. The electrolysis current was delivered by a Metrohm constant-current coulometer (type E 211).

Current integration was done with an electronic integrator constructed from a Keithley operational amplifier type K 301. A schematic diagram of the equipment is given in Fig. 1.

Coulometric titration of acids

The bridge section and the auxiliary electrode compartment of the coulometric

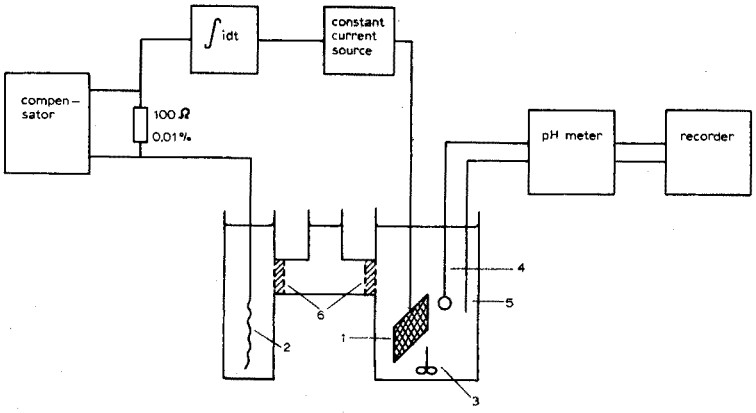

Fig. 1. Schematic diagram of the equipment for coulometric titration of acids and bases in *m*-cresol. (1) Working electrode, (2) auxiliary electrode, (3) stirrer, (4) glass electrode, (5) Ag/AgCl reference electrode, (6, 7) G4 sintered glass disk.

cell were filled with 1 *M* TEAP in *m*-cresol. The titration compartment of the cell was filled with 15–20 ml of 0.1 *M* TEAP in *m*-cresol. After insertion of the electrodes, the glass electrode was equilibrated for 10 min in the solution. Then the acid sample dissolved in *m*-cresol (0.5–3 ml of 0.01 *N*) was introduced from a piston burette. The titration was started when the pH meter gave a stable reading, by switching on the current (working cathode) and simultaneously starting the recorder. During titration the current i (A) was monitored by a compensating galvanometer with an accuracy of $\pm 0.01\%$. From the recorded titration curve, the time t(s), necessary to reach the equivalence point was determined. The amount of acid present in the sample was calculated from the formula:

$$\text{eq. acid} = ti/96500 \qquad (1)$$

The cell was cleaned and refilled after each determination. When not in use, the glass electrode was stored in aqueous buffer pH 7.

Coulometric titrations of bases

For the coulometric titration of bases, a somewhat different procedure was followed. The working electrode was operated as the anode. The cell fillings were the same, except the filling of the titration compartment. Here 0.1 *M* TEAP with 0.2 *M* urea in *m*-cresol was used. After the 10-min equilibration period for the glass electrode, a small amount of sample was introduced in the titration cell and a test titration was started when the pH meter showed a stable reading. From the recorded titration curve, the pH value in the equivalence point was determined. By changing the polarity of the working electrode and the auxiliary electrode and switching on the current again, the pH of the solution in the titration compartment was brought back to the value of the equivalence point. Then a sample of base dissolved in *m*-cresol was introduced from a piston burette (0.5–3 ml of 0.01 *N*). The actual titration was performed with the working electrode as anode in the circuit. In the vicinity of the equivalence point, the current was decreased and finally stopped when the pH of the solution reached the pH value of the

equivalence point. Then the integrator was read and the amount of base present in the sample was calculated from the formula

$$\text{eq. base} = Q/96.500 \qquad (2)$$

where Q is the integrator reading in coulombs. Up to 4 determinations were made with the same cell fillings.

RESULTS

Titration of acids

A typical coulometric titration curve is given in Fig. 2 for the titration of 6.85 μeq of 2,4-dinitro benzenesulfonic acid. To determine the standard deviation

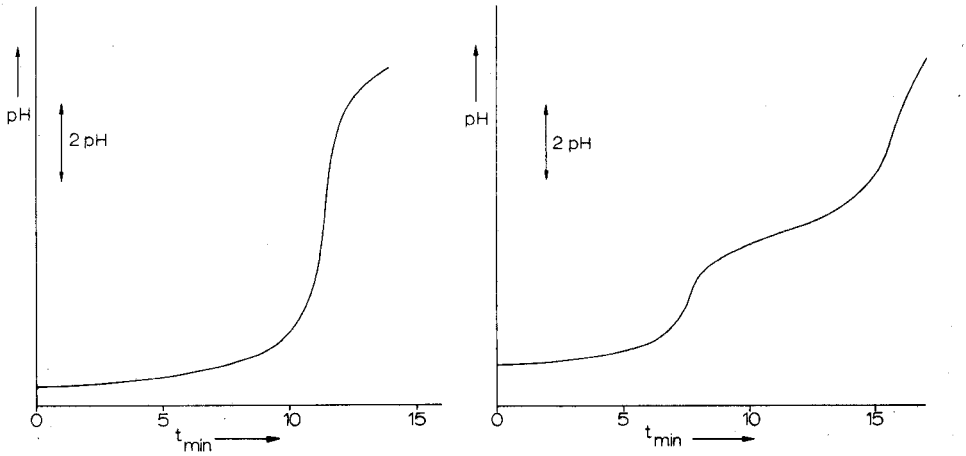

Fig. 2. Curve for the coulometric titration of 6.85 μeq of 2,4-dinitrobenzenesulfonic acid in *m*-cresol. Current, 0.965 mA.

Fig. 3. Curve of the coulometric titration of a mixture of 4.60 μeq of benzenesulfonic acid and 4.80 μeq of picric acid in *m*-cresol. Current, 0.960 mA.

TABLE I

COULOMETRIC TITRATION OF PICRIC ACID IN *m*-CRESOL

μeq. Added	*μeq. Found*	*% Recovery*	*Current eff. (%)*
9.44	9.46	100.2	99.8
9.44	9.43	99.9	100.1
9.44	9.40	99.6	100.4
9.44	9.40	99.6	100.4
9.44	9.46	100.2	99.8
9.44	9.37	99.3	100.7
9.44	9.43	99.9	100.1
14.16	14.23	100.5	99.5
18.88	18.62	98.6	101.4
18.88	18.80	99.6	100.4

TABLE II

COULOMETRIC TITRATION OF ACIDS IN *m*-CRESOL

Compound	*μeq. Added*	*μeq. Found*	*% Recovery*	*Current eff. (%)*
2,4-Dinitrobenzene sulfonic acid	8.51	8.53	100.2	99.8
2,4-Dinitrobenzene sulfonic acid	8.51	8.53	100.2	99.8
2,4-Dinitrobenzene sulfonic acid	8.51	8.55	100.5	99.5
2,4-Dinitrobenzene sulfonic acid	17.02	17.04	100.1	99.9
2,4-Dinitrobenzene sulfonic acid	17.02	17.04	100.1	99.9
Benzenesulfonic acid	9.39	9.52	101.4	98.6
Benzenesulfonic acid	9.39	9.49	101.1	98.9
Benzenesulfonic acid	9.39	9.52	101.4	98.6
Benzenesulfonic acid	9.39	9.62	102.4	97.6
Benzenesulfonic acid	18.78	18.92	100.7	99.3
Bromochlorophenol blue	7.78	7.81	100.4	99.6
Bromochlorophenol blue	7.78	7.78	100.0	100.0
Bromochlorophenol blue	7.78	7.77	99.9	100.1
Bromochlorophenol blue	15.56	15.40	99.0	101.0
Bromochlorophenol blue	15.56	15.40	99.0	101.0
Iodoacetic acid	50.05	49.95	99.8	100.2
Iodoacetic acid	50.05	49.80	99.5	100.5
Iodoacetic acid	50.05	50.50	100.9	99.1

for the method, ten titrations of picric acid were performed (Table I). The standard deviation was $\pm 0.6\%$. The other results are summarized in Table II. An example of a differential titration of two acids is given in Fig. 3 for the titration of a mixture of benzenesulfonic acid and picric acid.

Titration of bases

In Fig. 4 the coulometric titration of n-butylamine is given as an example. The results for various bases are summarized in Table III.

DISCUSSION AND CONCLUSIONS

As reported earlier[10], the electrode reaction in the coulometric titration of bases is the oxidation of the *m*-cresolate ion. When 0.2 *M* urea is present in the supporting electrolyte, the important steps in the titration are:

$$\text{urea} + \text{Hcres} \rightleftharpoons \text{ureaH}^+\text{cres}^- \rightleftharpoons \text{ureaH}^+ + \text{cres}^+ \quad (3)$$

$$\text{cres}^- \rightarrow \text{cres}^{\cdot} + e \quad (4)$$

The net result is the production of ureaH^+. For a successful titration, the base to be titrated should react with the ureaH^+, which means that the equilibrium constant of the reaction

$$\text{ureaH}^+ + \text{B} \rightleftharpoons \text{urea} + \text{BH}^+ \quad (5)$$

should be 10^5 or higher. From the pK_b value of 13.8 for urea in water[11], the pK_a value for ureaH^+ in *m*-cresol is estimated[12] to be about 6. Thus the method

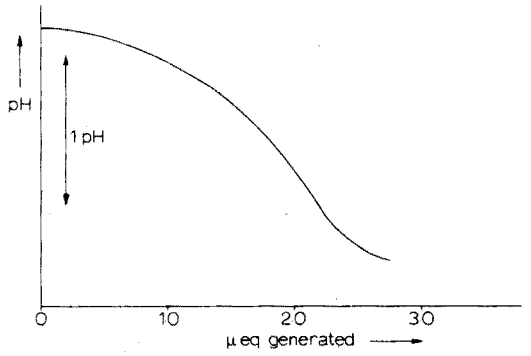

Fig. 4. Curve of the coulometric titration of 2.16 μeq of n-butylamine in *m*-cresol. Current, 1.000 mA.

TABLE III

COULOMETRIC TITRATIONS OF BASES IN *m*-CRESOL

Compound	*μeq. Added*	*μeq. Found*	*% Recovery*[a]	*Current eff. (%)*	s_r[a]
Tribenzylamine	30.0	30.15	100.5	99.5	1.0
n-Butylamine	35.61	34.49	96.8	103.2	0.8
Diphenylguanidine	30.0	30.06	100.2	99.8	0.8
Triethylamine	43.20	43.29	100.2	99.8	0.7
Tetramethylguanidine	37.8	37.62	99.4	100.6	0.4

[a] Mean of 10 determinations with relative standard deviation (s_r).

is suitable for bases with pK_a values above 11 in *m*-cresol or with pK_a values above 6 in water. From Table III, it can be seen that the accuracy of the titrations increases with increasing strengths of the bases. No explanation can be offered for the low current efficiency in the determination of *n*-butylamine.

In the titrations of the acids, the electrode reaction most likely is:

$$2\,HCres + 2e \rightarrow H_2\uparrow + 2Cres^-$$

as gas evolution can be observed at the working electrode during titration. The weakest acid that could be titrated was iodoacetic acid (pK_a in *m*-cresol = 13).

Of the two methods used in the end-point determination, that used for the titration of bases, *i.e.* titration to a fixed end-point, has the advantage that the cell solution can be used more than once. However, a pre-titration is necessary to establish the value of the end-point. The accuracy of the two methods is about the same.

The authors are indebted to A. H. J. Tijhuis, Btw. who performed part of this work for his B.Sc. degree. They also thank Mrs. B. Verbeeten-v. Hettema who prepared the manuscript and Mr. R. H. Arends who made the drawings.

SUMMARY

A method is described for the coulometric titration of acids and bases in

the solvent *m*-cresol. The method is suitable for bases with pK_a values greater than 11 in *m*-cresol, or for acids with pK_a values below 13 in *m*-cresol. Amounts of 5–50 μeq of acid or base can be determined with a relative accuracy of $\pm 1\%$.

REFERENCES

1 J. Dubbeling, C. M. van den Enk-van Twillert and E. A. M. F. Dahmen, *International Symposium on Analytical Chemistry, Birmingham (U.K.), July, 1969.*
2 B. Karlberg, *Anal. Chim. Acta*, 66 (1973) 93.
3 V. J. Vajgand and R. Mihajlović, *Talanta*, 16 (1969) 1311.
4 W. B. Mather and F. C. Anson, *Anal. Chim. Acta*, 21 (1959) 468.
5 B. G. Cooksey, B. Metters, J. M. Ottaway and D. W. Whymark, *Talanta*, 20 (1973) 371.
6 C. A. Streuli, *Anal. Chem.*, 28 (1956) 130.
7 G. S. Fritz and F. E. Gainer, *Talanta*, 15 (1968) 939.
8 C. E. Champion and D. G. Bush, *Anal. Chem.*, 45 (1973) 640.
9 M. Bos and E. A. M. F. Dahmen, *Anal. Chim. Acta*, 63 (1973) 325.
10 M. Bos and E. A. M. F. Dahmen, *Anal. Chim. Acta*, in press.
11 R. C. Weast, *Handbook of Chemistry and Physics*, 45th edn., The Chemical Rubber Co., 1964, p. D76.
12 M. Bos and E. A. M. F. Dahmen, *Anal. Chim. Acta*, 57 (1971) 361.

Analytica Chimica Acta, 72 (1974) 353–364

ENZYMATIC ANALYSIS BY MEANS OF THE AIR-GAP ELECTRODE DETERMINATION OF UREA IN BLOOD

ELO H. HANSEN and JAROMIR RŮŽIČKA

Chemistry Department A, The Technical University of Denmark, Building 207, 2800 Lyngby (Denmark)

(Received 3rd May 1974)

During the last decade, several potentiometric methods have been suggested for measurements of nitrogen-containing organic compounds via enzyme-catalysed ammonium ion-releasing reactions[1–4]. This approach is attractive not only for its potential simplicity and speed, but also because it allows highly selective determinations of a number of clinically and biochemically important species[3]. Provided that suitable experimental procedures and conditions for chemical reactions are found, either the amount of substrate or the enzyme activity may be determined. Thus, for determination of various substrates, different enzyme electrodes have been suggested[4–12]; of these the urea electrode, based on the urease-catalysed release of ammonium ions, has been most frequently investigated[4,13–16]. The reason for this particular interest is not only the importance of urea determination in blood, urine, tissues, fertilizers, and animal fodder, but also because this assay may serve as a model system for development of methods for enzymatic determinations of other nitrogen-containing compounds.

The purpose of the present work is to introduce a new potentiometric gas sensor, the air gap electrode[17] into the enzymatic assay. This required a new approach and resulted in a method which was developed to a point where determination of urea can be performed on a routine basis.

Enzyme electrodes

Any sensor of this type is a sensitized electrode, measuring a species of an interposed chemical reaction. Thus, the already classical urea electrode of Guilbault and Montalvo[4] uses immobilized urease imbedded in a layer of acrylamide gel covering the surface of a glass electrode. The ammonium ion, produced from the urea in the sample solution:

$$CO(NH_2)_2 + H_3O^+ + H_2O \xrightarrow{\text{urease}} 2\,NH_4^+ + HCO_3^- \qquad (1)$$

is sensed by the glass cation-sensitive electrode. Since then, electrodes sensitive to L-amino acids[6], D-amino acids[7], asparagine[7], and arginine[11] have been suggested. When these papers are studied in conjunction with further experimental material gathered with newer versions of urease electrodes[13–16], it becomes evident that various requirements must be fulfilled in order to obtain a sensor with reproducible parameters. This is because the organic molecule to be determined has to diffuse from the bulk of sample to the surface of the gel layer, enter it, and react there in the presence of enzyme; and then the reaction product has to diffuse further

towards the surface of the sensing electrode until a steady-state response has been achieved. The reaction products must also be able to rediffuse easily from the electrode surface so that the electrode recovers quickly before the next measurement. Thus a thin enzyme-containing layer seems essential, yet such electrodes are less stable and have a non-linear response at high substrate concentration[13,18], because the thin layers cannot contain enough enzyme to catalyse all the substrate diffusing from concentrated sample solutions. Therefore, in order to achieve a linear response up to bulk substrate concentrations higher than the Michaelis constant of the enzyme, cellophane layers have been used to limit the substrate diffusion into the gel layer[13,18]. The protective cellophane layers also help to retain sufficient enzyme within the electrode, and if the enzyme does not become denatured, the electrode response ought to remain unchanged over longer periods of time. Unfortunately, electrodes with such an "onion-like" structure of layers have longer response times[18]. To summarize, it is the enzyme content, the enzyme-retaining properties, the thickness, the porosity, and other physical parameters of the enzyme-containing layer, which affect the performance of any enzyme electrode.

The other set of critical properties depends on the ion-sensing electrode used. Unfortunately, none of the electrodes used so far has been selective enough to allow direct measurements in biological fluids. The originally used[1–4,6,7,12–14] Beckman 39137 cationic electrode (said to have the glass composition 27% Na_2O, 4% Al_2O_3, and 69% SiO_2)[3] has the selectivity series $Ag^+ > H^+ > K^+ > NH_4^+ > Na^+ > Li^+ \gg Mg^{2+} > Ca^{2+}$, yet this order may, in respect to NH_4^+ to Na^+, even change from one batch to another[3,19]. This imposes a severe limitation on the use of this electrode in biological fluids (*e.g.*, human serum contains 0.14 *M* Na^+, $5 \cdot 10^{-3}$ *M* K^+ and $5 \cdot 10^{-3}$ *M* urea), hence the newer ammonium ion-sensor is now generally used. This electrode, developed by Simon and Scholer[20] utilizes nonactin (72%) and monactin (28%) in tris(2-ethylhexyl)phosphate, and has selectivities of 10 over K^+ and 500 over Na^+. This liquid-membrane electrode, however, cannot be sensitized for urea measurements because the immobilized enzyme layer would be destroyed by contact with the organic solvent of the membrane. In order to overcome this difficulty Guilbault and Nagy[15] incorporated nonactin directly into a silicone rubber matrix and then covered this solid-state ammonium electrode by the enzyme layer. The selectivity constants for this ammonia sensor are 6.5 for NH_4^+/K^+ and 750 for NH_4^+/Na^+, which is a substantial improvement over the cationic glass electrode, but the contribution of the potassium present in normal human serum is equivalent to about 1 mmol of NH_4^+. Therefore, Guilbault *et al.*[16], when determining urea in blood sera, had to use a special compensation technique for which the interference level was monitored by means of an ammonia electrode, and the potassium level was adjusted to that at which the urea calibration curve had been prepared, before the final urea measurement with the urease electrode was performed. They also concluded that the stability of any enzyme electrode depends on (a) the stability of the electrochemical sensor; (b) the physical stability of the enzyme reaction layer (as it may swell to various thicknesses depending on its age and the ionic strength of the measured solution); and (c) the durability of the catalytic reactivity of the enzyme. It is therefore difficult to prepare a stable electrode because the essential properties of physical stability and enzyme-coupling capacity of the gel seem to be antagonistic[16].

Thus, owing to lack of selectivity of the electrochemical sensor and instability of the enzyme layer, none of the present urea electrodes seem to be suitable for routine measurements in body fluids. It might therefore be useful to adopt an admittedly less elegant, yet perhaps more reliable concept of potentiometric enzyme assay, that is, separating the catalytic and sensing reactions so that they can each be performed under strictly controlled optimal conditions. This will also allow use of a newly developed, highly selective gas sensor, the air-gap electrode.

The air gap electrode

Gas-sensing electrodes generally utilize a glass electrode and a reference electrode joined by an electrolyte the pH of which changes whenever an alkaline (or acid) reacting gas diffuses into it. The construction of these sensors is derived from the original design of the CO_2 electrode except that the recent sulphur dioxide and ammonia electrodes employ different electrolytes and gas-permeable membranes[21,22]. When such a gas electrode is used for, *e.g.*, ammonia measurements, the sensor is dipped into the sample solution and the ammonia gas present or generated there diffuses through the gas membrane into the ammonium chloride electrolyte solution. The higher the content of ammonia, the higher the pH, provided that the gas-permeable membrane permits free diffusion of gas, but totally prevents any diffusion of the sample solution into the inner electrolyte. The main advantage of this type of ammonia sensor is its extremely high selectivity, but practical difficulties—such as poor mechanical properties of the membrane and the possible clogging of the pores when measuring in *e.g.*, serum samples[23]—seems to limit its utility. Besides, as observed by Guilbault and Nagy[15], the ammonia gas electrode cannot be used as part of an urea enzyme sensor because it must be operated at pH values so high that the urease is denatured.

The recently developed air-gap electrode[17] is based on the same principle as other gas sensors, except that it does not have any gas-permeable membrane. The membrane is replaced by an air gap which separates the electrolyte layer from the sample solution, the entire system being contained in a gas-tight measuring chamber. The electrolyte itself is adsorbed as a very thin film on the surface of the indicator (pH) electrode. The greatest advantage of this design is that the electrode is never in direct physical contact with the sample solution which therefore may contain proteins, blood cells, surfactants, and other components that normally affect the function of any electrode. The simplicity of design, the easy renewal of electrolyte, and the fast response are further advantages of the air gap. It has been shown[17] that the air-gap electrode responds to ammonium ion concentrations according to the equation:

$$pH_e = \log[NH_4^+]_s - \log[NH_4^+]_e + pH_s + C \qquad (2)$$

from which it follows that the signal (pH_e) is proportional to the ammonium ion concentration of the sample ($[NH_4^+]_s$) provided that the electrolyte concentration on the surface of the glass electrode ($[NH_4^+]_e$), the pH of the sample (pH_s), and the geometry of the experimental set-up, the temperature, the ionic strength of the samples, and the atmospheric pressure are constant (combined in the constant C). Depending on the choice of pH_s, the ammonium ions of the sample can be either quantitatively or partially converted to ammonia. For a given concentration of

ammonium ion in the electrolyte, $[NH_4^+]_e$, quantitative conversion, obtained at $pH_s \geqslant 10.5$ (see Fig. 1A), will yield a calibration curve encompassing the largest possible $[NH_4^+]_s$ range (Fig. 1B, curve b). At lower pH_s values a less pronounced response will be obtained, while in the near neutral solutions ($pH_s = 7.5$, $[NH_4^+]_e = 10^{-2}$ *M*; Fig. 1B, curve a) the measuring range of the electrode will be severely restricted. Thus, at the pH values at which the catalytic effect of urease is greatest (Fig. 1C; TRIS buffer system; the position of the maximum depends slightly on the pH buffer used), a very poor signal is obtained. This happens because only a small fraction of the total ammonium content is volatilized as ammonia, and because the electrode surface already holds a significant amount of ammonia, originating from the hydrolysis of the electrolyte (Fig. 1A, point ▲). Theoretically, the sensitivity limit (c_L) could be extended to the point where the autoprotolysis of water would interfere (intersection of the H_3O^+ and the OH^- lines, Fig. 1A); but in practice such dilution of the electrolyte is impossible, because even 10^{-4} *M* ammonium chloride gives a noisy signal. Furthermore, no calibration curve can be used for precise evaluation close to the limit of sensitivity, c_L. Thus the practical limit of sensitivity is at best equal to log $c_L + 1$ (Fig. 1B, line c_p); only above this value can the curve can be linearized precisely. The limit for an electrode with a 10^{-2} *M* ammonium chloride electrolyte solution is thus $10^{-4.8}$ *M* ammonia for quantitative conversion, and 10^{-3} *M* ammonia for partial conversion (*e.g.*, $pH_s = 7.5$). The last, but equally serious objection to the method of partial conversion is that any pH_s below 10.5 must be very well fixed in order to achieve the same degree of conversion each time, since a deviation in pH_s of 0.01 pH unit corresponds to *ca.* 2.4% deviation in the measured sample content (compare eqn. (1) and Fig. 1A and B). These computations are, of course, valid not only for the air-gap electrode, but hold also for any gas membrane type ammonia sensor, if the membrane allows unobstructed passage of ammonia.

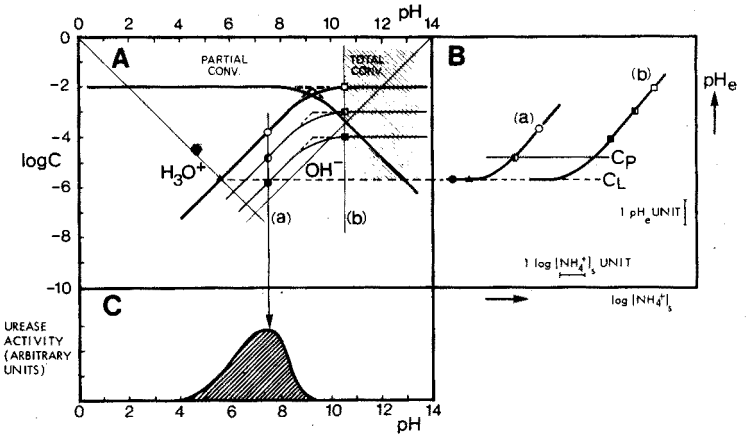

Fig. 1. (A) Logarithmic diagram (Hägg diagram) for the NH_4^+/NH_3 system. (B) Calibration curves for an ammonia electrode with an electrolyte solution of $[NH_4^+]_e = 10^{-2}$ *M*, operated by (a) the partial conversion method, and (b) the total conversion method. (○),(□) $= 10^{-2}$ *M*, (◐),(◧) $= 10^{-3}$ *M*, and (●),(■) $= 10^{-4}$ *M* $[NH_4^+]_s$; c_L denotes the theoretical limit of sensitivity while c_p represents the practical limit. (C) The activity of urease as a function of pH in TRIS buffer. For detailed explanation of this figure, see text.

On the basis of these considerations, it was decided to perform the urea assay in two separate operations, that is, to let the catalytic reaction occur at pH 7.0 (optimal enzyme activity, and as $pH_e < pK_a - 2$ there is no loss of ammonia), and then to carry out the actual ammonia measurements after addition of an excess of strong base, at the conditions of quantitative conversion. Thus parameters such as temperature, time of incubation, amount of enzyme, and volume, could be optimized and then strictly controlled.

EXPERIMENTAL

Apparatus

The air gap electrode described here is a modified design which allows better precision than the original[17]. Figure 2 shows a partial longitudinal sectional view of the cylindrical Teflon body (1) (diameter 50 mm; height 60 mm) accommodating the glass (2) and reference (3) electrodes in a common Perspex tube (4). For this purpose, a smooth coaxial hole (diameter 10 mm) was drilled and furnished with an O-ring (5). The Ag/AgCl reference electrode (3) is surrounded by the electrolyte solution (6) contained within the Perspex tube, the solution being introduced through the small hole (7). The same solution covers the pH-sensitive surface of the glass electrode (8). In this way an electrochemical cell consisting of a glass electrode and a silver chloride electrode is constructed, in which the liquid junction potential is minimized. Thus, an O-ring, which has been degreased and made hydrophilic in a strong detergent, can be used to prevent any leakage of electrolyte from the reference compartment.

The sample chamber (10) (the macrochamber) was cylindrical (Perspex; diameter 50 mm; height 35 mm) with a smooth coaxial hole (diameter 23 mm; depth 30 mm) and was fitted with a soft O-ring (11) serving as a gasket.

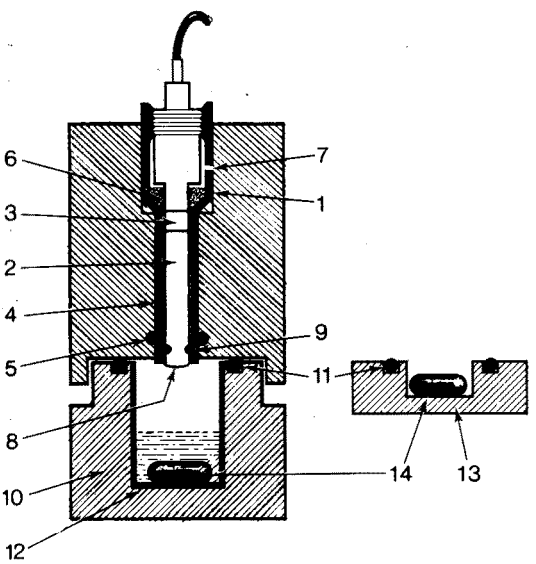

Fig. 2. The construction and the mode of operation of the air gap electrode (for details see text).

Polyethylene vials (12) fitting closely into the chamber cavity were used to hold the samples so that both incubation and measurement could be done in the same container.

The microchamber (13) was cylindrical (Perspex; diameter 42 mm and height 12 mm, provided with a cavity of diameter 13 mm and depth 8 mm) and fitted with an O-ring (11). The cavity was well polished and had rounded corners at the bottom as it was used directly as sample container both for incubation and measurement.

Teflon-coated magnetic stirring bars (14) (15 × 5 mm) were used in both types of chambers.

The electrolyte layer was applied to the electrode by means of a Perspex electrode holder which had a cavity containing the electrolyte solution. The electrode was rested on the holder between measurements, and as the holder was closed by the electrode body, the system was simply turned upside down after each measurement, so that the electrolyte film on the electrode surface was renewed; to remove excess of electrolyte from the surface, a coil of nylon thread was placed in the holder cavity. Alternatively, the electrolyte layer may be applied by touching the electrode surface on a cone-shaped polyurethane sponge in a suitable holder, the sponge being well soaked with the electrolyte. Both surface-renewal techniques[17] yield identical results.

The glass electrode (Radiometer E5036/0) had a flat pH-sensitive surface (area *ca.* 12 mm^2) and combined reference electrode consisting of a silver chloride-covered silver strip. The ammonium chloride electrolyte solution also served as reference solution.

A digital pH meter (Radiometer PHM 52) and a recorder (Servogor RE 520) were used for measuring and recording the electrode response.

All pipetting was done by means of MLA Precision Pipettes (Medical Laboratory Automation, Inc.).

Computations. All calibration curves were calculated by means of linear regression analysis on the linear part of the curves on a WANG 700B Programmable Electronic Calculator provided with a WANG 702 Plotting Output Writer.

Reagents

The electrolyte solution was $1.0 \cdot 10^{-2}$ *M* ammonium chloride (BDH, AnalaR), saturated with wetting agent (Victawet 12, Stauffer Chemical Company, U.S.A.).

The urease enzyme (Calbiochem) had an activity of 74 IU mg^{-1}.

The buffer solution was 0.1 *M* TRIS (tris-(hydroxymethyl)-aminomethane); adjusted to pH 7.0 with hydrochloric acid in which the enzyme was dissolved. This enzyme solution was prepared freshly each day.

The urea used for preparing the standard solutions was a chemically pure quality (Riedel–De Haën).

Serum and blood samples

The serum samples were supplied by the University Hospital of Copenhagen. The serum was freshly sampled and concurrently analyzed at the Hospital (by the AutoAnalyzer method) and at this University. During transportation from the Hospital to the University, the serum samples were kept at 4°C..

The whole blood used was sampled from a nomal, healthy human subject and stabilized with sodium heparine; the blood was analyzed within 1 h of sampling. In order to obtain the plasma, the blood was centrifuged for 5 min at 3000 r.p.m. A portion of this sample was concurrently analyzed at the University Hospital.

Procedure with macrochamber

The calibration of the electrode and the actual serum analyses in the larger sample chamber (macrochamber) were done in an identical manner: 1.00 ml of TRIS buffer containing *ca.* 7.4 units of urease was pipetted into the polyethylene vial containing the magnetic stirring bar, and 200 μl of urea standard solution (or 200 μl of serum) was added. The polyethylene vial was then placed in a water bath (26°C), incubated for at least 2 min, and then transferred to the sample chamber which was placed on a magnetic stirring table. After addition of 1.00 ml of 0.2 *M* sodium hydroxide, the chamber was immediately closed with the electrode body. Only then was the magnetic stirrer started (the stirrer was adjusted to a moderate speed, and switched on and off by a separate switch so that all samples were agitated in approximately the same manner). The signal was followed on the recorder, and when a steady state was reached, the pH_e was read on the digital pH meter within 0.001 pH_e unit.

Procedure with microchamber

The TRIS buffer solution (100 μl containing *ca.* 4 units of urease) was pipetted into the microchamber followed by 100 μl of the standard solution of urea (or 100 μl of the serum sample). The stirring bar was added, and the sample was agitated for *ca.* 20 s, placed in a water bath (26°C) and incubated for at least 2 min. Then it was again placed on the magnetic stirring table and 100 μl of 0.2 *M* sodium hydroxide was added. The chamber was immediately closed with the electrode body and the stirrer was switched on so that it was running at a preadjusted speed. Measurements were completed as above.

RESULTS

The shape of a typical response curve for the macrochamber method is shown in Fig. 3(b), and the calibration curve in Fig. 4(b). For more precise statistical evaluation, a larger number of calibration points was chosen within the physiologically important range (*i.e.*, 0.5, 1.0, 1.25, 2.5, 5.0, and 10.0 mmol/l) and each of these data points was then plotted against the obtained pH_e values. This was done on a minicomputer with a programme which, through linear regression analysis, yielded a calibration curve, which in turn was used for evaluation of the serum samples. For each standard three determinations were performed. Within the physiological range of standards, log [urea] as a function of pH_e yielded a straight-line relationship with a slope of 1.01, the standard error being 0.01 pH_e (corresponding to 2.4%). The regression coefficient was 0.9996. The results of the actual serum analyses are given in Table I, where the urea contents obtained by the AutoAnalyzer method are recorded for comparison. The blank value in all these determinations was less than 0.1 mmol l^{-1}.

A typical response curve for the microchamber method is shown in Fig. 3(a),

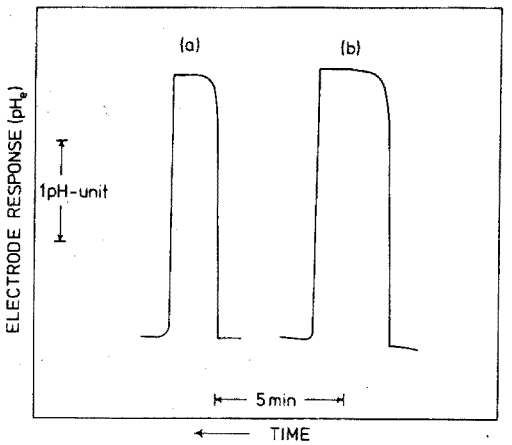

Fig. 3. Response signals for $5 \cdot 10^{-3}$ *M* urea. The electrode was used with (a) the microchamber, and (b) the macrochamber.

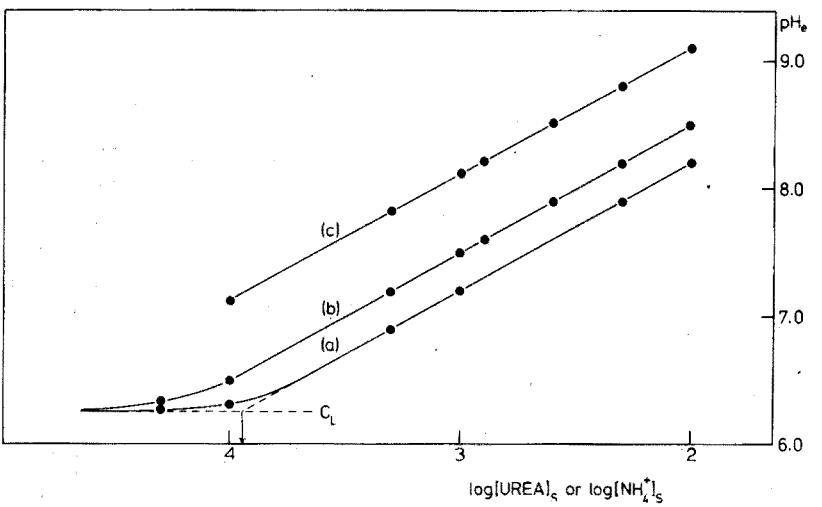

Fig. 4. Calibration curves recorded with standards of (a) ammonium chloride, and (b) urea (both in the macrochamber); and (c) urea (microchamber). The vertical distance between curve (a) and (b) is 0.297 pH$_e$ units.

and the calibration curve in Fig. 4(c). The section of the calibration curve within the physiological range had a slope of 1.086 log [urea]/pH$_e$ unit and a standard error of 0.0093 pH$_e$ (corresponding to 2.2%). The regression coefficient was 0.9998. The results of the serum analyses are reproduced in Table I, which also shows the corresponding values obtained by the AutoAnalyzer method. The blank value was again less than 0.1 mmol l^{-1}. In order to reduce the time needed for a series of analyses, two identical microchambers were used in turn for incubation and measurements.

To establish the yield of the enzymatic reaction and to check the ammonia response of the air-gap electrode, experiments were run with the macrochamber,

TABLE I

DETERMINATION OF UREA IN SERUM SAMPLES

Procedure	*Sample no.*	pH_e	*[Urea] (mmol l^{-1})*		*Calibration curve* $log\,[urea] = a(\theta) + a(l)pH_e$
			Average	*AutoAnalyzer (Univ. Hosp. Cop.)*	
Macro chamber	1	7.872 7.856	2.3	2.3	$a(0) = -7.6132$
	2	8.290 8.281	6.3	5.9	$a(1) = 1.0152$
	3	8.216 8.208	5.3	4.9	$r = 0.9996$[a]
	4	8.413 8.428	8.6	8.2	$S = 0.0103$[b]
	5	8.210 8.224	5.4	5.5	(corresp. to 2.4%)
	6	8.315 8.301	6.6	6.1	
	7	8.206 8.194	5.1	5.3	
	8	8.059 8.054	3.7	4.0	
Micro chamber	9	9.010 8.994	7.7	7.8	$a(0) = -8.2832$
	10	8.643 8.641	3.3	3.7	$a(1) = 1.0186$
	11	8.868 8.874	5.7	5.9	$r = 0.9998$
	12	8.819 8.823	5.0	5.3	$S = 0.0093$
	13	8.842 8.840	5.3	5.4	(corresp. to 2.2%)
	14	9.023 9.017	8.0	8.5	
	15	8.796 8.803	4.8	5.0	

[a] r = Correlation coefficient.
[b] S = standard error.

in which the urea standard solutions were replaced with standard solutions of ammonium chloride of exactly the same molar concentrations. The calibration curve is shown in Fig. 4(a). A parallel displacement of the calibration curves for urea and ammonium chloride of 0.297 pH_e was observed, which according to eqn. (1) corresponds to better than 99% yield for the enzymatic reaction. Over the range $10^{-4} - 10^{-2}$ *M*, the slope of curve (a) was 1.0125 and of curve (b) 1.0109; thus it is obvious that the response of the air-gap electrode is Nernstian both for ammonia as well as for urea.

The standard curves obtained with the macrochamber bend at *ca.* 10^{-4} *M* urea (Fig. 4). Since the standard solutions during the measuring procedure actually were diluted 10 times, the limit of sensitivity of the electrode is thus *ca.* 10^{-5} *M*

urea in the measured solutions. This is in excellent agreement with Fig. 1, according to which a c_p value of *ca.* 10^{-5} was to be expected when 10^{-2} *M* ammonium chloride was used on the electrode surface.

Finally, the microchamber assembly was used for the determination of urea in whole blood and plasma. The procedure was similar to that described above, *i.e.*, 100 µl of TRIS buffer, containing *ca.* 4.5 units of urease, and 100 µl of sample (standard, whole blood or plasma) were introduced into the microchamber and mixed for *ca.* 10 s; the chamber was then left for incubation in a water bath (32°C) for 2 min. After addition of 200 µl of 0.2 *M* sodium hydroxide, the chamber was closed with the air-gap electrode and the stirrer was started. The section of the calibration curve within the physiological range had a slope of 0.9759 log [urea]/pH_e unit with a standard error of 0.0040 pH_e (corresponding to 1.0%).

TABLE II

DETERMINATION OF UREA IN WHOLE BLOOD AND PLASMA

Sample	pH_e	*[Urea] (mmol l^{-1})*			*Calibration curve*[c] *log [urea] = a(0) + (1) pH_e*
		Aver.	*Calc.*	*AutoA.*	
	8.413				$a(0) = -7.7217$
Whole blood	8.413	3.10	—	—	$a(1) = 0.9759$
	8.421				$r = 0.9999$
	9.068				$S = 0.0040$
Spike 1[a]	9.077	13.44	12.71	—	(corresp. to 1.0%)
	9.062				
	9.310				
Spike 2[b]	9.315	23.38	21.45	—	
	9.321				
	8.492				
Plasma	8.487	3.64	—	3.7	
	8.484				
	9.067				
Spike 1[a]	9.065	13.31	13.23	—	
	9.061				
	9.294				
Spike 2[b]	9.293	22.10	21.95	—	
	9.285				

[a] 1.00 ml of sample + 50 µl of 0.2050 *M* urea.
[b] 1.00 ml of sample + 100 µl of 0.2050 *M* urea.
[c] The glass electrode used here was not the same as the one used for Table I.

The results of the whole blood and the plasma analyses are given in Table II. In all cases a stable signal of pH_e was reached within 1–2 min. In order to check the method further, the blood and plasma samples were spiked with known amounts of urea and then measured again (Table II). While excellent agreement between found and calculated urea contents was observed for plasma, the spiked whole blood samples were found to yield higher results than calculated. This is probably due to the presence of the erythrocytes which do not allow the urea added to become evenly distributed throughout the blood sample.

DISCUSSION

The experimental results confirm that it is indeed possible to find suitable conditions and to develop a simple method for the determination of urea so that the response of the air-gap electrode reflects the concentration of analyte in the Nernstian manner:

$$pH_e = \log[\text{urea}] + \text{const.} \quad (3)$$

Owing to the high selectivity of volatilization of ammonia into the air gap and the specificity of the enzymatic reaction, the determination is specific in the absence of ammonia. This is the case in freshly sampled plasma or blood assays where the ammonia content is[24] about 50 μmol l^{-1}, *i.e.*, less than 1% of the ammonia which can be liberated from urea in a typical serum sample. The low standard error (*ca.* 0.01 pH_e, corresponding to about 2.4%) obtained by both procedures is sufficient for clinical purposes, yet it might be further improved by thermostating of the electrode, as the ambient temperature in the laboratory varied about ± 1°C during the measurements. The discrepancy between the results obtained by the AutoAnalyzer and the air-gap electrode (an average of 0.29 mmol l^{-1} of urea with the macrochamber and 0.17 mmol l^{-1} with the microchamber) is either a systematic one or due to standardization. The standard addition method will be used at a later date to find the true source of this discrepancy.

The present construction of the electrode allows the use of the same solution on the electrode surface (8) and within the Perspex tube (4) surrounding the reference system (3). Thus, when an ammonium chloride solution is used, a cell without junction is established and an out-flow of electrolyte from the reference compartment can be stopped without the danger of creating a significant junction potential. This arrangement, which substantially improves the stability of the reference potential, also facilitates an easy exchange of the electrolyte solution, if for instance the electrode were to be used for measuring CO_2 or SO_2 (in which case $NaHCO_3$–NaCl and $NaHSO_3$–NaCl electrolyte solutions must be used, respectively). The conventional gas sensors[21,22], furnished with a gas membrane, could possibly also be used in the air-gap mode of operation. Thus the difficulties associated with blocking of the membrane pores would be avoided and the presence of wetting agents in the sample would no longer impair the electrode function[23]. However, the electrode response and recovery would be slower, not only because the gas still would have to penetrate the membrane, but also because the electrolyte layer could not be renewed after each measurement.

As to further use of the air-gap electrode in enzymatic assays, two aspects could be considered: determination of other substrates and determination of enzymes and their activity. For analyses of glutamine, asparagine, etc., the present procedure probably could be modified simply by using the particular enzyme instead of urease, but the cost of asparaginase or glutaminase per assay could be prohibitive. Therefore, a practical method must be devised by which such rare enzymes, insolubilized and firmly attached to solid carriers, could be used repeatedly. The determination of the enzyme activity is done by measuring the rate of the catalytic reaction in the presence of an excess of substrate[25]. From the previous discussion on the operating range of the air-gap electrode and that of urease, it

might appear that the electrode may not be suitable for such a direct measurement as these two pH ranges do not coincide (Fig. 1). In rate analysis, however, where *e.g.*, 0.1 *M* urea solutions would be used, sufficiently strong signals would be obtained even at pH 7, which of course would make direct measurements feasible. Besides, when the rate of reaction is being measured, the electrode response does not need to be as strictly linear as when direct measurements of substrate concentrations are carried out.

The authors wish to express their appreciation to G. G. Guilbault for his interest in this work, for many valuable discussions and also the gift of the urease; to Inge Marie Johansen for her conscientious technical assistance; and to the Danish Natural Research Council for financial support. Finally the authors extend their thanks to Jørgen Melchior Rasmussen from the University Hospital of Copenhagen for his help in providing the serum samples.

SUMMARY

The newly developed air-gap electrode has been used for enzymatic assay of urea in serum and whole blood; analyses can be done accurately, reliably, simply and quickly. The determination is highly selective because the electrode senses only the ammonium ion, which is selectively released from urea by urease in a preliminary rapid incubation step. The reproducibility of the determination (standard deviation less than 2.4%) is sufficient for clinical purposes; the linear range of the method is 10^{-2}–10^{-4} *M* urea. Since the electrode actually never touches the sample solution, the problems caused by the presence of proteins, blood cells etc. do not arise.

REFERENCES

1 S. A. Katz and G. A. Rechnitz, *Anal. Chem.*, 196 (1963) 248.
2 S. A. Katz, *Anal. Chem.*, 36 (1964) 2500.
3 G. G. Guilbault, R. K. Smith and J. G. Montalvo, Jr., *Anal. Chem.*, 41 (1969) 600.
4 G. G. Guilbault and J. G. Montalvo, Jr., *J. Amer. Chem. Soc.*, 91 (1969) 2164.
5 S. Updike and G. Hicks, *Nature (London)*, 214 (1967) 986.
6 G. G. Guilbault and E. Hrabankova, *Anal. Lett.*, 3 (1970) 53.
7 G. G. Guilbault and E. Hrabankova, *Anal. Chim. Acta*, 56 (1971) 285.
8 G. Baum and F. B. Ward, *Anal. Biochem.*, 42 (1971) 487.
9 G. G. Guilbault and G. J. Lubrano, *Anal. Chim. Acta*, 60 (1972) 254.
10 G. A. Rechnitz and R. Llenado, *Anal. Chem.*, 43 (1971) 283.
11 T. A. Neubecker and G. A. Rechnitz, *Anal. Lett.*, 5 (1972) 635.
12 G. G. Guilbault and G. Nagy, *Anal. Lett.*, 6 (1973) 301.
13 G. G. Guilbault and J. G. Montalvo, Jr., *Anal. Lett.*, 2 (1969) 283.
14 G. G. Guilbault and J. G. Montalvo, Jr., *J. Amer. Chem. Soc.*, 92 (1970) 2533.
15 G. G. Guilbault and G. Nagy, *Anal. Chem.*, 45 (1973) 417.
16 G. G. Guilbault, G. Nagy and S. S. Kuan, *Anal. Chim. Acta*, 67 (1973) 195.
17 J. Ruzicka and E. H. Hansen, *Anal. Chim. Acta*, 69 (1974) 129.
18 P. Racine and W. Mindt, *Experientia, Suppl.*, 18 (1971) 525.
19 G. Eisenman, *The Glass Electrode*, Wiley–Interscience, New York, 1962.
20 R. P. Scholer and W. Simon, *Chimia*, 24 (1970) 372.
21 *Orion Research Specification List for Ammonia Electrode, Model 95-10, Form DS 95-10*, 1711.
22 *Leaflet No. 8002-2/3*, Electronic Instruments Limited.
23 H. F. Proelss and B. W. Wright, *Clin. Chem.*, 10 (1973) 1162.
24 R. L. Coleman, *Clin. Chem.*, 18 (1972) 867.
25 N. W. Tietz, *Fundamentals of Biochemistry*, W. B. Sanders, Philadelphia, 1970, p. 374.

Analytica Chimica Acta, 72 (1974) 365–373

SELECTRODE—THE UNIVERSAL ION-SELECTIVE ELECTRODE

PART VIII. THE SOLID-STATE LEAD(II) SELECTRODE IN LEAD(II) BUFFERS AND POTENTIOMETRIC TITRATIONS

E. H. HANSEN and J. RŮŽIČKA

Chemistry Department A, The Technical University of Denmark, Building 207, 2800 Lyngby (Denmark)

(Received 10th April 1974)

Since the development of the solid-state lead(II) ion-selective electrode by Ross[1], several similar electrodes have been described[2,3,4]. The common feature of these sensors is a membrane consisting of a mixture of PbS and Ag_2S made either by sintering[1] or melting[2] these components or by incorporating them into an inert binder such as polyethylene[3]. The mechanism of the electrode function, as suggested by Ross[1], has been further confirmed by Mascini and Liberti[3], who demonstrated that the electrode does not respond to lead(II) ions unless silver sulphide is present in the membrane mixture. Besides the sulphide-based electrodes, metal chalcogenide electrodes employing lead(II) selenide and lead(II) telluride membranes made by sintering[5] or from monocrystals[6] have been prepared and tested for activity measurements of lead(II) ions[5] and in complexiметric titrations[5,6].

The practical applications of lead(II) electrodes have mainly been in titrimetric procedures, these sensors being used as indicator electrodes, although there have been some reports on their use in direct measurements of lead(II) in *e.g.*, paints[7]. Lead(II) electrodes have been used for determinations of lead in plating baths by titration with ammonium fluoride, of sulphate in soil extracts[8], and of sulphur in organic compounds[9], in coal[10] and in petroleum[11] after combustion and oxidation to sulfate. Sulphur dioxide in flue gases has been determined after collection in hydrogen peroxide followed by titration as lead sulphate[12].

In the present paper, the function of the solid-state Selectrode[13] operating as a lead(II) ion-sensing device is described on the basis of calibration curves obtained in lead(II) buffered solutions. The capacity of the electrode as a function of pH is demonstrated by means of potential–pH diagrams, and potentiometric titrations are discussed.

The concepts of metal buffers and their use for calibration of ion-selective electrodes have previously been described in detail[14,15]. Based on the principles of conditional stability constants and side-reaction coefficients, it was shown that at constant ionic strength, the pM value in a solution of the metal ion M^{n+} and the Ligand L^{m-} forming the 1:1 complex $ML^{(n-n)+}$, at equilibrium is expressed by the equation:

$$pM = \log K_{ML} + \log \frac{\alpha_{ML}}{\alpha_L} + \log \frac{[L']}{[ML']} \qquad (1)$$

where K_{ML} is the stability constant at the ionic strength used, [L′] is the total concentration of uncomplexed ligand, [ML′] is the total concentration of complex formed, and α_i denotes the side-reaction coefficient for the *i*th component.

Thus, for a given metal/ligand system the pM may be varied by varying the [L′]/[ML′] ratio and the α values. The side-reaction coefficients are inherently functions of all the side reactions in which the individual species participate. Often, however, side reactions with H^+ (or OH^-) are dominant, so that other side-reactions may be neglected. If this is indeed the case and if the ratio of [L′]/[ML′] is chosen to be unity, *i.e.*, the last term of eqn. (1) is zero, pM will be a particular function of pH. This relationship constitues a very important curve of a potential–pH diagram. Thus, if the pH of a solution containing equal concentrations of EDTA and Pb(EDTA) is continuously increased by automatically controlled addition of strong base to an originally acidified solution, the potential of a lead(II) ion-sensitive electrode immersed in the solution will reflect the corresponding increase of the pPb value. This function may then serve for evaluation of the electrode performance and for selecting the optimal conditions for titration of lead(II) with EDTA, since the relationship (1) can be considered to represent the electrode response in a 100% over-titrated solution. Thus, at that pH value where there is the largest span between this curve and that recorded by a similar technique in a 10^{-b} *M* lead(II) solution, the maximum change of potential at the equivalence point will be obtained.

Furthermore, the maximum measurable pPb values in the lead(II) buffers prepared by mixing lead(II) ions and EDTA at fixed molar ratios followed by adjustment of pH and the ionic strength, may inherently be considered as individual points on the PbEDTA/EDTA curve in the potential–pH diagram.

EXPERIMENTAL

Equipment

The instruments, the glass electrode and the reference electrode were the same as used previously[15]. For automatic pPb/pH measurements, an automatic scanning potentiometer, an autoburette ABU 13, and two pH-meters PHM 51 (Radiometer A/S, Copenhagen) together with a Watanbe WX 431 X–Y recorder were used.

Electroactive materials

A number of PbS/Ag_2S mixtures of molar ratios ranging from 10:1 to 1:10 were prepared using controlled excesses of either metal or sulphide ions for precipitation. It was found that PbS/Ag_2S precipitates of the molar ratio 2:1 or 1:1 were most suitable as electroactive materials, provided that they were prepared with a 20% excess of sodium sulphide. The following preparatory procedure was used.

A solution of sodium sulphide (*ca.* 0.1 *M*) was standardized against silver nitrat (0.100 *M*) by potentiometric titration, with a silver Selectrode as indicator. A lead nitrate solution (0.10 *M*) was standardized by means of EDTA with xylenol orange as indicator. Appropriate quantities of the metal nitrate solutions in the required ratios were then mixed (*e.g.*, 100.0 ml of 0.10 *M* lead nitrate and 100.0 ml of 0.10 *M* silver nitrate for preparation of the 2:1 precipitate), and

the mixture was slowly poured into the calculated volume of a vigorously stirred solution of sodium sulphide. The slurry was left for *ca.* 30 min, whereupon the supernatant liquid was decanted and the precipitate was repeatedly washed with cold redistilled water until the reaction of the washings was neutral. The slurry was then centrifuged and the precipitate was dried *in vacuo*. The electroactive material was subsequently applied on the Selectrode surface as previously described[13].

Conditioning of the activated Selectrodes was accomplished by storing them in solutions of pPb 3 at pH 3. Although the electrodes may be used immediately after preparation, the optimal sensitivity is reached after one day of conditioning (see Table I). The conditioned electrodes should be stored in redistilled water where they can be kept up to 25 days. If left in contact with the air, the ion-sensitized surface becomes oxidized and the response deteriorates (see also refs. 1, 3 and 16).

E I

NFLUENCE OF CONDITIONING AND STORAGE ON THE LEAD(II) SELECTRODE[a]

Prepared	*Conditioned*[b]				*Stored*[c]		
	3 h	*5 h*	*20 h*	*48 h*	*6 days*	*12 days*	*21 days*
44.4	48.8	49.9	51.0	52.1	54.0	53.9	56.1
17.8	20.6	20.4	22.1	24.2	25.2	25.8	26.3
−2.9	−1.9	−5.7	−5.6	−3.6	−0.1	2.0	−1.8
−19.2	−15.0	−28.0	−29.3	−27.3	−25.5	−21.7	−28.2
−132.1	−130.9	−160.4	−155.4	−152.4	−151.5	−146.7	−157.3
−153.3	−154.2	−190.3	−188.4	−177.2	−180.5	−172.0	−182.7
−160.5	−154.1	−192.4	−191.2	−177.4	−184.2	−172.2	−200.7
−164.9	−153.9	−191.0	−191.2	−177.4	−184.7	−174.1	−204.2

Ag_2S 1:1; all values in mV *vs.* SCE.
Pb 3 and pH 3.
rode conditioned for 20 h and then stored in water.

Preparation of lead buffers

Four series of lead(II) buffers were prepared: (a) the pH was adjusted to 4.8 by addition of acetate buffer; (b) the pH was adjusted to *ca.* 6.8 by maleate buffer; (c) the pH was adjusted to *ca.* 9 by borate buffer; and (d) the pH was adjusted to *ca.* 10 by ammonia buffer. All these series were prepared so as to contain a total concentration of uncomplexed ligand, [L′], of 10^{-3} *M*. These buffers totally covered a pPb range of approximately 5–18. In the pPb region of 2–4, it was found that solutions prepared by the normal dilution technique were satisfactory. The ionic strength in all buffered and unbuffered solutions was made up to 0.10 by addition of the calculated amount of potassium nitrate.

The pPb value of each buffer was computed according to eqn. (1). The buffer series (a) to (c) all comprised two sub-series, each containing 3 buffers in which the [L′]/[PbL′] ratio was 1:10, 1:1 and 10:1, respectively. In the first

TABLE II

LEAD(II) BUFFERS AND CALCULATED pPb VALUES

Series	*Ligand*	*NTA*			*EDTA*		
	[L]/[PbL]	*1:10*	*1:1*	*10:1*	*1:10*	*1:1*	*10:1*
a	pH	4.78	4.82	4.80	4.72	4.82	4.82
	pPb	5.78	6.82	7.80	9.84	11.04	12.04
b	pH	6.05	6.87	7.02	6.75	6.70	6.90
	pPb	7.05	8.87	10.02	13.25	14.18	15.46
c	pH	8.68	9.12	9.02	8.80	9.02	9.03
	pPb	9.61	10.98	11.91	15.42	16.62	17.63
d	pH	—	—	—	9.98	10.02	10.15
	pPb	—	—	—	16.48	17.55	18.56

sub-series, the ligand L was NTA (nitrilotriacetic acid) and in the second L was EDTA (ethylenediaminetetraacetic acid). Series (d) consisted of only three buffers where L was EDTA. The calculated pPb values are summarized in Table II (log $K_{PbNTA} = 11.8$; and log $K_{PbEDTA} = 18.0$)[17].

Measurement techniques

pPb response. The Selectrodes were activated in the usual manner[13], by rubbing the precipitate to be tested into the electrode surface. All potential measurements were executed at 25°C and they are referred to the saturated calomel electrode (SCE). The testing of the Selectrodes was done by immersing them into 100 ml of well-stirred lead buffer solutions, and the potentials were continuously recorded until equilibrium had been reached. This occurred within 90 s in the pPb range of 2–4, within 5 min at pPb 5–11, and within 8–10 min at higher pPb values.

Computations. All slopes were calculated by means of regression analysis on the linear part of the calibration curves, with a Wang 700 B Programmable Electronic Calculator provided with a Wang 702 Plotting Output Writer.

The potential–pH curves (Reilley diagrams). These were recorded automatically as described previously[14,15], and so were the potentiometric titrations of lead ions by EDTA. The other potentiometric titrations were performed manually. In all cases, 25.00 ml of 0.010 *M* analyte was mixed with 10–15 ml of an appropriate pH buffer[14] (no buffers were used in the titrations of the anions), and the volume was made up to *ca.* 100 ml. The solutions were then titrated with standard titrant (0.100 or 0.200 *M* lead nitrate).

RESULTS AND DISCUSSION

In the search for an electroactive material which would allow preparation of a lead(II) Selectrode with optimal parameters, several precipitates were made according to a procedure similar to that used in providing the copper(II) and cadmium(II) electrodes[14,15]. The result of these experiments can be briefly summarized in the following way.

(1) Pure PbS yields a Selectrode sensitive to changes of pPb, but the slope of the calibration curve is poor (only *ca.* 22 mV/pPb) and the electrode deteriorates rapidly during use.

(2) Mixtures of PbS/Ag_2S of molar ratios 1:1 and 2:1 yield the best Selectrodes, with almost Nernstian response and good lifetime.

(3) The use of a well controlled excess of sodium sulphide ($30 \pm 10\%$) is essential in order to obtain an electroactive material with maximal sensitivity and speed of response. After preparation, this material has to be dried *in vacuo* at room temperature before use on the Selectrode surface.

(4) Conditioning of the activated Selectrodes further improves their characteristics, which can be maintained by storing the electrodes in water. Storage in air results in slow deterioration.

Based on these observations, a procedure for making a precipitate with optimal parameters was devised (see Experimental) and then used for preparing a PbS/Ag_2S precipitate (1:1) which reproducibly yielded a lead(II) Selectrode with the following properties.

The calibration curve (Fig. 1A) showed a straight linear part within the pPb range of 2–11 with a slope of 26.26 mV/pPb as calculated by linear regression analysis. The observed limits of sensitivity, which in the pPb buffers mainly are limited by the pH of the particular solution series, are in reasonably good agreement with the corresponding conditional solubility products of PbS. $K'_{PbS} = [Pb'][S']$, *i.e.*, the pPb values calculated from this relationship are given by the equation[14]:

$$pPb = \tfrac{1}{2}(pK_{PbS} - \log \alpha_{S(H)} + \log \alpha_{Pb(H,Ac)}) \qquad (2)$$

where $pK_{PbS} = 25.8$ (ref. 17) and $\alpha_{Pb(H,Ac)}$ denotes that this side-reaction coefficient in the acetate buffers is a function of the acetate concentration, while in the other buffers it is a function of the pH only. Thus, in the acetate-buffered solutions of pH 4.8 and $[Ac^-] = 0.05$ *M*, a limit of sensitivity of pPb = 8.2 was observed compared to a value of pPb = 8.5 calculated by eqn. (2). In the maleate buffers (pH 6.8) the corresponding values were $pPb_{found} = 10$ and $pPb_{calc.} = 10$; in the borate buffers (pH 9), the values were 10.6 and 11.8, respectively; while in the ammonia buffers (pH 10) a maximum sensitivity of pPb = 11.3 was reached, not much different from the value pPb = 12.9 imposed by eqn. (2). It is therefore evident that the lead(II) Selectrode properly responds to lead(II) ion activities to an extent limited only by the solubility of the electrode material, and indeed it can be used for activity measurements down to *ca.* 10^{-11} *M* lead(II). It should be noted, however, that this high sensitivity was obtained in pPb buffers of relatively high buffering capacity, that is, in solutions where the total lead content was 10^{-2}–10^{-4} *M*. Thus, although the electrode undoubtedly can be used for measurements of total lead contents down to 10^{-4} *M* (see dilutions), and probably down to 10^{-5} *M*, any attempts to measure even lower total quantities should be discouraged. The reason is not so much the question of the quality or the capability of a particular lead(II) sensor, but the interfering effect of various complexing agents which will disturb the measurement, even if present in only trace amounts. Though careful calibration and meticulous work may lead to reasonable agreement between total amounts and measured activities also above pPb 5, the practical value of measurements performed to that end in this range is

doubtful, as for each actual sample material the content and the nature of complexing species present must be considered.

It might consequently appear that the wide measuring range of the lead(II) Selectrode is not of any particular utility in practical analysis where usually the determination of total amounts rather than activities are required. This is, however, not the case, as the electrode is very useful as an indicator electrode in potentiometric titrations. This is readily demonstrated by comparing the calibration curve (Fig. 1A) and the potential–pH diagram (Fig. 1B) obtained with the lead(II) Selectrode. For instance, if the titration of $1 \cdot 10^{-3}$ *M* lead(II) solution with EDTA is considered and it is assumed that the titrant is added in 100% excess at the end-point, a total change of 150 mV should be expected at pH 5 (the difference between line 10^{-3} and line PbEDTA/EDTA in Fig. 1B); the change should be 185 mV at pH 7, and 170 mV at pH 9. As can be seen from the potential–pH diagram, the maximal potential span is obtained around pH 6.5, while at higher pH values the span decreases again as the starting potential is lowered by hydrolysis of the lead ions. A series of titrations of lead(II) ions with EDTA were done at various pH levels, and in all cases excellent agreement was found between the expected and the actually recorded potential jumps.

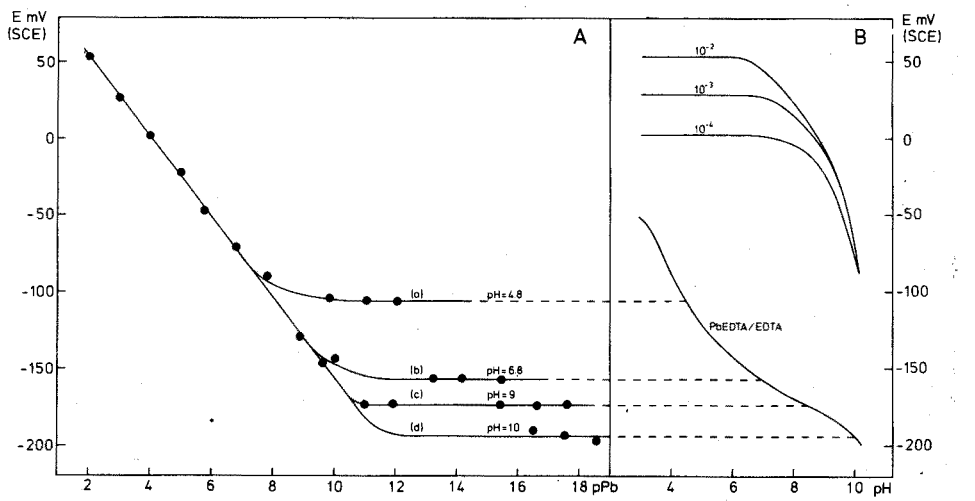

Fig. 1. (A) Calibration curve for the lead(II) Selectrode (PbS/Ag_2S 1:1) measured in PbS buffers. (B) Potential–pH diagram for the lead(II) Selectrode; the uppermost curves represent pPb 2, 3 and 4, respectively; for curve PbEDTA/EDTA, $[PbEDTA] = [EDTA] = 10^{-3}$ *M*.

Solutions of lead(II) nitrate have traditionally been used for the determination of anions such as sulphate, chromate and tungstate, and various electrodes[18–20] including the recently developed ion-selective ones[1, 2, 3, 5] have been applied in these potentiometric titrations. The lead(II) Selectrode can also be used for this purpose (Fig. 2). Here again, the theoretically maximum obtainable potential jumps at the equivalence point were observed because of the high sensitivity of the lead(II) Selectrode, the span of the titration curves being solely determined by the solubility of the precipitates formed during the titrations, *in*

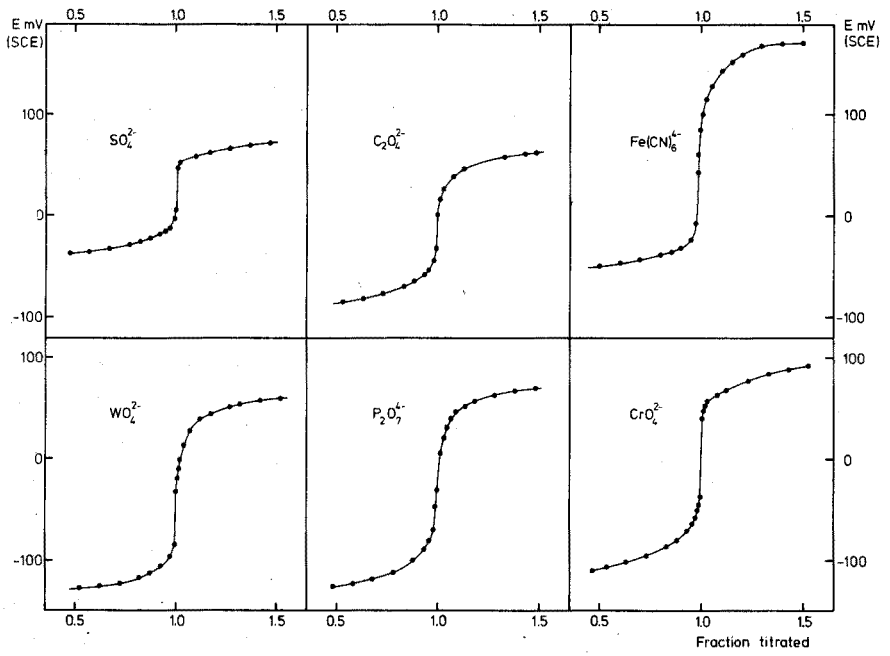

Fig. 2. Potentiometric titrations of 6 anion species by lead(II) nitrate monitored with the lead(II) Selectrode. The titrations were performed in aqueous solutions except the sulphate determination which was done in (1+1) ethanol/water medium.

casu $PbSO_4$, PbC_2O_4, $Pb_2(Fe(CN)_6)$, $PbWO_4$, $Pb_2P_2O_7$ and $PbCrO_4$. As lead sulphate is rather soluble in water (0.00425 g/100 ml of water at 25°C), the titration of the sulphate had to be made in a partially non-aqueous medium.

In conclusion, some remarks should be made about the mechanism by which the lead(II) Selectrode operates. This mixed metal sulphide-based electrode is an electrode of the third kind, and its performance is governed by the solubility products of the respective components. Thus an electrochemical chain is established in which the silver ion activity is affected by the sulphide ion activity which in turn depends on the activity of the divalent metal ion activity in the sample solution:

$$E = Const. + \frac{RT}{2F}\ln(K_{Ag_2S}/K_{MS}) + \frac{RT}{2F}\ln[M^{2+}] \qquad (3)$$

where the symbols have their usual meaning. In the classical electrode of the third kind, with metallic silver as a conductor (and as the first member of the electrochemical chain), the value of the constant *Const.* will be identical with the potential of a silver electrode measuring in a solution where the activity of silver ions is unity (558 mV *vs.* SCE). Since Ross suggested a similar mechanism for the solid-state membrane electrodes[1], the same equation has been applied for the mixed sulphide membranes in which the metallic silver is replaced by silver sulphide. In membrane electrodes, however, the value of the *Const.* term depends on the particular construction of the ion-selective electrode, that is, on the inner reference system,

the inner electrolyte and its components, and it therefore becomes complex and does not allow comparison between potentials of Ag_2S/MS electrodes where M is Cu, Cd or Pb. It is therefore interesting to observe that the Selectrodes activated by Ag_2S/CuS (ref. 14), Ag_2S/CdS (ref. 15) and Ag_2S/PbS give the following values of the term $Const. + RT/2F \ln(K_{Ag_2S}/K_{MS})$: 369 mV for Cu(II), 100 mV for Cd(II) and 113 mV for Pb(II) (at 20°C *vs.* SCE), which in turn yield the value of the term $Const. = 770$ mV. A very similar value (769 mV) has been obtained for the Selectrode activated by pure Ag_2S (ref. 21) by extrapolation of the data attained in solutions of silver nitrate. Because this potential differs as much as 212 mV from that of the Selectrode activated by metallic silver, the electrochemical chain is obviously not based on metallic silver. Nevertheless, the value of the *Const.* term agrees well with that computed by Sato[22] (768 mV) for the potential of a silver sulphide-based electrode having the maximal sulphur activity which the silver sulphide can possess in equilibrium with its neighbouring stable phase which is relatively rich in sulphur (S). Indeed, all these functional electrodes are invariably made of materials prepared with an excess of sulphide (or sulphur) during the precipitation. Furthermore, although copper and cadmium sulphides alone can be made into somewhat functional electrodes, the presence of silver sulphide in the electrode material is a necessity in order to attain good performance and potential stability. Thus, it can be concluded that the mixed sulphide electrodes are indeed electrodes of the third kind relying on a particular modification of silver sulphide as the first member of the electrochemical chain. It remains a matter of conjecture if this compound serves as an ionic[20,23] or an electronic conductor[24], as this, besides modification and temperature, also depends on whether the membrane made of it is in contact with an electrolyte on both sides[25]. In the Selectrode construction, an electronic conductance is assumed since the electroactive material forms a discontinuous film on the teflon–graphite surface and not a continuous thin body separating two liquid phases.

CONCLUSION

The lead(II) Selectrode exhibits an almost Nernstian slope within the pPb range of 2–11, and its sensitivity in lead(II)-buffered solutions is close to the theoretical limit imposed by the conditional solubility product of lead sulphide. The sensor is suitable for measurements of lead(II) ion activities and can also be used for indicating the equivalence point in all potentiometric titrations during which the lead(II) ion activity increases or decreases. Thus titration of lead(II) by EDTA or NTA, and titrations of anions such as SO_4^{2-}, CrO_4^{2-}, WO_4^{2-}, $C_2O_4^{2-}$, $Fe(CN)_6^{4-}$ and $P_2O_7^{4-}$ can be performed with the aid of the lead Selectrode.

The authors wish to express their thanks to Miss I. M. Johansen for valuable technical assistance; and to Dr. O. J. Jensen of Radiometer A/S for critical discussions. This work was in part supported by the Danish Natural Research Council.

SUMMARY

A new lead(II) Selectrode, activated with PbS/Ag_2S, has been calibrated in

lead(II) buffers and found to exhibit an almost Nernstian response within the pPb range of 2–11. The linear part of the calibration curve extends to a pPb level close to the theoretical limit imposed by the conditional solubility product of PbS. EDTA titrations of lead(II) as well as titrations of sulfate, tungstate, pyrophosphate, dichromate, oxalate and hexacyanoferrate(II) ions by lead(II) nitrate have successfully been monitored with the lead(II) Selectrode.

REFERENCES

1 J. W. Ross in R. A. Durst (Ed.), *Ion-Selective Electrodes*, NBS Spec. Publ. 314, Washington, 1969, Chapter 2.
2 A. V. Gordievski, V. S. Shtermen, A. Ya. Syrchenkov, N. I. Savvin, A. F. Zhukov and Yu. I. Urusov, *Zh. Anal. Khim.*, 27 (1972) 2170.
3 M. Mascini and A. Liberti, *Anal. Chim. Acta*, 60 (1972) 405.
4 H. Hirata, K. Higashiyama and K. Date, *Anal. Chim. Acta*, 54 (1971) 415.
5 H. Hirata and K. Higashiyama, *Talanta*, 19 (1972) 391.
6 J. Vesely, private communication.
7 *Analytical Methods Guide*, 5th edn., Orion Research, Mass., U.S.A., 1973.
8 J. O. Goertzen and J. D. Oster, *Soil Sci. Soc. Amer., Proc.*, 36 (1972) 691.
9 W. Selig, *Mikrochim. Acta*, (1970) 168.
10 J. E. Hicks, J. E. Fleenor and H. R. Smith, *Anal. Chim. Acta*, 68 (1974) 480.
11 R. N. Heistand and C. T. Blake, *Mikrochim. Acta*, (1972) 212.
12 J. N. Driscoll, K. Mahoney and M. Young, *Anal. Chem.*, 45 (1973) 13.
13 J. Ruzicka, C. G. Lamm and J. Chr. Tjell, *Anal. Chim. Acta*, 62 (1972) 15.
14 E. H. Hansen, J. Ruzicka and C. G. Lamm, *Anal. Chim. Acta*, 59 (1972) 403.
15 J. Ruzicka and E. H. Hansen, *Anal. Chim. Acta*, 63 (1973) 115.
16 *Orion Newsletter*, Vol. V, No. 2, (1973) p. 14.
17 A. Ringbom, *Complexation in Analytical Chemistry*, Interscience, New York, 1963.
18 A. Ringbom, *Acta Acad. Aboensis*, 8 No. 5 (1934).
19 C. W. Robbins, D. L. Carter and D. W. James, *Soil Sci. Soc. Amer., Proc.*, 37 (1973) 212.
20 G. C. Cortelessa, *Analyst (London)*, 93 (1968) 546.
21 J. Vesely, O. J. Jensen and B. Nicolaisen, *Anal. Chim. Acta*, 62 (1972) 1.
22 M. Sato, *Electrochim. Acta*, 11 (1966) 361.
23 C. Wagner, *J. Chem. Phys.*, 21 (1953) 1819.
24 P. Rahlfs, *Z. Phys. Chem., Abt. B*, 31 (1936) 157.
25 K. S. Fletcher III and R. F. Mannion, *Anal. Chem.*, 42 (1970) 285.

Analytica Chimica Acta, 72 (1974) 375–380

POTASSIUM-SELECTIVE ELECTRODES BASED ON MACROCYCLIC POLYETHERS

THE EFFECT OF STRUCTURE OF THE NEUTRAL CARRIER ON SELECTIVITY

J. PETRÁNEK and O. RYBA

Institute of Macromolecular Chemistry, Czechoslovak Academy of Sciences, 160 06 Prague 6 (Czechoslovakia)

(Received 17th April 1974)

Owing to their remarkable ability to form complexes with the alkali metal cations[1], macrocyclic polyethers come under the group of synthetic neutral carriers with properties similar to those of some natural antibiotics. The complexing properties of these so-called crown compounds have been dealt with in a number of papers[2] since they were first described by Pedersen. These studies showed that in most cases the crown compounds form more stable complexes with potassium ions than with sodium ions. The preference for potassium indicates the possibility of their application in practice as the active components of membranes for potassium ion-selective electrodes. Similarly to the valinomycin electrode[3], the first experiments in this respect[4,5] were carried out with conventional liquid membranes. In these electrodes, the neutral carrier dissolved in a hydrophobic solvent is held on an inert porous supporting membrane. The electrochemical behaviour of such liquid membranes can be affected by the character of the inert support, owing to the ill-defined interface. Another drawback of liquid membrane electrodes is their short lifetime. These disadvantages may be overcome by using polymeric membranes containing the active component in the plasticizer of the polymer used[6]. The applicability of this method for neutral carriers has been demonstrated for the valinomycin-based potassium electrode with a polyvinyl chloride membrane plasticized with dipentyl phthalate[7]. The satisfactory properties of the valinomycin electrode based on polyvinyl chloride have been reported recently by several authors[8–10]. The first results obtained with some basic types of the crown compounds in a PVC matrix[7] showed a considerable dependence of the K/Na selectivity on the structure of the crown compound used. In this paper, the structural effects in a series of twenty crown compounds having macrocyclic rings of different size and carrying different substituents (I–XX), are described in detail.

EXPERIMENTAL

Chemicals

Cyclic polyethers I–VI and XI–XIV (Table I) were synthesized from pyrocatechol, or from its 4-methyl-, 4-n-propyl-, 4-tert-butyl- or 4-nitro derivative, and

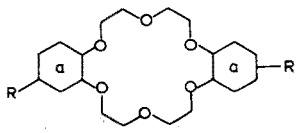

I a = benzo, R = H
II a = benzo, R = CH_3
III a = benzo, R = n-C_3H_7
IV a = cyclohexyl, R = H
V a = cyclohexyl, R = CH_3
VI a = cyclohexyl, R = n-C_3H_7

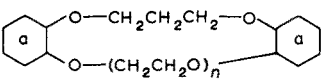

VII a = benzo, $n = 2$
VIII a = benzo, $n = 3$
IX a = cyclohexyl, $n = 3$
X a = benzo, $n = 4$

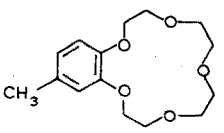

XI

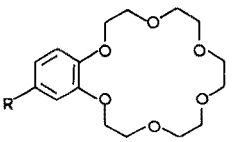

XII R = H
XIII R = NO_2

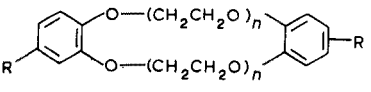

XIV $m = 3$, $n = 3$, R = CH_3
XV $m = 4$, $n = 4$, R = H
XVI $m = 4$, $n = 4$, R = CH_3
XVII $m = 4$, $n = 4$, R = tert-C_4H_9
XVIII $m = 4$, $n = 4$, R = NO_2
XIX $m = 5$, $n = 4$, R = tert-C_4H_9
XX $m = 5$, $n = 5$, R = H

the respective dichloro derivatives of ethers by using the methods described by Pedersen[11]. The crown compounds with a thirty-membered ring and larger rings (XV–XVII,XX), as well as asymmetrical dibenzocrown compounds (VII–X,XIX) were prepared by a two-step synthesis from monobenzyl ethers of the respective pyrocatechols[12]. Dinitrodibenzo-30-crown-10 (XVIII) was prepared by nitration of dibenzo-30-crown-10 (XV) with 65% nitric acid in anhydrous acetic acid at room temperature for 15 min. All products were purified chromatographically on alumina (Woelm) by elution with a (1 + 1) benzene–diethyl ether mixture. All crown compounds thus obtained gave satisfactory elemental analyses, as well as the appropriate molecular ions in the mass spectra.

The following new compounds were prepared among the crown compounds used in this work: 4-methylbenzo-15-crown-5 (XI), m.p. 46.5–49°C; dicyclohexyl-19-crown-6 (IX), oil; dibenzo-22-crown-7 (X), oil; ditert-butyldibenzo-30-crown-10 (XVII), m.p. 71–73°C; dinitrodibenzo-30-crown-10 (XVIII), m.p. 129°C; ditert-butyldibenzo-33-crown-11 (XIX), oil; and dibenzo-36-crown-12 (XX), m.p. 73–74°C. Properties of the other crown compounds used corresponded to literature data (I,IV,VII,VIII,XII,XV[11]; II,III,V,VI,XIV[7]; XVI[12]; XIII[13]).

Polyvinyl chloride (molecular weight about 200,000) was prepared by polymerization of vinyl chloride with tert-butyllithium[14]. Dipentyl phthalate was prepared from phthalic anhydride and n-pentanol (b.p. 175–178°C at 0.1 torr). Cyclohexanone and the other chemicals used were of reagent grade (Lachema).

Preparation of electrodes

The crown compound (10 mg) dissolved in 1 ml of dipentyl phthalate was mixed with 10 ml of a 5% (w/v) solution of polyvinyl chloride in cyclohexanone. The solution was poured on a horizontal glass plate (7 × 15 cm). The cyclohexanone evaporated at room temperature, and an elastic membrane about 0.15

mm thick was obtained, from which suitable discs for the electrodes were cut out. The discs were fixed between rubber rings in a teflon electrode body, or were heat-welded by means of a hot brass annular jig to the end of a PVC tube. The diameter of the effective surface of the membrane was 5–8 mm. Electrode units were completed with a silver–silver chloride wire internal reference electrode and a 10^{-3} *M* KCl filling solution.

Evaluation of the electrode behaviour

The response of the electrodes to potassium and sodium cations was measured as described earlier[1,2]. The selectivity constants $K_{K,Na}$ were determined by the equipotential method in mixed solutions: potentials were measured in solutions containing a fixed amount of sodium ions and a variable amount of potassium ions. The constants were calculated from the relationship $K_{K,Na} = a_K/a_{Na}$, where a_K and a_{Na} are the activities of the potassium and sodium ions, respectively, which produce the same electrode potential in the mixed solutions. The particular activity of the potassium ions, a_K, was obtained graphically as a value corresponding to the intercept of the extrapolated Nernstian response line with that of the horizontal total interference of the sodium ion having a constant activity a_{Na}.

RESULTS AND DISCUSSION

Membrane electrodes based on the crown compounds investigated here usually exhibited a linear response to the activity of potassium ions within the concentration range 10^{-1} or $10^{-1.5}$–10^{-5} *M* KCl. The slopes of the calibration plots for the electrodes were generally 59 ± 1 mV per decade change in activity at 25°C. However, for dibenzo-18-crown-6 (I), the linear response region was only $10^{-2.5}$–10^{-5} *M* KCl with a slope of 51 mV, and for dinitrodibenzo-30-crown-10 (XVIII), the slope was 56 mV. The selectivity constants measured for concentration levels of the interfering sodium ion of 10^{-1} and 10^{-2} *M* exhibited in some cases a dependence on the relative potassium–sodium ion concentration. Table I summarizes the constants $K_{K\ Na}$ together with their reciprocals $K_{Na\ K}$ obtained at a constant background concentration of 0.1 *M* sodium chloride.

The papers published so far on the crown compounds have proved that their complexing properties depend considerably on their structure. When these compounds are used as active components in the membranes of ion-selective electrodes, a pronounced effect of the structural parameters on the potassium–sodium selectivity can also be observed. The basic structural feature of the crown compounds is the size of the macrocyclic ring and the number of oxygen atoms. The selectivity constants (Table I) indicate that, for the compounds investigated, the highest K/Na selectivities are obtained in the group of crown compounds with eighteen-membered or nineteen-membered rings containing six oxygen atoms each, and for thirty-membered rings with ten oxygen atoms. Poor K/Na selectivity was displayed by 4-methylbenzo-15-crown-5(XI); with dibenzo-16-crown-5(VII), there was practically no difference between the responses to potassium and sodium ions. Obviously, in both cases the ring sizes and the number of binding sites represented by the oxygen atoms do not permit formation of a cavity suited for complex formation with potassium.

TABLE I

SELECTIVITY CONSTANTS OF CROWN COMPOUNDS IN PVC MEMBRANES

	Crown compound	$K_{K,Na}(\cdot 10^{-2})$	$K_{Na,K}$
I	Dibenzo-18-crown-6	7.7	13
II	Dimethyldibenzo-18-crown-6	6.7	15
III	Di-n-propyldibenzo-18-crown-6	6.3	16
IV	Dicyclohexyl-18-crown-6	1.1	97
V	Dimethyldicyclohexyl-18-crown-6	1.1	97
VI	Di-n-propyldicyclohexyl-18-crown-6	1.6	62
VII	Dibenzo-16-crown-5	100	1
VIII	Dibenzo-19-crown-6	2.2	45
IX	Dicyclohexyl-19-crown-6	1.5	66
X	Dibenzo-22-crown-7	3.3	30
XI	4-Methylbenzo-15-crown-5	6.7	15
XII	Benzo-18-crown-6	0.53	190
XIII	4-Nitrobenzo-18-crown-6	0.28	360
XIV	Dimethyldibenzo-24-crown-8	10	10
XV	Dibenzo-30-crown-10	0.85	117
XVI	Dimethyldibenzo-30-crown-10	0.22	450
XVII	Ditert-butyldibenzo-30-crown-10	0.24	417
XVIII	Dinitrodibenzo-30-crown-10	0.95	105
XIX	Ditert-butyldibenzo-33-crown-11	1.2	85
XX	Dibenzo-36-crown-12	1.6	62

The selectivity constants $K_{K,Na}$ of the group of crown compounds with six oxygen atoms in the ether ring indicate that the selectivity is not determined by the number of binding sites only, but also by the magnitude of the conformational changes accompanying the formation of the equilibrium cavity necessary for complexing the potassium ion. The x-ray diffraction data[15] for the dibenzo-18-crown-6 complex show that the cation is bound by six oxygen ligands lying in one plane. It appears that the closer the conformation of the oxygen atoms in the free crown compound lies to a planar arrangement of the complex, then the higher the stability of the potassium complex and the greater the selectivity of the electrode. Courtod's atomic model of dibenzo-18-crown-6 (I) shows that of the six oxygen atoms only four lie in one plane. Consequently, complex formation must bring about a considerable change in the molecular conformation. An increase in the conformational energy is probably the cause of the low K/Na selectivity of this compound. The hydrogenation of aromatic rings in the case of dicyclohexyl-18-crown-6 (IV) increases the mobility of the oxygen atoms in the macrocyclic ring, so that they can very readily attain a planar arrangement and form an equilibrium cavity of the appropriate parameters needed for the formation of the potassium complex. Accordingly, the K/Na selectivity of this compound increases almost by an order of magnitude. The planar arrangement of the oxygen atoms of the macrocyclic ring is also facilitated by increasing the ring by one methylene group, as in the case of dibenzo-19-crown-6 (VIII). This compound also exhibits a higher K/Na selectivity than dibenzo-18-crown-6 (I). A similar effect occurs in the case of benzo-18-crown-6 (XII) where, owing to the presence of only one benzene ring, the

oxygen atoms occupy an almost ideal position as shown by the atomic model. The K/Na selectivity of this compound is the highest among the crown compounds with six oxygen ligands. The presence of the methyl and n-propyl substituents in the molecules of crown compounds II, III, V and VI did not affect their selectivity, but resulted in more rapid electrode responses. Substitution of benzo-18-crown-6 (XII) with a nitro group in compound XIII led to an almost twofold increase in the K/Na selectivity.

For membrane electrodes based on macrocyclic polyethers, it has been suggested[5] that their selectivities may be approximated by the ratio of the stability constants of the complexes of the respective metals with the given crown compound. However, as has been stressed[16], the basic requirement needed to justify the use of such a relationship for neutral carriers is that the ligand should be able to enclose the complexed cation completely and evenly, so that the interactions of the complex with the surrounding medium are then independent of the central ion. In such a case, the membrane selectivities are independent of the solvent used as the plasticizer of the membrane and correspond quantitatively to the selectivity of the ligand in the outer solution given by the ratio of the stability constants of the complexes in water or a water-like solvent. However, for compounds XII and XIII, the high K/Na selectivity cannot be adequately expressed by the ratio of the stability constants of the potassium and sodium complexes[13]. The electrode selectivities found are approximately sixty times higher. This discrepancy is probably due to the crown compounds of this group being unable to replace completely the coordinated solvation shell of the cation in the respective complexes[16]

Unlike the group of crown compounds with six oxygen atoms in the ring, 30-crown-10 compounds with a pronounced K/Na selectivity are characterized by a high flexibility of the macrocyclic ring. These flexible macrocyclic ligands are able to complex the given cation by wrapping around it[17] with a change in conformation, similarly to valinomycin. Substitution of dibenzo-30-crown-10 (XV) with the methyl or tert-butyl groups (derivatives XVI and XVII) favourably affected not only the speed of the electrode response, but also the K/Na selectivity, which increased more than threefold. The cause of this increase in the selectivity is not clear; the effect of alkyl substituents on changes in the conformational energy on complexation cannot be ruled out. Substitution with nitro groups (derivative XVIII) had no influence upon selectivity, in contrast to crown compound XIII. The K/Na selectivities of electrodes with XV and XVI are roughly given by the ratio of the stability constants of the potassium and sodium complexes[13]. The experimentally determined selectivity of the electrodes is only three to four times higher than these ratios. The fact that selectivity in this case is in better accordance with the ratio of the stability constants of the complexes is associated with their structure, and is in agreement with the finding that in the complexes of 30-crown-10 there are no interactions of the bound cation other than those with the macrocyclic ligand[17].

The further increase in the size of the macrocyclic ring and in the number of oxygen atoms for ditert-butyldibenzo-33-crown-11 (XIX) and dibenzo-36-crown-12 (XX), is accompanied by a decrease in the K/Na selectivity. For complexes of these compounds a similar wrap-around structure may be assumed as for 30-

crowns-10. Owing to the greater number of atoms in the ligand rings, one may expect the necessity of a certain contraction of the cavity formed in the process of the potassium complex formation, which leads to partial destabilization of the complex because of intraligand repulsive forces. In accordance with this hypothesis, the determined stability constant of the potassium complex of dibenzo-36-crown-12 (log $K_s = 3.16$, methanol) is lower by an order of magnitude than the corresponding constants of the 30-crown-10 compounds.

The low K/Na selectivity of crown compounds X and XIV with medium sized rings may be explained on the basis of the above ideas. On the one hand, their macrocyclic ring is too large to form a cavity suitable for a potassium complex having a planar structure; on the other, it is still too small to wrap itself around the complexed cation.

Although electrodes based on macrocyclic crown compounds do not attain the K/Na selectivity of valinomycin, they can in certain cases because of their good properties[1,2] be applied in practice. The results of this study also indicate possibilities of increasing the electrode selectivity by appropriate substitution of the basic skeletons of the crown compounds.

SUMMARY

The K/Na selectivity of electrodes with a plasticized polyvinyl chloride membrane containing neutral carriers of the macrocyclic polyether type has been investigated. The results obtained for twenty different crown compounds showed that the highest selectivities are obtained for polyethers with six oxygen binding sites in an eighteen-membered ring ($K_{K,Na}$ up to $1.1 \cdot 10^{-2}$) and for thirty-membered rings with ten oxygen atoms ($K_{K,Na}$ up to $2.2 \cdot 10^{-3}$). Possible explanations of the effect of the structure of the basic macrocyclic ring on selectivity, and the effects of some substituents, are discussed.

REFERENCES

1 See, *e.g.*, C. J. Pedersen and H. K. Frensdorff, *Angew. Chem., Int. Ed. Eng.*, 11 (1972) 16.
2 J. Koryta, *Anal. Chim. Acta*, 61 (1972) 329.
3 L. A. R. Pioda, V. Stankova and W. Simon, *Anal. Lett.*, 2 (1969) 665.
4 *Orion Res. Newsl.*, 2 (1970) 14.
5 G. A. Rechnitz and E. Eyal, *Anal. Chem.*, 44 (1972) 370.
6 G. J. Moody, R. B. Oke and J. D. R. Thomas, *Analyst (London)*, 95 (1970) 910.
7 O. Ryba, E. Knižáková and J. Petránek, *Collect. Czech. Chem. Commun.*, 38 (1973) 497.
8 U. Fiedler and J. Růžička, *Anal. Chim. Acta*, 67 (1973) 179.
9 J. Pick, K. Tóth, E. Pungor, M. Vašák and W. Simon, *Anal. Chim. Acta*, 64 (1973) 477.
10 M. D. Smith, M. A. Genshaw and J. Greyson, *Anal. Chem.*, 45 (1973) 1782.
11 C. J. Pedersen, *J. Amer. Chem. Soc.*, 89 (1967) 7017.
12 O. Ryba and J. Petránek, *J. Electroanal. Chem.*, 44 (1973) 425.
13 J. Petránek and O. Ryba, *Collect. Czech. Chem. Commun.*, 39 (1974) 2033.
14 V. Jíšová, M. Kolínský and D. Lím, *J. Polym. Sci., Part A-1*, 8 (1970) 1525.
15 D. Bright and M. R. Truter, *Nature (London)*, 225 (1970) 176; *J. Chem. Soc. B*, (1970) 1544.
16 H.-R. Wuhrmann, W. E. Morf and W. Simon, *Helv. Chim. Acta*, 56 (1973) 1011.
17 M. A. Bush and M. R. Truter, *Chem. Commun.*, (1970) 1439.

Analytica Chimica Acta, 72 (1974) 381–390

NITRATE AND AMMONIUM ION-SELECTIVE ELECTRODES AS SENSORS

PART I. IN BACTERIAL GROWTH CURVES FOR ISOLATION OF NITRATE AND NITRITE REDUCTASES FROM *ESCHERICHIA COLI*

W. R. HUSSEIN and G. G. GUILBAULT

Department of Chemistry, University of New Orleans, (formerly L.S.U. in New Orleans), A Member of the L.S.U. System, New Orleans, Louisiana 70122 (U.S.A.)

(Received 1st May 1974)

Nitrate and ammonium ions are the main nitrogen sources for both plants and microorganisms. In microorganisms, ammonium is more readily utilized than nitrate[1]. On a much smaller scale, nitrate can be utilized by certain dentrifying microorganisms as the only nitrogen source; ammonium ion is the final product and NO_2^-, NO, N_2O, and NH_2OH are the possible intermediates[2]. Other organisms such as *Escherichia coli (E. coli)* can use nitrate as a terminal hydrogen or proton acceptor when grown under anaerobic conditions. In such a case, nitrate will be reduced to nitrite only. More than one known enzyme system is responsible for the process of nitrate respiration and assimilation[3]. These enzyme systems can be summarized as follows:

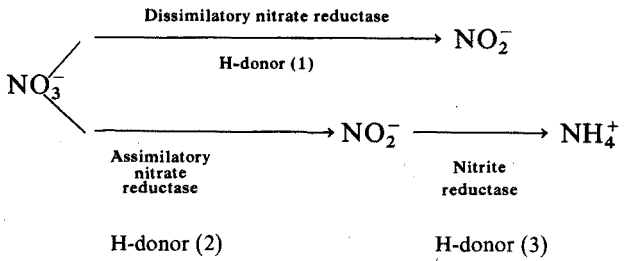

where H-donor (1) = formate, succinate, lactate
(2) = NADH, NADPH
(3) = NADH, NADPH, flavin (FMN-reduced), viologen.

The nitrate and nitrite reductase systems in Escherichia coli

Dissimilatory (respiratory) nitrate reductase. Quastel and Wetham[4], in 1925, were the first to demonstrate nitrate respiration in nondenitrifying bacteria such as *E. coli* (Reaction 1). Green and Tarr[5] were the first to show that nitrate reduction occurred in cell-free extracts from *E. coli.* After intensive studies, it was suggested that *E. coli* possesses several kinds of nitrate reductases which are dependent in part on the condition of growth[6].

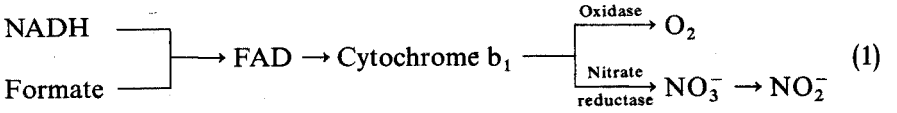

(1)

Assimilatory nitrate reductase and nitrite reductase. In addition to respiratory nitrate reductase, the presence of an assimilatory nitrate reductase in *E. coli*, which depends on the conditions of growth of the organism, has been reported[7]. Assimilatory nitrate reductase is responsible for the first step in the reduction of nitrate for the ultimate biosynthesis of nitrogen-containing cell constituents[8], while nitrite reductase is responsible for the reduction of nitrite to ammonium[9]:

$$NO_2^- + 6\,e^- + 8\,H^+ \xrightarrow[\text{reductase}]{\text{Nitrite}} NH_4^+ + 2\,H_2O \qquad (2)$$

In the present studies, nitrate reductase (dissimilatory) and nitrite reductase were induced and isolated from *E. coli*, strains B and Bn, respectively. For verification of the various phases of the growth curves, a new continuous potentiometric technique was developed and used instead of the conventional turbidimetric method. In this technique, nitrate ion-selective electrodes were used as sensors to follow the decrease in nitrate concentration used as substrate during growth. And ammonium ion-selective electrodes were used to measure the increase in ammonium ion concentration. The tedious sampling process for turbidimetric measurements was thus eliminated. The potentiometric results obtained were compared with spectrophotometric and turbidimetric data and were found to be in excellent agreement.

The enzymes nitrate and nitrite reductases were isolated for the purpose of developing new potentiometric techniques for the assay of both enzyme activities. The ultimate aim of this study was to develop analytical procedures for the assay of nitrate and nitrite ions with the enzymes. This aspect will be reported in Part II.

EXPERIMENTAL

Instrumentation

All potentiometric measurements were made with the Orion Digital pH-meter (Model 801) and the signal was displayed on a recorder (Sargent, Model SRLG). As sensors, the Orion nitrate ion-selective electrode (Liquid type – Model 92-07) was used, while the ammonium ion-selective electrode (Simon type)[10] was prepared in this laboratory. The antibiotic nonactin (SW 15859 – Batch No. LBH-3599-90-10, Squibb Institute for Medical Research) was the active ingredient in the sensitive membrane. The modified solid ammonium electrode[11] was used, with silicone rubber (no. 3140 RTV, Dow-Corning Corp., Midland, Mich.) as the solid supporting phase.

For spectrophotometric measurements, the Beckman DB spectrophotometer was used with an attached Sargent recorder (Model SRLG).

All chemicals used were reagent grade. The isolated dissimilatory nitrate reductase and nitrite reductase from *E. coli* strains B and Bn, respectively, were used as the stock solutions.

Analytical procedures

Potentiometric measurements. The Orion nitrate ion-selective electrode and the ammonium ion-selective electrode were used with a saturated calomel electrode for potentiometric measurements of nitrate and ammonium ions, respectively.

Spectrophotometric measurements. The brucine–sulfanilic method[12] was used for the determination of nitrate. This was necessary to follow the decrease in nitrate concentration during the growth of *E. coli* strains B and Bn. The Griess method[12] was used for assay of nitrite as it accumulated in the culture media. For ammonium ion measurements, the phenol–sodium nitroprusside procedure[13] was used. The Folin–Ciocalteu method was used[14] for the determination of proteins.

Induction and isolation of the nitrate and nitrite reductases from Escherichia coli (strains B and Bn)

Dissimilatory (respiratory) nitrate reductase (formate–nitrate reductase). For the purpose of this research, dissimilatory nitrate reductase was induced and isolated from *E. coli* strain B (E 11303, obtained from ATCC), which was chosen for its luxuriant growth and ability to mutate. The procedure of McNamara *et al.*[15] was followed for the enzyme preparation. The bacterial cells were harvested at the end of the log phase by batch centrifugation at 4000 *g* for 5 min (centrifuge model Sorvall, Superspeed, RC2-B). The precipitated bacterial cells were washed several times by resuspension in small volumes of 1% sodium chloride solution and recentrifugation. The precipitated whole cells were stored at −15 °C.

The frozen bacterial cells were ground for 30 min in a cold mortar and pestle in the presence of alumina powder in an approximate ratio of 1:2 w/w (cells: Al_2O_3). To the homogenate, cold 0.1 *M* phosphate buffer at pH 7.25 was added gradually (ratio of 1:5, w/v) with continuous grinding for approximately 10–15 min. The homogeneous suspension was then centrifuged in the cold at 2000 *g* for 20 min. The precipitate, which contained the cell debris and the alumina, was discarded, while the supernate was recentrifuged for 40 min at 20,000 *g*. The sediment contained nitrate reductase and formic dehydrogenase, and was used as the enzyme preparation.

Nitrite reductase (NADH–nitrite oxidoreductase EC 1. 6. 6. 4.). Nitrite reductase was induced and isolated from *E. coli* strain Bn, which was obtained by mutation of the parent organism *E. coli* strain B. The isolation of this mutant, Bn, was first reported by McNall and Atkinson in 1956[16]. Their procedure, with slight modifications, was followed for the isolation of the mutant.

E. coli strain B (E 11303, obtained from ATCC) was maintained on glucose agar slants with 0.01 *M* ammonium sulfate as the nitrogen source. For isolation of strain Bn, the parental strain B was successively transferred from the stock culture to yeast agar slants containing 10^{-3} *M* nitrate. After eight serial transfers, the new mutant strain Bn was isolated. The mineral media used for growth contained the following (in g l^{-1}): KNO_3, 1; glucose, 10; Na_2SO_4, 5; K_2HPO_4, 10; NaCl, 5; and (in mg l^{-1}): $(NH_4)_6Mo_7O_{24}\cdot 4H_2O$, 10; $FeCl_2$, 5; $CaCl_2$, 10; $CoCl_2$, 1; Na citrate, 50; $MgSO_4$, 200; $MnCl_2$, 10. Nitrate was used as the only source of nitrogen.

Attempts to grow the isolated mutant strain Bn in relatively large quantities

(500–1000 ml) on mineral media were not successful and the yield was extremely low. In order to improve the yield, the growth was started with liquid mineral media to which small quantities of yeast extract (50 mg/50 ml) were added, and then the amount of yeast extract was gradually decreased until it was completely absent in the fourth transfer; strain Bn from the last transfer of the stock culture was inoculated and successively transferred into the liquid media. The growth was conducted in sterile 50-ml test tubes, and rubber stoppers were used to eliminate possible contamination through cotton plugs in such long experiments. After 8 serial transfers, the growth proceeded reasonably well and the eighth transfer was used to grow the starter colony. Hydrogen gas was bubbled through a sterile trap into the liquid medium to provide anaerobic conditions and to serve as the hydrogen source for the reduction of nitrate to ammonium ion. The culture tubes were incubated at 37 °C for 24 h before the next transfer was made.

Starter cultures were grown under similar conditions (*i.e.*, nitrate was the only source of nitrogen, hydrogen gas was continuously bubbled through, and the temperature was maintained at 37 °C) in 250-ml sterile Erlenmeyer flasks. A sterile syringe needle was left permanently in the rubber stopper for frequent sampling. Samples were taken approximately every 6 h for nitrate, nitrite, ammonium ions, turbidity and pH measurements. The pH was maintained at 7.2. At the end of the log phase, *ca.* 300 ml of the starter culture were used to inoculate 3 l of mineral growth media in a deep standing culture which had been previously saturated with hydrogen. The growth temperature was 37 °C and the pH 7.2. Samples were taken frequently to follow the changes in nitrate, nitrite, ammonium ions, turbidity and pH with time.

At the end of the log phase, the bacterial cells were harvested by centrifugation at 4000 *g* for 10 min. The cells were then washed by resuspension in 1% sodium chloride several times and recentrifuged until a negative test for both nitrite and ammonium ions was obtained. The bacterial whole cells were then frozen overnight for isolation of the enzyme.

The washed frozen cells were ground with alumina powder, extracted with 0.1 *M* phosphate buffer at pH 7.25, and centrifuged at 2000 *g* for 20 min, as described for the isolation of nitrate reductase. The precipitate was discarded, and the supernate was recentrifuged at 144,000 *g* for 60–90 min. The precipitate which contained the flavine-specific part and most (95%) of the $NADH_2$–oxidase activity[9,17] was discarded. The supernate contained the partially purified nitrite reductase and was used as the enzyme preparation. The partially purified enzyme was frozen until use.

RESULTS AND DISCUSSION

According to reactions 1 and 2, the nitrate and nitrite reductases catalyze the formation of nitrite and ammonium ions from nitrate, respectively, in the presence of a suitable hydrogen-donor under optimum conditions. Spectrophotometric techniques seem to have been the only methods applied for the assay of the enzyme activities, as well as for bacterial growth investigations during the induction of the enzymes.

In the present investigations, ion-selective electrodes (nitrate and ammonium)

were applied as a new analytical technique for the assay of enzyme activities and in studies of the growth curves. Spectrophotometric methods were also used and results from the two methods were compared.

Growth curves

Nitrate and ammonium ion-selective electrodes were used to follow, respectively, the decrease in nitrate concentration as it is utilized by *E. coli* during growth, and the simultaneous increase in ammonium ions. A special arrangement was necessary for such a technique as shown in Fig. 1. A three-neck flask was used for the bacterial growth. One neck was used for the insertion of the indicating nitrate or ammonium ion-selective electrode while the second neck was used for the reference calomel electrode (A and B, Fig. 1). Two capillaries were fitted into the central neck which were used as an inlet and outlet for nitrogen or hydrogen gas bubbled through the medium (D). A magnetic stirrer (C) was used to provide proper potentiometric measurements and for the continuous agitation necessary for growth. The glassware was sterilized by autoclaving at 120 °C for 10 min while the electrode surfaces were disinfected with ethanol. The whole arrangement was maintained at a constant temperature of 37 °C. The electrodes were connected to the pH meter described under Experimental.

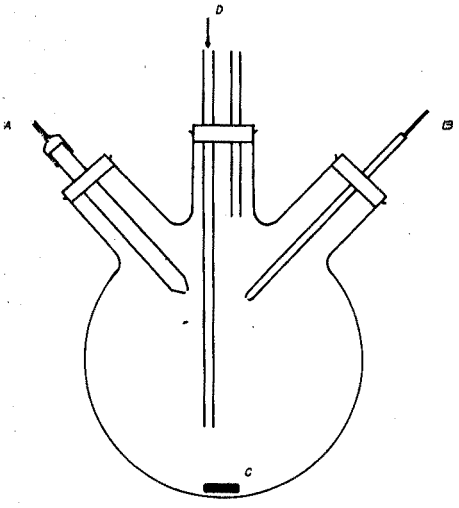

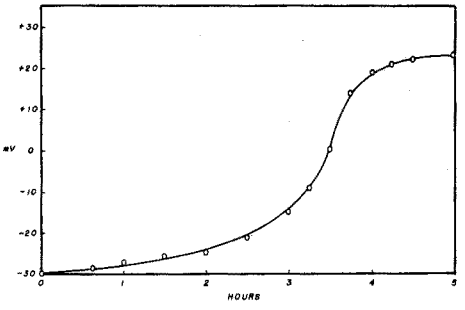

Fig. 1. Apparatus for potentiometric determination of the bacterial growth curves. A, nitrate ion-selective electrode; B, SCE reference electrode; C, magnetic stirrer; D, nitrogen inlet and outlet.

Fig. 2. The growth curves of *E. coli* strain B as indicated by the nitrate electrode response.

Figure 2 shows the nitrate ion-selective electrode response, demonstrating the decrease in nitrate concentration as a function of time during the growth of *E. coli* strain B. A maximal decrease in nitrate concentration was observed in the period 3–4 h after initiation, which can be correlated to the maximum turbidity observed by McNamara *et al.*[15] within the same period of time.

Figure 3 shows the corresponding decrease in nitrate concentration obtained

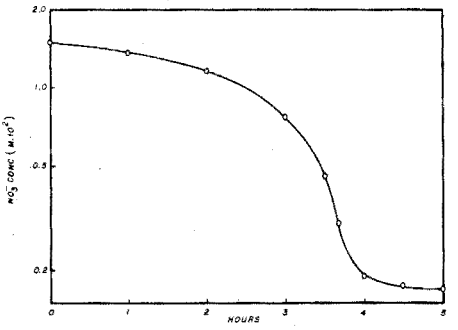

Fig. 3. The decrease in nitrate concentration during the growth of *E. coli* strain B (spectrophotometric).

by a colorimetric procedure (brucine–sulfanilic acid method). From Figs. 2 and 3, it was concluded that the end of the logarithmic phase for *E. coli* strain B is between 3 and 4 h, which is in agreement with previously reported data[16]. The harvest time was determined when the nitrate concentration remained almost constant with time (*ca.* 3.5 h).

Figure 4 shows the growth of strain Bn in the starter culture. In order to follow the changes in nitrate, nitrite and ammonium ion concentrations, as well as turbidity, spectrophotometric techniques were used. The brucine method was used for nitrate, the Griess method for nitrite, and the phenol–nitroprusside method for ammonium ion, while the absorbance was measured at 520 nm for turbidity estimation. As indicated by Fig. 4, it was found that a period of approximately three days elapsed before any change in nitrate or nitrite concentration was observed. The maximum changes, *i.e.*, decrease in nitrate and increase in nitrite concentrations, took place after almost six days, indicating an unexpectedly lengthy lag period. Furthermore, the ammonium concentration in the medium remained constant over a period of about 10 days. During this period no significant change in turbidity was observed. As the ammonium ion concentration began to rise, a parallel increase in turbidity took place and a corre-

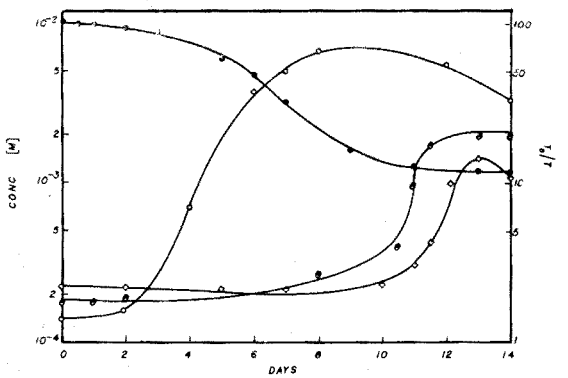

Fig. 4. Growth curves of *E. coli* strain Bn in the starter culture. (●) NO_3^- Concentration (*M*), (○) NO_2^- concentration (*M*), (◇) NH_4^+ concentration (*M*), (◓) turbidity (T_0/T).

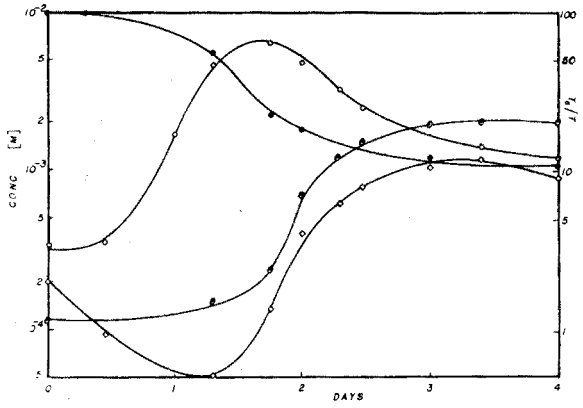

Fig. 5. Growth curves of *E. coli* strain Bn in the inoculum colony. (●) NO_3^- Concentration (M), (○) NO_2^- concentration (M), (◇) NH_4^+ concentration (M), (◓) turbidity (T_0/T).

sponding decrease in nitrite concentration was noticeable.

Figure 5 represents the growth of *E. coli* strain Bn in the inoculum colony. Compared with Fig. 4, the lag period drastically diminished to 24–36 h. During this period, a maximal increase in nitrite concentration with a decrease in nitrate concentration was observed. Under the anaerobic conditions, nitrate was reduced to nitrite during respiration in taking the role of oxygen. It was also observed that an initial decrease in ammonium concentration took place. Simultaneously, a gradual increase in turbidity was found, which explains the decrease in ammonium concentration. Afterwards, a sharp increase in ammonium concentration together with maximal turbidity occurred after 36 h, while at the same time, a sharp decrease in nitrite concentration took place as it was reduced to ammonium at the expense of hydrogen.

An ammonium ion-selective electrode was used in a similar fashion to the nitrate ion-selective electrode in following the growth curve. Figure 6 shows the change in electrode response caused by increase in ammonium concentration during the growth of *E. coli* strain Bn in the inoculum colony. The total change

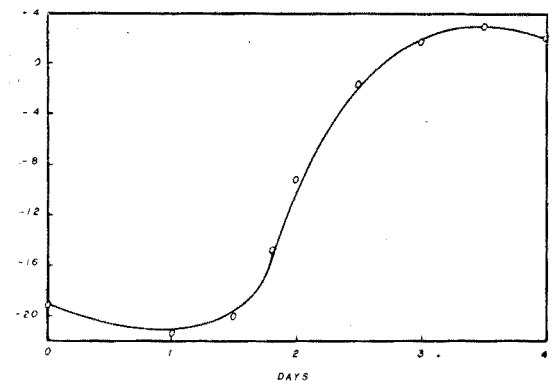

Fig. 6. Growth curve of *E. coli* strain Bn in the inoculum colony as indicated by the ammonium electrode response.

in mV was *ca.* 30, which is of the order caused by a one decade increase in ammonium concentration. These results agreed reasonably well with those obtained spectrophotometrically (Fig. 5), which indicated a change in ammonium concentration from 10^{-4} to 10^{-3} *M*. The harvest time was determined by the maximal change in the ammonium ion concentration.

According to McNall and Atkinson[16], although the inoculum colony was grown on nitrate, a lag period was observed during which nitrite accumulated in the growth medium which contained nitrate as the only nitrogen source. There was little nitrite reduction and little growth until the concentration ratio of nitrate to nitrite was markedly reduced. The lag was more pronounced when a higher concentration of nitrate was used.

MEASUREMENTS OF NITRATE REDUCTASE ACTIVITY

Potentiometric assay

The liquid exchanger nitrate-selective electrode was calibrated in stationary standard nitrate solutions in the concentration range 10^{-1}–10^{-4} *M* in 0.5 *M* phosphate buffer at pH 7.25, against a reference saturated calomel electrode. The calibration graph was linear over the range 10^{-1}–10^{-4} *M* and gave a slope of 58 mV/decade. The value of the slope, however, decreased with time and the electrode had to be recalibrated once a week. After approximately one month, a new electrode had to be prepared.

For potentiometric measurements, the nitrate indicating electrode and the reference electrode were immersed in a beaker containing 20 ml of 10^{-3} *M* nitrate solution prepared in 0.5 *M* phosphate buffer at pH 7.25 and 1 ml of 1 *M* formate solution. For reaction rate measurements by the slope method, 3 ml containing various concentrations of the enzyme preparation were injected into the substrate solution. The reaction rate was followed as the change in potential at the indicating electrode surface as the nitrate concentration decreased because of the enzymatic reduction of nitrate to nitrite. From the nitrate electrode calibration graph, the corresponding decrease in the molar concentration of nitrate was calculated. Hence, the activity units of nitrate reductase were determined (Table I). One specific activity unit equals one μmole of nitrite produced or nitrate reduced per min per mg of protein. The reaction temperature was maintained at 38°C.

The activity units of the stock nitrate reductase preparation were deter-

TABLE I

COMPARISON OF NITRATE REDUCTASE ACTIVITY ASSAY BY POTENTIOMETRIC AND SPECTROPHOTOMETRIC METHODS

mg of protein	ΔE *min*$^{-1}$	*Calculated units*	
		Potent.	*Spect.*
7.43	15.4	0.45	0.47
4.95	8.2	0.41	0.44
2.89	3.9	0.44	0.48

mined potentiometrically in stationary solution and the results were compared with those determined spectrophotometrically by a standard procedure.

Spectrophotometric assay

The standard procedure described in *Methods in Enzymology*[18] was followed. To 20 ml of 10^{-3} *M* nitrate solution prepared in 0.5 *M* phosphate buffer at pH 7.25 plus 1 ml of 1 *M* formate was added 3 ml of the enzyme preparation. The reaction mixture was incubated at 38 °C for 15 min and the nitrite produced was determined spectrophotometrically. The reaction was stopped by the addition of 1 ml of sulfanilic acid followed by 1 ml of 1-naphthylamine hydrochloride. The color was allowed to develop for 20 min and the absorbance was measured at 520 nm. From the standard nitrite calibration curve, the nitrite concentration was calculated. Knowledge of the total protein concentration is essential for the calculation of the activity units. Proteins were measured spectrophotometrically according to the Folin–Ciocalteu method. The calculated spectrophotometric activity units are shown in Table I.

It was found that the enzyme activity units calculated potentiometrically agreed well with the spectrophotometric values (5% error calculated; three runs were made for each enzyme concentration).

Conclusions

The application of nitrate and ammonium ion-selective electrodes as sensors in following bacterial growth for the isolation of nitrate and nitrite reductases provides a rather superior method when compared with the conventional turbidimetric technique. The potentiometric method is continuous, and sampling for turbidity measurements is eliminated. For the assay of enzyme activity, the electrochemical determination of nitrate reductase with a nitrate ion-selective electrode proves to be a sensitive and accurate method which compares favorably with the standard spectrophotometric techniques.

The financial assistance of the National Science Foundation (Grant No. GI 32995) and the Army Research Office (Grant No. DA-ARO-D31-124-70-G-69) is gratefully acknowledged.

SUMMARY

Ammonium and nitrate ion-selective electrodes were applied as sensors in bacterial growth curves for the isolation of nitrate and nitrite reductase. A nitrate ion-selective electrode was used as a successful new technique for the assay of nitrate reductase activity: the decrease in nitrate concentration was followed continuously. Likewise, an ammonium ion-selective electrode was used to follow the increase in ammonium ion concentration. Excellent agreement with spectrophotometric procedures ($<5\%$) was obtained.

REFERENCES

1 K. Mosback, *Scientific American*, 224 (1971) 26.

2 M. A. Azim and E. R. Toberts, *Biochim. Biophys. Acta*, 21 (1956) 308.
3 M. Dixon and E. C. Webb, *Enzymes*, Academic Press, New York, 2nd edn., 1966.
4 J. H. Quastel and M. D. Wetham, *Biochem. J.*, 19 (1925) 304.
5 D. E. Green and H. La. Tarr, *Biochem. J.*, 28 (1934) 1812.
6 P. D. Boyer and K. Myrback, *The Enzymes*, Academic Press, New York, 2nd edn., 1963.
7 D. J. D. Nicholas and A. Nason, *J. Bacteriol.*, 69 (1955) 580.
8 H. R. Garret and A. Nason, *Biochemistry*, 58 (1967) 1603.
9 J. D. Kemp and D. Atkinson, *J. Bacteriol.*, 92 (1966) 628.
10 R. P. Scholer and W. Simon, *Chimia*, 24 (1972) 372.
11 G. G. Guilbault and G. Nagy, *Anal. Chem.*, 45 (1973) 417.
12 F. J. Welcher, *Standard Methods of Chemical Analysis*, Vol. 2, Part B, 1968.
13 N. W. Tietz, *Fundamentals of Clinical Chemistry*, W. B. Saunders, Philadelphia, 1970.
14 G. Litwack, *Experimental Biochemistry*, Wiley, New York, 2nd edn., 1963.
15 A. L. McNamara, G. B. Meeker, P. D. Shaw and R. H. Hageman, *J. Agr. Food Chem.*, 19 (1971) 229.
16 E. G. McNall and D. Atkinson, *J. Bacteriol.*, 72 (1956) 226.
17 R. Lazzarini and D. Atkinson, *J. Biol. Chem.*, 236 (1961) 3330.
18 S. Colowick and N. Kaplan, *Methods in Enzymology*, Vol. XXII, Part A, Academic Press, New York, 1971.

Analytica Chimica Acta, 72 (1974) 391–399

DOSAGE AMPÉROMÉTRIQUE DES ACIDES AMINOPOLYACÉTIQUES NTA, HEDTA ET EDTA, ÉVENTUELLEMENT EN PRÉSENCE DE LANTHANIDES

J. VANDEGANS, E. MERCINY et G. DUYCKAERTS

Laboratoire de Chimie Analytique, Université de Liège au Sart Tilman, B-4000 Liège (Belgique)

(Reçu le 18 avril 1974)

Les acides aminopolyacétiques trouvent des applications extrêmement nombreuses en chimie analytique, en chimie préparative et en chimie appliquée; néanmoins, les publications concernant leur dosage ne sont pas très nombreuses.

Lorsqu'il s'agit d'un seul complexant, éventuellement en présence de cation, on a proposé l'emploi d'indicateurs colorés[1,2], de méthodes cinétiques[3] ou potentiométriques[4–6]; la polarographie est également souvent préconisée[7–13].

Or, très souvent, on est amené à devoir analyser des solutions contenant plusieurs acides aminopolyacétiques, éventuellement en présence de cations métalliques: contrôle de la pureté d'un acide aminopolyacétique[14–16], analyse de complexes mixtes contenant deux acides différents[17–20], analyse de détergents ou d'eaux résiduaires contenant plusieurs complexants.

Nous nous sommes trouvés confrontés avec ce problème à l'occasion d'une étude de séparations chromatographiques de lanthanides sur résine anionique saturée en NTA par une solution d'EDTA ou de HEDTA[21,22].

Devant l'absence de méthode d'analyse adéquate, nous nous sommes efforcés de mettre au point une méthode ampérométrique de dosage de solutions contenant deux acides aminopolyacétiques en présence de lanthanides.

Principe de la méthode

La méthode consiste à titrer la solution à analyser avec un cation Me^{n+} dans des conditions de milieu et de pH où la réaction de substitution est pratiquement complète

$$LnY^{(m-3)-} + Me^{n+} \rightarrow MeY^{(m-n)-} + Ln^{3+} \quad (1)$$

Si le cation Me^{n+} et ses complexes avec les différents acides aminopolyacétiques donnent des vagues de réduction polarographiques bien distinctes, on peut suivre le titrage et apprécier, par ampérométrie, le terme des réactions successives de complexation des acides libres et de substitution suivant l'éqn. (1).

THÉORIE

Choix du réactif titrant

Les constantes thermodynamiques de dissociation des complexes des terres rares avec l'EDTA varient de $10^{-15,5}$ mol l^{-1} pour le lanthane à $10^{-19,8}$ mol l^{-1}

TABLEAU I

CONSTANTES DE DISSOCIATION DES CHÉLATS DE L'EDTA, DU HEDTA ET DU NTA[23,24]

Me	p_c *Me–EDTA*[a]	p_c *Me–HEDTA*	p_c *Me–NTA*	*Propriétés*
Co^{3+}	36,0	—[b]	—	Instable à l'état 3^+ $E^0_{Co^{3+}/Co^{2+}} = 1.84$ V
V^{3+}	25,9	—	—	S'oxyde facilement à l'air $E^0_{V^{3+}/VO^{2+}} = 0{,}36$ V
Fe^{3+}	25,1	19,8	15,9	La vague de Fe^{3+}/Fe^{2+} se situe dans la vague du mercure
In^{3+}	24,9	—	15,0	Peut convenir
Cr^{3+}	24,0	—	—	Complexes hydroxylés très stables et cinétique de complexation lente
Th^{4+}	23,2	—	—	Radioactif
Sc^{3+}	23,1	—	$\simeq 11{,}5$	p_c Sc–NTA trop faible
Bi^{3+}	22,8	—	17,5	Peut convenir
Sn^{2+}	22,1	—	—	S'oxyde facilement à l'air $E^0_{Sn^{2+}/Sn^{4+}} = -0{,}14$ V
Hg^{2+}	21,8	20,1	12,7	p_c Hg–NTA trop faible
Ti^{3+}	21,3	—	—	S'oxyde facilement à l'air $E^0_{Ti^{3+}/Ti^{4+}} = 0{,}0$ V

[a] Conventions: $p_c = -\log K_c$; EDTA, acide éthylènediaminotétraacétique; HEDTA, acide hydroxyéthyléthylènediaminotriacétique; NTA, acide nitrilotriacétique; DTPA, acide diéthylènetriaminopentaacétique.

[b] Constantes non déterminées.

pour le lutétium. Avec le NTA, ces constantes[23] vont de $10^{-10,4}$ à $10^{-12,5}$ mol l^{-1}. Seuls les cations repris dans le tableau I forment des complexes plus stables et sont donc éventuellement capables de déplacer les lanthanides suivant la reaction (1), à condition que la constante d'équilibre apparente ne soit pas trop affectée par le milieu (précipitation, complexation, hydrolyse du cation). Certains cations présentent des particularités chimiques ou électrochimiques qui rendent leur usage malaisé. Finalement, nous avons retenu le bismuth; l'indium peut convenir en théorie, même si sa constante de stabilité avec le NTA est faible; il s'agit cependant d'un métal trop rare pour une méthode d'analyse de routine.

Choix des conditions du titrage

Les conditions du titrage doivent être choisies de telle façon que:

(1) il n'y ait de précipitation du bismuth à aucun moment;

(2) la réaction (1) soit quantitative;

(3) la constante de dissociation apparente (K'_c) de Bi–NTA soit suffisamment faible (*ca.* 10^{-6} mol l^{-1}) pour que le terme ampérométrique soit assez net;

(4) le titrage de l'EDTA ou du HEDTA se fasse sans interférence avec le NTA.

On peut voir, d'après la figure 1 qui représente les valeurs de p'_c des complexes Bi–EDTA (a) et Bi–NTA (b) en fonction du pH, en tenant compte des composés hydroxylés du bismuth[23], que la dernière conditions ci-dessus n'est réalisée que pour autant que le pH soit plus grand que 4. Nous savons d'autre

)art que, en milieu chlorure, le bismuth forme des complexes $BiCl_4^-$, $BiCl_5^{2-}$. Outre lue ces réactions secondaires ont pour effet d'augmenter les constantes de lissociation apparentes des complexes du bismuth avec les acides aminopoly-cétiques et de déplacer l'équilibre (1) vers la gauche, il ne faut pas perdre de ue que le bismuth précipite très rapidement sous forme de sels basiques comme iiOCl en milieu chlorure ou $BiONO_3$ en milieu nitrique[25]. Cette précipitation lu titrant a lieu dès le terme et même éventuellement avant le terme.

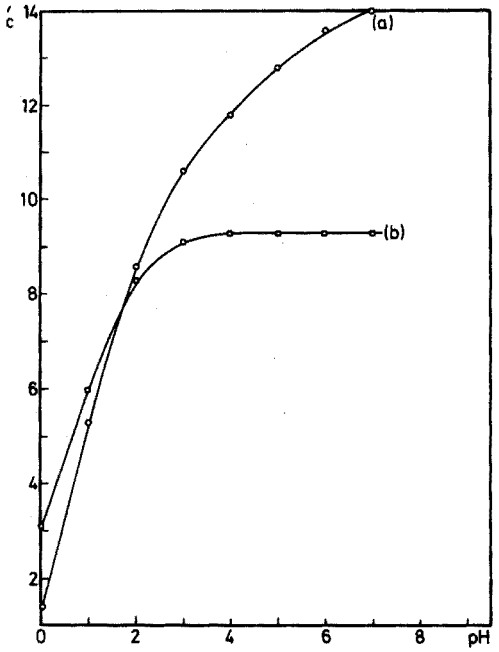

Fig. 1. Constantes de dissociation apparentes; (⊙) p'_c de Bi-EDTA, (⊡) p'_c de Bi–NTA, $[Bi^{3+}]_t = 10^{-3}$ *M*, $[NO_3^-]_t = 10^{-1}$ *M*, $[NTA]_t = [EDTA]_t = 10^{-3}$ *M*.

Si la concentration en ion chlorure est suffisamment élevée (2 *M* en NaCl), il est possible de maintenir le bismuth en solution jusque vers pH 5. Mais dans ces conditions, la formation des complexes chlorés dont nous venons de parler gêne; le terme du titrage du NTA n'est plus assez net, le p'_c de Bi–NTA étant beaucoup trop faible. Si, d'autre part, nous choisissons un milieu non complexant comme les nitrates, la précipitation du nitrate basique de bismuth empêche la réalisation de toute ampérométrie.

Les milieux complexants comme les milieux non complexants ne convenant pas, la solution de notre problème semblait vouée à l'échec lorsque nous avons constaté que le bismuth formait aisément des solutions sursaturées en milieu nitrique moyennant quelques précautions opératoires. La formation de ces solutions sursaturées résulte en fait d'une réaction d'olation[26], autrement dit, de la formation de polymères hydroxylés. Même sous agitation vigoureuse, une solution 10^{-3} *M* en nitrate de bismuth reste sursaturée à 10 °C et à pH 5.

Dans ces conditions, on peut conclure, d'après la figure 1, que la réaction (1) sera pratiquement quantitative et que toutes les conditions de titrage précitées

seront réalisées.

En conclusion, nous pouvons définir les conditions de titrage comme suit: solution titrante de $Bi(NO_3)_3$, température de 10 °C, et solution titrée tamponnée à pH 4,8 par du tampon acétique *M*.

Choix des potentiels de travail

La figure 2 montre l'enregistrement du polarogramme d'une solution contenant du Bi^{3+} et divers acides aminopolyacétiques en milieu nitrique à pH 4,5. Elle va nous permettre de définir nos conditions électrochimiques de travail.

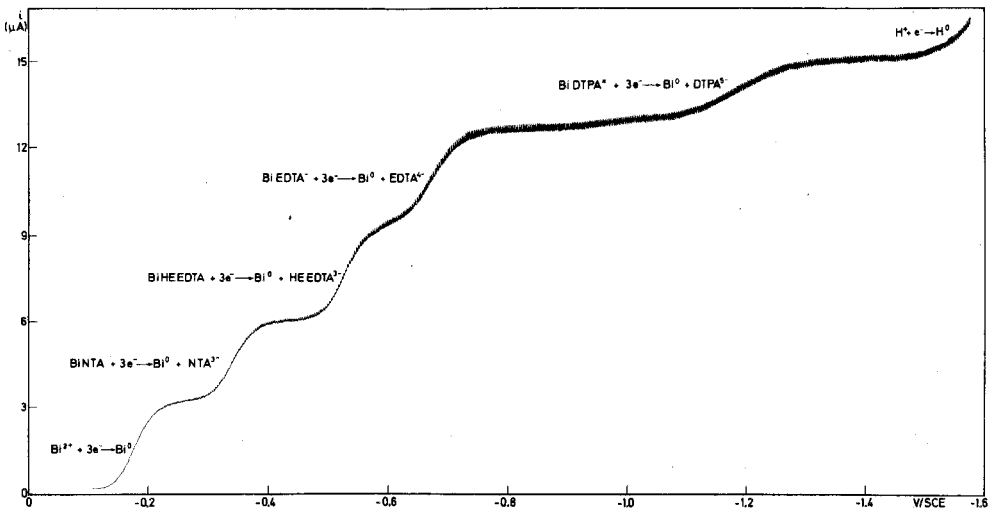

Fig. 2. Polarogramme d'une solution de complexes du bismuth avec divers acides aminopolyacétiques; pH = 4,5, $|Bi\text{–}NTA| = 3{,}522 \cdot 10^{-4}$ *M*, $|Bi\text{–}HEDTA| = 3{,}807 \cdot 10^{-4}$ *M*, $|Bi\text{–}EDTA^-| = 3{,}642 \cdot 10^{-4}$ *M*, $|Bi\text{–}DTPA^{2-}| = 3{,}660 \cdot 10^{-4}$ *M*, $|Bi^{3+}| = 3{,}922 \cdot 10^{-4}$ *M*. Électrode au calomel saturée en KCl; électrode à goutte tombante de mercure.

Prenons comme exemple le titrage d'une solution contenant le couple EDTA/NTA. Nous commençons le titrage ampérométrique en nous plaçant à un potentiel situé dans le palier de diffusion de la réduction de Bi NTA soit −0,43 V/SCE.

Dans ces conditions, le courant sera très faible jusqu'au terme du titrage de l'EDTA et comme la complexation du NTA se fera dès le premier terme, nous assisterons à une augmentation du courant au-delà de ce premier point équivalent. Pour pouvoir repérer le terme du titrage du NTA, nous changeons de potentiel; nous nous plaçons maintenant dans le palier de diffusion correspondant à la réduction de Bi^{3+} soit à −0,23 V/SCE. Au terme, nous enregistrons le courant de réduction de Bi^{3+} en excès par rapport à ces deux agents complexants.

Les autres cas de mélanges d'acides aminopolyacétiques peuvent se traiter d'une manière identique par simple examen de la figure 2.

CONDITIONS EXPÉRIMENTALES

Réactifs

L'acide éthylènediaminotétraacétique (EDTA, titriplex II pour le titrage des métaux, Merck), l'acide nitrilotriacétique (NTA, 99% minimum. Fluka), et l'acide hydroxyéthyléthylènediaminotriacétique (HEDTA; Sigma Chem. Corp.) sont utilisés. Le dernier a été purifié par cristallisation dans l'eau désionisée.

Les oxydes d'europium et de samarium (Eu_2O_3 et Sm_2O_3 très purs) proviennent de la firme Fluka. Le carbonate basique de bismuth ($(BiO)_2CO_3$-$1/2H_2O$ tout pur) est fourni par U.C.B.

Préparation des solutions

Dans un ballon jaugé d'un litre, on verse 500 ml d'eau et 5 ml d'acide nitrique 14 *M* pour analyse. D'autre part, on dissout 1297 g de carbonate basique de bismuth dans 5 ml d'acide nitrique 14 *M*. Ces deux solutions sont mélangées et amenées à 1 l. On obtient ainsi une solution $5 \cdot 10^{-3}$ molaire en Bi^{3+} (le carbonate basique de bismuth $(BiO)_2CO_3 \cdot 1/2H_2O$ peut être considéré comme une substance étalon).

Les solutions de LnY sont obtenues par dissolution des complexes solides préparés selon la méthode de zur Nedden et coll.[27].

Le tampon acétique *M* est préparé à partir d'acide acétique et d'acétate sodique (Merck pour analyse).

Une solution à 1% de gélatine (Merck) est utilisée comme suppresseur de maximum polarographique.

Appareillage

Les mesures sont effectuées au moyen d'un polarographe Metrohm Polarecord E. 261. Le pH est contrôlé avec un pH mètre Beckman Expandomatic.

La cellule de titrage à double paroi thermostatisée par circulation d'eau a un volume total de 100 ml et elle comporte cinq tubulures rodées par lesquelles on introduit: l'électrode à goutte de mercure, le pont électrolytique (agar-agar/KNO_3), l'électrode de verre, le barboteur à azote, et la burette. Afin d'éviter tout risque de précipitation de l'oxychlorure de bismuth par diffusion du KCl, l'électrode de référence est couplée à la cellule au travers d'un pont de jonction au KNO_3 saturé. Cette liaison n'a pas d'influence sur les potentiels de jonction.

Mesures

On introduit dans la cellule 20 à 50 ml de solution à analyser, 20 ml de tampon acétique et trois gouttes de la solution de gélatine à 1%. Avant chaque titrage, la solution est dégazée pendant 10 min par un courant d'azote, de même, après chaque ajout de la solution de $Bi(NO_3)_3$, on dégaze pendant 2 min.

La différence de potentiel entre l'électrode de mercure et la calomel est ajustée à ± 5 mV et les courants sont mesurés avec une sensibilité de $2 \cdot 10^{-8}$ A mm^{-1}.

RÉSULTATS ET DISCUSSION

La méthode proposée ci-dessus a d'abord été testée sur un mélange EDTA/NTA en l'absence de terre rare.

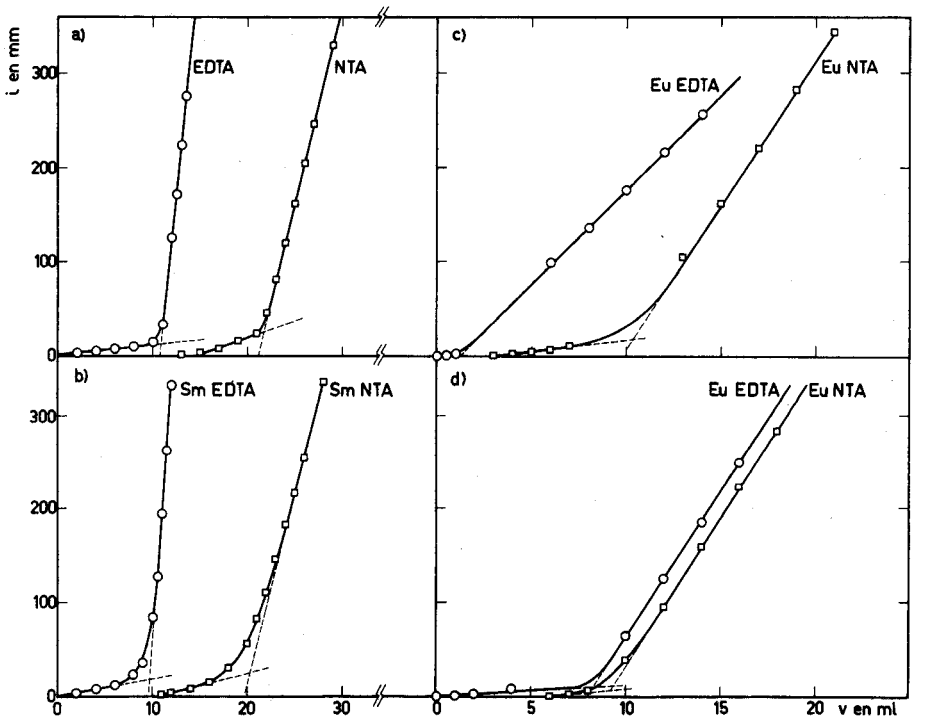

Fig. 3. Titrages ampérométriques de solutions complexantes; (a) EDTA $9{,}94 \cdot 10^{-2}$ *M* + NTA $9{,}94 \cdot 10^{-2}$ *M* par Bi^{3+} $1{,}002 \cdot 10^{-2}$ *M*, (b) Sm^{3+} + EDTA $8{,}83 \cdot 10^{-2}$ *M* + NTA $9{,}94 \cdot 10^{-2}$ *M* par Bi^{3+} $1{,}002 \cdot 10^{-2}$ *M*, (c) Eu^{3+} + EDTA $1{,}40 \cdot 10^{-4}$ *M* + NTA $5{,}20 \cdot 10^{-3}$ *M* par Bi^{3+} $5{,}102 \cdot 10^{-3}$ *M*, (d) Eu^{3+} + EDTA $4{,}26 \cdot 10^{-3}$ *M* + NTA $4{,}37 \cdot 10^{-4}$ *M* par Bi^{3+} $5{,}102 \cdot 10^{-3}$ *M*. Tampon acétique *M*; pH 4,8; température 10°C.

La figure 3a présente les courbes ampérométriques obtenues dans ce cas: le titrage de l'EDTA s'effectue dans d'excellentes conditions, la courbure au voisinage du terme est très faible et la zone de proportionnalité intensité–concentration est très rapidement atteinte. Pour le titrage du NTA, la valeur plus faible de la constante de stabilité du complexe Bi–NTA se traduit par une courbure plus prononcée au voisinage du terme; la zone de proportionnalité intensité–concentration n'est atteinte que beaucoup plus tard; il est néanmoins possible, grâce au phénomène de sursaturation, de maintenir le bismuth en solution suffisamment loin au-delà du terme.

La figure 3b présente les courbes ampérométriques obtenues lors du titrage d'une solution contenant du NTA et du Sm–EDTA. Comme il faut s'y attendre, la courbe de titrage de Sm–EDTA est un peu plus arrondie que celle de l'EDTA. Le titrage du NTA reste parfaitement possible à condition de pouvoir maintenir le bismuth en solution suffisamment loin au-delà du second point équivalent, car suite aux réactions (2), (3) et (4), nous titrons du NTA au moins partiellement complexé.

$$Sm(EDTA)^- + Bi^{3+} \rightleftharpoons Bi(EDTA)^- + Sm^{3+} \qquad (2)$$

$$Sm^{3+} + (NTA)^{3-} \rightleftharpoons Sm(NTA) \qquad (3)$$

$$Sm(NTA) + Bi^{3+} \rightleftharpoons Bi(NTA) + Sm^{3+} \quad (4)$$

Il s'ensuit une accentuation de la courbure au voisinage du terme.

Pour apprécier les limites de la méthode, nous avons fait varier le rapport des concentrations dans des proportions importantes. Les figures 3c et 3d présentent les résultats obtenus pour des mélanges en concentrations variables $C_{NTA}/C_{Eu-EDTA}$. Des expériences similaires ont été réalisées avec le couple Sm–HEDTA/NTA. Les performances obtenues dans ce dernier cas sont analogues si l'on travaille à −0,39 V/SCE pour le titrage de Sm–HEDTA.

L'erreur du titrage a été évaluée à 0,2% pour les complexants forts et à 1% pour le NTA. Cette précision reste valable, même pour des concentrations très faibles. Si la solution titrante de bismuth est 10^{-3} molaire, il est possible de doser des solutions 10^{-5} molaires en acides aminopolyacétiques même en présence de lanthanide (tableau II).

TABLEAU II

TITRAGES AMPÉROMÉTRIQUES DES ACIDES AMINOPOLYACÉTIQUES

Complexants	*Concentration théorique (M)*	*Concentration expérimentale (M)*
EDTA + NTA	$9{,}94 \cdot 10^{-2}$	$9{,}95 \cdot 10^{-2}$
	$9{,}94 \cdot 10^{-2}$	$9{,}85 \cdot 10^{-2}$
EDTA + NTA en présence de Sm^{3+}	$8{,}83 \cdot 10^{-2}$	$8{,}94 \cdot 10^{-2}$
	$9{,}94 \cdot 10^{-2}$	$9{,}76 \cdot 10^{-2}$
EDTA + NTA en présence de Eu^{3+}	$1{,}40 \cdot 10^{-4}$	$1{,}40 \cdot 10^{-4}$
	$5{,}20 \cdot 10^{-3}$	$5{,}17 \cdot 10^{-3}$
EDTA + NTA en présence de Eu^{3+}	$4{,}26 \cdot 10^{-3}$	$4{,}26 \cdot 10^{-3}$
	$4{,}37 \cdot 10^{-4}$	$4{,}34 \cdot 10^{-4}$
HEDTA + NTA	$9{,}87 \cdot 10^{-2}$	$9{,}88 \cdot 10^{-2}$
	$9{,}94 \cdot 10^{-2}$	$9{,}86 \cdot 10^{-2}$
HEDTA + NTA en présence de Sm^{3+}	$8{,}95 \cdot 10^{-2}$	$8{,}95 \cdot 10^{-2}$
	$9{,}94 \cdot 10^{-2}$	$9{,}82 \cdot 10^{-2}$

La méthode présente une limitation: elle trouve essentiellement son origine dans la réaction de déplacement (1). Si le complexe de terre rare devient trop stable —et cela se présente audelà du holmium—la réaction de substitution (1) ne se passe plus. Pour les terres plus lourdes, il faudrait utiliser l'indium(III) qui forme avec les acides aminopolyacétiques des complexes plus stables que le bismuth[12]

Nous ne voulons pas terminer cette discussion sans attirer l'attention sur un phénomène assez particulier déjà signalé antérieurement[28], relatif au déplacement des potentiels de demi-vague en fonction de la nature de l'agent complexant.

Koryta et Kossler[29] ont calculé le déplacement de potentiel de demi-vague pour les complexes du NTA d'après la relation

$$\Delta E^{\frac{1}{2}} = \frac{RT}{nF} \ln \frac{K_{cMeY}}{[Y]} \tag{5}$$

où $\Delta E^{\frac{1}{2}}$ représente la différence entre le potentiel de demi-vague de l'ion complexé et de l'ion libre. Ces résultats ont été comparés aux valeurs expérimentales de différents auteurs[30–32].

Lorsqu'ils introduisent dans cette relation (5) les valeurs de K_{cMeY}, ces auteurs[29] trouvent par calcul, à quelques exceptions près, toujours un $\Delta E^{\frac{1}{2}}$ plus petit que la valeur expérimentale.

Les complexes du bismuth avec les acides aminopolyacétiques à l'exclusion du NTA, présentent la même particularité. Pribil[28] attribue ce fait à l'irréversibilité des réductions des complexes. Il signale, en outre, que la vague de réduction de Bi–EDTA est irréversible dans tout le domaine de pH. La figure 2 montre d'ailleurs que les vagues de réduction deviennent de plus en plus irréversibles lorsque le pouvoir complexant augmente.

Ce comportement particulier présente un avantage considérable. En effet, la dimension des paliers de diffusion de chaque entité complexe s'en trouve fortement agrandie ce qui, pour la réalisation des titrages ampérométriques, est un avantage certain.

En conclusion, il semble donc que l'ampérométrie offre une solution simple, rapide et précise à un problème complexe auquel aucune autre méthode n'a encore apporté de réponse.

Signalons encore, pour terminer, que les conditions assez strictes de travail sont uniquement dues à la nécessité du titrage de NTA. Dans les autres cas, ces conditions peuvent être allégées si toutefois nous prenons soin d'ajouter à la solution un peu de NTA qui servira en somme d'indicateur ampérométrique tout en maintenant le bismuth en solution au-delà du terme.

RÉSUMÉ

Les auteurs décrivent le titrage ampérométrique d'acides aminopolyacétiques seuls ou en mélange et éventuellement en présence de lanthanide par une solution de nitrate de bismuth; la méthode est basée sur la complexation successive des différents acides aminopolyacétiques et l'existence de vagues polarographiques bien séparées pour Bi^{3+} et les différents complexes de Bi^{3+} avec ces acides. La méthode offre des limitations lorsque l'acide est moins complexant que le NTA et que le lanthanide éventuellement présent est au-delà du holmium.

SUMMARY

The amperometric titration of aminopolyacetic acids by a solution of bismuth nitrate has been studied in different conditions: alone, in mixtures, and eventually

in the presence of rare earth ions. The well-defined polarographic waves for bismuth(III) and the complexes of bismuth(III) with these chelating agents make it possible to study the complex formation. For ligands forming weaker complexes than NTA and for lanthanides heavier than holmium, the method is no longer applicable.

BIBLIOGRAPHIE

1 G. G. Clinckemaille, *Anal. Chim. Acta*, 43 (1968) 520.
2 D. L. Furhman, G. W. Latimer Jr. et J. Bishop, *Talanta*, 13 (1966) 103.
3 L. C. Coombs, J. Vasiliades et D. W. Margerum, *Anal. Chem.*, 44 (1972) 2325.
4 G. A. Rechnitz et N. C. Kenny, *Anal. Lett.*, 3 (1970) 509.
5 J. Horacek et R. Pribil, *Talanta*, 16 (1969) 1495.
6 S. Siggia, D. W. Eichlin et R. C. Reinhart, *Anal. Chem.*, 27 (1955) 1745.
7 J. Asplund et E. Wanninen, *Anal. Lett.*, 4 (1971) 267.
8 R. B. Le Blanc, *Anal. Chem.*, 31 (1959) 1840.
9 W. Hoyle et T. S. West, *Talanta*, 2 (1959) 158.
10 R. L. Daniel et R. B. Le Blanc, *Anal. Chem.*, 31 (1959) 1221.
11 W. Hoyle, I. P. Sanderson et T. S. West, *J. Electroanal. Chem.*, 2 (1961) 166.
12 J. P. Haberman, *Anal. Chem.*, 43 (1971) 63.
13 B. K. Afghan, P. D. Goulden et J. F. Ryan, *Anal. Chem.*, 44 (1972) 354.
14 C. N. Reilley, R. W. Schmid et F. S. Sadek, *J. Chem. Educ.*, 36 (1959) 619.
15 R. N. P. Farrow et A. G. Hill, *Analyst (London)*, 90 (1965) 210.
16 R. N. P. Farrow et A. G. Hill, *Analyst (London)*, 90 (1965) 241.
17 L. C. Thompson et J. A. Loraas, *Inorg. Chem.*, 2 (1963) 89.
18 G. Geier et O. Karlen, *Helv. Chim. Acta*, 54 (1971) 135.
19 V. Yugelik Uzer, *J. Inorg. Nucl. Chem.*, 32 (1970) 1279.
20 G. H. Carey et A. E. Martell, *Inorg. Chem.*, 3 (1964) 1288.
21 F. Schoebrechts, E. Merciny et G. Duyckaerts, *J. Chromatogr.*, 79 (1973) 293.
22 F. Schoebrechts, E. Merciny et G. Duyckaerts, à paraître.
23 A. Ringbom, *Les Complexes en Chimie Analytique*, Dunod, Paris, 1967.
24 B. P. Karadakov et D. I. Venkova, *Talanta*, 17 (1970) 878.
25 G. Charlot, *L'analyse qualitative et les Réactions en Solution*, Masson, Paris, 1965.
26 J. C. Bailar Jr., *The Chemistry of the Coordination Compounds*, Reinhold, New York, 1956.
27 P. zur Nedden, E. Merciny et G. Duyckaerts, *Anal. Chim. Acta*, 64 (1973) 197.
28 R. Pribil, *Analytical Applications of EDTA and Related Compounds*, Pergamon, Oxford, 1972.
29 J. Koryta et I. Kossler, *Collect. Czech. Chem. Commun.*, 25 (1950) 241.
30 J. Heyrovsky et D. I. Ilkovic, *Collect. Czech. Chem. Commun.*, 7 (1935) 198.
31 M. Stackelberg et H. V. Freyhold, *Z. Elecktrochem.*, 46 (1940) 120.
32 J. Lingane, *Chem. Rev.*, 29 (1941) 1.

Analytica Chimica Acta, 72 (1974) 401–406

VACUUM FUSION–ALUMINIUM BATH METHOD FOR THE DETERMINATION OF HYDROGEN IN COPPER

A. COLOMBO
Chemistry Division, Joint Nuclear Research Centre, Euratom Ispra Varese (Italy)
(Received 18th February 1974)

The effects of small amounts of gaseous impurities on the properties of metals and alloys were first discovered in the last century. A short summary of the effects of hydrogen in non-ferrous metals has been given by Hardie[1]; although the effects may be beneficial, they are much more often deleterious. It is therefore important to be able to establish accurately the hydrogen contents of metals at low levels.

Depending on the various steps of the manufacturing process, hydrogen may be present in solid metals as a solution, as the hydride, as elemental hydrogen in voids, or as water in voids. Provided that it is thermodynamically unstable towards the metal, water is converted to the metal oxide and to some of the other forms, if the metal is submitted to sufficiently high temperatures; water may be considered stable when the metal has easily reducible oxides.

Eborall[2] has given an excellent critical review of the methods used, and of the problems met, in determining hydrogen in various metals. The most frequently used methods are those based on classical vacuum or inert gas fusion, on tin fusion, and on hot extraction from the solid samples. According to Eborall, the relatively low temperatures employed in the hot extraction are often sufficient to release hydrogen from sources other than water* because these forms are readily decomposed and hydrogen diffuses quite rapidly through solid metals. But in the case of copper and its alloys, Eborall emphasizes that it is necessary, at least in the case of materials that have not been strongly reduced, to melt the samples in order to be sure of recovering all the hydrogen which may be present in the solid as stable, non-diffusing steam. Because of the difficulties generally associated with measuring evolved water vapour as such (adsorption on the walls of the apparatus, *etc.*), the final measurement must be made on gaseous hydrogen[2]. Eborall quotes some work by Sloman[3] which showed that after vacuum fusion of copper "the reaction with carbon converts the steam to hydrogen and no difficulties arise".

The following considerations contradict such a statement; they apply, unless specified, to vacuum or inert gas fusion in its simplest form, *viz.* in a graphite crucible without a bath; where statements involving reactions are made, the standard free energies of reaction used to validate them on a thermodynamical basis have been taken from the books of Kubaschewski and Evans[4] and of

* Water may be included if it is converted to other forms as described above.

Turovtseva and Kunin[5]. Molten copper dissolves only a few p.p.m. of carbon[6,7], whereas it may contain quite large amounts of oxygen in a dissolved or combined form[6]. Thus, because hydrogen easily reduces oxygen-bearing copper, it seems probable that not only the steam already present but also any hydrogen in the sample will eventually be evolved as water vapour from the melt. Depending on the contact time, the temperature, and the surface area and volume of the graphite crucible, *i.e.* the environmental conditions, and on the instrument chosen, any steam will subsequently revert more or less to hydrogen and carbon monoxide by reaction with the walls of the crucible.

Because most of the available instruments (including those used in present work) can measure hydrogen only when present in the elemental form, it is necessary to push the re-conversion of steam to hydrogen as near to 100% as possible. Various means to this end appear to exist, *e.g.* the use of high temperatures together with lidded crucibles of large inner surface area, baths containing an adequate amount of dissolved carbon, sample-containing graphite capsules to be dropped into the main crucible, and some means of recirculating the evolved gases over the hot crucible. However, in determining hydrogen in metals, the problem does not lie in its extraction, but in maintaining the errors at a low level, especially where, as in copper, the content is low; thus the total blank of the method and volatilization of the sample and of any bath material must be minimized[2]. On this basis, the above-mentioned methods appear either to be impractical, insofar as they require extensive modification of an existing apparatus, or they do not meet the desiderata for minimizing errors.

From thermodynamic considerations, the tin fusion procedure (which is free from the errors cited) would not seem to be able to solve the problem, as tin does not dissolve carbon to a great extent, and steam in contact with it at the temperatures used is far from being completely reconverted to hydrogen.

The simplest method of overcoming all these difficulties seems to be the use of an aluminium bath in which to drop the samples. Aluminium has some properties which make it unique; it has a relatively low melting point (659°C); its low density (2.7 g cm^{-3}) renders the penetration of the samples into the melt easy; it dissolves, in the liquid state, a considerable percentage of copper[6] (about 70% at 800°C). It does not dissolve carbon to a great extent[6], but its affinity for oxygen is so high that any water evolved from copper would be reconverted to aluminium oxide and to measurable hydrogen. In addition to this, prior experience suggested that its use in a graphite crucible up to a temperature of the order of 800°C is safe, and that under these conditions it does not volatilize even in a vacuum of 10^{-5}–10^{-6} mm Hg. At a temperature of 800°C, there is no adhesion between the aluminium and the crucible, so that the crucible can be recovered intact; at about 1000°C or higher, aluminium forms Al_4C_3 in a relatively short time, thus destroying the crucible.

These characteristics make aluminium an ideal bath for hydrogen determinations, and it is rather surprising that there appears to be no mention of it in the available literature, as it could be used in principle where troubles similar to those given by copper are expected, *i.e.* in the case of metals with easily reducible oxides.

Apart from problems of volatilization, the only condition to be fulfilled is

that at the lowest useful working temperature, the metal must dissolve in the bath or, if insoluble, must sink in the liquid state in the aluminium. Thus, it is possible to devise methods involving its application to metals of the copper subgroup, of the iron and platinum groups, and to indium, germanium and tin. The use of an inert-gas fusion apparatus, in which the presence of the carrier gas greatly depresses volatilization phenomena, should allow the application of aluminium baths to the analysis of thallium, lead, antimony and bismuth.

EXPERIMENTAL

Two commercial vacuum-fusion instruments were employed: the Feichtinger StRe 0583 (H. Feichtinger, Schaffhausen, Switzerland)[8] and the Heraeus VH6 (W. C. Heraeus GmbH, Hanau/Main, Germany)[9]. Both the instruments accommodate the analysed samples in graphite crucibles without lids, and for the determination of the extracted gases, both use gas chromatographs (argon carrier gas, molecular sieve column, thermal conductivity detection), which are calibrated by the injection of known amounts of hydrogen, nitrogen and carbon monoxide.

Whilst the Feichtinger instrument is currently used in this laboratory as purchased, the Heraeus instrument has been modified during the course of time: its gas chromatograph is now replaced by a home-made chromatograph with a thermistor detector giving a greatly increased linearity of response; fixed and known amounts of calibration gases are delivered by means of a system of magnetic valves. These modifications result in an overall increase in precision and accuracy.

The Feichtinger instrument was used only for comparison experiments of vacuum fusion without a bath at about 1150°C, as this could not be done on the Heraeus instrument, probably because of the different geometry and construction materials of the furnaces, the different type of heating, *etc.* The evaporation of copper at 1150°C caused, in the Heraeus instrument, the evolution of rather high and variable quantities of spurious hydrogen which prevented accurate and precise measurements on the samples.

The modified Heraeus instrument was employed for all other experiments of hot extraction and of vacuum fusion with tin and, especially, with the aluminium bath. The working temperatures, which will be indicated later, were such as to give no visible evaporation of materials, thus ensuring fairly low and constant hydrogen blanks. The small standard graphite crucible of the instrument was replaced with another of 26 mm internal diameter and 32 mm internal height, as the use of a crucible with a large cross-section allows, with the bath, a quick immersion of the samples by decreasing the possibility of collisions with the crucible walls.

The height of the aluminium baths tested ranged from 10 to 20 mm, and the highest concentration of copper was about 40% weight. No differences in the results or problems were observed in these ranges. For the tin bath a height of 10–12 mm was used and the highest copper concentration was much lower than that possible with aluminium.

For vacuum fusion without a bath and for hot extraction, the empty crucible was degassed at a temperature of the order of 1500°C, and the analyses were begun when the blank at the working temperature was low and constant. For vacuum fusion, the apparatus was preconditioned with 1–2 g of copper.

For vacuum fusion with a tin or aluminium bath, the crucible (if recovered from prior analyses) was charged directly with the necessary quantity of bath-metal and degassed for 2–3 h at the working temperature until a low and constant blank was reached. Before charging, a new crucible was previously degassed empty at about 1500–1600°C in order to expel the major part of the gases it contained, these were only slightly readsorbed on subsequent exposition to the atmosphere.

After preparation, the samples, weighing 0.5–1 g, were stored in the sample holder of the appropriate instrument at the same high vacuum as the furnace, and left there until the analyses were begun.

Whichever method was used, the sample degassing time was found to be less than 10 min, but was in general kept at 15 min in order to have a good safety margin. The blanks were then found to be practically constant, and only a very slight decrease with time was occasionally noticed.

RESULTS AND DISCUSSION

Table I presents the results obtained on copper samples from various origins, and on other materials which, although not fully investigated, were analysed in order to show the potentiality of the aluminium bath method; the results are expressed in p.p.m. hydrogen. The samples were obtained from small bars of different origin (Cu 1, 2 and 4), tube 1 mm thick (Cu 3), sheet 1 mm thick (Ni) and foil 0,03 mm thick (Pt). All were shown to contain oxygen (from 50 to 200 p.p.m. for copper, about 1200 p.p.m. for nickel and about 30 p.p.m. for platinum). As the Table shows, the results obtained with the aluminium bath are the highest, which seems to prove its superiority, and to confirm the speculations in the introductory paragraphs about the possibility of hydrogen being lost as water which cannot be measured. In order to check the blanks, and the satisfactory working of the instruments, zirconium hydride was analysed under the same operating conditions at the end of some series of vacuum fusion runs without a bath and with the aluminium bath. The powder samples (0.1–0.2 mg) were enclosed in light platinum containers. Within experimental error, quantitative recoveries of hydrogen were achieved, thus confirming proper functioning of the procedure.

Some comments on the sample preparation and on the results obtained with the aluminium bath method are needed. Sample Cu 4 was analysed both after cutting with pincers to appropriate dimensions and solvent cleaning, and after cutting, careful filing on all sides and solvent cleaning. The differences in the results found reflected the different conditions of the sample surface, which, in an unfiled sample, may contain water adsorbed in the oxide–carbonate surface layers. Accordingly, bulk hydrogen should always be determined on filed samples. All other samples were analysed after cutting and solvent cleaning only. In all cases, great care was taken during and after the preparation to avoid handling the samples with the fingers. Among the copper samples, Cu 1 and Cu 2 were not filed but showed a good bright pink surface; accordingly, they gave results of good precision, which compared well with those given by filed samples of Cu 4. The scattered results for the other samples (including nickel and platinum) were

TABLE I

ANALYTICAL RESULTS BY DIFFERENT METHODS

Sample	Feichtinger	Heraeus		
	Vacuum fusion without bath (~1150°C)	*Hot extraction (Cu ~900°C; Pt, Ni ~1150°C)*	*Vacuum fusion Sn bath (~800°C)*	*Vacuum fusion Al bath (~800°C)*
Cu 1	0.29 0.37 0.55 Av. 0.47 0.66			0.99 1.03 0.85 0.78 Av 0.89 0.88 *s* 0.095 0.87 s_r 10.7% 0.94 0.76
Cu 2	0.41 0.35 0.35 Av. 0.37 0.37			0.81 0.85 Av. 0.85 0.88
Cu 3	1.30 0.87 Av. 1.08			3.02 3.02 2.89 Av. 2.89 2.62
Cu 4	0.27 0.60 0.54 Av. 0.57 0.89			0.80 1.62 0.72 Av. 1.04 1.31 0.75
Cu 4 (filed)	0.19 0.21 0.44 Av. 0.28 0.27	<0.05 <0.05 <0.05 Av. <0.05 <0.05	0.24 0.16 0.15 Av. 0.17 0.15	0.53 0.40 0.42 Av. 0.47 0.42 *s* 0.064 0.53 s_r 13.6% 0.44 0.44 0.55
Ni		1.45 1.21 Av. 1.33	0.13 0.20 Av. 0.16	1.20 1.51 2.50 Av. 1.76 1.85
Pt		0.79 0.77 Av. 0.78	0.48 0.63 Av. 0.55	1.87 1.18 0.91 Av. 1.23 0.98

probably due to inhomogeneous surfaces.

Some tests were made in order to verify whether or not the conversion by aluminium of water to hydrogen was complete. Calcium hydroxide (0.1–0.2 mg) was analysed, after having been sealed in heavy copper containers so that it could be

rapidly submerged in the bath. Unfortunately, the gas evolution was so rapid, and violent, forming large gas bubbles, that only in a limited number of tests could a quantitative recovery of hydrogen be achieved. It is nevertheless thought that in the case of real samples, the conversion is complete, because the gas evolution is very smooth and without visible gas bubbles.

The limit of detection of the aluminium bath method is good. Under the working conditions described, the low constant hydrogen blank (about 0.2 μg of hydrogen in 15 min) coupled with the inherent high sensitivity of gas chromatography, allows the detection of 0.05 p.p.m. hydrogen on samples weighing 1 g.

SUMMARY

Conventional methods (hot extraction, tin fusion, vacuum fusion, inert gas fusion) for the determination of the hydrogen content of copper and of metals or alloys bearing easily reducible oxides, are often rather inaccurate. At the relatively low temperature which is essential to minimize total blanks (and therefore errors), not only hydrogen but also water vapour is evolved; the latter is not measured when gas chromatography is used to determine hydrogen, and is lost by adsorption in other techniques. These problems are overcome by the use of a vacuum fusion procedure with an aluminium bath. The affinity of aluminium for oxygen is so high that any water formed after sample dissolution is converted to measurable hydrogen. The method allows detection of 0.05 p.p.m. hydrogen on 1-g samples.

REFERENCES

1 D. Hardie, *J. Inst. Metals*, 95 (1967) 188.
2 R. Eborall, *Spec. Rep. no. 68*, The Iron and Steel Institute, (1960), p. 192.
3 H. A. Sloman, *J. Inst. Metals*, 71 (1945) 391.
4 O. Kubaschewski and E. Ll. Evans, *Metallurgical Thermochemistry*, Pergamon, Oxford, 1958.
5 Z. M. Turovtseva and L. L. Kunin, *Analysis of Gases in Metals*, Consultants Bureau, 1961.
6 M. Hansen, *Constitution of Binary Alloys*, McGraw-Hill, 2nd edn., 1958.
7 P. E. Rodney, *Constitution of Binary Alloys, First Supplement*, McGraw-Hill, 1965.
8 H. Feichtinger, H. Bächtold and W. Schuhknecht, *Schweiz. Arch.*, 12 (1959) 426.
9 R. Lesser and H. Gruber, *Z. Metallk.*, 51 (1960) 495.

Analytica Chimica Acta, 72 (1974) 407–413

DETERMINATION OF RIBOFLAVIN IN PHARMACEUTICAL PRODUCTS BY AUTOMATIC DISCRETE-SAMPLE ANALYSIS

J. RAMÍREZ-MUÑOZ
Beckman Instruments, Inc., Irvine, California 92664 (U.S.A.)
(Received 2 April 1974)

Riboflavin (vitamin B_2) is commonly determined manually by procedures described in the U.S. Pharmacopeia XVIII[1] and National Formulary XIII[2] which include final fluorimetric measurements of riboflavin.

Riboflavin is found either as the single active component of riboflavin tablets or as one of many active ingredients in polyvitamin oral dosages. The determination of riboflavin has been tested by means of a newly developed automatic analyzer working in the discrete-sample mode[3]. Instrumentation, operating conditions, final procedure and analytical results, as well as details on analytical methodology are discussed in this paper.

Methodology

Riboflavin can be determined in different ways: fluorimetric analysis (by means of the typical yellowish green fluorescence of riboflavin), polarographic analysis, spectrophotometric analysis (by using the yellow color of the compound), and by converting the riboflavin to lumiflavine (a method of high selectivity), which in turn can be determined by spectrophotometry or fluorimetry; this last method requires a number of rather involved operating steps. Direct spectrophotometric determination may be used when riboflavin is the only active compound in the preparation and the matrix produces no interference in the measurement of the yellow color of prepared solutions. A discussion of this and other methods has been given by Strohecker and Henning[4].

In the work described here, special attention is given to the fluorimetric determination of riboflavin, since this analytical method is more sensitive and suitable for application to manufactured and natural products. Three factors are critical in the determination of riboflavin: (a) sensitivity of riboflavin to light, (b) effect of temperature, which increases the rate of decomposition by light, and (c) influence of pH on the fluorescence intensity.

In manual operation, even if the operator takes extreme precautions and tries to standardize temperature, exposure to light and timing, it is difficult to achieve high accuracy and repeatability. However, with automatic operation, conditions are more easily standardized and repeated, with consequent improvements in accuracy and repeatability. This has been checked many times during the development of the automatic unit by comparing the accuracy and precision achieved by the same operator manually and by automatic techniques.

Since solutions in the automatic instrument are contained in plastic tubes

and containers with small orifices, the exposure of prepared solutions to light is minimal. Furthermore, any exposure to light is equal for all containers, and, consequently, for all solutions (standards, blanks and samples).

The heating of the solvent used in the automatic disruption is uniform for all treated samples, and cooling by dilution and time always follows the same schedule.

Automatic disruption successfully replaces manual operations such as the lengthy heating and constant shaking or stirring recommended to dissolve oral dosages. Automatic disruption in the presence of heated solvent reduces the disruption and dissolution process to only 1 min.

The intensity of fluorescence is a function of the concentration of the analyte and pH of the medium; a maximum is achieved between pH 6 and 7. Ohnesorge and Rogers[5] have mentioned the possibility of measuring riboflavin fluorescence at 530 nm with solutions adjusted to pH 7. Fluorescence shows less dependence on pH between 3 and 5. Fluorescence decays in the alkaline region, so that highly alkaline solutions should be avoided.

Good measuring conditions are achieved[2] when the sample is excited with 440-nm radiation, and the fluorescence is measured at about 565 nm. These conditions were therefore used here.

Spurious fluorescence may arise from sample components other than riboflavin. Therefore, the fluorescence arising from riboflavin should be eliminated, and the solutions read again. Fluorescence of riboflavin can be eliminated by transformation of riboflavin to non-fluorescent leucoflavine by treatment of solutions with sodium dithionite ($Na_2S_2O_4$). Treated samples are then read as individual blank solutions, and the relative net fluorescence is calculated by the difference between the two readings. Quenching by the reducing action of sodium dithionite may also affect other fluorescent components, which may be a source of individual blank distortion. Use of standard addition may help in such a case to establish the quenching effect on riboflavin in the presence of other fluorescent components, without the need of chromatographic separations or use of ion-exchange resins.

EXPERIMENTAL

Instrumentation

A Beckman Automated Materials Analyzer (AMA-40) equipped with a Ratio Fluorimeter, recorder, and teletype (via an intercoupler) as printer and tape puncher, was used.

Reagents

Solvent. 0.1 *M* hydrochloric acid was used as solvent for the tablet disruption.

Buffer solution, pH 7.9. 15.73 g of K_2HPO_4 and 0.523 g of KH_2PO_4 were dissolved in 800 ml of deionized–distilled water. The solution was adjusted to pH 7.9 with concentrated phosphoric acid, and diluted to 1 l with deionized–distilled water.

Sodium dithionite solution, 10%. 50.00 g of $Na_2S_2O_4$ were dissolved in 400 ml of deionized–distilled water and then diluted to 500 ml with the same solvent.

Diluent solution. Deionized–distilled water was used.

Operating conditions

Operating conditions are summarized in Table I.

Procedure

The procedure for the AMA-40 System is summarized in Figs. 1 and 2 corresponding respectively to the first and second experimental runs.

TABLE I

OPERATING CONDITIONS FOR RIBOFLAVIN

	First run	*Second run*
Disruption	Yes	No
Disruption speed	Position 20	Off
Disruption time	60 s	60 s
Incubation	No	No
Filter tubes	Yes	No
Filter vacuum	15 in	No
Operation	Auto	Auto
Analysis rate	Ca 40/h	Ca 40/h
Fluorimeter operation		As in first run
Attenuator	Out	
Filters:		
primary	Wratten 47B (or Corning 4-70)	
secondary	Corning 3-68 (or Corning 3-67)	
Sleeve	450 (or Hg)	
Zero adjustment	Adjusted	
100% adjustment	Minimum (no expansion)	
Bar	No. 4 (or no. 5)	
Sample volume	5 ml	5 ml
Recorder chart speed	5 in min^{-1}	5 in min^{-1}
Recorder span setting	100 mV	100 mV
Solvent pump	100 ml 0.1 *M* HCl (at 90°C)	Off
Sample vacuum	15 in	15 in
Sequence	3 Blanks, 4 standards, 30 samples, 3 blanks, standards in reference tubes	As in first run

Data evaluation

Data included here were evaluated by computer techniques. Numerical data collected on punched tape were processed by means of a time-shared terminal (IBM 360 System).

RESULTS

Repeatability

Tests with low numbers of repeated readings, as typically done when including in series duplicate or triplicate samples, were acceptable, as shown in Table II.

Linearity

Linearity of response was found with net fluorimeter readings, as shown in Fig. 3, over the riboflavin range 0–25 $\mu g\ ml^{-1}$.

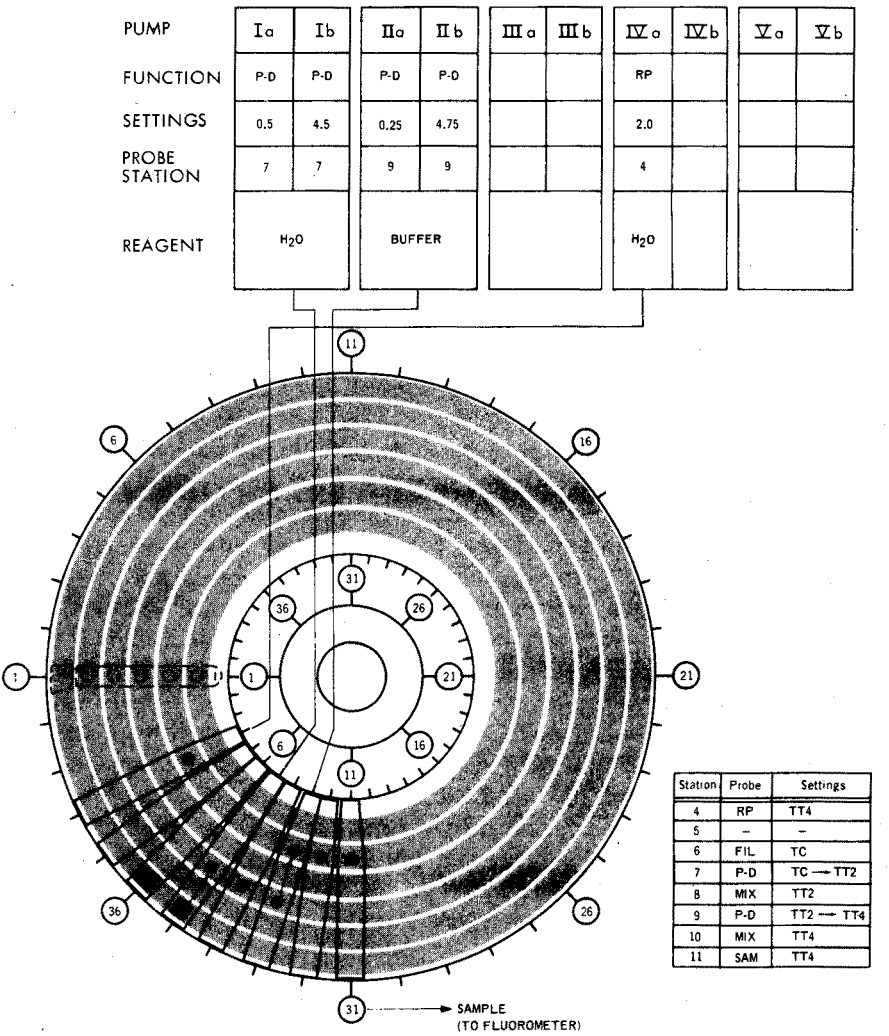

Station	Probe	Settings
4	RP	TT4
5	–	–
6	FIL	TC
7	P-D	TC → TT2
8	MIX	TT2
9	P-D	TT2 → TT4
10	MIX	TT4
11	SAM	TT4

Fig. 1. Set-up diagram for riboflavin determinations (1st run). P-D = pipetter–diluter, RP = reagent pump, SAM = sample probe, FIL = filter, MIX = mixer, TC = T-cup, TT = T-tube.

Tablet analysis

Tablets of different brands were assayed. A few results are summarized in Table III.

DISCUSSION

The automatic procedure described seems to be appropriate for the determination of riboflavin in single-component and multicomponent tablets.

The procedure described includes two consecutive runs: (a) measurement of total fluorescence, and (b) measurement of residual fluorescence after addition of sodium dithionite. Determinations may also be done in a single run: two sub-

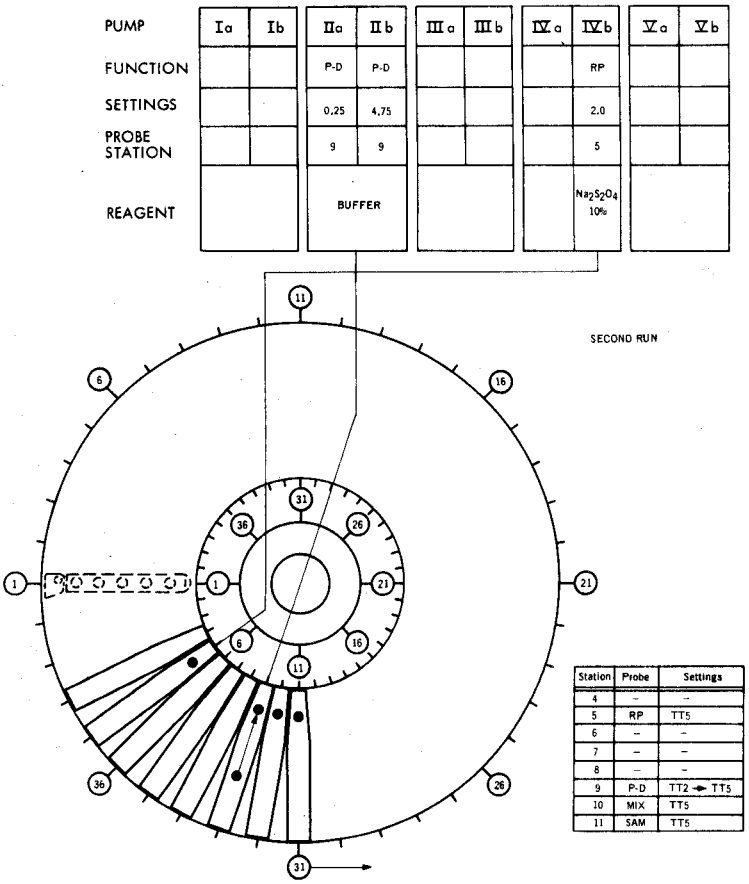

Fig. 2. Set-up diagram for riboflavin determinations (2nd run). Abbreviations as for Fig. 1. Arrow at station 31: sample to fluorometer.

TABLE II

REPEATABILITY FOR RIBOFLAVIN

Solutions tested	*Number of readings*	*Average*[a] *(Net readings)*	$s^{a,b}$	s_r
Standards	2	41.5	1.06	2.56
Pooled samples	3	45.9	2.27	4.97
Pooled samples	2	36.6	1.63	4.45
Pooled samples	2	11.2	0.85	7.58
Pooled samples	3	50.8	2.40	4.72
Pooled samples	3	18.0	0.30	1.67
Standards	10	47.2	0.37	0.77
Standards	10	47.1	0.29	0.61
Standards	10	47.2	0.21	0.44
Standards	10	47.4	0.53	1.11

[a] Readings in scale divisions.
[b] s = Standard deviation; s_r = relative standard deviation.

TABLE III

RESULTS OF DETERMINATIONS OF RIBOFLAVIN IN PHARMACEUTICAL DOSAGES

Type of dosage	*Content (mg)*		*Potency (%)*	
	Label	*Found*	*Calculated*	*Average*
Riboflavin tablets	25.0	26.1	104.2	
		28.3	113.2	110.5
		28.5	114.2	
Multivitamin tablets	25.0	21.3	85.4	88.1
		22.7	90.8	
Multivitamin tablets	10.0	10.7	106.8	
		11.1	111.0	108.8
		10.9	108.5	

```
LINEAR FIT.  SLOPE =        1.826237

PAIR    X VALUES    Y VALUES    Y CALCD.   DIFFERENCE     % ERROR

   1      5.5500     10.0000     10.1356      0.1356      1.3561
   2     10.0000     17.3000     18.2624      0.9624      5.5628
   3     13.6000     25.0000     24.8368     -0.1632     -0.6528
   4     16.7000     30.6000     30.4981     -0.1019     -0.3329
   5     19.2000     35.4000     35.0637     -0.3363     -0.9499


QUADRATIC FIT.  COEFFICIENTS:

T1 =        1.716105

T2 =        0.006879

PAIR    X VALUES    Y VALUES    Y CALCD.   DIFFERENCE     % ERROR

   1      5.5500     10.0000      9.7363     -0.2637     -2.6373
   2     10.0000     17.3000     17.8490      0.5490      3.1731
   3     13.6000     25.0000     24.6114     -0.3886     -1.5545
   4     16.7000     30.6000     30.5775     -0.0226     -0.0737
   5     19.2000     35.4000     35.4851      0.0851      0.2404
```

Fig. 3. Computer linearity data for riboflavin. In spite of the fact that differences found for TI are higher than 5%, errors in both fittings do not differ drastically; this effect may be due to the scattering of experimental points. The final computer output illustrating the linearity of the plot is not shown.

samples of each sample (diluted test solutions) are transferred to different positions of T-tubes in the chemical table and only one of them receives sodium dithionite. Both of them are aspirated at the same time (dual sampling probe) and transferred simultaneously to two flow cells. Readings are then related. The procedure described in this paper requires more total working time, but simpler equipment. In the double-run mode, the instrument can analyze 30 tablets with necessary blanks and standards in about 2 h (double reading required for each tablet, at the rate of about 40 readings/h).

The use of hot acid solvent for disruption (solvent heated at 90°C) was successful for disruption and dissolution in all the experimental tests.

No decomposition of riboflavin by light was observed in this work by automatic schedule, where light exposure was minimal; light conditions, temperature changes and timing can be perfectly standardized to be equal for all solutions processed.

The automatic procedure discussed is suitable for the routine quality control analysis (content uniformity and assay) of riboflavin in pharmaceutical dosages.

SUMMARY

The fluorimetric determination of riboflavin by an automated procedure is described. The procedure allows up to thirty samples plus standards and blanks to be analysed in each run. After measurement, sodium dithionite treatment is used to eliminate the riboflavin fluorescence, and a second reading makes it possible to calculate net fluorescence values which can be related with concentration of riboflavin in the original samples. Linear response to riboflavin is obtained over the range 0–25 $\mu g\ ml^{-1}$. Repeatability is satisfactory for content uniformity and assay tests of riboflavin in oral pharmaceutical dosages.

REFERENCES

1 *U.S. Pharmacopeia XVIII*, U.S. Pharmacopeia Convention, Inc., Bethesda, Maryland, 1970.
2 *National Formulary XIII*, American Pharmaceutical Association, Washington, D.C., 1970.
3 D. G. Rohrbaugh and J. Ramírez-Muñoz, *Anal. Chim. Acta*, 71 (1974) 311; J. Ramírez-Muñoz, *AMA-40 Chemical Operations Manual, Industrial Technical Report TR-581*, Beckman Instruments, Inc., 1973.
4 R. Strohecker and H. M. Henning, *Vitamin Assay. Tested methods*, Verlag Chemie GmbH, Weinheim/Bergstr., 1966.
5 W. E. Ohnesorge, and L. B. Rogers, *Anal. Chem.*, 28 (1956) 1017.

Analytica Chimica Acta, 72 (1974) 414–418

SHORT COMMUNICATION

The application of peak integration in flameless atomic-absorption spectrometry

P. SCHRAMEL

Gesellschaft für Strahlen- und Umweltforschung mbH., 8042-Neuherberg-München (German Federal Republic)

(Received 11th March 1974)

Detailed investigations of applicability of flameless atomic-absorption spectrometry for the determination of trace elements in biological materials have shown that the precision of the method is mostly very good but the accuracy often leaves much to be desired. Particularly the so-called matrix effects, which cause variation of the height of the absorption signals, have complicated the application of flameless atomic-absorption spectrometry in some routine measurements.

Careful investigations in the present work about the curve form of the recorded absorption signals have led to the conclusion that the method of utilizing peak height for evaluation is inadequate. Integration of the output signal which is normally connected to a recorder, makes it easy to determine the area of the absorption signal. This was done for the elements Al, Cd, Cr, Cu, Fe, Mn and Pb. The two evaluation methods—peak height and integration—were compared for calibration curves and for some practical biological samples.

Experimental

Instrumentation. The instruments used were a double-beam Perkin-Elmer Model 403 spectrometer, a graphite furnace Model HGA-72, a laboratory recorder, and a Perkin-Elmer peak integrator Model PSP-1. This integrator is normally used for the evaluation of signals from gas chromatographs, but is easily adapted for the absorbance signals of an atomic-absorption spectrometer. The spectrometer had a deuterium-arc background corrector. The special Perkin-Elmer graphite tubes were used, because the reproducibility was better than with normal tubes, although the sensitivity was somewhat poorer because of the smaller atom concentration caused by the larger cross-section of these tubes. But there were no differences in the shapes of the calibration curves with these two different tubes.

Preparation of standard solutions. Stock standard solutions of all the elements investigated were prepared, mostly in concentrations of about 1 mg ml^{-1}, which solutions can be stored for a reasonable time without adsorption effects. For work with the graphite furnace, standard solutions were prepared in suitable ranges, mostly between 0.1 ng and 10 ng per 10 μl in aqueous solution. Concentrated sulphuric acid (100 μl) was added to 10 ml of solution, because all

practical samples were wet-ashed in this matrix. This procedure and the temperature programme applied for the various elements has been described earlier[1].

Results

All calibration curves (Figs. 1–7) were obtained with 10-μl amounts of the standard solutions. In each case, curves for both peak height and peak area are drawn. The curves were obtained by least-squares approximation from the measured points, the evaluation being done on a HP-9820 A desk computer connected to a plotter. The effect of the absolute sample quantity on the absorb-

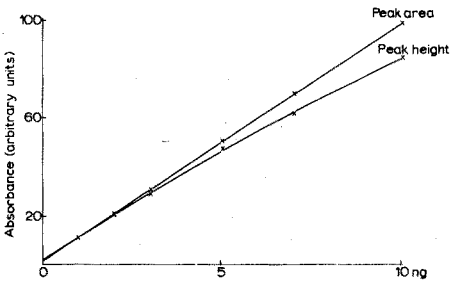

Fig. 1. Calibration curves for aluminium.

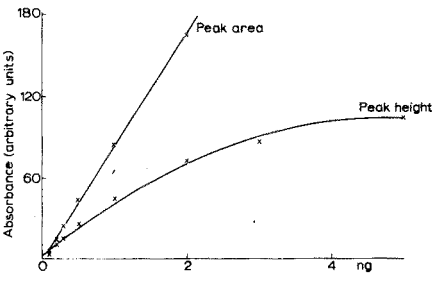

Fig. 2. Calibration curves for cadmium.

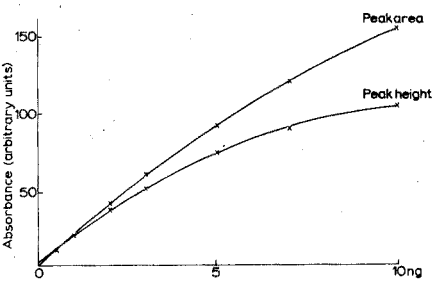

Fig. 3. Calibration curves for chromium.

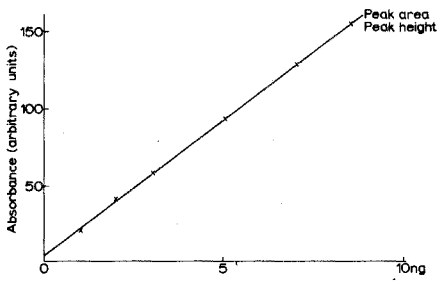

Fig. 4. Calibration curve for copper.

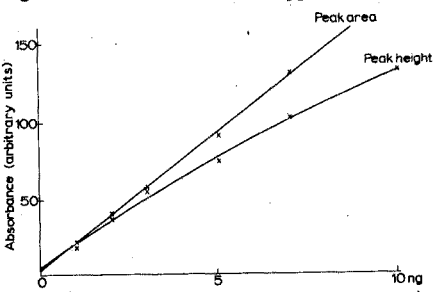

Fig. 5. Calibration curves for iron.

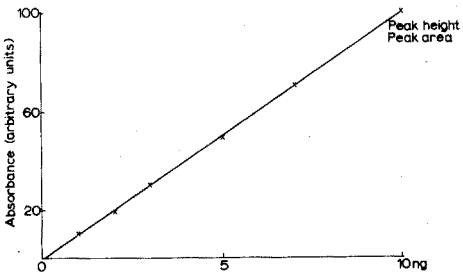

Fig. 6. Calibration curve for manganese.

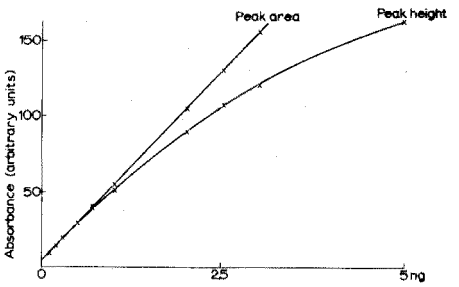

Fig. 7. Calibration curves for lead.

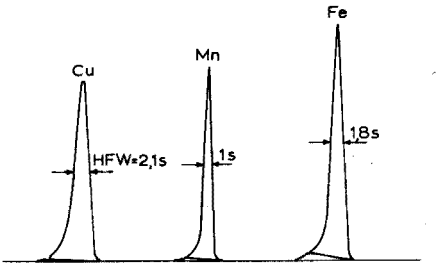

Fig. 8. Absorbance peaks for copper (7 ng), manganese (2 ng) and iron (7 ng).

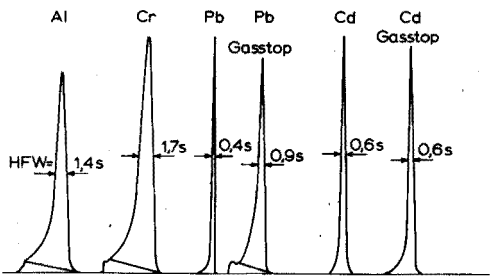

Fig. 9. Absorbance peaks for aluminium (5 ng), chromium (3 ng), lead (5 ng and 1 ng), and cadmium (0.5 ng and 0.1 ng).

ance signal was also tested. The signal for a certain amount of one element was obtained by pipetting 10 μl of a solution of a particular concentration, and then signals for the same quantity were obtained by pipetting appropriate volumes of less concentrated solutions. No differences in the signals were detected, hence no curves are drawn.

For the elements investigated here, the calibration curves obtained from the integrated values are usually linear over greater ranges than those from the peak-height values. Thus it appears peak-height detection is often inadequate for describing the absorbance signals from the graphite furnace. When the absorbance peaks are detected by a recorder with a chart speed of 240 mm min^{-1}, there are big differences in the peak shapes of the various elements, as shown in Figs. 8 and 9. The halfwidths of these signals varied between 0.4 s and 2.1 s for the pure element standards. Moreover, the reproducibility of the integration measurements is better than that of peak-height detection. Table I shows some results for copper as an example.

The halfwidth of the signal depends not only on the number of atoms in the sample but also on the matrix, as is shown in Figs. 10 and 11 for aluminium. There can be large differences between the results by the two evaluation methods as shown in Fig. 12. Clearly, the signal width depends on the absolute number of atoms and on the matrix. A planimetrical evaluation of the peaks confirms these results. In spite of equal peak heights, there can be large differences in the peak areas, as shown in Figs. 10 and 11. An example of a so-called matrix

TABLE I

COMPARISON OF THE REPRODUCIBILITY FOR COPPER

	Peak height (arb. units)	*Peak area (arb. units)*
Mean value (5 detns.)	61.2	11770
s_r	± 4.7%	±1.4%

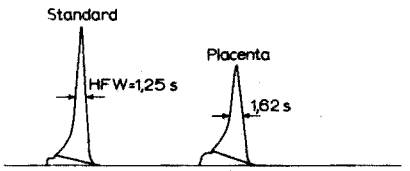

Fig. 10. Comparison of peak-height and peak-area detection for aluminium. Chart speed 240 mm min^{-1}. The results (in arbitrary units) are:

	0.7 ng (Standard soln.)	*Placenta*	
Peak height (A)	29.5	21	$R_1\ (A_s/A_p) = 1.4$
Peak area (B)	4985	4751	$R_2\ (B_s/B_p) = 1.05$
Planimetrical area (C)	40	38	$R_3\ (C_s/C_p) = 1.05$

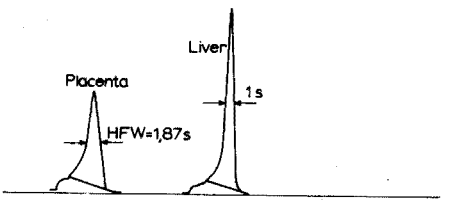

Fig. 11. Aluminium absorbance peaks for two different tissues. Chart speed 240 mm min^{-1}. The results are:

	Placenta tissue	*Liver tissue*	
Peak height (A)	21	39	$R_1\ (A_L/A_p) = 1.85$
Peak area (B)	4751	6256	$R_2\ (B_L/B_p) = 1.31$
Planimetrical area (C)	43	56	$R_3\ (C_L/C_p) = 1.30$

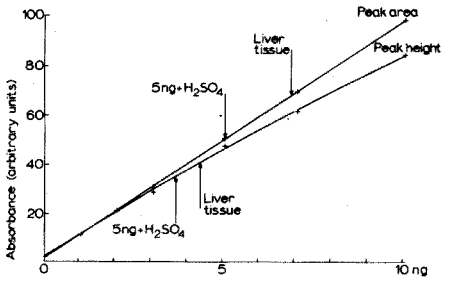

Fig. 12. Examples for the evaluation of some practical samples (aluminium).

effect is also shown in Fig. 12. A large difference exists between the peak heights of an aqueous standard aluminium solution (5 ng/10 μl) and a solution with concentrated sulphuric acid added in an mount of 100 μl/10 ml. But the peak areas are equal, so that the matrix effect in the case of integration disappears, and only the width of the signal increases.

Discussion

The results presented show that the peak-height method of evaluating absorbance signals in flameless work can lead—at least for the elements investigated—to inaccurate results. Integration of the signals leads to much better and more reproducible results. Not the peak height but the peak area is the correct measurement. Differences can exist in the length of an absorbance signal, especially for higher concentrations, so that the calibration curves are linear over a wide range of concentrations for peak-area detection. Some of the so-called matrix effects described in many papers (*e.g.* refs. 1, 2) can be attributed to the method of evaluation, as is shown for aluminium in this paper.

As a general rule, the integration method seems to be much more satisfactory in evaluation of flameless absorbance signals.

REFERENCES

1 P. Schramel, *Anal. Chim. Acta*, 67 (1973) 69.
2 L. Ebdon, G. F. Kirkbright and T. S. West, *Anal. Chim. Acta*, 58 (1972) 39.

Analytica Chimica Acta, 72 (1974) 419–422

SHORT COMMUNICATION

Extraction–spectrophotometric determination of silver traces in some thermoelectric materials

V. FANO and L. ZANOTTI
Laboratorio MASPEC del C.N.R., 43100 Parma (Italy)
(Received 25th March 1974)

The presence of silver in thermoelectric materials is particularly important for two reasons: (1) silver is a fundamental component of binary and ternary semiconductors which are used either as single crystals or as thin films; (2) silver is useful as a dopant in order to improve the efficiency of the p-type branch in the lead telluride-type of semiconductors. Because of this, it seemed of interest to develop a method for the determination of silver traces, which would be applicable to many tellurides and selenides with thermoelectric properties. This communication describes simple procedures suitable for binary and ternary semiconductor systems composed of selenium, tellurium, germanium, tin, lead, antimony and bismuth. The proposed method consists of solvent extraction of silver with dithizone in carbon tetrachloride and its subsequent spectrophotometric determination. The extraction procedure requires two delicate steps: the sample dissolution, and the masking of interfering elements.

Sample dissolution

Nitric acid is preferred as a common solvent for antimony, bismuth and lead tellurides and selenides. In fact, a small volume of nitric acid (2–3 ml) is sufficient to dissolve rapidly 0.1 g of finely powdered sample; silver remains in a soluble form, and any insoluble antimony compounds, precipitated during the sample dissolution process, are easily dissolved by adding ammonium citrate solution.

A similar treatment with nitric acid is not sufficient to dissolve germanium telluride and selenide samples, and halogen acids must be avoided because they could interfere in the final analysis. Mixtures of nitric and sulfuric acid are not appropriate, owing to the length of time required for an entire sample dissolution. A mixture of nitric acid and sodium oxalate proved to be the most suitable solvent for germanium compounds; germanium oxalate complexes[1] are very soluble in acidic medium. A (1+2) mixture of concentrated nitric acid and 10% sodium oxalate solution (10 ml) is enough to dissolve 0.1 g of sample in 10 min. Excessive heating must be avoided, because too much of the oxalate would be destroyed and germanium dioxide might precipitate.

Since halogen acids must not be used, dissolution of $Pb_xSn_{1-x}Te$ samples is best obtained with sulfuric acid. The addition of hydrogen peroxide greatly

facilitates the sample dissolution and reduces the volume of sulfuric acid required; 10 ml of a (1 + 1) 120-vol. hydrogen peroxide–concentrated sulfuric acid mixture was enough to dissolve a sample of 0.1 g in about 30 min at 70–80°C. The lead sulfate precipitate which appears when the sulfuric solution is diluted can be easily dissolved by an addition of ammonium citrate and ammonia solution.

In each of these dissolution procedures, great care is necessary in heating to avoid complete evaporation of the solution, otherwise difficultly soluble precipitates may be formed.

Masking

Extraction of silver dithizonate in highly acidic solutions is reasonably selective[2], but under these conditions tellurium[3,4] and selenium[5–8] react with dithizone and can interfere with the final spectrophotometric determination. In fact, the measured absorbances of blank solutions at 462 nm were high and irreproducible. At higher pH values, the interferences of tellurium and selenium decrease; at pH 4–5, no interference from tellurium and selenium was spectrophotometrically detectable in an ammonium citrate medium. Moreover, ammonium citrate was useful in preventing any precipitate formation of tellurium, antimony or bismuth salts. Citrate does not interfere with the extraction of silver dithizonate. However, in this medium the silver extraction is not selective and an appropriate amount of EDTA solution is necessary to prevent interferences from fundamental components and other possible impurities[2]. Under these conditions, only mercury[2] can interfere in silver extraction, but mercury is rarely present in the examined materials.

Experimental

Apparatus and reagents. Pear-shaped separatory funnels with Teflon stopcocks were used for extraction. Absorbances were measured with a Beckman model DU2 spectrophotometer with glass cells having a path length of 10 mm. A Sargent-Welch NX pH meter was used.

Antimony, bismuth, lead, germanium, tin, tellurium and selenium of 99.999% purity were used. All other reagents were of analytical grade.

Silver solution was prepared by dissolving silver nitrate in water. Dithizone was used as a $5.0 \cdot 10^{-5}$ *M* solution in carbon tetrachloride.

Ammonium citrate solution was prepared by adding ammonia to a 10% (w/v) solution of citric acid in water, until pH 9 was achieved. This solution was purified by shaking with dithizone. After purification the excess of dithizone dissolved in aqueous solution was back-extracted with carbon tetrachloride. An aqueous 10% (w/v) sodium oxalate solution in water was purified in the same manner. An aqueous EDTA (disodium salt) solution (0.1 *M*) was purified as described by Welcher[9].

The distilled water used was treated with dithizone and stored in quartz vessels over dithizone solution. The inorganic acids used (B.D.H. Aristar) were free of silver and mercury traces, as was shown by blank tests on the procedures involving nitric or sulfuric acid.

General procedure. Crush the sample in an agate mortar until it is reduced to a fine powder, and weigh a suitable amount into a quartz vessel. Add the correct volume of the appropriate solvent mixture (see above) and dissolve the sample by gentle

heating, being careful not to evaporate the solution completely. Then cool and dilute with water. Add 10 ml of 10% (w/v) ammonium citrate solution and 5 ml of 0.1 *M* EDTA solution for each 0.1 g of sample. Adjust the pH of the solution to 4–5 and transfer to a separatory funnel. Extract with a sufficient amount of dithizone solution. Measure the absorbances of the organic phase at 462 and 620 nm, relative to carbon tetrachloride. A reagent blank is carried out throughout the entire analysis.

Results

A silver calibration curve was prepared for the above analytical condi-

TABLE I

SILVER DETERMINATION IN SOME TYPICAL THERMOELECTRIC MATERIALS

Sample	*Ag added (p.p.m.)*	*Ag found (p.p.m.)*	*Standard deviation*
PbTe		1.2	
	1	1.0	0.15
		0.9	
		5.3	
	5	5.1	0.20
		4.9	
		10.4	
	10	9.8	0.30
		10.1	
		20.0	
	20	20.5	0.32
		19.8	
GeTe		0.8	
	1	1.0	0.20
		1.2	
		5.0	
	5	5.2	0.12
		5.2	
		10.0	
	10	10.2	0.26
		10.5	
		19.5	
	20	20.0	0.27
		19.6	
$Pb_xSn_{1-x}Te$		1.0	
	1	0.8	0.17
		1.1	
		5.2	
	5	5.3	0.20
		4.9	
		10.2	
	10	10.5	0.25
		10.0	
		20.0	
	20	20.1	0.06
		20.0	

tions. Beer's Law was obeyed over the range 0–4 μg of silver per ml of carbon tetrachloride. The procedure was checked by adding known amounts of silver nitrate solution to 0.1-g samples of the different powders. The results for different materials are shown in Table I. By using this procedure as little as 1 p.p.m. of silver can be determined with good accuracy. The absorbance of silver dithizonate is calculated from the absorbances of the organic phase and from the absorptivities of dithizone and silver dithizonate at 620 and 462 nm, respectively.

REFERENCES

1 N. H. Furman, *Standard Methods of Chemical Analysis*, Van Nostrand, Princeton, N.J., 1962.
2 J. Stary, *The Solvent Extraction of Metals Chelates*, Pergamon, Oxford, 1964.
3 H. Mabuchi, *Bull. Chem. Soc. Jap.*, 29 (1956) 842.
4 K. Marhenke and E. B. Sandell, *Anal. Chim. Acta*, 38 (1967) 421.
5 H. Mabuchi and H. Nakahara, *Bull. Chem. Soc. Jap.*, 36 (1963) 151.
6 D. P. Shcherbov, A. I. Ivankova and G. P. Gladysheva, *Zavod. Lab.*, 33 (1967) 683.
7 R. S. Ramakrishna and H. M. N. H. Irving, *Anal. Chim. Acta*, 49 (1970) 9.
8 J. Stary, J. Marek, K. Kratzer and F. Sebesta, *Anal. Chim. Acta*, 57 (1971) 393.
9 F. J. Welcher, *The Analytical Uses of Ethylenediaminetetraacetic Acid*, Van Nostrand, Princeton, N.J., 1958.

Analytica Chimica Acta, 72 (1974) 423–425

SHORT COMMUNICATION

A rapid method for the determination of total sulphur in refractory oxides and in steels

H. N. BAJPEI, C. S. P. IYER and M. SANKAR DAS
Analytical Chemistry Division, Bhabha Atomic Research Centre, Trombay, Bombay-400 085 (India)
(Received 18th April 1974)

Analyses for total sulphur in oxides of thorium and zirconium are often required in nuclear technology. The opening up of these samples calls for repeated treatment with acids, or fusion with a large excess of an alkaline flux. The method followed in this laboratory for this determination involves the dissolution of samples with concentrated nitric acid in the presence of a few drops of hydrofluoric acid followed by separation of sulphate on an alumina column; the adsorbed sulphate is later eluted with ammonia solution and determined turbidimetrically or by indirect microtitration of the precipitated lead sulphate with EDTA[1]. In this context, the use of tin(II)–phosphoric acid, reported by Kiba and other Japanese workers[2–5], appeared to be promising. A few preliminary experiments showed that even ignited thorium and zirconium oxides dissolve in this medium within a few minutes of heating. Moreover, in the process of dissolution, all compounds of sulphur are liberated as hydrogen sulphide, thus obviating the need for separation methods. The hydrogen sulphide is determined spectrophotometrically as methylene blue. The method has been extended to the determination of sulphur in carbon steels as well as alloy steels.

Experimental

Apparatus. The apparatus used was similar to the one used by Kiba *et al.* The reaction tube was a thick-walled Pyrex glass tube (15 cm high and 3.2 cm o.d.) with a 29/32 ground glass socket. The corresponding cone carried an inlet tube for the carrier gas, which reached to within a few cm of the bottom of the tube, and a horizontal outlet tube, which was attached via a ground-glass joint to a right-angled tube leading to the receiver (a 50-ml volumetric flask). Previous workers have used carbon dioxide with the necessary trains to purify the gas. Use of carbon dioxide directly from a cylinder was found satisfactory, as the blank values obtained were low (< 2 μg).

Tin(II)–phosphoric acid. Pour 250 g of dehydrated orthophosphoric acid, prepared by heating to 300°C, over 50 g of tin(II) chloride dihydrate (AnalaR) and again heat to 300°C. Cool and store in a desiccator.

p-Aminodimethylaniline (0.7% w/v). Dissolve 0.7 g of the reagent (E. Merck g.r.) in 100 ml of (1+1) sulphuric acid. Store in a dark glass bottle. The reagent is stable for about 6 months.

Standard sulphate solution (20 μg S ml^{-1}). Dissolve 2.2188 g of anhydrous sodium sulphate (AnalaR) in 200 ml of water and make up to 500 ml in a volumetric flask, to give solution (A) (1 mg S ml^{-1}). Pipette 20 ml of solution (A) and dilute to 1 l to give the working standard.

Procedure. Weigh an amount of sample, containing 10–40 μg of total sulphur, or pipette a suitable aliquot of solution, into the reaction vessel. Add 0.5 ml of 1% (w/v) barium chloride solution and dry over a water bath. Add 5 ml of tin(II)–phosphoric acid reagent. Use 10 ml of the reagent in the case of steel samples. Connect up the apparatus, flush the system with carbon dioxide for 5 min, and then reduce the flow rate to about 50–60 bubbles per min. Heat the reaction tube over a wire gauze for 15 min until white fumes of phosphoric acid appear, collecting the hydrogen sulphide evolved in 35 ml of aqueous 2% (w/v) zinc acetate solution (clarified if necessary with a little acetic acid) in a 50-ml volumetric flask. Discontinue heating and continue passing carbon dioxide for another 5 min. Disconnect the volumetric flask along with the delivery tube, and keep it for 30 min in a thermostatted bath at 25°C. Add 1.5 ml of *p*-aminodimethylaniline solution, slowly down the flask wall, followed by 0.5 ml of aqueous 10% (w/v) iron(III) chloride solution (containing a few drops of hydrochloric acid to stabilize the solution). Shake vigorously for 2 min and keep the flask at 25°C for another 15 min. Remove the delivery tube, make up to the mark with water, and measure the absorbance at 655 nm against a blank run through the procedure.

Results and discussion

The reaction between hydrogen sulphide and *p*-aminodimethylaniline in the presence of iron(III), leading to the formation of methylene blue is not quantitative[6,7] However, it is considered[6–8] to be sufficiently reproducible to be useful for the determination of hydrogen sulphide. It was found here that if the acidity is maintained at 0.27 *M* in sulphuric acid, and the temperature at 25 ± 1°C (observed variation), and if the *p*-aminodimethylaniline solution is added slowly down the vessel wall, the measured absorbance of methylene blue per μg S is reproducible in the range 10–40 μg S/50 ml. Earlier workers have shown that the reduction of sulphate to sulphide by tin(II)–phosphoric acid is quantitative, and this was confirmed in the present studies.

The results on the application of the method to refractory oxides of thorium and zirconium are given in Table I. The sample weights varied from 100 to 200 mg in the case of thorium oxide and from 10 to 40 mg for zirconium oxide. The results obtained by the proposed method agreed well with those obtained by microtitrimetry (thorium oxide) or gravimetry (zirconium oxide). The precision of the method is good, as is evident from the relative standard deviation of 2–3%.

Table I also shows some results for various types of steel. When the method was applied to an NBS steel sample (standard 121C), erratic and generally low results were obtained; this was found to be due to incomplete dissolution of the samples. When normal samples were taken in the form of fine turnings or thin chips, the dissolution was found to be complete and the results were reproducible. However, a major difficulty in the analysis of steels by the present method is that sample sizes of the order of 1–2 g, which are normally considered necessary from the point of view of homogeneity, cannot be handled. Considering this

TABLE I

COMPARISON OF SULPHUR VALUES IN OXIDES OF THORIUM, ZIRCONIUM AND IN STEELS

Matrix	*Present method (p.p.m.)*	*Other methods (p.p.m.)*
ThO_2	81, 81, 79, 85, 83, 85 Mean 82.3; s 2.8%	78
ZrO_2	900, 900, 951, 923, 930, 900 Mean 920; s 2.4%	930
NBS stainless steel 121 C	72, 61, 51	90
Carbon steel	330	310
Stainless steel (304)	95	110
Stainless steel (304)	140	120
Stainless steel (347)	100	90
Stainless steel (347)	45, 47, 48	60
Stainless steel (316)	65, 62, 62	75

limitation, the results compare favourably with those obtained by methods recommended by ASTM[9].

The method is simple, rapid and sensitive compared to conventional methods.

REFERENCES

1 B. L. Jangida, M. S. Varde and V. Venkatasubramanian, *Indian J. Chem.*, 2 (4) (1964) 149.
2 T. Kiba and I. Kishi, *Bull. Chem. Soc. Jap.*, 30 (9) (1957) 44.
3 T. Kiba, I. Akaza and N. Sughishita, *Bull. Chem. Soc. Jap.*, 30 (9) (1957) 972.
4 Y. Yamazaki, *Jap. Anal.*, 19 (2) (1970) 187.
5 S. Nagashima, M. Yishida and T. Ozawa, *Bull. Chem. Soc. Jap.*, 45 (11) (1972) 3346.
6 D. F. Boliz (Ed.), *Colorimetric determination of non-metals*, Interscience, New York, 1958, p. 273.
7 J. H. Karchmer (Ed.), *Analytical Chemistry of Sulphur and its Compounds, Part I*, Wiley–Interscience, New York, 1970, p. 296.
8 Lilly Gustaffson, *Talanta*, 4 (1960) 227.
9 *ASTM Standards, Part 32*, 1968, pp. 27, 64.

Analytica Chimica Acta, 72 (1974) 426–429

SHORT COMMUNICATION

Complexometric titration of metals with copper(II)–EDTA–TAR as indicator

H. YAMADA and T. MAEDA

Laboratory of Analytical Chemistry, Faculty of Engineering, Gifu University, Kagamigahara, Gifu 504 (Japan)

I. KOJIMA

Laboratory of Analytical Chemistry, Nagoya Institute of Technology, Showa-ku, Nagoya 466 (Japan)

(Received 28th January 1974)

Although many metallochromic indicators have been proposed for the titration of metals with EDTA, certain metals are still difficult to titrate because of a sluggish indicator transition or a narrow optimal pH range.

The present communication describes the complexometric titration of Mn^{2+}, Zn^{2+}, Cd^{2+}, Hg^{2+}, Pb^{2+}, Sc^{3+}, Fe^{3+}, and In^{3+} with the copper(II) EDTA–TAR system as indicator. As in the titration of gallium[1] and nickel[2] with this indicator system, the method is simple and accurate; it is especially useful for iron and manganese. A sharp and distinct color transition from red(lilac) to yellow or greenish yellow is obtained at the end-point over a rather wide pH range.

As described previously[2], the indicator transition with the copper(II)–EDTA–TAR system can be expressed as follows:

$$a = 1 - f_1 \frac{1-\phi}{\phi} + f_2 \frac{\phi}{1-\phi} - \frac{c_A}{c_M}(1-\phi)$$

where

$$a = (c_Y - c_{Cu})/c_M\,, \quad \phi = [A']/c_A\,,$$

$$f_1 = [\{(K_{CuY-M})^{-1}\, c_M/c_{Cu}\} + 1] \cdot [K_{Cu'A'(CuA)} \cdot c_M]^{-1}$$

and

$$f_2 = K_{CuY-A}\, c_{Cu}/c_M\,.$$

K_{CuY-M} and K_{CuY-A} are the equilibrium constant of the following substitution reactions, respectively:

$$(CuY)' + M' \rightleftharpoons (MY)' + Cu'\colon \; K_{CuY-M} = \frac{K_{MY}\,\alpha_{Cu}\,\alpha_{MY(H)}}{K_{CuY}\,\alpha_M\,\alpha_{CuY(H)}}$$

$$(CuY)' + A' \rightleftharpoons (CuA)' + Y'\colon \; K_{CuY-A} = \frac{K_{CuA}\,\alpha_{Y(H)}\,\alpha_{CuA(H)}}{K_{CuY}\,\alpha_{A(H)}\,\alpha_{CuY(H)}}$$

Effect of pH

Figure 1 shows the titration curves for manganese at various pH values. Of the metal ions studied in this paper, the conditional stability constant for manganese was the smallest, hence the titration of the other metals should also be successful. As is evident from the previous treatment[1,2] and from Fig. 1, the indicator transition becomes obscure as the pH decreases. At high pH values where the third dissociation of TAR is appreciable, the reddish shade of the indicator anion makes the end-point less sharp, and the titration should preferably be carried out at pH less than 6.5.

The potentiometric EDTA titration of mercury(II) with a mercury electrode (Fig. 2) suggests that the Hg–EDTA complex(HgY) reacts with hexamine to form a mixed ligand complex(HgYL) similar to Hg–EDTA–NH_3 (ref. 3). This mixed ligand

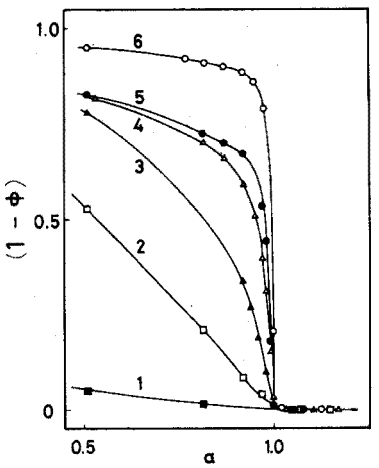

Fig. 1. Effect of pH on the indicator transition, $c_{CuY} = 2.5 \cdot 10^{-3}$ *M*, $c_{Mn} = 2.5 \cdot 10^{-3}$ *M*, $c_{OAc^-} = 0.25$ *M*. (1) pH = 3.91; (2) pH = 4.99; (3) pH = 5.46; (4) pH = 5.89; (5) pH = 6.19; (6) pH = 6.70 ($c_{Mn} = 5 \cdot 10^{-4}$ *M*).

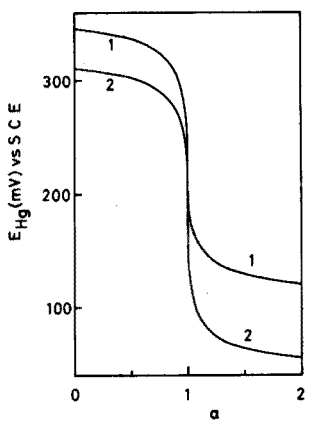

Fig. 2. Potentiometric titration curve of mercury(II) with a mercury electrode. $c_{Hg} = 1.09 \cdot 10^{-3}$ *M*, $c_{CuY} = 10^{-3}$ *M*, pH = 5.49. (1) Acetate (0.04 *M*); (2) hexamine (0.11 *M*), acetate (0.02 *M*).

complex formation makes the f_1 value smaller. However, it has been reported that ammonia accelerates the rate of the ligand substitution reaction of the mercury(II)–CPC complex with CyDTA[4]. Hexamine similarly accelerates the rate of the ligand substitution reaction of the Hg(II)–TAR complex with EDTA in the present system, so that the indicator transition in the presence of hexamine is sharper than in an acetate buffer. In the presence of a large amount of acetate, the side-reaction coefficient of lead, $\alpha_{Pb(OAc)}$, is inevitably large, and the optimal pH range for lead becomes narrow.

Effect of copper–EDTA concentration

Though f_1 becomes smaller with increasing concentrations of CuY, end-point detection becomes difficult owing to the deep color of CuY. Iron(III), which has a high stability constant, can be titrated to a sharp, distinct end-point over the pH range 2.5–5.5 for c_{CuY}/c_{Fe} ratios of 0.3–3.0, and even in the pH range 3.0–4.0 for c_{CuY}/c_{Fe} ratios of 0.1. However, manganese, which has a low stability constant, gives sharp end-points only in the pH range 5.5–6.5 for a c_{CuY}/c_{Mn} ratio of 3.0, or in the pH range 5.8–6.5 for c_{CuY}/c_{Mn} ratios of 0.5–2.0; no clear end-points are possible with ratios of 0.1–0.3 at any pH value.

Under the optimal conditions given in Table I, visual titrations of Mn^{2+}, Zn^{2+}, Cd^{2+}, Hg^{2+}, Pb^{2+}, Sc^{3+}, and In^{3+} are possible at room temperature; Fe^{3+} is titrated at about boiling point.

TABLE I

OPTIMAL TITRATION CONDITIONS FOR METAL IONS

Metal	*pH*	*Conditions*
Mn	5.5–6.5	Acetate or hexamine buffer
Ni	4–6	Acetate buffer, heat, titrate slowly
Zn	5–6.3	Acetate buffer
Cd	5–6.5	Acetate buffer
Hg	5.5–6.5	Hexamine buffer, titrate slowly
Pb	4–5	Depending on acetate
Sc	3.5–5.0	Acetate buffer
Fe	3–4	Acetate buffer, heat near end-point
Ga	3.5–4.0	Acetate buffer, heat, titrate slowly
In	3.5–4.5	Acetate buffer
Al[5]	4.2–5.4	Back-titration with Cu acetate buffer, titrate rapidly

Accuracy and precision. The average results obtained under the optimal conditions for each metal ion agreed within 0.01 mg with the amounts taken (Table II). The reproducibility of the present method were found to be satisfactory.

Experimental

Reagents. Standard EDTA solution was prepared from the disodium salt (G.R.) and was standardized with standard zinc solution with eriochrome black T as indicator. Standard solutions of manganese and zinc were prepared by dissolving pure metal (99.99%) in water containing perchloric acid. The other metal solutions

ABLE II

CCURACY AND PRECISION

Metal	*Taken (mg)*	*Found (mg)*	*Metal*	*Taken (mg)*	*Found (mg)*
Mn	1.07	1.06, 1.08, 1.07	Zn	5.37	5.36
	2.69	2.69, 2.66, 2.70		10.73	10.72
	5.37	5.36, 5.36, 5.38		16.08	16.08, 16.08, 16.07,
Cd	1.32	1.32, 1.29			16.07, 16.07
	2.63	2.64, 2.62, 2.65	Hg	21.97	21.96, 21.98, 21.97
	6.57	6.58, 6.58, 6.58		32.80	32.81, 32.80, 32.80
	13.15	13.15, 13.15, 13.12	Sc	0.440	0.441, 0.441, 0.441
Pb	2.06	2.03, 2.03, 2.05		0.880	0.877
	4.07	4.08, 4.07		2.200	2.196, 2.201, 2.201
	10.18	10.20, 10.16, 10.18	In	1.03	1.03, 1.02, 1.03
Fe	0.558	0.561		2.06	2.05, 2.05, 2.05
	1.12	1.10, 1.11, 1.12		5.16	5.16, 5.15, 5.17
	5.58	5.58, 5.58, 5.57			

were prepared by dissolving the metal perchlorate or nitrate in water containing a small amount of the corresponding acid, and were standardized by the accepted method for each metal ion[6]. Standard copper solution was prepared from purified copper perchlorate and was standardized with standard EDTA solution with TAR as indicator. Copper–EDTA solution was prepared by adding an equivalent amount of EDTA to recrystallized copper perchlorate. 4-(2-Thiazolylazo)-resorcinol (purity higher than 99%) was dissolved in alcohol. Acetate buffer solution or solid hexamine was used to adjust the pH value.

Recommended procedure. To a sample solution containing $0.1–3.0 \cdot 10^{-4}$ mole of metal ion, add 5–10 ml of 10^{-2} *M* Cu–EDTA solution. Adjust the pH value to the recommended value (see Table I) with acetate buffer solution or solid hexamine (for mercury). Add indicator (*ca.* 10^{-5} *M*), and titrate with standard 10^{-2} *M* EDTA solution. Near the end-point, titrate slowly, the solution being heated, if necessary (see Table I). Titrate to light green or yellow with no dark shade.

The authors would like to thank Prof. M. Tanaka of Nagoya University for valuable discussions, and Prof. T. Iwanaga of Gifu University and Prof. C. Iida of Nagoya Institute of Technology for their interest in this work.

REFERENCES

1 H. Yamada, I. Kojima and M. Tanaka, *Anal. Chim. Acta*, 52 (1970) 35.
2 I. Kojima, *Anal. Chim. Acta*, 57 (1971) 460.
3 F. S. Sadek and C. N. Reilly, *Anal. Chem.*, 31 (1959) 494.
4 M. Tabata, S. Funahashi and M. Tanaka, *Anal. Chim. Acta*, 62 (1972) 289.
5 S. Murate, G. Nakagawa and K. Kodama, *Bunseki Kagaku*, in press.
6 K. Ueno, *Chelate titration (Kireito Tekiteiho)*, Revised edition, Nankodo, Tokyo, 1972.

Analytica Chimica Acta, 72 (1974) 430–433

SHORT COMMUNICATION

Application of ion-selective electrodes to the analysis of silver-plating baths

LEONARD N. LAPATNICK

General Electric Co., Insulation Systems Laboratory Operation, 6901 Elmwood Ave., Philadelphia, Pa. 19142 (U.S.A.)

(Received 1st February 1974)

Wherever silver plating is performed, the bath must be maintained within certain rather broad concentration limits in order to assure trouble-free operation of the plating line. The parameters which are controlled are silver and "free" cyanide. Silver is determined either by titration with standard thiocyanate solution after evolution of hydrogen cyanide, or, as was the case in this laboratory, by electrodeposition at high current density from a cyanide-rich electrolyte. "Free" cyanide is customarily determined by titration with standard silver nitrate solution. These methods involve considerable handling of the samples, and, in the case of electro-deposition of silver, lead to intensification of the cyanide disposal problem. Ion-selective electrodes seem to present a rapid means of determining the two components of interest. The most promising method appears to be that of known increments[1,2].

Experimental

The apparatus and equipment used consisted of the following items: Leeds and Northrup Model 7415 pH/specific ion/millivolt meter; Orion electrodes, Models 94-16 (silver sulfide), 90-02 (double-junction reference), 94-06 A (cyanide) and 90-01 (single-junction reference); Drummond disposable calibrated capillary micropipets (100 μl).

The cyanide-selective electrode cannot be used for measurements on the actual bath because of the corrosive effect of high cyanide concentration on the sensing membrane. Furthermore, the pH of the measured solution must be high enough so that all of the "free" cyanide is truly free, *i.e.*, uncomplexed by hydronium species. In order to obviate these problems, the following procedure was developed.

A sample aliquot of 100 μl is added to approximately 100 ml of 0.25 *M* sodium hydroxide solution in a 150-ml beaker. The electrode pair is immersed while the solution is stirred magnetically at low speed. The indicator on the monovalent specific ion scale is set at 100 (the beginning of the second scale decade) and 100 μl of standard sodium cyanide solution is added. The new meter reading is noted, and the concentration of free sodium cyanide in the sample is

calculated from the relation $X(\mathrm{Na}) = 100\ S/(R-100)$, where $X(\mathrm{Na})$ = free sodium cyanide concentration (ounces/gallon), S = standard sodium cyanide concentration (ounces/gallon) and R = meter reading after standard addition.

When free potassium cyanide is being determined, the equation becomes $X(\mathrm{K}) = 133\ S/(R-100)$, where $X(\mathrm{K})$ = free potassium cyanide concentration (ounces/gallon).

TABLE I

REPRODUCIBILITY DATA

Run	*Concentration of free KCN (oz/gal)*	*Run*	*Concentration of Ag (oz/gal)*
1	13.2	1	0.54
2	13.2	2	0.47
3	12.9	3	0.54
4	13.4	4	0.54
5	13.0	5	0.54
6	13.3	6	0.58
Mean	13.15±0.10	*Mean*	0.54±0.03

TABLE II

COMPARISON OF RESULTS OF SILVER DETERMINATIONS

Sample no.	*Silver concentration (oz Ag/gallon)*			*% Error*	
	Referee	*I.S.E.*	*Deposition*	*I.S.E.*	*Deposition*
1[a]	0.42	0.50	0.33	+19.0	−21.4
2	11.9	11.8	11.6	−0.8	−2.5
3	1.29	1.34	1.12	+3.9	−13.2
4[a]	0.27	0.29	0.17	+7.4	−37.0
5	9.41	8.81	9.00	−6.4	−4.4
6	15.9	14.3	15.4	−9.5	−2.5
7	3.64	3.61	3.42	−0.8	−6.0
8	6.64	6.53	6.52	−1.7	−1.8
9	12.6	12.6	11.8	0	−6.3
10	10.7	10.5	10.2	−1.9	−4.7
11	10.1	10.2	9.69	+1.0	−4.0
12	14.7	14.6	13.5	−0.7	−8.1
13	9.90	9.84	9.55	−0.6	−3.5
14[a]	1.50	1.57	1.33	+4.7	−11.3
15[a]	0.58	0.63	0.50	+8.6	+13.8
16	3.29	3.34	2.98	+1.5	−9.4
17[a]	0.50	0.58	0.39	+16.0	−22.0
18	1.61	1.59	1.50	−1.2	−6.8
19	2.83	2.83	2.73	0	−3.5
Average error, over-all (%)				+2.0	−9.6
Average error, omitting strikes (%)				−1.2	−5.5
Average error, strikes only (%)				+11.1	−21.1

[a] Designates a strike solution.

The same technique can be applied to the silver analysis. The procedure calls for water to be used as diluent in place of sodium hydroxide, and for the use of $NaAg(CN)_2$ as the addition standard (in order to avoid upsetting the silver(I)–cyanide–dicyanoargentate(I) equilibrium). The calculation is $X(Ag) = 100\ S/(R-100)$ where $X(Ag)$ = silver concentration in sample (ounces silver/gallon), S = standard silver concentration (ounces silver/gallon), and R = meter reading after standard addition.

However, because of the range of silver concentrations involved, it is preferable in some cases to set the pointer at 10 initially (left-hand end of scale), so that the value of $X(Ag)$ is obtained from the relation $X(Ag) = 10\ S/(R-10)$. The reason for this is that the logarithmic scale on the meter covers only 1.4 decades, *i.e.*, from nominal 10 to nominal 250.

Results

A series of samples was analyzed by the usual methods, by the method outlined above and by careful (referee) titration. The referee method for cyanide was essentially the same as that used normally, but the titrations were performed with more attention to detail. For silver, the thiocyanate titration was used as the referee method.

Six readings on one sample in each set produced the data in Table I,

TABLE III

COMPARISON OF RESULTS OF FREE CYANIDE DETERMINATIONS

Sample no. and type	*Concentration of free NaCN or KCN (oz/gal)*			*% Error*	
	Referee	*I.S.E.*	*Titration*	*I.S.E.*	*Titration*
1 KCN	11.3	13.2	11.2	+16.8	−0.9
2 KCN	12.4	13.3	12.4	+6.3	0
3 KCN	11.7	13.3	11.6	+13.7	−0.9
4 KCN	11.3	11.8	11.2	+4.4	−0.9
5 KCN	11.5	12.9	11.2	+12.2	−2.6
6 KCN	12.9	13.4	12.9	+3.9	0
7 NaCN	16.6	19.4	17.0	+16.9	+2.4
8 NaCN	8.4	8.6	9.1	+2.4	+8.3
9 NaCN	8.6	8.9	8.9	+3.5	+3.5
10 KCN	10.9	11.5	10.8	+5.5	−0.9
11 KCN	12.1	13.5	12.5	+11.6	+3.3
12 KCN	12.1	13.2	12.0	+9.1	−0.8
13 KCN	17.6	18.3	16.8	+4.0	−4.5
14 KCN	11.4	13.5	11.4	+18.4	0
15 NaCN	13.1	13.7	13.4	+4.6	+2.3
16 NaCN	9.0	9.7	9.6	+7.9	+6.7
17 NaCN	6.2	6.8	9.4	+9.3	+52
18 NaCN	9.0	9.7	9.3	+8.5	+3.3
19 NaCN	7.1	7.7	7.2	+8.5	+1.4
20 NaCN	7.0	7.3	6.9	+5.2	−1.4
Average error (%)				+8.7	+1.0[a]

[a] Excludes result 17, obviously a mechanical error in the routine titration.

indicating good reproducibility among readings on a given sample.

The analytical results on a number of actual baths are presented in Tables II and III. The numbering corresponds only to the order in which the analyses were run, so that Sample 1 for silver is not the same bath designated by Sample 1 for free cyanide.

Conclusions

These results indicate that measurements by ion-selective electrodes provide results which are sufficiently accurate for plating bath maintenance. This analytical method permits the analyst to use much smaller samples than the ordinary methods and thus alleviates the problem of disposal of moderate quantities of cyanides. The number of titrations involved in bath maintenance is reduced to a single weekly standardization of the sodium cyanide solution used as an addition reagent.

REFERENCES

1 M. S. Frant, *Plating*, 58 (1971) 686.
2 J. U. Eynon, *Amer. Lab.*, 2 (9) (1970) 59.

Analytica Chimica Acta, 72 (1974) 434–436

SHORT COMMUNICATION

Amperometric back-titrations of traces of chromium

G. DEN BOEF and R. OOSTERVINK

Laboratory for Analytical Chemistry, University of Amsterdam, Nieuwe Achtergracht 166, Amsterdam (The Netherlands)

(Received 17th April 1974)

Chromium(III) reacts slowly with EDTA and other complexing agents at room temperature. This makes impossible the direct complexiметric titration of this element, except in the case of an amperometrically indicated "pseudo-titration" of chromium(III) with EDTA which has been described recently[1]. This method, in which no reaction occurs in the bulk of the solution but nevertheless the equivalence point can be detected at the indicator electrode, allows the determination of millimolar solutions of chromium(III).

Heating of a weakly acidic solution containing chromium(III) and an excess of EDTA, leads to complete complex formation within a reasonable period of time, which depends on the concentration of chromium(III) and the excess of EDTA[2]. This reaction forms the basis of several procedures for chromium at the millimolar level[3,4]. Determinations of 10^{-6} *M* solutions of chromium(III) have been successfully carried out by inverse voltammetry[5], although the selectivity is rather poor. Other determinations of traces of chromium in solution generally make use of the hexavalent state.

The present communication describes the amperometric back-titration of chromium(III) at the 10^{-6} *M* level. The best pH value for the complex formation is 3.5. A ten-fold excess of EDTA is required for complete complexation in 30 min on a boiling water bath. Such an excess of EDTA does not favour precision, but is inevitable in order to keep the time requirement within reasonable limits. In order to minimize interference by other metal ions, the back-titration was carried out in a solution as acidic as possible. Back-titration with bismuth(III) appeared to be appropriate. The end-point was indicated amperometrically at a rotating mercury electrode by means of the anodic wave of EDTA as described earlier[6].

Of course, metal ions which complex with EDTA at pH 2 and which are not displaced from their complexes by bismuth(III) will interfere[7]. Determination of chromium(III) in the presence of these metal ions can be carried out by means of a difference procedure, making use of the extremely slow formation of the chromium(III)–EDTA complex at room temperature. EDTA is added in excess to the sample solution containing chromium(III) and interfering metal ions. Two aliquots of the solution are taken. One of them is titrated directly with bismuth-

(III); the other after heating the solution in order to complex chromium(III) as well. The difference between the two titrant volumes corresponds to the amount of chromium(III). It is obvious that for the successful application of this difference method, two requirements must be fulfilled: (a) the interfering metal ion must react quickly with EDTA at room temperature; and (b) the approximate amount of interfering metal ion should be determined or known, in order to know the required amount of EDTA. This can be done easily.

Experimental

The rotating mercury electrode (1000 r.p.m.), consisting of a platinum wire (1 cm length, 0.5 mm diameter) sealed into glass and covered with mercury, was prepared by a modification of the procedure described by Neeb[8]. After cleaning with aqua regia, the platinum wire is covered with mercury by electrolysis of a solution which contains 0.05 *M* EDTA and 0.05 *M* ammonia, the platinum wire acting as cathode and a mercury pool as anode. The current is 2 mA and the time required is about 1 h. The result of the first titration often deviates considerably and is therefore discarded. After 10 titrations, the electrode is immersed in mercury in order to regain its sensitivity which gradually decreases. After a few months, the surface of the platinum wire is so affected that the electrode can no longer be used. All chemicals used were of analytical grade.

The titration cell and the electrical equipment are the same as described previously[5].

Procedure for normal back-titrations. Adjust the sample solution—about 10^{-6} *M* chromium(III)—to pH 3.5. Add a ten-fold excess of EDTA with respect to chromium(III). Heat for 30 min on a boiling water bath, cool and adjust to pH 2 with 0.5 *M* perchloric acid. Transfer the solution, or a 5-ml aliquot, to the 10-ml titration compartment of the H-cell containing the rotating mercury electrode, and titrate with 10^{-3} *M* bismuth(III) solution, the potential of the indicator electrode being set at 0.33 V *vs.* SCE.

Procedure for the difference titration method. Adjust two aliquots of the sample solution—about 10^{-6} *M* chromium(III)—to pH 3.5. Add enough EDTA so that complete complex formation of chromium(III) and metal ions interfering at pH 2 can take place, and so that a ten-fold excess with respect to chromium(III) is present. Heat one of the aliquots in order to form the chromium(III)–EDTA complex completely, and cool. Adjust both aliquots to pH 2 as in the previous procedure and back-titrate both aliquots with 10^{-3} *M* bismuth(III). The difference in the amount of bismuth(III) consumed by the two aliquots corresponds to the amount of chromium(III).

Results

Determinations of 5 ml of 10^{-6} *M* chromium(III), corresponding to 0.25 μg of chromium(III), were possible with a standard deviation of 5%.

The influence of the most important metal ions reacting with EDTA in acidic solution was investigated. The amount of other metal ions is mentioned on the basis of mole-to-mole ratio. No interference was observed by 5 × lead(II),

100 × cobalt(II), 1 × mercury(II), 100 × zinc(II) and 1 × copper(II). Iron(III) interfered because it reacts with EDTA even at pH 2. Nickel(II) interfered because its EDTA complex which is formed at pH 3.5 is rather inert. Aluminium(III) interfered, probably for the same reason. Vanadium(IV), manganese(II) and larger amounts of copper(II) interfered.

In order to circumvent these interferences, the difference procedure was developed. When this was applied, no interference was observed for 10-fold amounts of iron(III), copper(II), nickel(II) or vanadium(IV), but manganese(II) and aluminium(III) still interfered.

The interference by aluminium(III) can be overcome in this procedure by performing the back-titration at pH 3 instead of at pH 2; a ten-fold amount of this metal ion may then be present. When the different procedure is used, larger amounts of the metal ions mentioned above may be tolerated, but at some cost in precision.

REFERENCES

1 D. I. Bustin and I. Mocák, *Talanta*, 20 (1973) 1185.
2 R. Přibil and J. Klubalova, *Collect. Czech. Chem. Commun.*, 15 (1950) 42.
3 G. den Boef and B. C. Poeder, *Anal. Chim. Acta*, 30 (1964) 261.
4 L. Szekeres, *Microchem. J.*, 17 (1972) 360.
5 R. Neeb and I. Kiehnast, *Z. Anal. Chem.*, 268 (1974) 193.
6 F. Freese, H. J. Jasper and G. den Boef, *Talanta*, 17 (1970) 945.
7 Th. J. M. Pouw, G. den Boef, U. Hannema, J. M. van der Meer and S. Q. J. Zonneveld, *Anal. Chim. Acta*, 68 (1974) 137.
8 R. Neeb, *Inverse Polarographie und Voltammetrie*, Verlag Chemie, Weinheim, 1969, pp. 98–100.

Analytica Chimica Acta, 72 (1974) 437–442

SHORT COMMUNICATION

The determination of nitrate in waters at low p.p.m. levels by automatic discrete-sample analysis

J. RAMÍREZ-MUÑOZ
Beckman Instruments, Inc., Irvine, California 92664 (U.S.A.)
(Received 2nd April 1974)

The nitrate ion absorbs strongly in the u.v. region at 207 nm. Nitrate in water samples can be measured at this wavelength with or without preliminary dilution, depending on the nitrate concentration. Contributions by Navone[1,2] have clearly demonstrated the analytical capabilities of u.v. measurement of nitrates, even in the presence of nitrites, and the close correlation between experimental u.v. results and results of other recommended methods for nitrate determinations.

This type of determination is not subject to noticeable interferences by nitrites (much lower absorption in this region, even if present at similar concentrations), especially when potable waters are examined[2]. Attention should be given to possible interferences from organic matter absorbing at this low wavelength. Navone[1] has described the possibility of destroying the nitrate in a duplicate of each sample by means of a Zn–Cu couple, and measuring the sample against this duplicate, so that the net absorbance of nitrate is measured.

This paper describes the adaptation of this u.v. technique to an automatic discrete-sample system, the AMA-40 System (Beckman Automated Materials Analyzer[3]). Automatic handling of samples provides several advantages in the u.v. measurement, *e.g.* rapid sample preparation (addition of reagents and dilution processes), elimination of personal errors in manual handling, and standardization of the whole process with identical instrumental conditions (which leads to improved precision).

Experimental

The AMA-40 System is used without the disruption module. When preliminary dilution of the samples is needed, a pipette–diluter is used. Aliquots of diluted hydrochloric acid solution are added with a reagent pump. The resulting acidic solution is mixed and finally delivered to the Beckman Model 25 Spectrophotometer for the u.v. measurement. Readings are performed at 207 nm with a reference solution of distilled water and diluted hydrochloric acid prepared under the same conditions as the samples.

Standards and blanks. Aqueous solutions of potassium nitrate, also treated with diluted hydrochloric acid, serve as standards. Standards of 40, 20 and 10 mg NO_3^- l^{-1} (40, 20, and 10 p.p.m.) are used. These standards are diluted to

8, 4, and 2 mg l^{-1} concentrations by pipetter–diluter (dilution ratio 1:5) transfers.

A standard stock solution of 1,000 mg NO_3^- l^{-1} is prepared by dissolving 1.6305 g of anhydrous potassium nitrate in deionized–distilled water and diluting to 1 l. Alternatively, a 100 mg N l^{-1} solution can be used; this is prepared by dissolving 0.7218 g of the chemical with deionized–distilled water, and diluting to 1 l. Working standards are prepared by simple dilution.

Filtering. Samples can be filtered in the T-cups before aliquots are taken for dilution by the pipetter–diluter. A filter probe should be installed and filter tubes placed in the T-cups where filtering is desired.

Samples not requiring dilution. Pipetted aliquots (5 ml) are transferred from the sample T-cups to the T-tubes. Standards (pre-diluted standards) are also placed in the respective T-tubes (5 ml each). Samples and standards each receive an addition of 0.4 ml of diluted hydrochloric acid solution at pedestal position no. 6 (see Table I).

TABLE I

OPERATING CONDITIONS

Disruption timer[a]	15 s
Filter probe[b]	Pedestal position no. 4
Pipetter diluter	Pedestral position no. 5. Diluting soln.: water. Volumes: 1 ml + 4 ml. T-C to T-T 1
Reagent pump	Pedestal position no. 6. Reagent: 0.25 *M* HCl. Volume: 0.4 ml. T-T 1
Mixer	Pedestal position no. 7. T-T 1
Sampling probe	Pedestal position no. 8. T-T 1
Wavelength	207 nm
Reference cell	0.4 ml 0.25 *M* HCl + 5 ml water
Sampling timer	Position 3 (4.5 ml)
Slit program	Normal
Recorder chart speed	5 in min^{-1}
Recorder span setting	100 mV
Solvent pump	Not used
Sample vacuum	15 in
Model 25 Spectrophotometer operation	Double beam
Lamp	Deuterium
Setting	1 A

[a] Disruptor is not used. Disruption time is set at 15 s to perform each working cycle in 60 s (40 working positions in 48 min).
[b] Not used if samples are not to be filtered.

Samples requiring dilution. These samples are placed in T-cups. Their volume need not be measured and the pipetter–diluter will take a 1-ml aliquot from each and dilute this aliquot with 4 ml of water (dilution ratio 1:5). The pipetter–diluter is located in pedestal position no. 5 (see Table I).

Experimental set-up. The experimental set-up is shown in Fig. 1.

Results

Repeatability. The instrument was tested for repeatability by measuring a

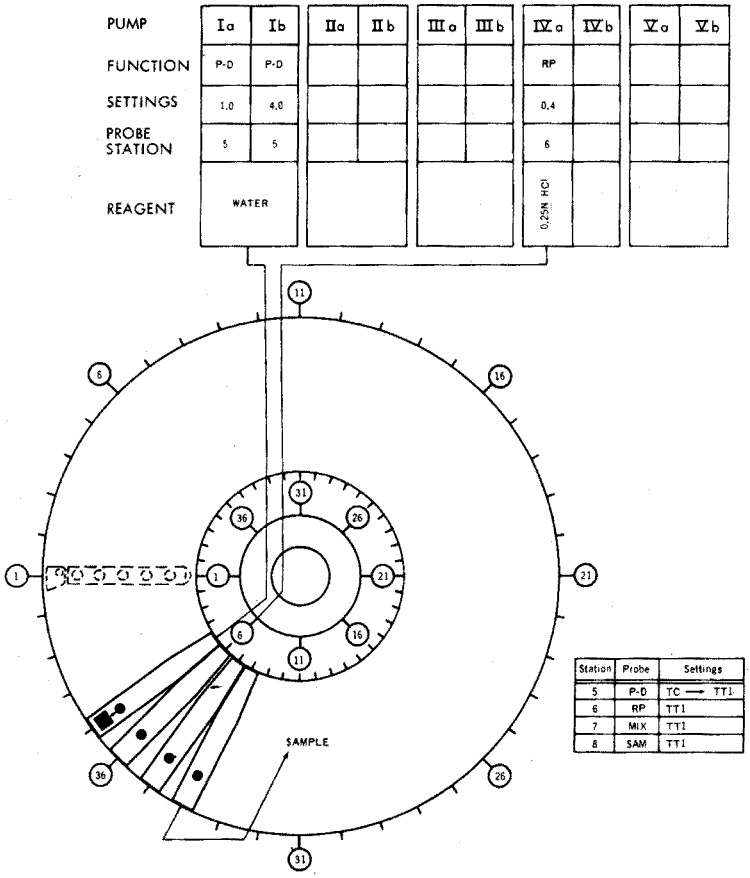

Fig. 1. Experimental set-up. P-D = Pipetter–Diluter; RP = reagent pump; MIX = mixer; SAM = sample probe; TT = T-tube; TC = T-cup.

standard solution (40 mg l^{-1} after dilution) several times in each run. The results are summarized in Table II.

If desired, aqueous solution without acid addition can also be measured, especially when the performance of the instrument is tested, or when the operator wishes to observe results after removing one working probe (reagent pump probe) from the work schedule. However, acid addition is recommended for reading water samples*. Readings obtained with a standard (40 mg l^{-1} after (1+4) dilution) without acid addition are also shown in Table II.

Measurement of nitrate concentration in water samples. Three water samples of low nitrate concentration were read in triplicate and compared with standards (three standards also read in triplicate). Two runs were conducted on different

* In preliminary tests the concentration of acid added to samples was much higher than that recommended in this report. Results appeared to be much more acceptable when the acid concentration was reduced to the levels recommended here.

TABLE II

REPEATABILITY TESTS FOR STANDARD SOLUTION

Series	*No. of readings*	*Average*[a]	*Standard deviation*[a]	*Relative standard deviation (%)*
With acid addition				
1	20	0.747	0.0037	0.49
2	20	0.746	0.0053	0.71
3	20	0.747	0.0030	0.41
Without acid addition				
4	16	0.807	0.0023	0.28

[a] In absorbance units.

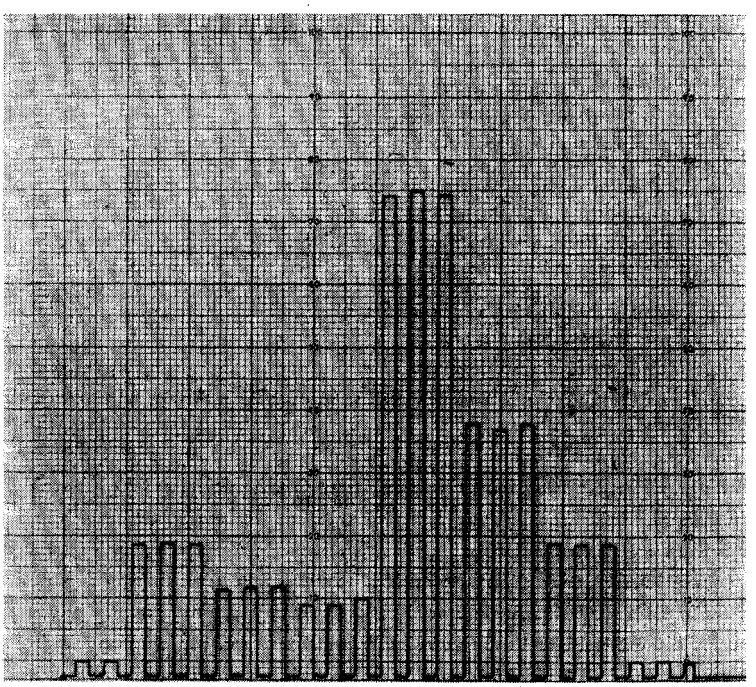

Fig. 2. Triplicate recordings of 3 standards (10, 20 and 40 p.p.m. nitrate) and 3 samples of low nitrate content.

days to test the repeatability of the method. In Fig. 2 one of the runs is reproduced. Table III summarizes the results of these tests. The calibration curve is linear up to at least 40 mg NO_3^- l^{-1}.

Discussion

An addition of 0.4 ml of 0.25 *M* hydrochloric acid has resulted in much

TABLE III

ANALYSIS OF WATERS: REPEATABILITY TESTS

(Triplicate readings in absorbance units)

Solutions	*I*			*II*			*III*		
	Ave.	S_r	NO_3^- *concn.* *(mg l^{-1})*	*Ave.*	S_r	NO_3^- *concn.* *(mg l^{-1})*	*Ave.*	S_r	NO_3^- *concn.* *(mg l^{-1})*
Standards									
10 mg l^{-1}	0.188	0.53		0.196	0.88		0.192		
20 mg l^{-1}	0.377	1.15		0.396	0.29		—		
40 mg l^{-1}	0.746	0.63		0.776	0.26		—		
Samples									
A	0.093	7.13	5.0	0.098	5.40	5.0	0.090	4.44	4.8
B	0.117	2.16	6.3	0.127	5.14	6.4	0.118	2.94	6.3
C	0.188	0.31	10.0	0.202	0.86	10.3	0.198	2.67	10.5

better repeatability in comparison with tests performed at higher acidities. Filtration is mandatory for turbid samples, since slight turbidity will affect readings at the working wavelength. The final volume should not be less than 5 ml since at least 4–4.5 ml of solution are needed for the flow cell.

If desired, reagent addition can be done at the same time as transfer and dilution by pipetting the water sample aliquot with a pipetter–diluter using a diluted solution of hydrochloric acid as diluent instead of water. A mixer probe should be used after the pipetter–diluter.

No attempt has been made to compare the method with accepted colorimetric methods, since the u.v. procedure is well-established[2].

In routine work only single readings per sample should be scheduled. One or two blanks, and the standards should be read at the beginning of the series. A blank or two can be located at the end. In this way, 30–36 samples can be examined in a full run.

The automated system proposed is easily applicable to routine determinations of nitrate in water samples. The repeatability of results is excellent, as potential sources of variability such as manual pipetting and operation bias are eliminated. For optimal accuracy, duplicate or triplicate readings are recommended for low nitrate concentrations. Single readings for medium and high levels are sufficient Good long-term repeatability has been found in multiple runs of samples of low nitrate concentration.

The experimental set-up is simple and can be programmed to provide a reading every minute, which speeds acquisition of multiple readings in laboratories dealing with a great number of samples for nitrate determinations.

Thanks are given to Mr. Fred Pearlman for his help in some preliminary tests done in the first stages of the work described.

REFERENCES

1 R. Navone, *J. Amer. Water Works Ass.*, 56 (1964) 781.
2 R. Navone, *J. Amer. Water Works Ass.*, 58 (1966) 1193.
3 J. Ramirez-Muñoz and D. G. Rohrbaugh, *Anal. Chim. Acta*, 71 (1974) 311.

Analytica Chimica Acta, 72 (1974) 443–449

BOOK REVIEWS

Instrumentation in Analytical Chemistry, an ACS Reprint Collection, collected by Alan J. Senzel, American Chemical Society, Washington, D.C., 1973, ix+428 pp., price $ 4.20 hardback ($ 3.36 paperback).

This is a collection of the monthly invited articles on instrumentation published in *Anal. Chem.* during the period January 1969 to July 1972. The articles are invariably well written and provide good technical reviews of pertinent facets of instrumental analysis. No effort has been made to provide a systematic coverage of any single analytical field, hence it would be unsuitable as a text-book for a comprehensive course in analytical chemistry. The subjects covered are randomly distributed and may provide a good choice for a "special topics" discussion course. The topics covered are varied, including nineteen articles in spectrometry on subjects as varied as "Ion Cyclotron Resonance Spectrometry, Recent Advances of Analytical Interest," by M. L. Groes and C. L. White, and "Infrared Detectors," by H. Levinstein. Three articles are devoted to chromatography and four to electrochemistry. Eighteen other articles are written on diverse subjects such as computers, superconductors, lasers and signal-to-noise level.

One of the attractions of this collection is the inclusion of the "Commentaries," by the late Ralph H. Müller. The penetrating scientific evaluations and the lucid presentations of these commentaries are worthy of collection themselves. The combination of the articles and the Müller commentaries constitutes a very readable book which is surely a collector's item.

J. W. Robinson (Baton Rouge)

J. G. Dick, *Analytical Chemistry*, McGraw-Hill, New York, 1973, viii+696 pp., price £6.85.

Although the title promises a much-needed comprehensive account of modern analytical chemistry, this is essentially an introductory undergraduate text, similar to many others already available. The main part of the text (376 pp.) follows the well-worn sequence from chemical equilibria via titrimetry to gravimetric analysis, and is preceded by discussions of concepts of concentration, chemical equations, standardization, and of statistical treatment of data (84 pp.). This section of the book, within the limitations outlined below, is one of the best of its type. It is detailed, comprehensive, and clear to understand. There is an abundance of problems at the end of each section, throughout the book.

The classical section is followed by a good account of electrochemical methods of analysis (120 pp.), which includes such relatively recent developments as ion-selective electrodes, and the mercury electrode for EDTA titrations. Absorptiometry and separation methods (solvent extraction, volatilization, chromatography

and ion-exchange) are squeezed into 48 pages, and the remainder of the text (68 pp.) is given over to (mainly classical) laboratory experiments, to appended tables of atomic weights, formula weights, equilibrium constants (including a useful section on metallochromic indicators and their metal complexes) and logarithms, and to a comprehensive subject index. There seem to be very few typographical errors.

The detailed treatment of the classical chemical methods is sufficient for self-tuition. However, any student learning analytical chemistry solely from this text would gain a rather curious impression of the subject. Firstly, he would assume that most analysis is done by gravimetry or titrimetry. This arises because the minor portion of the text devoted to instrumental techniques (other than electrochemistry) is out of all proportion to the relative importance of these methods. Gas chromatography, arguably the most used analytical technique today, is discussed in three pages, ion-exchange is allotted a single page, and atomic absorption nothing at all. Why should ionic equilibria and acid–base titrations receive such detailed theoretical treatment whereas the various chromatographic processes get so little?

Secondly, the student would be very confused as to the uses of these analytical techniques. There is a great dearth of examples of the applications of all the techniques, classical and instrumental. In some instances, this is extended to a lack of specific examples of even the reagents used. For example, the discussion of solution spectrophotometry is accomplished without reference to one example of an absorbing species; the widespread use of organic reagents for spectrophotometry is not even mentioned. Applications are the raison d'être for analytical chemistry, and any book claiming to discuss the subject without them is very incomplete.

In addition to these major faults, one is disappointed to find little mention of masking or catalysis, and such a brief treatment of precipitation from homogeneous solution. The use of volumetry synonymously with titrimetry should be discouraged, as should the use of two systems of nomenclature for oxidation states (for example, mercurous and iron(II)), and the term solubility product constant. N-Benzoylphenylhydroxamic acid should have been included in the list of common organic precipitants (perhaps by excluding quinaldinic acid), and the molybdate masking procedure should have appeared in the periodate oxidation section. Finally, metal ions are *not* metallic!

A. Townshend (Birmingham)

Automatic Air Quality Monitoring Systems, Proceedings of the Conference held at the National Institute of Public Health, Bilthoven, The Netherlands, 5–8 June 1973, Edited by T. Schneider, Elsevier, Amsterdam, 1974, 267 pp., price Dfl 42.00.

At first glance the title of this book might appear to suggest an up-to-date account of analytical procedures for monitoring air pollutants on an automatic basis. Alas, further inspection reveals that the volume actually contains the proceedings of an international conference held in the Netherlands in June 1973.

This conference was convened as a vehicle for the exchange of ideas and data on automatic air quality monitoring systems among the various countries which are presently concerned with the problem of air pollution.

As one would guess the largest contribution in this field has been made by the United States and in the first paper presented at the Symposium, F. J. Burmann, of the Environmental Protection Agency of the U.S.A., reviews the overall problems and summarizes the various analytical methods and techniques available for the more common atmospheric pollutants. This is the closest the book gets to the analytical problems. The remaining papers deal largely with the transfer of the data from the site to the data handling centre and the subsequent treatment and application of the results to such problems as the forecasting of high pollution levels in conjunction with meteorological data.

Occasionally one finds in the papers reference to the experimental limitations of the analytical measurements but there seems to be a tendency among those who interpret data on environmental pollutants to overlook these limitations.

It is difficult to see which sections of the environmentally aware scientific community would find sufficient interest in this book to justify its purchase, apart, of course, from those who attended the conference.

J. A. Kerr (Birmingham)

Microprobe Analysis, Edited by C. A. Anderson, John Wiley & Sons, New York, 1973, xi + 571 pp., Price £12.50.

This book on microprobe analysis is mainly devoted to the electron probe microanalyser but contains, also, sections on the laser microprobe and the ion microprobe. It consists of 17 chapters written by different authors who, with one exception, work in the U.S.A. The content of each chapter, presumably planned by the Editor, can hardly be faulted and both the instrumental and application sides of the subject are extremely well covered.

In many cases, the choice of author is beyond reproach and these chapters are clear, authoritative and of uniformly high standard. In other cases, the selection of contributor has been less felicitous and this fact more than any other has contributed to the slightly patchy quality of the book as a whole.

The Editor in his preface hopes that the book "will help to delineate the special advantages and areas of application of each of the techniques and instruments". A short chapter devoted entirely to a comparison between the three methods would have contributed greatly to this objective.

Apart from this omission, it is also surprising that so little is said about the combined electron microscope/microanalyser. There is one reference in the Index but unhappily it directs the reader to the wrong page. It could be argued that this topic was worth a chapter on its own, but when the actual reference is unearthed it amounts to no more than about two pages in a chapter on analysis of free particulates. Unfortunately, this also happens to be one of the chapters with no bibliography whatsoever.

The book as a whole is produced to a very high standard. With these minor

qualifications it can be commended as a most valuable account of the present state of these arts and the contributions they have made to man's study of the microstructure of his environment.

D. A. Melford (Saffron Walden)

K. Burger, *Organic Reagents in Metal Analysis*, (International Series of Monographs in Analytical Chemistry, Volume 54) Pergamon Press, Oxford, 1973, 268 pp., Price £5.80.

This book is the enlarged and translated edition of the author's book in Hungarian which appeared in 1969. The main emphasis in the book is on the determination of trace amounts of metal, with organic compounds as the ligands. There is an excellent chapter dealing with the analytical selectivity of reactions based on complex formation, which discusses the factors influencing the stabilities of complexes as well as the analytical selectivity of functional groups. This is a useful chapter for any worker in the field of organic reagents. It collects much of the important work published, and presents it in a very readable manner.

The second chapter deals with the application of selective organic reagents in quantitative analysis and indicates how the reagents are used in gravimetry, titrimetry, colorimetry, polarography and in a few cases, chromatography. This forms a very good basis for the remaining chapter which is a collection of tables summarizing what metal ions can be determined with a given reagent and by what method. The stability constants of the chelates of complexing agents used as analytical reagents are also listed. Whilst this is not new material, it is extremely useful to have the details of the reagents, and the information about complexes and their uses in one book. There are approximately 500 references quoted; this is itself indicative of the range of material covered. There are some errors, such as listing Daxime as a reagent for cobalt in the index but nowhere else, and not indicating what Komplexone III is, except that it is a popular reagent. But these do not seriously detract from the worth of the book; and for those research workers in these fields of analysis, it will be a very useful addition to the literature.

L. S. Bark (Salford)

Gerald H. Wagman and Marvin J. Weinstein, *Chromatography of Antibiotics*, Elsevier, Amsterdam, 1973, viii + 238 pp., price Dfl. 65.00.

This book was prepared as a consolidated reference volume for the chromatographic identification of antibiotics and forms Volume 1 of the *Journal of Chromatography* Library. It contains chapters on chromatographic classification and on the detection of antibiotics followed by an index of over 1200 compounds. The index contains, in some detail, information on paper and thin-layer chromatography, electrophoresis, counter-current distribution and gas chromatographic systems, including solvents, phases, voltages, flow rates, etc. and retention/mobility data.

Journal and Patent Literature references are given.

Only two blemishes to this otherwise excellent book were noted, an incomplete reference on p. 125 and trimming of half a column of R_F values on p. 181. Anyone concerned with antibiotics and their characterisation cannot afford to be without access to this book, which is definitive, and has been prepared by authors with great experience of the field.

D. Thorburn Burns (Loughborough)

Annual Reports on Analytical Atomic Spectroscopy, 1972, Vol. 2, Edited by D. P. Hubbard, Society for Analytical Chemistry, London, x+216 pp., price £5.00.

This second volume lives up to the high standard of its predecessor. It presents clearly the developments in all aspects of the subject in the same format as the previous volume, and should be invaluable to all who are working in analytical atomic absorption spectroscopy. The inclusion of material reported in lectures and at Conferences is an excellent feature, as is the inclusion of the titles of all the papers discussed (1123 papers) and the addresses of the authors. The standard of presentation remains high, and, considering the speed of publication, the number of errors seems very reasonable.

A. Townshend (Birmingham)

Quantitative Thin Layer Chromatography, Edited by Joseph C. Touchstone, Wiley–Interscience, New York, 1973, xiv+330 pp., price £7.50.

The book has its origins in two symposia, namely "Quantitative Thin Layer Chromatography" held in Philadelphia, Pennsylvania in December 1970, and a similar symposium sponsored by The American Oil Chemists Society in November 1971. The results of these have been collected in an attempt to fulfill the need for a volume on the quantitative aspects of thin-layer chromatography, although some of the participants of the symposia could not prepare their presentations and these have been replaced by other authors. Additionally, new subjects have been added in order to make the book more complete.

The penalty in producing a book of this type is that the material, which is generally of a research nature when presented, loses impact some 2–3 years after the original event and there is inevitably a deal of subject overlap. Additionally, the uninitiated reader is likely to get the impression that almost the whole of analytical chemistry can best be dealt with by the particular symposium technique.

There are numerous books on the quantitation of thin-layer chromatography and there is little that this particular book can contribute to the essential literature. However, an attempt is made to select chapters which present more of a review of the special area of interest. The original symposia were primarily devoted to *in situ* quantitation; many of the contributions are dominated by densitometry and attempt to show the ease and reliability of the technique. Some 16 contributions are presented

covering such varied subjects as polymer molecular weight distributions, several biochemical applications, pesticide and drug metabolite investigations and some aspects of air pollution measurements.

Those who have the need for an up-to-date review of thin-layer chromatography with special regard to aspects of quantitation will find the book of value. In general, it is not the type of book to hold a prominent position in a personal library.

R. M. Dagnall (Huntingdon)

W. W. Christie, *Lipid Analysis*, Pergamon Press, Oxford, xiv+338 pp., price £6.00.

This book presents a clear and logical approach to the field of lipid analysis. The first chapter gives an introduction to the chemistry and occurrence of these compounds, from the simple fatty acids to the complex lipids. The second chapter describes their isolation from tissues, first in a general manner and then with practical details of recommended methods. Here is much sound advice on precautions to be taken, and problems that the newcomer should be aware of are discussed.

Subsequent chapters deal with the techniques of value to the analyst, particular attention being paid to gas–liquid and thin-layer chromatography. The examination of fatty acids and the preparation of suitable derivatives are then dealt with in detail. This is followed by the analysis of simple then complex lipids. The subject matter is thus treated in a logical progress of increasing complexity. Two useful appendices give sources of standard lipids and further sources of information. The text is supplemented with over 600 references covering the literature to 1972. This is a book that will be of value to newcomers to the field of lipid analysis and appreciated by experts as a reference work.

J. Tillman (Loughborough)

Ralf Steudel, *Chemie der Nichtmetalle*, de Gruyter, Berlin et New York, 1974, 471 pp., prix DM49.—.

C'est un ouvrage d'enseignement, écrit en langue allemande, consacré plus spécialement à la chimie des non-métaux.

Les divers sujets traités ont été ordonnés d'une façon logique. Par rapport à la chimie descriptive détaillée des composés individuels, on a fait une place importante aux principes généraux essentiels et à la chimie comparative de ces éléments. L'auteur a rapproché les modèles théoriques des observations expérimentales, ce qui permet de montrer leur utilité et leurs limites.

C'est un ouvrage clair et bien conçu, dont la lecture attentive doit intéresser non seulement l'étudiant, mais aussi les enseignants de la branche concernée.

W. Haerdi (Genève)

D. J. David, *Gas Chromatographic Detectors*, Wiley–Interscience, New York, 1974, xii + 295 pp., price £10.20.

During the last decade there has been an increasing desire to improve the selectivity and sensitivity of analytical techniques. In gas chromatography, this demand has been met by many developments in the various modes of detection and the literature has expanded accordingly. *Gas Chromatographic Detectors* is a most useful survey of much of the work in this important field, for, in the words of the author, "without suitable and desired means of detection, the finest column separation would be useless".

The first chapter of the book gives a short introduction to the history and terminology of detectors. This is followed by seven chapters each of which deals with one of the common detectors: thermal conductivity, flame ionization, electron capture, thermionic, ultrasonic, helium ionization and flame photometric. Chapter 9 contains a discussion of the various types of electrochemial detectors. Some of the more unusual detection systems, which are less important at present owing to their newness, limited application or limited commercial interest, are described in Chapter 10. Ancillary devices, such as mass spectrometry and infrared spectrophotometry, which were not developed primarily as gas chromatographic detectors, are not included in this book.

Every chapter contains a discussion of the background and development of each type of detector together with the effects of the various operating parameters on the performance and response. Some important applications are described.

If the book was printed directly from typescript by photo offsett lithography in order to speed publication or to reduce the cost, then neither intention is fulfilled. It is unfortunate that for a book published in 1974 there are few references to work published even in 1971. However, there is good literature coverage before this date and good subject and author indices are included. A number of typographical errors occurs but the most serious criticism concerns the printing style. It is difficult to follow the text when figure legends tend to merge into it.

Nevertheless, *Gas Chromatographic Detectors* is a welcome addition to the tertiary literature on gas chromatography and should prove useful to workers involved in developing or applying the technique. Many useful practical points are included, although they may need some extracting from the text. At such a high price it is unlikely that the worker will buy his own copy, particularly if, like the reviewer, he dislikes the printing style.

R. Barratt (Birmingham)

W. H. McFadden, *Techniques of Combined Gas Chromatography/Mass Spectrometry: Applications in Organic Analysis*, Wiley–Interscience, New York, 1973, xv+463 pp., price £9.50.

It is probably considered by many that the technique of gas chromatography/mass spectrometry is sufficiently well known and proven not to warrant a text book on the subject. In this particular instance, however, the purpose of the book is achieved, that is to provide the organic chemist with a background and understanding of g.c./m.s. whilst considering each of the important associated technologies.

The discussion of gas chromatographic instrumentation is less extensive than that of mass spectrometry and each chapter attempts to illustrate some important facet of g.c./m.s. or a direct relationship to the overall theme of g.c./m.s. With the exception of a brief account of computer interpretation of g.c./m.s. data, the whole subject of mass spectral data interpretation has been avoided. The individual chapters deal with the relationships of components of a mass spectrometer to the requirements of g.c./m.s. analysis, fundamentals of gas chromatography pertinent to g.c./m.s. operation, application of elementary vacuum technology in g.c./m.s. systems, the g.c./m.s. interface, operational techniques of the g.c./m.s. system, the role of the computer in g.c./m.s. and applications of g.c./m.s. This last chapter is somewhat novel and consists of contributed reports from a number of g.c./m.s. users, illustrating applications from several fields of organic chemistry, biochemistry, geochemistry and clinical and forensic chemistry. Unfortunately, this section is in many instances too brief, although it cannot be argued that it fulfills the objectives of interesting and educating the reader.

In general, the text is clear and well illustrated and only in a few instances, *e.g.* those involving some computer generated data, could the presentation be improved. Because of its practical orientation this book will be of value and special interest to chemists in several areas of research, as well as a supplementary text book for graduate level courses in instrumental analysis and advanced mass spectrometry.

R. M. Dagnall (Huntingdon)

Computers in Chemistry (Topics in Current Chemistry, Vol. 39), Edited by F. Boschke, Springer–Verlag, Berlin, 1973, iii+195 pp., price DM 62,—.

This soft-cover monograph ranges widely over the applications of computers in chemistry. It begins with a discussion of computer-designed organic syntheses (Thakkar) and of the use of an algebraic model of constitutional chemistry as a basis for chemical computer programmes (Dugundji and Ugi). This is followed by consideration of the better-known applications of computers to information retrieval (Veal), and to identification of spectra and thus of organic compounds (Clerc and Erni), and of the use of computers for mass spectral interpretations (Delfino and Bucks) and in gas chromatography (Caesar). The final article is concerned with computer-assisted instruction in chemistry (Geist and Ripota).

The book as a whole gives a balanced account of how computers are becoming increasingly useful in many fields of chemistry, and all chemists who strive to keep up-to-date will find these chapters a relatively easy means of doing so.

A. Townshend (Birmingham)

Wolfgang Leithe, *The Analysis of Organic Pollutants in Water and Waste Water*, Ann Arbor–Wiley, New York, 1973, ix + 213 pp., price £8.75.

The German edition of this book was reviewed by Professor W. Haerdi (*Anal. Chim. Acta*, 65 (1973) 486). This English edition is an efficient translation, and is to be recommended to anyone interested in the analysis of trace effluents and potable waters.

Analytica Chimica Acta, 72 (1974) 452–453

ANNOUNCEMENT

XXV th International Congress of Pure and Applied Chemistry

At the invitation of the Israel Chemical Society, the 25th IUPAC Congress will be held in Jerusalem on 6–11 July, 1975, under the auspices of His Excellency, The President of the State of Israel, Professor Ephraim Katzir, and under the sponsorship of the Israel Academy of Sciences and Humanities, the National Council for Research and Development, and the Hebrew University of Jerusalem.

Tentative Scientific Programme

A. Organic Chemistry

1. New theoretical insights into organic molecules. 2. Chemistry of excited states. 3. Novel instrumental methods of structure determination. 4. Computers in organic synthesis and structure determination. 5. Novel synthetic applications of organometallic compounds. 6. Ylid chemistry. 7. Prebiotic chemistry and organic geochemistry. 8. Approaches to the structure of biological receptors. 9. Stereochemical aspects of biogenesis.

B. Physical Chemistry

1. Condensed phases. 2. Lasers in chemistry. 3. Molecular spectroscopy. 4. Molecular dynamics. 5. Interfacial electrochemistry. 6. Molecular structure. 7. Molecular conformations. 8. Symposium: 50 years of quantum chemistry.

C. Medicinal Chemistry

1. Prostaglandins. 2. Chemistry and biochemistry of ageing. 3. Chemistry of memory. 4. Chemistry of pain relief. 5. Chemotherapy of tropical diseases. 6. Molecular pharmacology. 7. Drugs and toxins from marine sources. 8. Histochemistry. 9. Immunosuppression.

D. Applied Chemistry

1. Processes for future chemical industries. 2. Chemical aspects of future energy sources. 3. Food resources through chemistry. 4. Surface chemistry and surface activity. 5. Chemical processes for water desalination. 6. Industrial use of water. 7. Recycling and re-use of wastes. 8. Chemical means for reduction of environmental pollution.

In conjunction with the 25th IUPAC Congress, the following symposium will be held jointly with the Division of Macromolecular Chemistry of IUPAC, in the week following the IUPAC Congress:

E. Macromolecular Chemistry—The Tihlrd Aharon Katzir-Katchalsky Conference.

1. Developments in polymer theory. 2. Surface- and electrochemistry of macromolecules. 3. Ions in polymeric systems. 4. Polymeric reagents. 5. Membranes—synthesis and function. 6. Biomedical applications of macromolecules. 7. Specialized polymeric systems in structural materials. 8. Polymers in pollution abatement.

The following distinguished scientists have already agreed to deliver plenary lectures at the Congress: Herbert C. Brown, Egbert Havinga, Dudley Herschbach, Ephraim (Katchalsky) Katzir, E. Bright Wilson.

The Congress will be held in the Jerusalem Convention Center (Binyanei Ha'ooma). The official language of the Congress is English. Papers may be presented in any language but the use of a widely understood one is recommended.

Social events will be provided for all participants during the Congress. In addition to the general social activities, a diversified programme will be offered to the accompanying ladies during session time. Post-Congress tours will provide an opportunity to visit all parts of the country. PELTOURS Ltd. are the official travel agents and will provide all the necessary services to participants. Further information can be obtained from "KENES", Organizers of Congresses and Special Events Ltd. P.O. Box 16271, Tel Aviv, Israel.

ERRATA

V. Fano, F. Licci and L. Zanotti, A simple microtitrimetric method for alkaline earth metals, *Anal. Chim. Acta*, 71 (1974) 218–221.
Page 219, on the last but one line of the *Results* section,
"650 nm for copper" should read "605 nm for copper".

Fu Chung Chang, Hui-Tuh Tsai and Shaw-Chii Wu, Determination of Th–U and U–Zr alloy composition with a fluoride-selective electrode, *Anal. Chim. Acta*, 71 (1974) 477–481.
Page 481, Table III should read as follows:

TABLE III

DETERMINATION OF URANIUM(VI), THORIUM(IV) AND ZIRCONIUM(IV) IN MIXTURES

F^- added ($\cdot 10^{-2}$ M)	Th^{4+} ($\cdot 10^{-4}$ M)		UO_2^{2+} ($\cdot 10^{-4}$ M)		Zr^{4+} ($\cdot 10^{-5}$ M)		Relative error (%)		
	Added	Found	Added	Found	Added	Found	Th^{4+}	UO_2^{2+}	Zr^{4+}
1.90	4.0	4.0	6.5	6.4			0	3.0	
1.90	4.0	4.1	7.1	6.9			2.5	2.3	
1.90	3.9	4.0	3.6	3.5			2.0	1.4	
0.30			9.0	8.9	3.5	3.5		1.1	0
0.30			9.0	8.8	4.5	4.4		1.7	2.2
0.30			9.0	8.9	5.5	5.3		1.1	3.6
							Mean 1.5	1.8	1.9

ANALYTICA CHIMICA ACTA, VOL. 72 (1974)

AUTHOR INDEX

ANALYTICA CHIMICA ACTA, VOL. 72 (1974)

SUBJECT INDEX

(Continued from page 4 of cover)

CONTENTS

(Continued on inside page of cover)